Extra-corporeal Carbon Dioxide Removal as an adjunct to Non-Invasive Ventilation in Acute Exacerbations of Chronic Obstructive Pulmonary Disease

Barrett, Nicholas

Awarding institution:
King's College London

Extra-corporeal Carbon Dioxide Removal as an adjunct to Non-Invasive Ventilation in Acute Exacerbations of Chronic Obstructive Pulmonary Disease

Nicholas Anthony Graham Barrett

(1271068)

Supervisors: Dr Luigi Camporota

Professor Nicholas Hart

Centre for Human & Applied Physiological Sciences,

School of Basic & Medical Biosciences,

Faculty of Life Sciences & Medicine,

King's College London

This dissertation is submitted for the degree of

Doctor of Philosophy

August 2023

Dedication

This thesis is dedicated to the patients with COPD who have severe and life limiting disease but who also volunteered to be part of a study to advance our understanding of COPD and its therapies. This thesis and the studies described within could not have occurred without the help and support of the team in the intensive care unit at Guy's and St Thomas' NHS Foundation Trust. The nurses, perfusionists, physiotherapists, dieticians, doctors and support staff of the ICU who provide the dedicated care for patients and their families. The work could not have been undertaken without Dr Eirini Kostakou and the clinical and research nurses. A special thanks to Dr Luigi Camporota and Professor Nicholas Hart who supervised this thesis. Finally, words cannot express the debt that I owe to my family – Bryony, Tomos and Aneira – without whose love and support this work would never have been completed.

Sumus humaniores homines et gerunt braccas

"Man has always assumed that he is more intelligent than dolphins because he has achieved so much – the wheel, New York, wars and so on – while all the dolphins had ever done was muck about in the water having a good time. But conversely, the dolphins had always believed that they were far more intelligent than man – for precisely the same reasons."

Douglas Adams, So Long, and Thanks for All the Fish.

Declaration

I hereby declare that except where specific reference is made to the work of others, the contents of this dissertation are original and have not been submitted in whole or in part for consideration of any other degree or qualification in this or any other University. This dissertation is my own work and contains nothing which is the outcome of work done in collaboration with others, except as specified in the text and acknowledgements. This dissertation contains fewer than 50,000 words and has 35 figures.

Nicholas AG Barrett

August 2023

Acknowledgements

This work could not have occurred without the contributions of others:

Dr Luigi Camporota and Professor Nicholas Hart who supervised and guided me throughout all stages of this work;

Dr Eirini Kostakou who helped with the initial set up of the study including the introduction of oesophageal pressure measurement into the ICU at Guy's and St Thomas';

Dr Patrick Murphy who taught me parasternal electromyography, including the data analysis;

Dr Francesco Murgolo who guided me through the technical analysis of the raw oesophageal pressure data;

The team at Glasgow Royal Infirmary who enrolled one patient into the study and the teams at Chelsea and Westminster and Manchester Royal Infirmary who were prepared to do so;

ALung Inc who funded the work, but had no role in the design, conduct, analysis, presentation or publication of the results;

and the Guy's and St Thomas' ICU team who cared for the patients 24/7 and undertook all the clinical care and changes to therapies.

Abstract

Introduction

Chronic obstructive pulmonary disease (COPD) is a common condition, with a worldwide prevalence of 10.1% and is the third leading cause of death worldwide. Approximately half of patients experience at least one exacerbation per year, with 15% of patients with an exacerbation requiring hospitalisation. Besides the pharmacological management, patients with an acute exacerbation of COPD commonly require respiratory support, most commonly in the form of non-invasive ventilation (NIV). Although NIV provides significant survival benefit, 20-30% of patients tolerate NIV poorly, or do not respond to NIV and require invasive mechanical ventilation, which is associated with a significant increase in mortality. One potential approach to improve patient outcome and to avert invasive ventilation is the use of extracorporeal carbon dioxide removal ($ECCO_2R$), where carbon dioxide is removed directly from the venous blood. Reports of the use of $ECCO_2R$ are from animal and retrospective or observational clinical studies. However, there are significant gaps in the knowledge about $ECCO_2R$.

Carbon dioxide clearance across an artificial membrane lung is relatively well understood however there is limited data available relating to the CE marked device used in this study. There are no data available confirming the CO_2 clearance from the device, nor is there data relating to the relationship between sweep gas flow and CO_2 clearance. Consequently, the first element of the study is a series of bench tests exploring the in vitro clearance across the membrane. The next phase of the underpinning work is the in vivo exploration of CO_2 clearance and its relationship with sweep gas flow rate which is analogous to the minute ventilation of the natural lung.

The second element of the study was to compare NIV and $ECCO_2R$ in patients with an acute exacerbation of COPD (AECOPD) at risk of failing NIV. NIV failure is complex and relates to severity of illness, patient factors including agitation, delirium, tendency to claustrophobia and distress as well as NIV device factors, especially relating to device settings and mask fit/comfort. If patients fail NIV, they commonly require tracheal intubation and mechanical ventilation. In AECOPD, this can result in prolonged

periods of mechanical ventilation leading to a tracheostomy and is often punctuated by recurrent episodes of hospital acquired infection. Patients receiving mechanical ventilation are at significant risk of muscular deconditioning and ICU acquired weakness as well as delirium. All these potential sequelae have significant impacts on long term outcomes. At present studies using $ECCO_2R$ in AECOPD have been limited to observational studies without a contemporaneous control group. Hence there is a need for a randomised, controlled trial comparing outcomes for patients with AECOPD receiving NIV or $ECCO_2R$.

There has been minimal work on the impact of $ECCO_2R$ on respiratory physiology, especially in patients with AECOPD.

The key aims of this thesis are:

1. to assess the CO_2 removal by the device;
2. to assess whether $ECCO_2R$ is of benefit to patients compared with NIV;
3. and to assess the impact of $ECCO_2R$ on work of breathing.

Methods

In vitro and in vivo studies of CO_2 clearance across the membrane

The in vitro component tested the device in accordance with regulatory requirements for extracorporeal devices. This required the development of a circuit with several membranes in series and one in parallel. The circuit was arranged to grossly mimic human physiology with blood flow (provided by an extracorporeal membrane oxygenation pump and providing the surrogate for cardiac output), CO_2 production (provided by CO_2 instillation via a dedicated membrane) and ventilation (CO_2 clearance provided by the study device). The study was based on the physiology seen in AECOPD and created the conditions of a hypercapnic respiratory acidosis using expired human packed red cells. CO_2 clearance was calculated using the trans-membrane CO_2 content difference and the CO_2 content in the gases from the exhalation port at each change in sweep gas flow rates. This data was then compared with the CO_2 removal reported by the device.

The second phase of the basic investigation of the device and the kinetics of CO_2 clearance was an in vivo study. In this study, subjects commenced on $ECCO_2R$ had

serial trans-membrane samples measured as sweep gas flow was increased and transmembrane CO_2 clearance was calculated at each step. The CO_2 reported by the device was also recorded. The two methods were directly compared to ascertain the accuracy of the device. The relationship between sweep gas flow rate and CO_2 clearance in vivo was also explored.

Clinical study

The second component of the thesis was the performance of a prospective, randomised controlled trial of NIV alone compared with NIV and $ECCO_2R$. Patients were included if they were over 18 years of age, had a history of COPD presenting with an acute exacerbation and with a persisting pH <7.30 due to hypercapnia after initial medical therapy and at least one hour of NIV. Patients were excluded if they had acute multiple organ failure, intolerance, allergy or contraindication to heparin, a contraindication to NIV or were receiving chronic domiciliary NIV.

The study was designed for a primary endpoint of time to cessation of NIV with a power calculation performed based on reduction in NIV use of at least 12 hours. Secondary outcomes included physiological measurements, intensive care and hospital length of stay and outcomes at 90-days including quality of life. Adverse outcomes included incidence of major haemorrhage, thrombosis, haemolysis, mechanical complications, need for invasive mechanical ventilation and mortality. Subjective discomfort and dyspnoea were measured using a visual analogue scale. $ECCO_2R$ was delivered using the Hemolung device. All care not directly relating to $ECCO_2R$ was in accordance with standard clinical protocols.

Physiological study

Three different methods were explored simultaneously in the physiological study which included a subset of patients who consented for these elements. The first was oesophageal pressure measurement using an oesophageal balloon. This was used to both measure oesophageal pressure and calculate muscular pressure and transpulmonary pressure. Work of breathing and the pressure time product of each breath was calculated. The second method was electrical impedance tomography where a small current is injected across the thorax using a dedicated device and a

belt placed at the 4th intercostal space anteriorly which measures the changes in impedance with each breath and over time. The impedance change is used to generate changes in tidal impedance change, surface volume, inspiratory time, homogeneity and end expiratory lung impedance. These measurements allow insight into the distribution and timing of aeration both globally and regionally within the lungs. The final method was parasternal electromyography which measures the electrical signal in the intercostal muscles in the upper thorax and is a surrogate for work of breathing. This is achieved through electrodes placed in the second intercostal space anteriorly.

Results

In vitro and in vivo studies of CO_2 clearance across the membrane

The in vitro study demonstrated that firstly the membrane was capable of clearing CO_2 and secondly that the CO_2 clearance reported by the device accurately reflected the CO_2 clearance using the other methods. Finally, there is a clear and consistent relationship between sweep flow rate and CO_2 clearance. CO_2 clearance increases rapidly as sweep flow increases from 0 to 2 L/min. Thereafter the rate of rise of clearance decreases with a plateau between 4 and 6L/minute giving a maximum ventilation/perfusion ratio of approximately 10-15:1 as the limit of efficiency for this artificial membrane lung. These results were replicated by the in vivo study.

Clinical study

The randomised controlled trial demonstrated a significant reduction the duration of NIV with the addition of $ECCO_2R$ (7 hours compared with 30 hours in the NIV group). Additionally, there was a more rapid reduction in respiratory rate and faster resolution of respiratory acidosis with $ECCO_2R$ than with NIV alone, but there was a small increase in respiratory work after commencement of $ECCO_2R$ and removal of NIV. Intensive care and hospital lengths of stay were both approximately 117 hours longer in the $ECCO_2R$ group than with NIV. Symptomatic dyspnoea resolved rapidly with commencement of $ECCO_2R$. The $ECCO_2R$ group had a higher incidence of haemolysis however overall, NIV-related complications were more common than $ECCO_2R$ -related complications.

Physiological study

It was demonstrated that oesophageal pressure pressure indices, work of breathing and pressure time product were lower in the NIV group initially and paradoxically increased as the clinical condition improved. Work of breathing and pressure time product were discordant with NIV, especially on day 2 of the study indicating an elevated isometric work. Electrical impedance tomography demonstrated progressive improvements in aeration in the NIV group. The parasternal electromyogram showed an elevated neural respiratory drive in the NIV group which decreased over time. In the $ECCO_2R$ group the oesophageal pressure measurements indicated that work of breathing and pressure time product remained elevated throughout the study but were concordant without evidence of isometric work. The neural respiratory drive remained elevated than $ECCO_2R$ group throughout the study. Electrical impedance tomography demonstrated a more dorsal distribution of ventilation with $ECCO_2R$, and that aeration was more inhomogeneous than with NIV. The lowest work of breathing and most homogeneous ventilation was found with the combination of NIV and $ECCO_2R$.

Conclusion

In vitro and in vivo studies of CO_2 clearance across the membrane

The important clinical implication of the in vitro and in vivo testing is that the relationship between CO_2 clearance and sweep gas flow rate is non-linear. At the onset of therapy with only 1L/minute of sweep gas, a substantial amount of CO_2 amounting to approximately a third of CO_2 production is cleared (assuming that 3mL/kg/min CO_2 is produced). A plateau is reached at around 4L of sweep gas flow giving a ventilation/perfusion ratio of approximately 10:1 as the limit of efficiency for this artificial membrane lung. It is reasonable to assume that the relationship between sweep flow rate and clearance shows no hysteresis, and consequently during device weaning there remains a significant CO_2 clearance at low sweep low rates. Given this, it is important that a period of slow weaning of the last elements of sweep flow gas occurs and that a period of observation following cessation of sweep flow gas should be undertaken to prevent rebound respiratory failure. The study also

showed that the CO_2 clearance reported by the device is accurate and can be used instead of recurrent sampling from the circuit.

Clinical study

The randomised, controlled trial demonstrated that there was earlier cessation of NIV by approximately 30 hours. The trial also demonstrated a physiological benefit associated with $ECCO_2R$ with a more rapid improvement in respiratory acidosis and tachypnoea with minimal complications. Additionally, there was a patient symptomatic benefit with rapid improvement in discomfort and dyspnoea after the addition of $ECCO_2R$. However, this data also indicates that there was a longer ICU and hospital length of stay for patients commenced on $ECCO_2R$. The study was not powered to demonstrate a mortality benefit or a difference in the need for intubation and these need to be explored in future larger trials. Although many patients did cease NIV shortly after commencing $ECCO_2R$, given that there was a deterioration in gas exchange after removal of NIV, this suggests that there may be a benefit in the combination of $ECCO_2R$ and NIV.

Physiological study

The data from oesophageal pressure measurements, electrical impedance tomography and parasternal electromyography demonstrate differential effects of NIV and $ECCO_2R$ on work of breathing and the distribution of ventilation. NIV provides mechanical support for breathing with improvements in work of breathing, increases in tidal volume and more homogeneous ventilation but in the first 24-48 hours of severe exacerbations there is a persisting dynamic hyperinflation which results in neuromechanical dissociation and increased isometric work despite the use of NIV. $ECCO_2R$ provides clearance of carbon dioxide from the blood which results in a lower minute ventilation, reducing dynamic hyperinflation which in turn reduces neuromuscular dissociation and isometric work but results in an increase in overall work of breathing. The combination of $ECCO_2R$ and NIV allowed elimination of a proportion of the metabolic CO_2 and a reduction in the requirements of alveolar ventilation and was also associated with a lower work of breathing, better neuromechanical coupling and more homogenously distributed ventilation.

Overall conclusion

This thesis has demonstrated the nature of gas exchange across a specific $ECCO_2R$ device and explored its efficiency of gas exchange.

The clinical and physiological data supports different but complementary impacts of NIV and $ECCO_2R$ in patients with AECOPD. NIV provided direct respiratory support but during the early phase of the exacerbation patients remained at end expiratory lung volumes close to total lung capacity and were unable to generate significant pleural pressures or provide adequate aeration of the lungs resulting in isometric contraction and neuromechanical dissociation along with respiratory acidosis. Over time as the exacerbation started to resolve, the ongoing physical support with NIV resulted in improved aeration which was homogenously distributed across the lung. As hyperinflation reduced, and higher muscular pressures were able to be generated, acidosis was corrected and sensations of dyspnoea reduced. $ECCO_2R$ removed CO_2 from the venous blood and allowed early reduction in dyspnoea with reduced respiratory rate, lower dynamic hyperinflation and improvement in neuromechanical dissociation and isometric work.

The combination of $ECCO_2R$ and NIV provided particular benefit early in the course of an exacerbation with elimination of a significant proportion of the metabolic CO_2 and a reduction in the requirements of alveolar ventilation and was also associated with a lower work of breathing, lower neural drive and more homogenously distributed ventilation than $ECCO_2R$ alone.

Table of contents

List of figures

List of tables

List of equations

Glossary of terms

AECOPD	acute exacerbation of COPD
ARDS	acute respiratory distress syndrome
ATP	ambient temperature and pressure
AU	arbitrary units
AV	arterio-venous
BF	blood flow
BMI	body mass index
BTPS	body standard temperature (37°C) and saturated with water vapour
CAT	COPD assessment test
CGVD	centre of gravity of ventilation distribution
COPD	chronic obstructive pulmonary disease
$CtCO_2$	CO_2 content in blood
CtO_2	O_2 content in blood
dEELI	change in end expiratory lung impedance
dP_{ES}	change in oesophageal pressure
dTID	change in tidal impedance distribution
DZ	change in impedance
E	elastance
$ECCO_2R$	extracorporeal carbon dioxide removal
ECMO	extracorporeal membrane oxygenation
EELI	end expiratory lung impedance
EELV	end-expiratory lung volume
EIT	electrical impedance tomography
$EMG_{paramax\%}$	percentage of maximal parasternal electromyelogram signal
GF	gas flow
GI	global inhomogeneity
GOLD	global Initiative for chronic obstructive lung disease
LOS	length of stay
MP	mechanical power

NDRI	Neural respiratory drive index
NIV	non-invasive ventilation
P_{AW}	airway pressure
PEEP	positive end-expiratory pressure
pEMG	parasternal electromyelography
P_{ES}	oesophageal pressure
P_{MUS}	muscular pressure
PTP	pressure time product
R	resistance
RMS	root mean square
RVD	regional ventilation distribution
SGRQ	St George's respiratory questionnaire
STPD	standard temperature (0°C), pressure and dry
SURF	surface of aerated volume
τ_E	expiratory time constant
TID	tidal impedance distribution
TPP	transpulmonary pressure
V/Q	ventilation/perfusion ratio
VCO_2	CO_2 production
VCO_2/VO_2	respiratory quotient
VR	ventilatory ratio
WOB	work of breathing

Chapter 1: Introduction

Chronic obstructive pulmonary disease (COPD) is a common condition, with a worldwide prevalence of 10.1% and is the third leading cause of death worldwide accounting for 3.2 million deaths in 2017 (Celli & Wedzicha, 2019). Globally, COPD is a major cause of morbidity, mortality and health care expenditure (Nguyen et al., 2021). In the USA, there are approximately 500,000 inpatient stays with AECOPD annually with an average hospital length of stay of 4.7 days at an estimated cost of US$3.8 billion (Wier et al., 2011). The cost is even greater in patients with co-morbidities including heart failure and hyperlipidaemia (Shah et al., 2021). The annual cost of hospital admissions relating to AECOPD in the UK is approximately £320 million (NICE, 2011). Patients requiring invasive ventilation for the management of respiratory acidosis are responsible for a disproportionate amount of that cost.

In the UK, approximately 1.9% of the population has been diagnosed with COPD (PHE, 2023), although the true incidence is thought to be significantly higher (Gruffydd-Jones, 2008). Approximately half of patients experience at least one exacerbation per year, with 15% of patients requiring hospitalisation (Raluy-Callado et al., 2015; Whittaker et al., 2022). Patients with a moderate or severe exacerbation are more likely to have a further exacerbation and have a significantly increased risk of death compared with patients with COPD but without exacerbations (Raluy-Callado et al., 2015; Whittaker et al., 2022). Patients with more severe underlying disease, with higher Global Initiative for Chronic Obstructive Lung Disease (GOLD) stage, higher modified Medical Research Council dyspnoea scale and lower body mass index (BMI) are more likely to have more severe exacerbation (Whittaker et al., 2022). Patients with severe exacerbations are 2-5 times more likely to die from their exacerbation (Raluy-Callado et al., 2015; Whittaker et al., 2022).

Besides the pharmacological management (Vasques et al., 2020), patients with an acute exacerbation of COPD (AECOPD) require respiratory support, usually non-invasive ventilation (NIV) (Brochard et al., 1995). NIV provides significant survival benefit with a mortality reduction from approximately 30% to 10% (Brochard et al., 1995; Lightowler et al., 2003). However, 20-30% of patients tolerate NIV poorly, or

do not respond to NIV and require invasive mechanical ventilation, which is associated with a significant increase in mortality (Brochard et al., 1995; Duan et al., 2019; Echevarria et al., 2020; Lightowler et al., 2003).

The acute and severe airflow obstruction increases the respiratory work but is associated with inefficient gas exchange which leads to hypercapnia, which in turn increases respiratory drive. One potential novel approach to interrupt this vicious cycle is the use of extracorporeal carbon dioxide removal ($ECCO_2R$), where carbon dioxide is removed directly from the venous blood in a manner analogous to removal of creatinine in dialysis for renal failure. This method directly reduces arterial carbon dioxide tension and content and improves acidaemia. Although this technique has shown promising results from uncontrolled case series, there is no prospective, randomised data supporting its use in association with or instead of NIV (Burki et al., 2013). Furthermore, there is limited physiological data explaining how $ECCO_2R$ changes respiratory mechanics.

The key aims of this thesis are to assess:

1 The ability of a commonly used $ECCO_2R$ device to remove carbon dioxide;
2 Benefits of $ECCO_2R$ is compared with NIV alone in AECOPD;
3 The impact of $ECCO_2R$ on work of breathing and regional distribution of ventilation.

1.1 Chronic Obstructive Pulmonary Disease

COPD is a syndrome characterised by progressive and not fully reversible expiratory airway flow limitation (Halpin et al., 2021; Vestbo et al., 2013). COPD is commonly caused by cigarette smoking and the number of pack-years directly correlates with the severity of illness (Halpin et al., 2021). COPD may also be caused by other conditions including alpha-1 anti-trypsin deficiency, atmospheric pollutants and occupational exposure to a variety of noxious substances (Halpin et al., 2021; Vestbo et al., 2013). The underlying pathophysiology of COPD is the progressive destruction of the elastic and alveolar tissue within the lung (Halpin et al., 2021). This results in reduced expiratory flow rates, maldistributed ventilation, gas trapping and

hyperinflation, which in turn leads to diaphragmatic flattening and inefficient respiration.

The clinical sequelae of COPD are chronic dyspnoea, cough and sputum production, punctuated by recurrent exacerbations, on average 2 to 3 times annually. GOLD defines an exacerbation of COPD as an acute event characterised by a worsening of the patient's dyspnoea, cough and/or sputum production beyond day-to-day variations (Halpin et al., 2021). Exacerbations are triggered by any stimulus that increases the inflammatory burden in the airways, including bacterial or viral infections and environmental pollution (Halpin et al., 2021; Sapey & Stockley, 2006). Acute exacerbations are an important cause of hospital admission and impact on patients' quality of life (Anzueto, 2009; Garcia-Aymerich et al., 2003; Kessler et al., 2006; Spencer et al., 2004). Exacerbations also accelerate disease progression leading to a progressive stepwise functional decline (Ankjaergaard et al., 2017; Anzueto et al., 2009; Donaldson et al., 2002; Kanner et al., 2001; Kesten et al., 2011; Seemungal & Sykes, 2008; Seemungal et al., 2000). It is not known whether this is solely because of the exacerbation itself or whether the therapy, including higher inspired oxygen and mechanical ventilation or other consequences of hospital admission, including antibiotic exposure and colonisation by resistant organisms, also contribute. As the underlying disease and functional status declines, a vicious cycle develops where exacerbations become increasingly common and more severe, leading inexorably to death (Pauwels et al., 2001). It has recently been demonstrated that this cycle can be interrupted through the addition of domiciliary non-invasive ventilation for patients with persistent hypercapnic respiratory failure following an acute exacerbation (Ankjaergaard, Maibom, et al., 2016; Ankjaergaard, Tonnesen, et al., 2016; Murphy et al., 2017).

1.2 Regulation of arterial carbon dioxide

The development of respiratory acidosis is a key element in the need for hospital admission and the clinical sequelae of COPD exacerbations. To understand its development, the carriage and control of CO_2 in health and disease as well as the physiological impact of exacerbations needs to be considered.

1.2.1 Carbon dioxide carriage in the blood

Carbon dioxide (CO_2) is carried in the blood in three forms – in solution as a gas, as bicarbonate and bound to proteins, particularly haemoglobin, as carbamino compounds (Cherniack & Longobardo, 1970; O'Neill & Robbins, 2017). The concentration of CO_2 dissolved is determined by Henry's law of solubility (PCO_2 x solubility coefficient = concentration of CO_2 in solution), where the solubility coefficient at 37 degrees Celsius is 0.231 mmol L^{-1} kPa^{-1} (Arthurs & Sudhakar, 2005). The major proportion of CO_2 in the blood is carried as bicarbonate ion, which is formed from carbonic acid in a reaction catalysed by carbonic anhydrase ($H_2CO_3 \rightleftharpoons H^+ + HCO_3^-$) (O'Neill & Robbins, 2017; West, 2011). This reaction occurs within the red cell due to the presence of carbonic anhydrase. CO_2 can also be carried as carbamic acid which is a direct reaction between α-amino groups and CO_2. The major protein carrying CO_2 is haemoglobin, with CO_2 binding at α-amino groups of both α and β chains. Carriage of CO_2 on haemoglobin is modified by both 2,3-diphosphoglycerate which competes with CO_2 for the α-amino groups of the β chains and the Haldane effect. The Haldane effect is the increase in CO_2 carriage in de-oxygenated compared with oxygenated blood (O'Neill & Robbins, 2017; West, 2011). This difference is due to deoxyhaemoglobin having a higher affinity for hydrogen ions and hence drives a shift in the bicarbonate from carbonic acid increasing total CO_2 content. The Bohr effect also occurs. The Bohr effect describes a decreased affinity of haemoglobin for oxygen with increasing CO_2 and H^+ concentrations due to conformational changes in the haemoglobin molecule (O'Neill & Robbins, 2017; West, 2011).

As the red cell traverses from the arterial to the venous side of the capillary, oxygen is rapidly offloaded into the tissues. Simultaneously CO_2 is taken up and moves into the red cell. The conformational changes in haemoglobin result in increased carbamino carriage and at the same time, increased bicarbonate is formed through the hydration and subsequent dissociation of CO_2, catalysed by carbonic anhydrase. The increased concentration of hydrogen ions is buffered by binding to de-oxygenated haemoglobin. The increased concentration of bicarbonate ions is managed by a chloride exchange transport protein from the red cell into the plasma, known as the Hamburger shift (O'Neill & Robbins, 2017; West, 2011). The Hamburger

shift is facilitated by a membrane bound protein – band 3 – which sequentially exchanges bicarbonate for chloride ions. In the pulmonary capillary, CO_2 passes down its concentration gradient into the alveolus and oxygen is taken up and the processes reverse.

The Henderson-Hasselbalch equation, derived from the equilibrium equation for the dissociation of carbonic acid, is shown in Eq 1.1.

$$pH = pKa + log_{10}\frac{[HCO_3]}{\alpha PCO_2} \quad \text{[Eq 1.1]}$$

Equation 1.1: Henderson-Hasselbalch equation. pKa is the equilibrium constant (~6.1 at 37°C and pH 7.4), $[HCO_3]$ is the total concentration of bicarbonate and αPCO_2 is the solubility coefficient of CO_2 multiplied by its partial pressure in plasma.

Rearranging this gives:

$$[HCO_3] = \alpha PCO_2.\left(10^{(pH-pK)}\right) \quad \text{[Eq 1.2]}$$

Equation 1.2: Rearranged Henderson-Hasselbalch equation.

Since total plasma CO_2 content is the sum of that carried as bicarbonate and that in solution, we have:

$$Ct_{CO2,\,(plasma)} = [HCO_3] + \alpha PCO_2 = \alpha PCO_2.\left(10^{(pH-pK)}\right) + \alpha PCO_2 \quad \text{[Eq 1.3]}$$

Equation 1.3: Total plasma CO_2 content

Which rearranges to:

$$Ct_{\mathrm{CO2,\,(plasma)}} = \alpha \mathrm{PC}O_2.\left(1 + 10^{(pH-pK)}\right) \quad \text{[Eq 1.4]}$$

Equation 1.4: Rearranged total plasma CO_2 content

It was shown by Visser (1960) (Visser, 1960), and modified by McHardy (1967) (McHardy, 1967) that the whole blood CO_2 content can be calculated by multiplying

the plasma CO_2 content by a 'factor'. Not surprisingly, given the previous discussion on the capacity of haemoglobin to buffer protons, this factor is itself a function of both the total haemoglobin concentration, and its oxygen saturation. It can be seen below that both McHardy's 1967 version of this factor (transcribed from Van Slyke's 1932 nomogram (Van Slyke et al., 1932)), and that derived empirically by Douglas in 1988 are structurally similar, but with minor differences in the input constants (Douglas et al., 1988; McHardy, 1967).

$$Ct_{CO2,\,(blood)} = Ct_{CO2,\,(plasma)}.F \qquad \text{[Eq 1.5]}$$

Where,

$$F(McHardy) = 1 - \frac{0.02924[Hb]}{(2.244 - 0.422.SO2) - (8.74 - pH)}$$

$$F(Douglas) = 1 - \frac{0.0289[Hb]}{(3.352 - 0.456.SO2) - (8.142 - pH)}$$

Equation 1.5: Total CO_2 in blood with variation using the methods of McHardy (McHardy, 1967) and Douglas (Douglas et al., 1988).

I adopt the Douglas calculation for work in this thesis.

1.2.2 Control of respiration

Respiration is under the control of the dorsal and ventral respiratory groups in the medulla oblongata responsible for inspiratory and expiratory initiation respectively (Adler & Janssens, 2019; Ikeda et al., 2017; Krohn et al., 2023; Smith, 2022). A respiratory group in the pons then modulates the frequency and intensity of the neuronal signals from the medulla (Adler & Janssens, 2019; Ikeda et al., 2017; Smith, 2022). Input into the respiratory control centre is received from mechanoreceptors in the airways, lung and pulmonary vasculature which provide signals relating to lung volume, pulmonary irritants and interstitial oedema respectively (Adler & Janssens, 2019; Mortola, 2019). Peripheral (carotid body and aortic) and central (medullary) chemoreceptors exert significant influence over respiratory drive. Carbon dioxide is

a potent determinant for respiratory drive. CO_2 is a highly soluble molecule and readily crosses the blood brain barrier. Rising CO_2 leads to a fall in the pH within the cerebrospinal fluid stimulating respiration (Adler & Janssens, 2019). Hypoxaemia is also an important stimulant for respiration however it is significantly less potent than hypercapnia (Javaheri & Kazemi, 1987). Distress, changes in temperature, pain and panic provide further input into respiratory drive (Krohn et al., 2023; Tipton et al., 2017).

A model that describes the control of breathing and which describes the relationship between $PaCO_2$ and alveolar minute ventilation has been proposed (Collins et al., 2023; Spinelli et al., 2020; Vaporidi et al., 2020). This model links neural factors, ventilatory changes achieved by the change in respiratory centre outflow and the metabolic changes in CO_2 production to relate alveolar minute ventilation to $PaCO_2$. The $PaCO_2$ that results from the respiratory centre set point is the eupneic $PaCO_2$. In health the eupneic $PaCO_2$ and the actual $PaCO_2$ are identical, however this is not the case in respiratory disease when the respiratory centre set-point is not able to be achieved contributing to the development of neuromechanical dissociation (Collins et al., 2023; Spinelli et al., 2020; Vaporidi et al., 2020).

1.2.3 Determinants of alveolar minute ventilation

The three-compartment model of Riley and Cournand (1949) (Riley & Cournand, 1949, 1951) indicates that the arterial blood gas is impacted by the presence of shunt, dead space and ideal alveolar units, where ventilation and perfusion are optimally matched. In health, there is a scatter of ventilation/perfusion ratios within the lung, for example those due to the impact of gravity (West, 2011; West et al., 1964). Dead space is the proportion of the total tidal volume that does not participate in gas exchange and in health is approximately 30% of tidal volume (Lumb, 2017; West, 2011). Alveolar ventilation is minute ventilation minus deadspace ventilation (Lumb, 2017; West, 2011).

The total physiological dead space is made up of 1) *anatomical dead space* – the volume of the naso-oropharynx, trachea and conducting airways and 2) *alveolar dead space* – the proportion of inspired gas that passed through the anatomical dead space

and ventilates non perfused alveoli and therefore does not contribute to gas exchange. The alveolar gas composition of these alveoli is the same as inspired air (Lumb, 2017; West, 2011).

Physiological dead space was first described by Bohr using the alveolar partial pressure of CO_2 ($PACO_2$) and mixed expired partial pressure of CO_2 ($PeCO_2$) (Bohr, 1891; Lumb, 2017). Since $PACO_2$ cannot be measured, arterial $PaCO_2$ is substituted into Bohr's equation as a reasonable approximation of it (Enghoff, 1938; Lumb, 2017).

$$\text{physiological dead space} = V_T*(PaCO_2 - PeCO_2)/PaCO_2 - \text{apparatus dead space}$$

Equation 1.6: Enghoff's modification of the Bohr equation (Lumb, 2017). V_T is tidal volume, $PaCO_2$ is arterial partial pressure of CO_2, $PeCO_2$ is the mixed expiratory partial pressure of CO_2.

It is also important to consider the impact of perfused but not ventilated alveolar units (shunt) when considering calculation of dead space (Tusman et al., 2012; Tusman et al., 2011) as the arterial PCO_2 cannot be considered equivalent to the alveolar PCO_2 in the presence of shunt.

Although Enghoff's modification is a good approximation for dead space calculated by the Bohr calculation in health, in conditions where there is significant venous admixture or shunt, Enghoff's modification provides a higher estimate of physiological dead space than the true value (Bourgoin et al., 2017; Riley & Cournand, 1949, 1951; Suarez-Sipmann et al., 2013; Wagner, 2008).

1.2.4 Impact of COPD

In COPD, there is a chronic increase in alveolar dead space fraction that results from destruction of alveolar walls with enlargement of the alveolar spaces and loss of surface area in combination with obliteration of the pulmonary capillaries and unequal ventilation of alveolar units (Brusasco & Martinez, 2014). The under-ventilated alveolar units results in ventilation/perfusion (V/Q) inequality and leads to the development of venous admixture and arterial hypoxaemia (Marthan et al., 1985; Wagner et al., 1977). The hypoxic alveolar units are also accompanied by hypoxic

pulmonary vasoconstriction (Cooper & Celli, 2008; Dunham-Snary et al., 2017; Nagaraj et al., 2017). Hypercapnia is thought to develop as a response to the decreased ventilatory efficiency leading to a progressive increase in respiratory work (Adler & Janssens, 2019; Gorini et al., 1996; Mathews et al., 2020; Roussos & Koutsoukou, 2003; Similowski et al., 1991). The high inspiratory muscle load to overcome increased airway resistance, degree of obstruction and the mechanical disadvantage caused by the shortening of the muscles of respiration, especially diaphragmatic flattening, all contribute to high respiratory work and an increase in CO_2 production (Mathews et al., 2020; Saure et al., 2012). Consequently, there is a downregulation of respiratory drive that results in relative hypoventilation to reduce overall respiratory work which leads to chronic hypercapnia (Adler & Janssens, 2019; Gorini et al., 1996; Mathews et al., 2020; Roussos & Koutsoukou, 2003; Similowski et al., 1991).

1.3 Exacerbations of COPD

1.3.1 Clinical presentation

An exacerbation of COPD is defined as an increase in symptoms above the normal variation for that patient that results in a treatment change (Halpin et al., 2021; Vestbo et al., 2013). An exacerbation of COPD starts with a trigger, for example a bacterial or viral respiratory infection or changes in air pollutants (Wedzicha & Seemungal, 2007). Symptoms include increased dyspnoea, sputum load or cough. Exacerbations may be mild and require only a change in outpatient management or moderate to severe and require hospitalisation, parenteral medication or respiratory support (Halpin et al., 2021; Vestbo et al., 2013).

The standard initial management of COPD exacerbations consists of inhaled bronchodilator therapy (short-acting β2 agonists in combination with short-acting anticholinergics) (Celli & MacNee, 2004; Halpin et al., 2021; Vasques et al., 2020; Vestbo et al., 2013), oral and/or inhaled corticosteroids (Davies et al., 1999; Maltais et al., 2002; Niewoehner, 2008; Niewoehner et al., 1999; Thompson et al., 1996) and antibiotics (Quon et al., 2008). Respiratory support is initially provided using

supplemental oxygen aiming for peripheral haemoglobin saturation (SpO_2) of 88-92% (Austin et al., 2010).

1.3.2 Pathophysiology of a COPD exacerbation

Exacerbations result in increasing airway and systemic inflammation (Bhowmik et al., 2000; Hurst et al., 2006). Airway inflammation causes worsening oedema, bronchospasm and sputum production (D. E. O'Donnell & C. M. Parker, 2006a), resulting in progressive airway narrowing. In accordance with Poiseuille's law, airway narrowing leads a significant increase in airway resistance and increased expiratory time constants (figure 1.1).

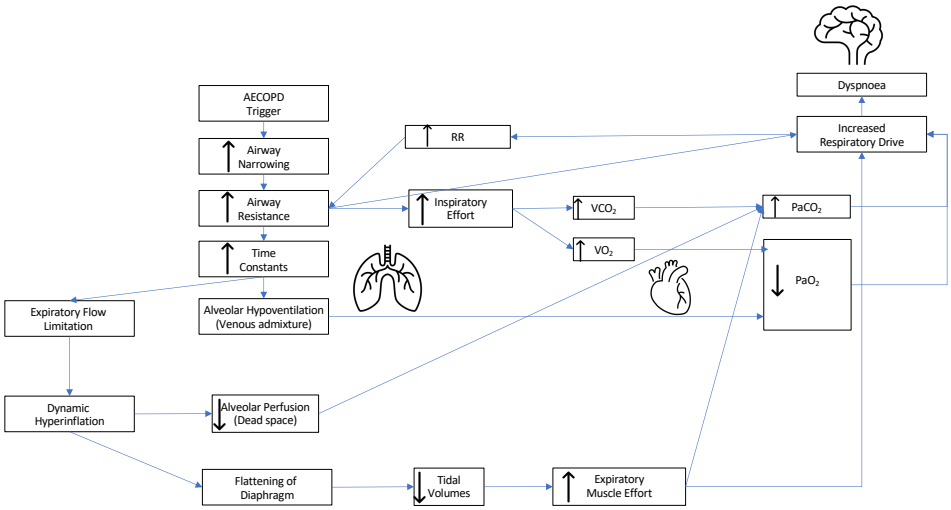

Figure 1.1: The pathophysiology of COPD exacerbations.

The expiratory time constant (τ_E) is the time taken for the lungs to deflate by 63% and is the product of compliance and resistance. Increasing airway resistance lengthens τ_E for the entire lungs, however, given the heterogenous nature of COPD there is significant regional variability in expiratory time constants (Al-Rawas et al., 2013; Banner & Lampotang, 1988; Engel, 1986). As τ_E increases, the underlying V/Q heterogeneity also progressively worsens with an increase in the proportion of low V/Q alveolar units (Al-Rawas et al., 2013; Banner & Lampotang, 1988; Engel, 1986). As discussed above, low V/Q alveolar units lead to systemic hypoxaemia, although this can be relatively easily overcome through supplemental oxygen (Barbera et al.,

1997; Calverley, 2003; Riley & Cournand, 1949, 1951). Increasing τ_E results a need for expiration to lengthen to allow expiration to complete, without this, dynamic hyperinflation will occur (Calverley, 2003; Pellegrino et al., 1993). Dynamic hyperinflation also reduces alveolar perfusion leading to an increase in dead space (Laghi & Goyal, 2012; West & Wagner, 1998). This leads to wasted respiratory effort as alveolar ventilation becomes a progressively lower proportion of minute ventilation (West & Wagner, 1998). By reducing venous return, dynamic hyperinflation also reduces cardiac output which decreases oxygen delivery to tissues, worsening respiratory muscle fatigue (Cardoso et al., 2020; Lukacsovits et al., 2023). Prolonged near maximal loading of the muscles of respiration combined with hypoxia, hypercapnia, acidosis, and reduced cardiac output worsens fatigue and contributes to progressive hypercapnia (Ranieri et al., 1997).

Expiratory flow varies with lung volume and when expiratory flow approaches the maximum that can be generated for any given lung volume, expiratory flow limitation will occur (Calverley, 2003; D. E. O'Donnell & C. M. Parker, 2006b). Dynamic hyperinflation occurs when expiratory time is insufficient to allow end-expiratory lung volume (EELV) to fall to baseline (Calverley, 2003; Pellegrino et al., 1993). As EELV increases, it approaches total lung capacity and there is a rightward shift of the pressure/volume relationship of the lung, reducing pulmonary dynamic compliance (Macklem et al., 1965; Wagers & Jaffe, 2003). As EELV increases, the diaphragm shortens leading to functional diaphragmatic weakness and increased work for the muscles of respiration (Laghi & Tobin, 2003; Orozco-Levi et al., 1999; M. Orozco-Levi et al., 2001; M. I. Polkey et al., 1996; Similowski et al., 1991). The increasing work performed by respiratory muscles results in increasing oxygen demand and carbon dioxide production by approximately a quarter (Ranieri et al., 1997). The increase in EELV is strongly correlated with subjective dyspnoea, increasing distress and sympathetic stimulation (Lougheed et al., 1995; Lougheed et al., 1993).

Expiratory flow limitation due to increasing airway resistance leads to the development of intrinsic positive end-expiratory pressure (PEEP) (Laghi & Goyal, 2012). The inspiratory muscles must overcome the airway resistance and the inward recoil of the lung and chest wall prior to initiating inspiratory flow, effectively

providing an inspiratory threshold load (Haluszka et al., 1990; Pare et al., 1982). Inspiratory threshold load accounts for up to 60% of static inspiratory work of breathing during an exacerbation (Broseghini et al., 1988; Guérin et al., 1993; Tantucci et al., 1991; Terry et al., 1978). The overall effect of loading already weak muscles is that the effort for inspiration is a significant proportion of maximal effort and this is perceived as dyspnoea and distress (Chen et al., 1992). Tachypnoea reduces inspiratory time, exacerbates dynamic inspiratory work and adds to the patient's perception of distress. Increasing inspiratory and expiratory muscle effort along with tachypnoea increases CO_2 production, which is estimated to be 25% higher than normal value of 200 to 250 mL/min (Ranieri et al., 1997).

The neural drive to breathe is preserved and can increase during exacerbations of COPD (A. De Troyer et al., 1997; Sinderby et al., 2001). Hypercapnic acidosis, hypoxaemia, fever from infection, sympathetic load and distress all increase neural drive. As the expiratory flow does not increase in proportion to the neural drive, neuromechanical dissociation occurs (James et al., 2022; Jolley et al., 2009; Moxham & Jolley, 2009; O'Donnell et al., 2020; Reilly et al., 2011). Neuromechanical dissociation worsens patient perceptions of dyspnoea further increasing distress and sympathetic load (Chen et al., 1992; A De Troyer et al., 1997; O'Donnell et al., 1997; O'Donnell et al., 2001; Sinderby et al., 2001).

Arterial hypoxaemia also develops during a COPD exacerbation (Barbera et al., 1997). Arterial hypoxaemia is contributed to by high oxygen consumption by respiratory muscles. Increasing oxygen consumption leads to lower mixed venous oxygen saturation which, in the presence of V/Q mismatch and venous admixture further exacerbates systemic hypoxaemia (Barbera et al., 1997). The addition of supplemental oxygen reduces hypoxic pulmonary vasoconstriction and increases the perfusion of underventilated alveoli which increases venous admixture and therefore CO_2 transfer from right to left contributing to the development of hypercapnia (Aubier et al., 1980; O'Donnell et al., 2002; Robinson et al., 2000). Another important factor in the worsening hypercapnia associated with oxygen therapy is the Haldane effect which describes the upward shift of the CO_2 dissociation curve as blood is deoxygenated (Abdo & Heunks, 2012; Aubier et al., 1980; Hanson et al., 1996).

The pathophysiological effects of AECOPD can be potentially reversed by the use of NIV or $ECCO_2R$ which can potentially reduce arterial CO_2 through differing physiological mechanisms (figure 1.2). NIV provides support through the application of positive pressure which should reduce inspiratory effort and improve alveolar ventilation. $ECCO_2R$ provides support by reducing arterial CO_2 directly. It is possible that these different approaches result in reductions in inspiratory drive and dyspnoea which in turn reduce tachypnoea and the deleterious impacts of expiratory flow limitation on respiratory mechanics.

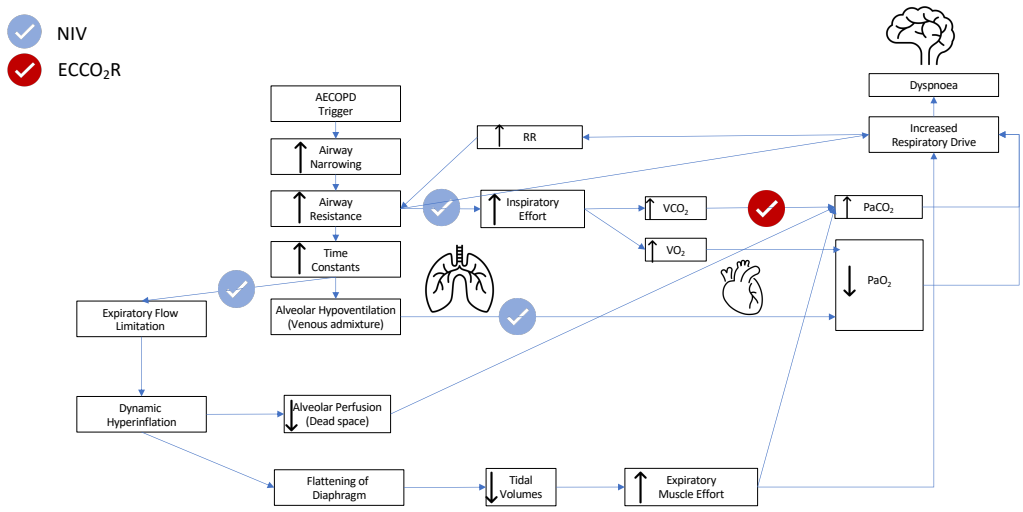

Figure 1.2: The pathophysiology of COPD with the potential impacts of NIV and $ECCO_2R$

1.4 Non-invasive ventilation

Non-invasive ventilation is a form of mechanical ventilation which provides positive pressure during inspiration and expiration most commonly via a tight-fitting facemask. Enhanced FiO_2 can also be provided and titrated to patient requirements.

1.4.1 Pathophysiological rational of non-invasive ventilation

NIV impacts the pathophysiology of exacerbations of COPD at several different points (figure 1.2). The application of extrinsic PEEP balances the effects of intrinsic PEEP and splints open unstable or collapsing airways (Appendini et al., 1994; Girault et al.,

1997; Ranieri et al., 1997). This increases expiratory flow, decreases expiratory muscle activation and reduces end-expiratory lung volume and dynamic hyperinflation which reduces the inspiratory threshold load and improves the pressure/volume relationship of the lung to improve compliance (Appendini et al., 1994; Girault et al., 1997; Osadnik et al., 2017; Ranieri et al., 1997).

The application of inspiratory pressure provides significant physiological benefits. Positive pressure offloads the inspiratory work for the respiratory muscles and enhances tidal volume (Appendini et al., 1994; Girault et al., 1997; Ranieri et al., 1997). The enhanced tidal volume improves alveolar ventilation to improve both PaO_2 and $PaCO_2$/pH (Brochard et al., 1990; Brochard et al., 1995; Díaz et al., 2002; Diaz et al., 1997). Higher inspiratory pressures have been shown to provide greater benefit with reduced diaphragmatic fatigue, reduced diaphragmatic oxygen consumption, larger tidal volumes and lower respiratory rates, although at the expense of greater discomfort and a higher likelihood of mask leaks (Díaz et al., 2002; Dreher et al., 2011; Dreher et al., 2010; Elliott et al., 1994; Field et al., 1984; Jubran et al., 1995; Köhnlein et al., 2014; Prinianakis et al., 2004; Windisch et al., 2015).

Although supplemental oxygen can result in a worsening hypercapnoea due to the release of hypoxic pulmonary vasoconstriction combined with low alveolar ventilation, these impacts are limited at a peripheral saturation of around 90% (Abdo & Heunks, 2012). Supplemental oxygen, combined with enhanced alveolar ventilation, overcomes the arterial hypoxaemia induced by low V/Q units and provides improved oxygen delivery for tissues which is important given the marked increase in oxygen consumption of the respiratory muscles (Brochard et al., 1990; Diaz et al., 1997).

1.4.2 Evidence for non-invasive ventilation

Patients with hypercapnic respiratory failure with respiratory acidosis ($PaCO_2$ > 6kPa and pH < 7.35) have a severe and potentially life-threatening respiratory failure and NIV is considered standard of care (Burge & Wedzicha, 2003; Halpin et al., 2021; Osadnik et al., 2017; Ram et al., 2004; Rochwerg et al., 2017; Vestbo et al., 2013). Randomised controlled trials have demonstrated that NIV provides significant clinical

benefit averting intubation in 70-80% of patients (Brochard et al., 1995; Lightowler et al., 2003; Osadnik et al., 2017; Ram et al., 2004). NIV decreases mortality, ICU and hospital length of stay, the need for tracheostomy and complications associated with invasive mechanical ventilation (Brochard et al., 1995; Carrera et al., 2009; Conti et al., 2002; Kramer et al., 1995; Plant et al., 2000; Ram et al., 2004). However, despite the strong evidence that therapy with NIV is beneficial for patients with AECOPD, 15-30% of patients commencing NIV fail to improve and require intubation and mechanical ventilation (Abroug et al., 2017; Demoule et al., 2006; Ozsancak Ugurlu & Habesoglu, 2017). There are several contributors to NIV failure. NIV may cause discomfort (30-50%), claustrophobia (5-20%) and noise (up to 100%) that impacts patient tolerance (Carron et al., 2013; Osadnik et al., 2017). Other acute complications include pneumothorax, caused by a combination of the direct effects of positive inspiratory pressure and the increased in lung volume and pressure due to airflow limitation and gas trapping; hypotension due to a positive pressure reducing venous return and worse right heart failure; nasal/facial pressure areas caused by the tight interface; and dyssynchrony due to leaks or improper NIV settings (Carron et al., 2013). Complications relating to air flow are significant and include nasal/oral/airway dryness, aerophagia with gastric insufflation and emesis and air leaks due to a combination of mask fit and air pressure (Carron et al., 2013). The frequency of some of these complications can be reduced, but not eliminated, by staff with expertise and equipment selection. Ventilator dyssynchrony can be particularly problematic and is a major cause of NIV failure. It is contributed to by both patient (respiratory drive, degree of dynamic hyperinflation, muscle strength) and mechanical factors (mask fit, air leaks, inspiratory/expiratory pressure settings, inspiratory flow rate and trigger and autotriggering from either cardiac oscillations or excessive water in the circuit) (Carron et al., 2013).

NIV failure has several specifically identified risk factors include obtundation, higher APACHE II score (>28), and lack of improvement in the first 1-2 hours of therapy with persisting respiratory acidosis (pH <7.30), tachypnoea (>29) (Carratu et al., 2005; Confalonieri et al., 2005; Contou et al., 2013; Kumar et al., 2013; Ozsancak Ugurlu & Habesoglu, 2017). Factors that also contribute to NIV failure include significant co-

morbidities, mask intolerance, significant hypoxia, high secretion load and absent dentition (Schettino et al., 2008; Soo Hoo, 2010; Soo Hoo et al., 1994; M. Stefan et al., 2015).

Over the last decade, the proportion of patients with AECOPD requiring any form of respiratory support has remained relatively constant at 7-8% and the in-hospital mortality of patients with AECOPD requiring NIV as the sole supportive therapy has fallen to 5-7% (Chandra et al., 2012). However, patients requiring invasive mechanical ventilation have a significantly higher mortality (Chandra et al., 2012; Demoule et al., 2006; Schnell et al., 2014; Tabak et al., 2009; Toft-Petersen et al., 2017). The mortality is highest for patients who commence on NIV, fail to improve, and are transitioned to mechanical ventilation (Chandra et al., 2012). The absolute number of patients transitioning from NIV to mechanical ventilation has increased over the last decade and the mortality in this group has progressively risen, from approximately 20% to 30% (Chandra et al., 2012). Mechanical ventilation is known to have a wide range of complications including ventilator induced lung injury, ventilator associated pneumonia, muscular deconditioning, delirium, laryngeal dysfunction, and the need for tracheostomy to facilitate weaning from mechanical ventilation. This is particularly common in patients with AECOPD and leads to longer ICU and hospital lengths-of-stay, increased morbidity and increased mortality (Makris et al., 2011; Mamary et al., 2011; Nava et al., 1998; Penuelas et al., 2011; Schnell et al., 2014; Toft-Petersen et al., 2017).

1.5 Extracorporeal CO_2 removal

Extracorporeal CO_2 removal ($ECCO_2R$) is the use of an extracorporeal circuit with a gas exchange membrane to clear CO_2 directly from venous blood. $ECCO_2R$ uses the same technology as extracorporeal membrane oxygenation (ECMO), which was first successfully used in 1972 (Hill et al., 1972). ECMO requires large cannulae (25-33 French gauge) with a pump to provide a high blood flow (3-7L/minute) to provide adequate systemic oxygen delivery and CO_2 removal (Terragni et al., 2010). $ECCO_2R$ uses the same basic approach as ECMO, however because of the properties of CO_2 carriage in the blood, CO_2 can be removed at much lower blood flows (0.3-1L/minute)

(Kolobow et al., 1977).

1.5.1 Pathophysiological rationale of $ECCO_2R$

CO_2 is present in the blood in dissolved form, as bicarbonate, and carbamino compounds (Arthurs & Sudhakar, 2005). It is important to recognise that dissolved CO_2 is only a small portion of the total CO_2 content in whole blood and consequently small changes in the partial pressure of CO_2 can be associated with large changes in total CO_2 content (Douglas et al., 1988; O'Neill & Robbins, 2017; Siggaard-Andersen, 1971; West, 2011). The most consistent effect of $ECCO_2R$ in both clinical and pre-clinical studies is to improve arterial pH through the direct removal of CO_2 from the blood (figure 1.2) (Abrams & Brodie, 2013; Burki et al., 2013; Kluge et al., 2012; Moss et al., 2016; Sklar et al., 2015; Wearden et al., 2012). By removing CO_2 from the blood, $ECCO_2R$ reduces hypercapnic acidosis and reduces the neural drive to breathe (Diehl, Piquilloud, et al., 2020; Karagiannidis, Strassmann, et al., 2019), which results in reduced respiratory rate and minute ventilation (Braune et al., 2016; Del Sorbo et al., 2015; Karagiannidis, Hesselmann, et al., 2019; Karagiannidis et al., 2014; Moss et al., 2016; Sklar et al., 2015).

$ECCO_2R$ has consistently been shown to reduce PaO_2 requiring the administration of supplemental oxygen (Fitzgerald et al., 2014; Gattinoni, Kolobow, Tomlinson, Iapichino, et al., 1978; Moss et al., 2016; Sklar et al., 2015). The mechanism for this is increased venous admixture secondary to reduced hypercapnic pulmonary vasoconstriction (Domino et al., 1983; Fanelli et al., 2016; Gattinoni, 2016).

Right ventricular impairment due to acute pulmonary hypertension is common in COPD exacerbations due to the impact of hypercapnia, acidosis and hypoxaemia on the pulmonary circulation (Bouferrache & Vieillard-Baron, 2011; Mekontso Dessap et al., 2009). Improving pulmonary arterial PO_2, PCO_2 and pH lead to reductions in pulmonary arterial pressure and improvement in right ventricular function and cardiac output, thereby improving tissue oxygen delivery (Cherpanath et al., 2016; Reis Miranda et al., 2015).

There is limited data available about the impact of $ECCO_2R$ on other aspects of pulmonary physiology. A small pilot study reported on the changes associated with $ECCO_2R$ in patients with COPD weaning from a ventilator and found that intrinsic PEEP, inspiratory pulmonary resistance and work of breathing were all reduced (Pisani et al., 2015). It is possible that reductions in respiratory rate improve the time available for expiration and better match this to the lengthening of expiratory time constants. In turn this could reduce dynamic hyperinflation resulting in improved ventilatory efficiency, improved muscle fatigue and reduced dyspnoea (Lund & Federspiel, 2013; Morelli et al., 2017; Sklar et al., 2015).

1.5.2 Evidence for $ECCO_2R$

The development of $ECCO_2R$ equipment has followed several stages. One early approach to $ECCO_2R$ was a pumpless arteriovenous (AV) device (Ohtake et al., 1983). This required the placement of a femoral arterial and venous cannulae with the patient's cardiac output providing the pressure to drive blood through the membrane. A number of case reports and case series have been published using pumpless AV $ECCO_2R$ at a blood flow of >500mL/minute in the management of hypercapnic respiratory failure either to facilitate lung protective ventilation or manage primary hypercapnic respiratory failure (Bein et al., 2006; Bein et al., 2009; Elliot et al., 2007; Fischer et al., 2008; Mallick et al., 2007; Zimmermann et al., 2009; Zimmermann et al., 2006; Zwischenberger & Alpard, 2002; Zwischenberger et al., 2001; Zwischenberger et al., 2002). In the reported series, there was a statistically significant decrease of arterial CO_2, with an increase in arterial pH and an associated hospital survival of 36-70%. No randomised trials of AV $ECCO_2R$ have been reported. Complications of AV $ECCO_2R$ are significant, particularly bleeding (18-47% of patients), limb ischaemia (4.5-22%) circuit thrombosis (0-20%) and cardiac arrest or arrhythmia (5-14%) (Bein et al., 2006; Brunet et al., 1993; Gattinoni et al., 1986; Morris et al., 1994).

The development of pumped systems allowed the use of veno-venous (VV) $ECCO_2R$ (Terragni et al., 2012). These systems avoid the complications associated with arterial cannulation (Garcia et al., 2011; Terragni et al., 2009). Pumped systems use either

two single lumen cannulae or one double lumen cannulae with a centrifugal pump to achieve blood flows of 300-1000mL/minute. A variable gas flow is then run through the membrane to clear CO_2. Animal studies have consistently demonstrated that this approach is efficacious in controlling arterial CO_2 with blood flow under 500mL/minute and over 500mL/minute (Batchinsky et al., 2011; Cardenas et al., 2009; Dorrington et al., 1989; Livigni et al., 2006; Ruberto et al., 2009). Uncontrolled case series in humans have also demonstrated efficacy of VV $ECCO_2R$ for CO_2 control, including in patients with AECOPD (Cardenas et al., 2009; Garcia et al., 2011; Gattinoni et al., 1986; Kluge et al., 2012; Wearden et al., 2012) (Engel et al., 2016; Hilty et al., 2017; Ontario, 2010). However, a retrospective propensity matched case-control study using VV $ECCO_2R$ in COPD found no significant difference in outcome was associated with the use of $ECCO_2R$ (Braune et al., 2016). Recently VV $ECCO_2R$ has been shown to be safe when combined with renal replacement therapy platforms for patients with acute respiratory distress syndrome (Husain-Syed et al., 2020; Schmidt et al., 2018) and AECOPD (Consales et al., 2021). However, prospective randomised outcome data are lacking.

1.5.3 Study device

The Hemolung $ECCO_2R$ device is CE marked for VV $ECCO_2R$ and has blood flow of under 500mL/minute. In work by Batchinsky (2011) using a healthy swine model, $ECCO_2R$ using the Hemolung device enabled a 50% reduction in native lung CO_2 clearance that reduced native lung minute ventilation and maintained arterial normocapnoea (Batchinsky et al., 2011). In a case series using the Hemolung device in 20 patients with hypercapnic respiratory failure due to AECOPD, including 7 receiving NIV, the device restored arterial CO_2 and pH to the patient's baseline within 24 hours and maintained the arterial CO_2/pH until the conclusion of the study protocol (Burki et al., 2013). Patients remained on Hemolung for a mean of 104 hours (0.2-192 hours) and had a mortality of 7/20. Furthermore, in the patients with COPD at risk of failing NIV there were no patients who required intubation (Burki et al., 2013). Other series of patients with AECOPD managed with VV $ECCO_2R$ have demonstrated reduced respiratory rate with increasing CO_2 removal in a series of 6 patients with COPD, although work of breathing was not directly measured (Spinelli

et al., 2013). Use of the device has also been explored as an addition to invasive mechanical ventilation with resulting improvement in respiratory acidosis (Diehl, Piquilloud, et al., 2020). There have been no trials exploring the physiological impact of VV $ECCO_2R$ in AECOPD. There have been no randomised controlled trials of the impact of VV $ECCO_2R$ on patient outcomes in AECOPD.

1.6 Rationale for the thesis

Exacerbations of COPD remain a significant clinical problem with NIV providing significant benefits but with up to 30% of patients failing to improve with NIV.

$ECCO_2R$ shows promise as a technique to remove CO_2 but currently robust evidence from prospective randomised trial data is lacking. In addition, there is scanty data on the physiological consequences on gas exchange, respiratory effort and dyspnoea of $ECCO_2R$ in comparison with NIV.

Using the physiological model illustrated in figure 1.2, the main aims of this thesis are to describe: the efficiency of a $ECCO_2R$ device in CO_2 removal (chapter 2), the effects of $ECCO_2R$ compared with NIV in patients with AECOPD (chapter 3) and the impact of $ECCO_2R$ compared to NIV on work of breathing and the regional distribution of ventilation (chapter 4).

Chapter 2: Carbon dioxide transfer across artificial membranes

2.1 Introduction

Carbon dioxide carriage in the blood has been considered in section 1.2.1. Transfer across membranes, membrane efficiency and both in vitro and in vivo performance will be considered in this chapter.

2.1.1 Membranes

$ECCO_2R$ membranes enable gas exchange (mainly CO_2 removal) in a manner analogous to the native lung with a capillary network within the membrane allowing a flow of gas and blood through separate channels (Kolobow & Bowman, 1963). The blood flow through the artificial lung can be considered analogous to the perfusion of the native lung, while the sweep gas flow rate can be considered analogous to minute ventilation – in practice increasing sweep gas flow rate increases CO_2 clearance (Federspiel & Hattler, 1996). Hollow-fibre membranes are constructed of polymethylpentene or siloxane which have been demonstrated to be more durable and have a lower impact on the blood than silicon membranes (Horton et al., 2004).

The Hemolung is the membrane used in the current study. The Hemolung membrane is composed of a cylindrical bundle of siloxane and heparin-coated hollow-fibre membrane positioned around a spinning core which centrifugally pushes blood through the cartridge resulting in mixing of the blood. CO_2 removal is achieved by passing sweep gas (air or 100% O_2) through the gas channel. The total surface area of the membrane is 0.59 m^2. The priming volume of the circuit is 280mL.

2.1.2 Carbon dioxide clearance through membrane oxygenators

Carbon dioxide clearance by the native lung is affected by numerous factors including CO_2 production, mixed venous carbon dioxide content, minute ventilation, acid-base equilibrium, dead space and shunt within the lungs, cardiac output and tissue stores of carbon dioxide (Cherniack & Longobardo, 1970; Ramos et al., 2013). Carbon dioxide transfer across the membrane lung is affected by the same factors but is also dependent upon the diffusion gradient, transit time across the membrane, the

membrane material, blood flow rate and sweep flow rate (Park et al., 2013; Sun et al., 2018). The diffusion gradient is maintained by clearance of CO_2 using the sweep gas (air, oxygen or CO_2/O_2 mix - carbogen) flowing across the semi-permeable membrane with a higher sweep gas rate maintaining a higher diffusion gradient which in turn leads to a greater degree of CO_2 clearance from any given volume of blood (Cove & Federspiel, 2015; Park et al., 2013). This means that at a fixed blood flow, sweep gas blood flow rate can be considered analogous to minute ventilation in the native lung. Blood flow through the membrane is analogous to cardiac output with a higher blood flow delivering a greater volume of CO_2 per minute to the membrane and consequently resulting in higher clearance (Karagiannidis et al., 2017).

Membrane lungs are affected by inequalities in the distribution of sweep gas and blood flows leading to regional ventilation-perfusion mismatch (Bartlett, 2017). This may be considered, superficially, as being analogous to dead space and shunt within the native lung. “Shunt” in the membrane lung is commonly caused by a blockage of the gas capillaries (eg through water saturation due to water transfer from the blood to the gas capillary), whilst “dead space” is commonly caused by a blockage within the blood path (eg through thrombus formation). Although rare, gas exchange membrane layers can fail, caused, for example, by lipid saturation of the interface. Gas transfer across the membrane is dependent upon blood flow and can be measured in mL/minute of O_2 or CO_2.

Oxygen transfer across the membrane can be calculated from the transmembrane differences in oxygen content (equations 2.1 and 2.2).

$$VO_{2\,ML}\ (mL/min) = (CtO_{2\,(post)} - CtO_{2\,(pre)}\ (mL/dL))*10*\text{blood flow}\ (L/min) \qquad [Eq\ 2.1]$$

Equation 2.1: Oxygen transfer across the membrane. $CtO_{2\,(post)}$ is the O_2 content in blood after the membrane, $CtO_{2\,(pre)}$ is the O_2 content in blood before the membrane.

$$CtO_2 = (Hb*1.39*SO_2*0.01) + (PO_2*0.0231) \qquad [Eq\ 2.2]$$

Equation 2.2: Oxygen content of blood (mL/dL). Hb (g/dL) and PO_2 (kPa).

Carbon dioxide transfer across the membrane can be calculated either from the trans-membrane CO_2 content difference (equation 2.3) or from the CO_2 partial pressure in the effluent gas (equation 2.4).

$$VCO_{2\ ML} = (CtCO_{2\ (pre)} - CtCO_{2\ (post)})*\text{blood flow}*22.414 \qquad \text{[Eq 2.3]}$$

Equation 2.3: Carbon dioxide transfer across the membrane calculated from the trans-membrane CO_2 content difference. $CtCO_{2\ (post)}$ is the CO_2 content in blood after the membrane, $CtCO_{2\ (post)}$ is the CO_2 content in blood before the membrane (equation 1.2). $VCO_{2\ ML}$ is measured in mL/min, blood flow is measured in L/min, $CtCO_2$ is measured in mmol/L and the correction factor is in mL/mmol. The correction factor is for gases at standard temperature, pressure and without water vapour (STPD) rather than at body temperature, pressure and saturated (BTPS).

$$VCO_{2\ ML} = (PCO_{2\ ML\ (exp)})*(7.5/760)*(\text{sweep gas flow rate}*1000) \quad \text{[Eq 2.4]}$$

Equation 2.4: Carbon dioxide transfer across the membrane calculated from the partial pressure of CO_2 in the effluent gas. $PCO_{2\ ML\ (exp)}$ is the partial pressure of CO_2 in the effluent gas (kPa). $VCO_{2\ ML}$ is measured in mL/min, the correction factors are 7.5mmHg/kPa and 760mmHg, sweep gas in L/min.

The total CO_2 content of venous blood, including dissolved CO_2, bicarbonate and carboxyhaemoglobin, is approximately 500mL/litre, compared with 400-450mL/litre in arterial blood (Arthurs & Sudhakar, 2005). CO_2 exhibits biphasic clearance kinetics, with an initial rapid decline in $PaCO_2$ followed by a slower decline over time (Sun et al., 2018). This is caused by the rapid removal of dissolved CO_2, enzymatic catalytic conversion of bicarbonate to CO_2 via carbonic anhydrase and a slower equilibration of blood and tissues stores of CO_2 (Muller et al., 2009). Although the conversion of bicarbonate to CO_2 is relatively rapid, CO_2 removal has been shown to be enhanced by the acidification of blood immediately prior to the membrane lung using infusions of lactic acid, coating the membrane in carbonic anhydrase or using an acidified sweep gas (Arazawa et al., 2015; Zanella et al., 2013; Zanella et al., 2009). In a

perfectly efficient system where all dissolved CO_2 is removed, the total VCO_2 of approximately 250mL/minute could be achieved from a blood flow of 0.5L/minute. In practice this is not achievable during the membrane transit time of 15-30 seconds (Gattinoni, Kolobow, Agostoni, et al., 1979; Gattinoni, Kolobow, Damia, et al., 1979; Gattinoni, Kolobow, Tomlinson, Iapichino, et al., 1978; Gattinoni, Kolobow, Tomlinson, White, et al., 1978; Karagiannidis et al., 2017). This is due to diffusion limitation within the membrane lung and consequently a reduced mass transfer of CO_2 with higher V/Q (Turri & Yanagihara, 2011).

Although V/Q inequalities as described above can occur within the membrane lung, in practice the ventilation substantially exceeds the blood flow by up to 10-20 times depending on the device, leading to wasted ventilation. CO_2 transfer at low sweep gas flows relative to blood flow (V/Q <1) equilibrates with inlet PCO_2 before the end of the capillary indicating that CO_2 transfer is gas flow limited (Turri & Yanagihara, 2011). At high sweep gas flow rates relative to blood flow (V/Q>2), equilibration does not occur, rather CO_2 transfer occurs along the full length of the capillary and hence there is diffusion limitation (Turri & Yanagihara, 2011). Diffusion limitation can be described in terms of the effectiveness of mass transfer – the fraction of the maximum transfer of CO_2 that could be transferred should it have fully equilibrated (Turri & Yanagihara, 2011).

To calculate the proportion of wasted ventilation or mass transfer effectiveness of the membrane lung, measurement of the partial pressure of CO_2 in the effluent gases is required.

$$Ef_{CO2} = PECO_2 / PCO_{2\ ML\ (pre)} \qquad \text{[Eq 2.5]}$$

Equation 2.5: Mass transfer effectiveness (Ef_{CO2}) in the membrane lung (%). $PECO_2$ is the partial pressure of CO_2 in the effluent gas, $PCO_{2\ ML(pre)}$ is the partial pressure of CO_2 in the pre-membrane blood.

The relationship between CO_2 clearance and blood flow in extracorporeal circuits due to the change in mass transfer effectiveness is non-linear with a plateau reached with a ventilation/perfusion ratio of 10:1 (Cove & Federspiel, 2015; Gattinoni et al., 1983;

MacLaren, 2012; Pesenti et al., 2010; Sun et al., 2018; Terragni et al., 2012; Terragni et al., 2010). In practice this means that for any given blood flow rate, the proportional change in CO_2 clearance is greater when changes are made at lower sweep flow rates than when they are made at higher sweep flow rates (Federspiel & Hattler, 1996; Lehle et al., 2014).

There is limited published data on the CO_2 removal which can be achieved using the Hemolung membrane (Wearden et al., 2012). Furthermore, the available data reports measurements from the device without independent confirmation of the accuracy of these measurements. The method of assessment and validation of the device VCO_2 measurement is not in the public domain. It is unknown whether the device measures VCO_2 at standard temperature (0°C), pressure and dry (STPD), body standard temperature (37°C) and saturated with water vapour (BTPS) or ambient temperature and pressure (ATP). The differing measurement conditions have been shown to make a significant difference to the calculations of VCO_2 (D'Albo et al.).

To explore this, two separate studies were undertaken – an in-vitro study using human blood and exogenous CO_2 (Barrett et al., 2020b) and in-vivo in patients with AECOPD (Barrett et al., 2020a).

2.2 In vitro CO_2 clearance across the membrane

2.2.1 Introduction

A blood and crystalloid primed circuit using packed red cells was used to understand the impact of $ECCO_2R$ clearing CO_2 from blood. The guidelines suggest that tests are undertaken using an approximation of clinical conditions. To achieve this, it is suggested that the following blood inlet conditions occur: blood oxygen saturation of 65 ± 5 %; haemoglobin, 8 ± 2 g/dL; base excess, 0 ± 5 mmol/L; partial pressure of carbon dioxide in blood, PCO_2, 6.0 ± 0.7 kPa. The circuit temperature should be maintained at 37°C. The device should be run at the manufacturer's specified blood flow rate attached to an appropriate test circuit and last 6 hours (ISO, 2016). Given the requirement to use the device in patients with hypercapnic respiratory failure, a model providing an elevated PCO_2 with a respiratory acidosis was developed.

2.2.2 Method

2.2.2.1 Ethical approval

The study was approved by the Guy's and St Thomas' NHS Foundation Trust transfusion review committee. Anonymous donor packed red blood cells which had expired, were scheduled for destruction and were unable to be used for human transfusion were used. Other blood components (plasma, platelets and white blood cells) were not available. Need for informed consent was waived.

2.2.2.2 Circuit

The experimental set-up was designed to form a steady state between CO_2 addition and removal. To achieve this, three separate membranes were used. The adult ECMO circuit provided a pump and membrane to drive total flow through the circuit and clear CO_2/add O_2 in a constant manner. A paediatric membrane was used to add CO_2, representing the metabolic CO_2 load. The test $ECCO_2R$ circuit then provided variable sweep gas with a constant blood flow to assess membrane VCO_2. The set-up was formed using a Quadrox HLS oxygenator on a Cardiohelp circuit (Gettinge, Stockholm, Sweden), paediatric Quadrox oxygenator (Gettinge, Stockholm, Sweden), priming bag

(Gettinge, Stockholm, Sweden) and a Hemolung circuit (ALung, Pittsburgh, USA). The priming bag was added as a reservoir to allow removal of fluid from the circuit for analysis. The total surface area of the test membrane is 0.59 m^2. Only one experimental circuit was set-up. The circuit schematic is described in figure 2.1.

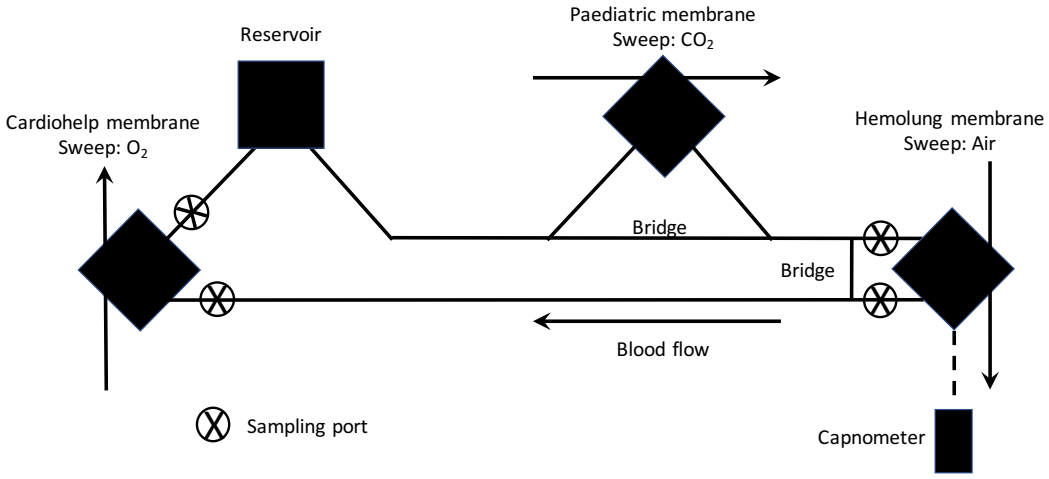

Figure 2.1: Circuit schematic

Bridge connections were formed using 3/8"/1/4" y-connectors (figure 2.1 and 2.2). Bridge connections were used to allow most of the blood to bypass the paediatric and $ECCO_2R$ membranes. The paediatric membrane is rated to 500mL/minute, the $ECCO_2R$ circuit operates at 350-450mL/minute and the ECMO circuit is rated at 3-7L/minute. The circuit was primed with 1L balanced crystalloid solution (plasmalyte[1] (Baxter, Illinois, USA)), 1052mL packed red blood cells (4 units, compatible, O negative, human, expired) and 120mL 8.4% sodium bicarbonate (figure 2.9). The pH of the circuit without CO_2 running was 6.98 and the pH of the circuit with CO_2 added was 7.02, the HCO_3 was 25mmol/L, base excess -5mEq/L, the haemoglobin was 7g/dL. Although the packed cells contained citrate, given that plasmalyte contains calcium ions, additional anticoagulation was provided with 10000 units of heparin.

Blood flows through the different circuit components were measured. Total circuit flow was measured using the Cardiohelp integrated monitoring (4000mL/min), the

[1] 1L Plasmalyte contains: 140 mmol sodium, 5 mmol potassium, 3 mmol magnesium, 98 mmol chloride, 27 mmol acetate, and 23 mmol gluconate EMC. (2018). *Summary of product characteristics: Plasmalyte solution for infusion*. Retrieved 14/7/2023 from https://www.medicines.org.uk/emc/product/1795/smpc#gref

paediatric membrane flow was measured using an ultrasonic flowmeter (Spectrum Medical, South Carolina, USA) (430mL/min) and the flow through the Hemolung was measured using integrated monitoring controller (400mL/min). Blood flows remained constant for the duration of the experiment.

Carbogen was not available, consequently CO_2 addition and O_2 addition had to be managed separately. The sweep gas used by the paediatric oxygenator was 100% medical CO_2 at a constant 0.5L/min via a ball flow meter. The sweep gas used by the Cardiohelp was 100% medical O_2 at a constant 2L/min via a ball flowmeter. The sweep gas used by the Hemolung was room air with a variable rate controlled by the device (0-10L/min). Medical nitrogen was not available and consequently pre-membrane saturations of 65±5% were not able to be achieved.

One quarter inch (¼") connectors with high flow pigtails and 3-way taps were cut into the Hemolung circuit before and after the membrane to allow measurement of pre-$ECCO_2R$ and post-$ECCO_2R$ circuit gases. Another ¼" connector was cut into the effluent line on the Hemolung (figure 2.3) and connected to a PC-900B capnograph (Creative Industries, Shenzen, China) via a 3-way tap. The capnograph measured the concentration of CO_2 averaged over 10 seconds in kPa and drew 100mL/min from the effluent gas line. The 3-way tap was opened intermittently to the circuit to prevent saturation of the capnometer. In the ECMO circuit, high flow pigtails with 3-way taps were added to the existing pre-membrane and post-membrane access points to facilitate ECMO circuit gases. Constant circuit temperature of 37°C was maintained using a Paratherm heater-cooler (Chalice Medical, Nottinghamshire, UK)..

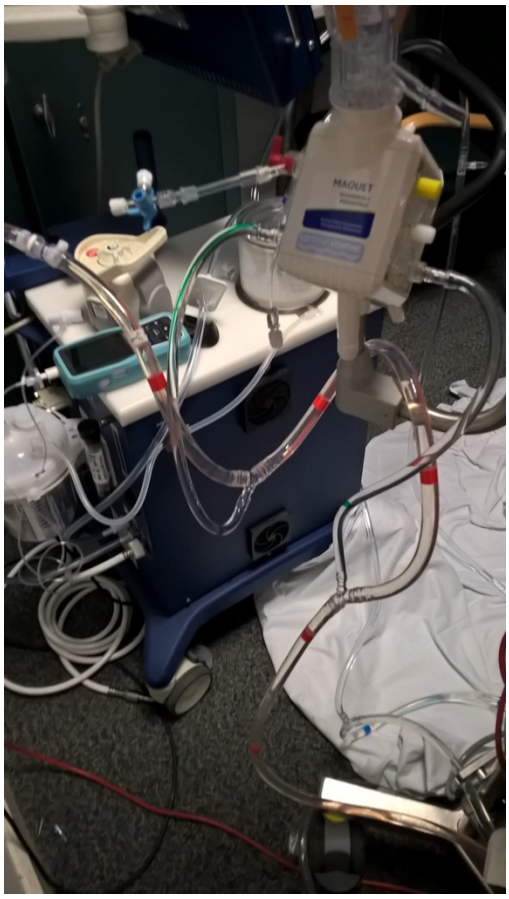

Figure 2.2: The paediatric membrane connected via a bridge.

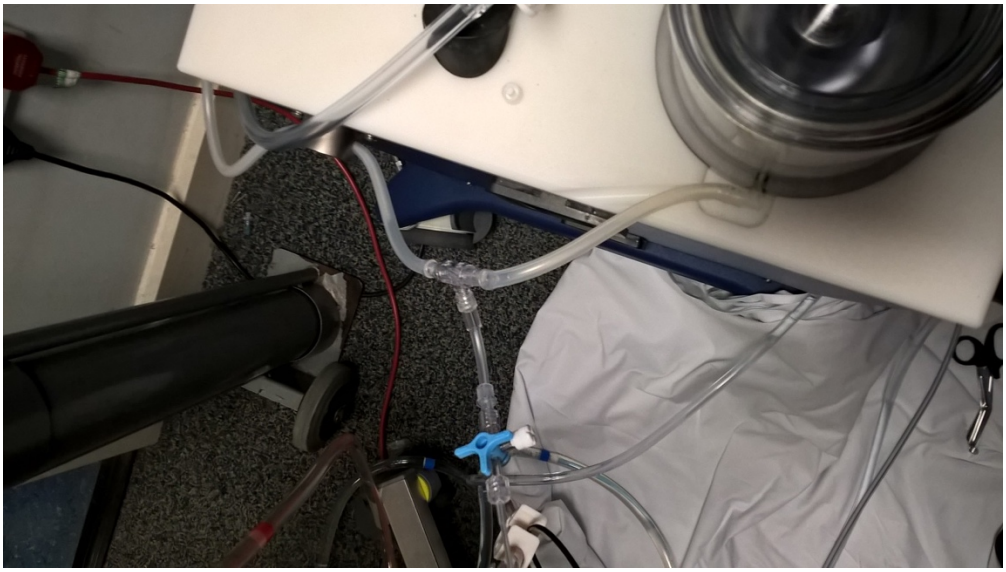

Figure 2.3: The ¼" connector cut into the gas effluent line on the Hemolung to allow connection to the capnograph.

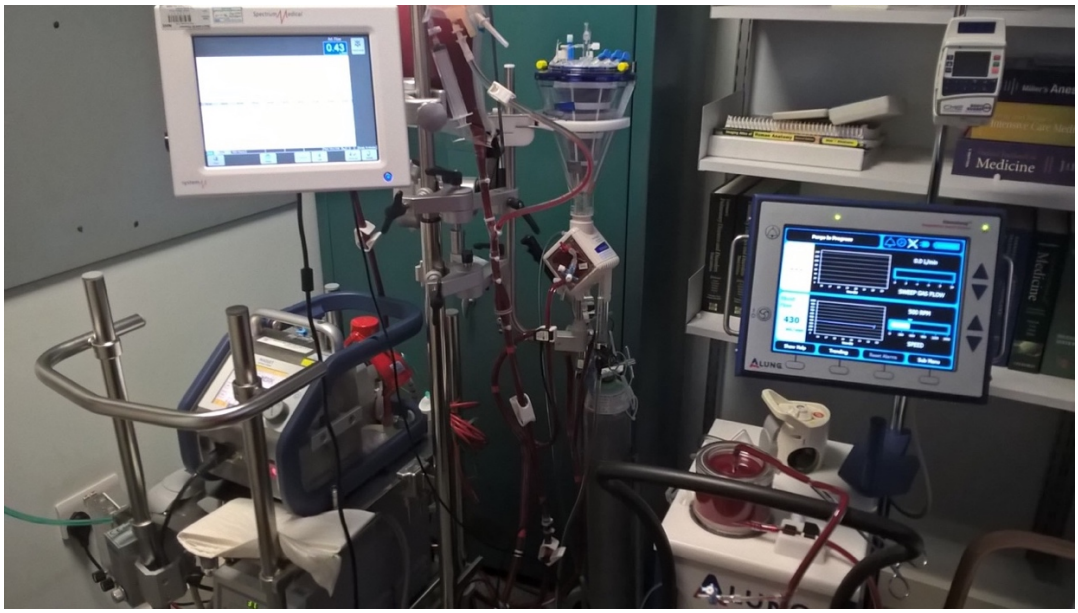

Figure 2.4: The blood primed circuit

The total duration of the study was 6 hours. For the first hour, the $ECCO_2R$ sweep gas flow rate was 0 L/minute. Following this the $ECCO_2R$ sweep gas was increased by 1L/minute every 30 minutes until the $ECCO_2R$ device maximum of 10L/minute was reached. The fraction of inspired oxygen of the $ECCO_2R$ sweep gas was 0.21. The following measurements were recorded every 15 minutes after a change in sweep gas flow rate:

1. Pre-ECMO circuit blood gas
2. Post-ECMO circuit blood gas
3. Pre-$ECCO_2R$ circuit blood gas
4. Post-$ECCO_2R$ circuit blood gas
5. Concentration of CO_2 in the $ECCO_2R$ effluent gas
6. The CO_2 removal reported by the $ECCO_2R$ device
7. The $ECCO_2R$ sweep flow rate.

All blood gases were measured using a Cobas B 221 blood gas analyser (Roche, Basel, Switzerland). Blood gases were performed in the following manner: 10mL of fluid was withdrawn and discarded to ensure clearance of the dead space within the 3-way connector and high-flow pigtail (dead space volume of 2.6 mL); 2mL of fluid was withdrawn into a heparinised blood gas syringe.

2.2.2.3 Data measurement

For each gas, the following data was recorded: pH, PCO_2, PO_2, HCO_3, base excess, Hb, SO_2.

CO_2 content was described in mmol/L using equation 1.5

VCO_2 was described in mL/min using three separate methods:

1. VCO_2 was recorded directly from the $ECCO_2R$ device.
2. Calculated from the trans-membrane CO_2 difference (equation 2.3)
3. Calculated from the partial pressure of CO_2 in the effluent gas (equation 2.4)

Mass transfer effectiveness (%) was calculated using equation 2.5.

2.2.2.4 Statistical analysis

Data was recorded in Microsoft Excel database. Statistical analysis was performed in Prism 9.1 for Mac (Graphpad, California, USA). Gas flow was plotted against VCO_2 (calculated from trans-membrane difference). Comparison of VCO_2 measured by the trans-membrane CO_2 difference and calculated from the effluent gas was compared with that reported by the device using a Bland-Altman analysis (Bland & Altman, 1986). A linear regression of mass transfer effectiveness for CO_2 transfer compared with gas flow was undertaken. One-way Analysis of Variance (Kruskal-Wallis) was used to compare the different methods to obtain VCO_2:

1. VCO_2 calculated as a trans-membrane CO_2 content difference from calculations using the Douglas equation vs VCO_2 (E) measured by the $ECCO_2R$ device.
2. VCO_2 (E) measured by the $ECCO_2R$ device vs VCO_2 (P) calculated from the partial pressure of CO_2 in the effluent gas.

2.2.3 Results

Results of the $ECCO_2R$ circuit gases demonstrate a constant inlet PCO_2 (table 2.1). The impact of sweep gas flow on CO_2 content is also demonstrated (table 2.2). Results of the ECMO circuit gases demonstrate that a steady state has been achieved (tables 2.3). The different VCO_2 calculations are compared using a Bland-Altman analysis in figures 2.5-2.6. The relationship between VCO2 and gas flow is demonstrated in figure 2.7. The relationship between mass transfer effectiveness with gas flow is demonstrated in figures 2.8.

The comparison VCO_2 measured by the $ECCO_2R$ device is compared with the VCO_2 calculated as a trans-membrane CO_2 content there is a strong, linear correlation with minimal bias (figure 2.5). VCO_2 measured by the $ECCO_2R$ device and the VCO_2 calculated from the partial pressure of CO_2 in the effluent gas (figure 2.6) also shows a strong, linear correlation with minimal bias (R^2 = 0.99, bias -6.1, SD 4.3). The relationship between gas flow and VCO_2 measured by the $ECCO_2R$ device is described in figure 2.7. There is a rapid increase in CO_2 removal from crystalloid which plateaus after 4L/min sweep gas flow. Mass transfer effectiveness for CO_2 is demonstrated in figure 2.8.

BF(E)	GF(E)	BF(P)	GF(P)	BF(EC)	GF(EC)	pH (pre)	pH (post)	PCO_2 (pre)	PCO_2 (post)	$CtCO_2$ (pre)	$CtCO_2$ (post)
4	2	0.43	0.5	0.41	0	7.019	7.057	16.58	14.52	32.9	31
4	2	0.43	0.5	0.41	1	7.011	7.325	15.15	6.24	29.5	23.3
4	2	0.43	0.5	0.41	2	7.025	7.269	15.09	7.24	30.3	24
4	2	0.43	0.5	0.41	3	7.018	7.35	15.08	5.78	31.2	22.8
4	2	0.43	0.5	0.41	4	7.01	7.357	16.33	5.62	31.8	22.4
4	2	0.43	0.5	0.41	5	7.008	7.365	16.05	5.42	31.1	22.7
4	2	0.43	0.5	0.41	6	7.006	7.373	16.07	5.21	31	22
4	2	0.43	0.5	0.41	7	7	7.376	16.36	5.25	31.3	21.7
4	2	0.43	0.5	0.41	8	6.995	7.38	16.77	5.09	30	21.3
4	2	0.43	0.5	0.41	9	7.003	7.386	16.19	4.96	31.1	21.1
4	2	0.43	0.5	0.41	10	7.003	7.378	16.38	5.14	31.4	21.4

Table 2.1: $ECCO_2R$ transmembrane gas measurements. BF(E) is blood flow via ECMO membrane (L/min), GF(E) is gas flow via ECMO membrane (L/min), BF(P) is blood flow via paediatric membrane (L/min), GF(P) is gas flow via paediatric membrane (L/min), BF(EC) is blood flow via $ECCO_2R$ membrane (L/min), GF(EC) is gas flow via $ECCO_2R$ membrane (L/min). PCO_2 is partial pressure of CO_2 (kPa) and $CtCO_2$ is CO_2 content (mmol/L), all of which are measured directly/calculated by the gas analyser. The nomenclature pre/post refers to the inlet and outlet of the Hemolung membrane respectively.

BF(EC)	GF(EC)	$CtCO_2$ (pre)	$CtCO_2$ (post)	VCO_2 $dCtCO_2$	$PECO_2$	VCO_2 (P)	VCO_2 (E)
0.41	0	33.6	33.2	4.3	0	0.0	0.0
0.41	1	31.5	25.2	57.9	4.9	48.4	50.0
0.41	2	32.3	25.9	58.5	3.4	67.1	66.0
0.41	3	33.1	24.7	77.1	2.3	68.1	72.0
0.41	4	33.9	24.4	87.4	1.9	75.0	84.0
0.41	5	33.1	23.9	84.5	1.5	74.0	86.0
0.41	6	33.0	23.4	88.6	1.4	82.9	92.0
0.41	7	33.3	23.7	88.2	1.2	82.9	91.0
0.41	8	33.8	23.2	96.7	1.1	86.8	95.0
0.41	9	33.1	22.9	94.0	1	88.8	96.0
0.41	10	33.5	23.3	94.0	0.9	88.8	98.0

Table 2.2: $ECCO_2R$ circuit transmembrane CO_2 content: $CtCO_2$ (pre) is the plasma content of CO_2 in the pre-membrane sample (mmol/L). $CtCO_2$ (post) is the plasma content of CO_2 in the post-membrane sample (mmol/L). $dCtCO_2$ is the content difference of the samples (mmol/L). VCO_2 ($dCtCO_2$) is calculated from the CO_2 content difference between the pre-membrane and post-membrane samples (mL/min). $PECO_2$ is the partial pressure of CO_2 measured in the effluent gas (kPa). VCO_2(P) is the CO_2 transfer derived from equation 2.8 (mL/min). VCO_2(E) is the CO_2 transfer measured by the $ECCO_2R$ circuit (mL/min).

BF(E)	GF(E)	BF(P)	GF(P)	BF(EC)	GF(EC)	pH (pre)	pH (post)	PCO_2 (pre)	PCO_2 (post)	$CtCO_2$ (pre)	$CtCO_2$ (post)
4	2	0.43	0.5	0.41	0	7	7.116	16.57	12.08	31.7	29.1
4	2	0.43	0.5	0.41	1	7.033	7.159	14.77	10.46	30.1	27.5
4	2	0.43	0.5	0.41	2	7.038	7.143	14.7	10.85	30.3	27.7
4	2	0.43	0.5	0.41	3	7.014	7.117	15.15	11.11	29.7	26.8
4	2	0.43	0.5	0.41	4	7.049	7.132	14.21	11.03	29.8	27.4
4	2	0.43	0.5	0.41	5	7.04	7.131	14.76	10.84	30.5	26.9
4	2	0.43	0.5	0.41	6	7.035	7.135	14.77	11.02	30.2	27.6
4	2	0.43	0.5	0.41	7	7.029	7.124	14.95	11.24	30.3	27.5
4	2	0.43	0.5	0.41	8	7.024	7.116	15.04	11.4	30	27.4
4	2	0.43	0.5	0.41	9	7.037	7.127	14.75	11.16	30.2	27.5
4	2	0.43	0.5	0.41	10	7.033	7.122	14.93	11.27	30.4	27.5

Table 2.3: ECMO transmembrane gas CO_2 measurements: BF(E) is blood flow via ECMO membrane (L/min), GF(E) is gas flow via ECMO membrane (L/min), BF(P) is blood flow via paediatric membrane (L/min), GF(P) is gas flow via paediatric membrane (L/min), BF(EC) is blood flow via $ECCO_2R$ membrane (L/min), GF(EC) is gas flow via $ECCO_2R$ membrane (L/min). PCO_2 is partial pressure of CO_2 (kPa) and $CtCO_2$ is CO_2 content (mmol/L). $CtCO_2$ (pre) is the plasma content of CO_2 in the pre-membrane sample (mmol/L). $CtCO_2$ (post) is the plasma content of CO_2 in the post-membrane sample (mmol/L).

Bias	0.11
SD of bias	4.7
95% Limits of Agreement	
From	-9.1
To	9.3

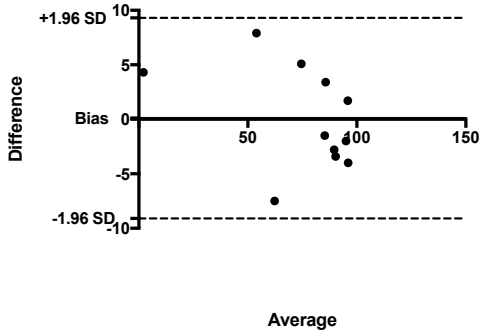

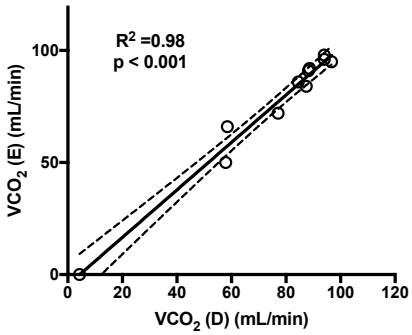

(a) (b)

Figure 2.5: (a) Bland-Altman analysis of the VCO_2 (mL/min) measured by the $ECCO_2R$ device (VCO_2(E)) vs VCO_2 (mL/min) calculated from trans-membrane CO_2 content difference (VCO_2(D)) in blood in vitro and (b) linear regression comparing the VCO_2 (mL/min) measured by the $ECCO_2R$ device (VCO_2(E)) vs VCO_2 (mL/min) calculated from trans-membrane CO_2 content difference (VCO_2(D)) in blood in vitro.

Bias	-6.1
SD of bias	4.3
95% Limits of Agreement	
From	-15
To	2.3

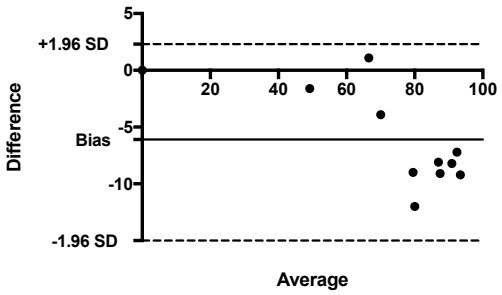

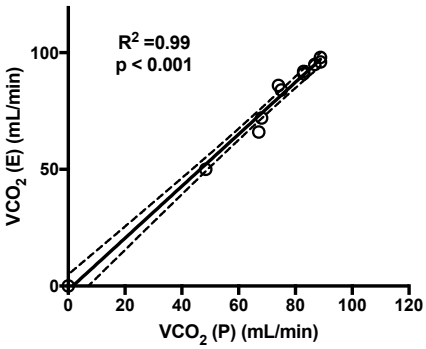

(a) (b)

Figure 2.6: (a) Bland-Altman analysis of the VCO_2 (mL/min) measured by the $ECCO_2R$ device ($VCO_2(E)$) vs VCO_2 (mL/min) calculated from the partial pressure of CO_2 in the effluent gas ($VCO_2(P)$) in blood in vitro and (b) linear regression comparing the VCO_2 (mL/min) measured by the $ECCO_2R$ device ($VCO_2(E)$) vs VCO_2 (mL/min) calculated from the partial pressure of CO_2 in the effluent gas ($VCO_2(P)$) in blood in vitro.

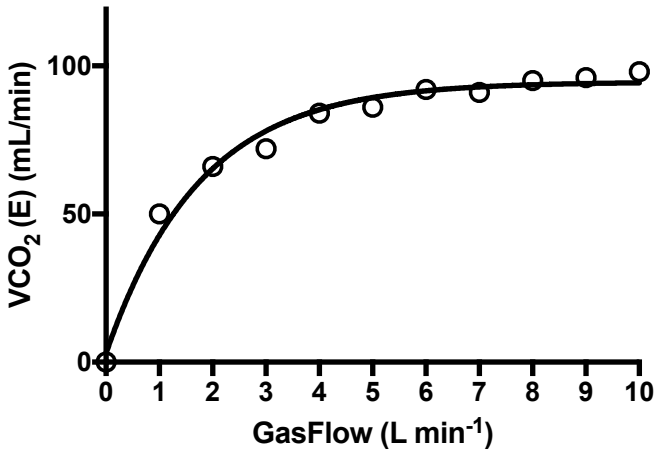

Figure 2.7: VCO_2 (E) (mL/min) measured by the $ECCO_2R$ device vs gas flow (L/min) in blood in vitro.

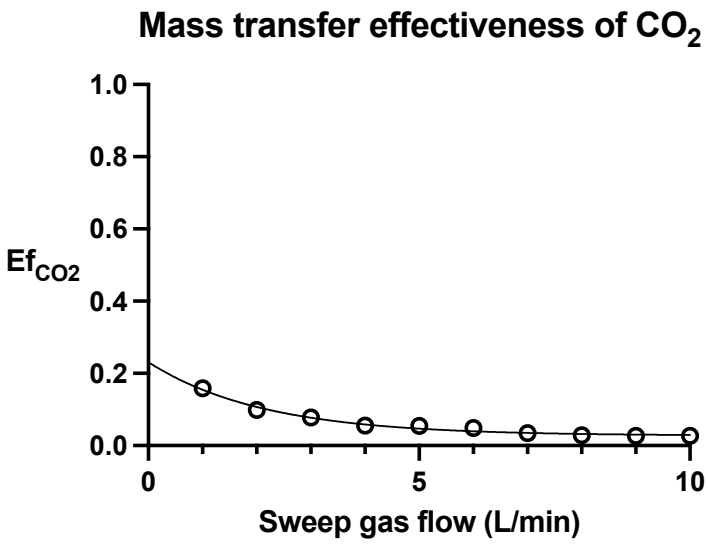

Figure 2.8: Mass transfer effectiveness of CO_2 across the Hemolung membrane. Ef_{CO2} is mass transfer effectiveness of CO_2.

2.2.4 Discussion

The in vitro testing undertaken in the current study provides an independent demonstration of a dedicated low flow $ECCO_2R$ device characteristics using a blood prime. The results indicate that there is a strong correlation between the different methods of VCO_2 calculation and, importantly, demonstrate a strong linear relationship with minimal bias between the measurement of VCO_2 through the device with methods using trans-membrane blood gases and partial pressure CO_2 in the effluent gas. The experimental set-up provided steady state conditions at the $ECCO_2R$ inlet and across the ECMO membrane with the only variable being the $ECCO_2R$ sweep gas flow rate. The results of in vitro testing have been published (Barrett et al., 2020b).

Gas exchange membranes are expected to conform with the International Standards Organisation standard 7199:2016 (ISO, 2016). For clinical testing, this standard requires a haemoglobin concentration of 8±2g/dL, inlet PCO_2 of 6±0.7kPa and base excess of 0±5 mEq/L. Regulators need to be informed of results, however there is no requirement for this data to be available to end-users. Corporate data measuring VCO_2 using this device from expiratory port gases (Jeffries et al., 2014; Wearden et al., 2012) is available, however neither independent in vitro measurements nor

comparisons with transmembrane gases are available in the literature. The baseline conditions were generally in accordance with the European testing regime but had some important differences to demonstrate CO_2 clearance in a model closer to that of patients with severe respiratory failure (Di Lascio et al., 2017; Jiang et al., 2017). The pH was lower, and CO_2 content higher than in guidelines and the haemoglobin chosen (7g/dL), is in keeping with current British Society of Haematology guidelines for transfusion in critical illness (Retter et al., 2013).

Although the relationship between CO_2 clearance and both blood and sweep gas flow in this extracorporeal circuit is highly sensitive to changes in gas flow rate at low gas flow rates, it becomes less sensitive at high sweep flow rates, similar to other reports in the literature (Federspiel & Hattler, 1996; Gattinoni, Kolobow, Agostoni, et al., 1979; Gattinoni, Kolobow, Damia, et al., 1979; Gattinoni, Kolobow, Tomlinson, Iapichino, et al., 1978; Gattinoni, Kolobow, Tomlinson, White, et al., 1978; Lehle et al., 2014; Sun et al., 2018). This differs to the relationship described in healthy humans where relationship between CO_2 clearance is linear over physiological ranges. However, the situation in humans is more complex with changes in minute ventilation, pulmonary blood flow, venous blood CO_2 content and respiratory drive. The relationship between sweep gas flow rate and VCO_2 at a constant blood flow has been demonstrated to plateau at approximately 4L/minute sweep flow for 0.4L/minute blood flow (figure 2.7). The ventilation/perfusion ratio of approximately 10:1 is reported as representing the limit of efficiency for an artificial membrane lung, unless alternative means of increasing CO_2 removal from the blood are used (e.g. exogenous acidification) (Federspiel & Hattler, 1996; Gattinoni, Kolobow, Agostoni, et al., 1979; Gattinoni, Kolobow, Damia, et al., 1979; Gattinoni, Kolobow, Tomlinson, Iapichino, et al., 1978; Gattinoni, Kolobow, Tomlinson, White, et al., 1978; Lehle et al., 2014; Scaravilli et al., 2016; Scaravilli et al., 2015; Sun et al., 2018). To gain further increases in CO_2 clearance an increase in blood flow is required (de Villiers Hugo et al., 2017; Joyce et al., 2018; Karagiannidis et al., 2017; Muller et al., 2009).

The mass transfer effectiveness of this membrane lung is 0.15 at 1L sweep gas flow rate indicating that equilibration does not occur at the lowest possible sweep gas flow rate (Turri & Yanagihara, 2011). Membrane lungs can be affected by inequalities in

the distribution of sweep gas and blood flows leading to regional ventilation-perfusion mismatch thereby reducing their efficiency (Bartlett, 2017). However the mass transfer efficiency of CO_2 in the current membrane likely relates to the V/Q relationship, which at even the lowest gas flow available on the device is over 2:1. Consequently due to the blood flow achieved by the device, there is a diffusion limitation which results in a low mass transfer effectiveness of CO_2 and incomplete equilibration of CO_2 at all gas flow rates in keeping with other membranes with similar V/Q relationships (Turri & Yanagihara, 2011).

This study has several limitations. The experiment was performed in only one low-flow system (0.59m^2 membrane surface area, blood flow 0.35-0.45L/min) and results cannot be extrapolated to different devices, however results are in keeping other studies using different devices (de Villiers Hugo et al., 2017; Joyce et al., 2018; Karagiannidis et al., 2017; Muller et al., 2009; Sun et al., 2018). The conditions used, particularly haemoglobin, pH and PCO_2 were not those recommended for the bench testing (ISO, 2016), however they are within the spectrum seen in clinical practice (Di Lascio et al., 2017; Jiang et al., 2017; Retter et al., 2013). Another limitation is that it is not known whether the device measures VCO_2 at standard temperature (0°C), pressure and dry (STPD), body standard temperature (37°C) and saturated with water vapour (BTPS) or ambient temperature and pressure (ATP). This introduces a source of potential error (D'Albo et al.). Only one circuit was able to be set up and only one set of blood gases at sweep gas flow rate was used in the analysis. Expired human packed red cell concentrates were used and it is possible that the lack of other components of whole blood (plasma and cellular) or the performance of expired red blood cells is not the same as blood in vitro. It is acknowledged that the CO_2 compartments in this model include dissolved CO_2, bicarbonate and carbamino compounds, there is no renal compensatory mechanisms, nor are there any tissue stores of CO_2, however given the relatively slow turnover, it is unlikely to have significantly contributed over the time scale of the present study (Muller et al., 2009). The present study also used a constant CO_2 load, whereas in vivo there is a variable load depending on metabolic demands (Cabello & Mancebo, 2006; Moxham & Jolley, 2009). Many of these limitations can be addressed by measuring VCO_2 in vitro.

2.3 In-vivo CO_2 Gas exchange across the membrane

2.3.1 Introduction

In-vitro testing of the Hemolung device using a blood prime has demonstrated that the VCO_2 reported by the device is accurate within the limitations of testing. It also demonstrated that a V:Q relationship of 10:1 (i.e., 4L/minute sweep gas flow) represents the limit of CO_2 clearance using the device, in keeping with the literature (de Villiers Hugo et al., 2017; Hout et al., 2000; Karagiannidis, Hesselmann, et al., 2019). Other factors relevant in clinical practice include the PCO_2 gradient between the venous blood and the sweep gas; the transit time across the membrane; the membrane surface area and the membrane material (Cove & Federspiel, 2015; Park et al., 2013). There is no clinical data available in devices with a blood flow of under one litre per minute, although there is for devices of blood flow of more than 1L/minute (Muller et al., 2009).

2.3.2 Methods

2.3.2.1 Ethical approval

The trial received prospective ethical approval from the UK Human Research Authority (14/E/0109). Informed written consent was obtained from patients or their designated legal representative.

2.3.2.2 Inclusion criteria

Patients were included if they had confirmed AECOPD, the arterial pH remained less than 7.30 due to hypercapnia after medical therapy, a minimum of 1-hour NIV, were over 18 years of age and were randomised to and commenced on $ECCO_2R$ as part of the randomised controlled trial of $ECCO_2R$ in AECOPD (ClinicalTrials.gov: NCT02086084). A subset of 8 patients were included.

2.3.2.3 Study procedures

Patients allocated to the $ECCO_2R$ limb in the study were commenced on $ECCO_2R$ in accordance with the method described in chapter 3. Patients were breathing spontaneously, and systemic arterial blood gases were recorded prior to commencing $ECCO_2R$. Sweep gas was 100% oxygen and titrated up from 0 to 10L/min in 1L/min increments every 15-20 minutes. Blood flows remained constant throughout the study period. Blood gases were taken prior to a change in sweep gas flow rate before and after the membrane via high-flow pigtails and 3-way taps. 10mL of blood was discarded before sampling at each port.

The following measurements were recorded prior to every change in sweep gas flow rate:

1. Pre-$ECCO_2R$ circuit blood gas
2. Post-$ECCO_2R$ circuit blood gas
3. The CO_2 removal reported by the $ECCO_2R$ device
4. The $ECCO_2R$ sweep flow rate.

Blood gases were measured using a Cobas B 221 blood gas analyser (Roche, Basel, Switzerland). Blood gases were performed in the following manner: 10mL of fluid was withdrawn and discarded to ensure clearance of the dead space within the 3-way connector and high-flow pigtail (dead space volume of 2.6 mL); 2mL of fluid was withdrawn into a heparinised blood gas syringe.

2.3.2.4 Data measurement

For each gas, the following data was recorded: pH, PCO_2, PO_2, HCO_3, base excess, Hb, SO_2.

CO_2 content was described in mmol/L using equation 1.5

VCO_2 was described in mL/min using three separate methods:

1. Recorded directly from the $ECCO_2R$ device.
2. Calculated from the trans-membrane CO_2 difference (equation 2.3)

3. Corrected to a constant inlet blood PCO_2 using data from the trans-membrane CO_2 difference calculated using the Douglas equation ($VCO_{2\,(D)\,(corr)}$) (equation 2.9)

$$VCO_{2\,(D)\,(corr)} = VCO_{2\,(D)} * 6kPa / PCO_{2\,ML\,(pre)} \quad \text{[Eq 2.6]}$$

Equation 2.6: Carbon dioxide transfer across the membrane calculated from the trans-membrane CO_2 content difference using the Douglas equation corrected for an inlet PCO_2 of 6kPa ($VCO_{2\,(D)\,(corr)}$). $VCO_{2\,(D)\,(corr)}$ is measured in mL/minute. $PCO_{2\,ML\,(pre)}$ is the partial pressure of CO_2 content in blood before the membrane (kPa).

2.3.2.5 Statistical analysis

Data was recorded in a Microsoft Excel database. Statistical analysis was performed in Prism 9.1 for Mac (Graphpad, California, USA). Results are described as mean (SD). Gas flow was plotted against the mean (SD) VCO_2 calculated from trans-membrane CO_2 difference. VCO_2 was also corrected to a normalised inlet PCO_2 of 6kPa (equation 2.10) and plotted against sweep gas flow. A Bland-Altman plot and linear regression of the trans-membrane VCO_2 compared with the VCO_2 in the expiratory gas measured by the device were performed (Bland & Altman, 1986).

2.3.3 Results

2.3.3.1 Patient Demographics

There were 8 participants in this study, 4 of whom were female, with a median age of 67.5 years (71-73). Initial median arterial pH was 7.27 (range 7.24-7.29) and median $PaCO_2$ was 8.1kPa (range 7.4 – 11.3kPa).

2.3.3.2 Trans-membrane gas exchange

The extracorporeal blood flow was constant for the duration of this study with a median blood flow (range) of 0.39 (0.38-0.4) L/minute. The transmembrane PCO_2, CO_2 content and VCO_2 calculated using equation 1.5 ($VCO_{2\,(D)}$) or measured directly from the device ($VCO_{2\,(E)}$) are displayed in table 2.4.

The relationship between sweep gas flow and VCO_2 across the membrane lung calculated from the difference in CO_2 content in whole blood is described in table 2.4 and figure 2.9, with the VCO_2 corrected for an inlet PCO_2 of 6kPa in Figure 2.10. The figures show that there was an increase in CO_2 removed with each step increase in VCO_2 ($p<0.0001$, repeated measures ANOVA), however 85% of membrane $VCO_{2\ max}$ was removed at a gas flow of 4 L/min. The relationship between calculated VCO_2 across the membrane lung and that reported by the device is described in figure 2.11. The Bland-Altman plot demonstrates a bias [95% limits of agreement] of 6.5 [-11 to 24] ml/min.

Gas Flow (L/min)	Pre pH (SD)	Pre PCO_2 (kPa) (SD)	Pre $CtCO_2$ (mmol/L) (SD)	Post PCO_2 (kPa) (SD)	Post pH (SD)	Post $CtCO_2$ (mmol/L) (SD)	$VCO_{2\ (D)}$ (mL/min) (SD)	$VCO_{2\ (E)}$ (mL/min) (SD)
1	7.27 (0.03)	9.19 (1.38)	26.63 (3.5)	5.29 (0.43)	7.43 (0.02)	22.33 (2.2)	39.7 (17)	48.20 (17.0)
2	7.23 (0.04)	8.94 (1.45)	26.60 (3.1)	4.75 (0.59)	7.48 (0.04)	21.83 (2.1)	45.8 (19)	61.25 (18.9)
3	7.31 (0.46)	8.35 (1.72)	25.35 (3.7)	3.77 (0.61)	7.53 (0.04)	19.11 (2.9)	62.9 (13.3)	70.50 (14.1)
4	7.31 (0.43)	9 (1.79)	27.00 (3.1)	3.93 (0.59)	7.55 (0.03)	20.50 (2.3)	63.1 (7.4)	78.50 (14.3)
5	7.32 (0.06)	8.28 (1.9)	25.34 (3.6)	3.44 (0.51)	7.55 (0.04)	18.08 (2.3)	72.9 (14.1)	84.50 (18.3)
6	7.31 (0.04)	9.15 (1.7)	27.87 (3.6)	3.63 (0.45)	7.57 (0.02)	19.66 (2.1)	79.6 (16.2)	86.00 (11.2)
7	7.32 (0.06)	8.54 (2.13)	26.39 (3.6)	3.39 (0.62)	7.58 (0.03)	18.54 (2.5)	82.2 (5.6)	87.00 (11.8)
8	7.31 (0.05)	8.96 (1.61)	27.28 (3.1)	3.48 (0.46)	7.58 (0.03)	19.14 (1.8)	78.5 (10.3)	90.60 (6.9)
9	7.32 (0.05)	8.51 (1.71)	26.25 (3.3)	3.4 (0.48)	7.58 (0.03)	18.88 (1.7)	78.3 (16.2)	96.33 (21.2)
10	7.31 (0.04)	9.11 (1.68)	27.51 (3.6)	3.45 (0.47)	7.58 (0.03)	19.07 (2.2)	82.2 (13.7)	94.80 (9.6)

Table 2.4: Trans-membrane mean (SD) changes in pH, PCO_2 (kPa), CO_2 content ($CtCO_2$) (mmol/L), and CO_2 clearance using the Douglas equation ($VCO_{2\ (D)}$) or measured by the device ($VCO_{2\ (E)}$) (mL/min) measured at each sweep gas flow rate (L/min).

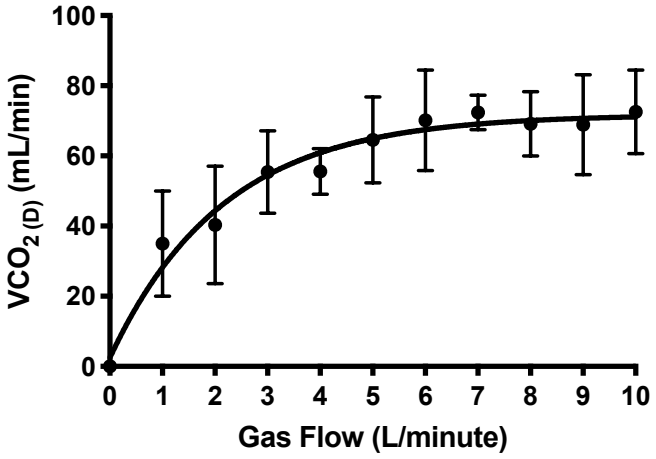

Figure 2.9: The relationship between gas flow and VCO_2 calculated from the trans-membrane CO_2 difference using the Douglas equation ($VCO_{2(D)}$).

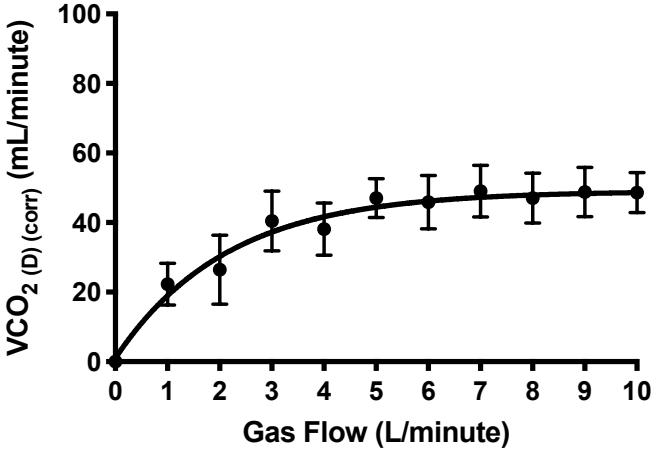

Figure 2.10: The relationship between gas flow and VCO_2 calculated from the trans-membrane CO_2 difference using the Douglas equation corrected to a normalised inlet PCO_2 of 6kPa using equation 2.6 ($VCO_{2(D)(corr)}$).

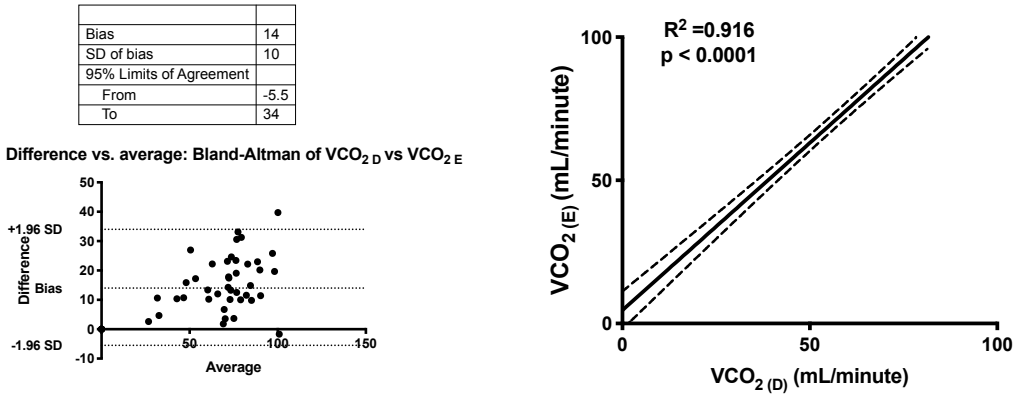

Figure 2.11: Bland-Altman plot of the relationship between VCO_2 calculated from the transmembrane CO_2 content difference ($VCO_{2(D)}$) compared with VCO_2 reported by the $ECCO_2R$ device ($VCO_{2(E)}$) and the linear regression analysis between VCO_2 calculated from the transmembrane CO_2 content difference (Douglas equation) ($VCO_{2(D)}$) compared with VCO_2 reported by the $ECCO_2R$ device ($VCO_{2(E)}$).

2.3.4 Discussion

This study describes the kinetics of CO_2 removal in vivo in a device with a blood flow of 0.4L/minute in patients with an acute exacerbation of COPD. The data demonstrates that there is a non-linear relationship between sweep gas flow and VCO_2 with a rapid increase in VCO_2 between 0 and 2 L/minute of gas flow which then reaches a plateau at a sweep gas flow rate of 4-6 L/minute. Nearly two thirds of CO_2 clearance occurred below a sweep gas flow rate of 2 L/minute. This correlates with the pre-clinical literature which explored VCO_2 in-vitro and in animal models (Federspiel & Hattler, 1996; Gattinoni, Kolobow, Agostoni, et al., 1979; Gattinoni, Kolobow, Damia, et al., 1979; Gattinoni, Kolobow, Tomlinson, Iapichino, et al., 1978; Gattinoni, Kolobow, Tomlinson, White, et al., 1978; Lehle et al., 2014). In these models there was a limit to CO_2 clearance at a ventilation to perfusion ratio of 10:1. Membrane VCO_2 reached a plateau at a ventilation/perfusion ratio of around 10:1 to 15:1 (figure 2.16). However, this was closer to 10:1 with inlet PCO_2 corrected to 6kPa, thereby reducing the interindividual variation in venous PCO_2 (figure 2.10). The absolute amount of CO_2 removed is higher for a blood flow of approximately 0.4 L/minute and a membrane surface area of 0.59 m^2 than has been reported in previous

studies (Jeffries et al., 2017; May et al., 2018; Strassmann et al., 2019). It is likely that this is due to the far higher PCO_2 in patients' venous blood than in the in vitro models as it is known that the PCO_2 and total CO_2 content in venous blood are important determinants of the CO_2 which can be removed (Jeffries et al., 2017). An additional important factor in CO_2 clearance is the blood flow, as for any given sweep flow, a higher blood flow results in a greater CO_2 clearance (Strassmann et al., 2019), however with the Hemolung device the blood flow is fixed to 0.35-0.45L/min making variable blood flow less impactful. A progressive increase in sweep gas flow does not achieve clearance of additional CO_2, rather with increasing sweep flow there is decreased lower incremental change in VCO_2 in keeping with diffusion limitation due to reduced mass transfer effectiveness (Bartlett, 2017; Turri & Yanagihara, 2011).

Carbon dioxide clearance was calculated using both the transmembrane CO_2 content difference and the CO_2 clearance reported by the device. The two methods demonstrated a linear relationship and agreement with low bias and high precision (figure 2.19). This supports the use of the CO_2 clearance reported by the device in routine clinical care which has the advantage of not requiring blood sampling.

The study has the advantage that it was undertaken in a population of patients with AECOPD providing a relatively homogenous population with systemic arterial and membrane blood gases performed in a structured protocolised manner. One of the key limitations is that all patients were spontaneously breathing, hence it is likely that the venous/pre-membrane CO_2 load will have varied during the measurements. This has been accounted for by normalizing the inlet CO_2 6kPa.

2.4 Conclusions

The series of experiments has demonstrated some key factors that are consistent across both the in-vivo and in-vitro study results. Firstly, there is a linear relationship with minimal bias between the VCO_2 measured by the device and VCO_2 measured by calculating transmembrane gas exchange in all experiments. Consequently, the VCO_2 measured by the device can be used as a measure of CO_2 clearance in clinical studies. Secondly, there is a clear and consistent relationship between sweep flow rate and VCO_2, with a rapid increase in clearance at sweep flow rates below 2L/minute and a

plateauing between 4 and 6L/minute giving a ventilation/perfusion ratio of approximately 10:1 as the limit of efficiency for an artificial membrane lung. This is consistent with the linear rise in dead space fraction indicating rising inefficiency and wasted gas flow. These factors have significant implications for the clinical management of the device. At the onset of therapy, a substantial amount of CO_2 amounting to approximately a third of CO_2 production is cleared by the device (assuming that 3mL/kg/min CO_2 is produced). Although untested, it is reasonable to assume that the relationship between sweep flow rate and clearance shows no hysteresis, and consequently during device weaning there is significant CO_2 clearance at low sweep low rates. Given this it is important that a period of slow weaning of the last elements of sweep flow gas occurs and further that a period of observation following cessation of sweep flow gas should be undertaken to prevent rebound respiratory failure.

It is important to note that in the spontaneously breathing patient with AECOPD, that there will be a variation in respiratory rate, oxygen consumption/carbon dioxide production and potentially changes in work of breathing and respiratory drive. Demonstration of the relationship between sweep gas flow rate and VCO_2 does not equate to clinical benefit.

Chapter 3: A randomised, controlled trial of the addition of $ECCO_2R$ to NIV in acute exacerbations of COPD

The trial was conducted in accordance with the standards set by the International Committee for Harmonisation of Good Clinical Practice and overseen by King's College London, carried out in the Department of Critical Care at Guy's and St Thomas' NHS Foundation Trust and was approved by the Cambridge Research Ethics Committee (reference: 14/EE/0109). The full trial protocol has been published (Barrett, Kostakou, et al., 2019). The data has been presented in abstract format at the ELSO congress (virtual), 30th September – 1st October 2021 and published in a peer-reviewed journal (Barrett et al., 2022). Previous chapters have described the underlying pathophysiology of COPD and demonstrated the impact of $ECCO_2R$ on CO_2 clearance in vitro and in vivo. The focus for this chapter is to explore the impact of $ECCO_2R$ on patient outcomes ascertained in a randomised controlled trial. This chapter therefore describes the conduct, methods, results and conclusions of the randomised controlled trial of the addition of $ECCO_2R$ to NIV in patients with AECOPD with a persisting pH of less than 7.30 after at least 1 hour of NIV.

3.1 Introduction

Patients with AECOPD have hypercapnic respiratory failure (arterial partial pressure of carbon dioxide ($PaCO_2$) > 6.5 kPa with an arterial pH <7.35) (Davidson et al., 2016). In these patients, non-invasive ventilation (NIV) has been consistently shown to provide a significant survival benefit (Osadnik et al., 2017). However, 15-30% of patients on NIV experience treatment failure and require tracheal intubation and invasive mechanical ventilation (Ozsancak Ugurlu & Habesoglu, 2017). The risk factors for NIV treatment failure include device or mask intolerance and discomfort, or persisting respiratory acidosis or tachypnoea after at least 1 hour of NIV (Plant et al., 2001) (Ozyilmaz et al., 2014; Steriade et al., 2019). When NIV failure occurs and patients require invasive mechanical ventilation, they are at a significantly higher risk of death (Martin-Gonzalez et al., 2016).

$ECCO_2R$ with a blood flow of around 400mL/minute can remove around a third of CO_2 from venous blood (Barrett & Camporota, 2017; Camporota & Barrett, 2016). $ECCO_2R$ has been shown to have physiological benefits in pre-clinical trials (Batchinsky et al., 2011) and uncontrolled case series in AECOPD (Burki et al., 2013; Kluge et al., 2012; Moss et al., 2016). To date, there have been no randomised controlled trials on the role of $ECCO_2R$ in AECOPD.

The hypothesis for this trial is that $ECCO_2R$ results in faster correction of hypercapnia and earlier cessation of NIV. Time to cessation of NIV is an important outcome as a longer duration of NIV is associated with increased complications, including NIV failure (Ozyilmaz et al., 2014; Steriade et al., 2019). Consequently, if NIV duration was reduced by at least 12 hours, this would be clinically meaningful.

3.2 Methods

3.2.1 Population

This study was a randomised, open-label, parallel-arm trial comparing standard therapy using NIV (NIV arm) with $ECCO_2R$ added to NIV ($ECCO_2R$ arm) in adults with AECOPD. Patients were included if they were over 18 years of age, had a history of COPD presenting with an acute exacerbation and had a persisting pH <7.30 due to hypercapnia after initial medical therapy and at least one hour of NIV. Patients were excluded if they had acute multiple organ failure, intolerance, allergy or contraindication to heparin or a contraindication to NIV. Patients were also excluded if they required domiciliary NIV as the primary endpoint (cessation of NIV) would not be able to be achieved.

3.2.2 Randomisation

Patients were randomised following written informed consent by the patient or nominated legal representative. Randomisation was computer-generated and allocation was concealed in opaque, sealed envelopes.

3.2.3 Outcomes

The primary outcome was time to discontinuation of NIV. Time to cessation of NIV was either patient preference or based on an improvement in respiratory rate to less than 25 with an arterial pH of more than 7.35. Short breaks for meals or patient comfort did not count as discontinuing NIV.

Secondary outcomes included physiological measurements, ICU and hospital length of stay (LOS) and outcomes (90-day mortality). Adverse outcomes included incidence of major haemorrhage (according to the International Society for Thrombosis and Haemostasis bleeding score) (Schulman & Kearon, 2005)), thrombosis, haemolysis, mechanical complications and need for IMV. Subjective discomfort and dyspnoea were measured using a visual analogue scale (VAS) (0-100mm). A higher score indicated greater subjective discomfort or dyspnoea. Quality-of-life measurements, including the COPD assessment test (CAT) (Jones et al., 2009), the St George's respiratory questionnaire (SGRQ) (Jones et al., 1991) and the EuroQuol-5D-5L (Devlin et al., 2018) were administered at the 90-day follow-up visit.

3.2.4 Sample size calculation

Sample size was calculated to achieve a mean population difference of 12 hours with a standard deviation of 10 hours (SEL, 2012). The estimated sample size with a 1:1 enrolment ratio was 12 patients in each arm. This would achieve 80% power to reject the null hypothesis of equal means with an alpha error of 5% and a loss to follow-up of 10%.

3.2.5 Trial conduct

Patients were randomised to continuation of NIV alone or to the addition of $ECCO_2R$ to NIV. NIV was delivered using an ICU ventilator in NIV mode (Draeger V500, Germany) with a mask specifically designed for dual limb ventilators (Freemotion, Fisher and Paykel, New Zealand). NIV was ceased when the respiratory rate was 25 or less and an arterial pH 7.35-7.45 or at patient request. When patients in the NIV

arm had ceased NIV, they were transferred to the medical ward the same day, as per ICU policy.

$ECCO_2R$ was delivered using the Hemolung Respiratory Assist System (ALung Technologies, USA) described in chapter 2. Cannulation was with a dual lumen cannula inserted in the femoral vein using previously published methods (Moss et al., 2016). Membrane VCO_2 reported by the device was recorded. $ECCO_2R$ and heparin were managed in accordance with institutional protocols. $ECCO_2R$ was weaned in increments of 1L/minute provided the respiratory rate was maintained at 25 breaths/minute or less and arterial remained pH 7.35-7.45. Once the sweep gas flow rate was reduced to 1L/minute for at least 4 hours, the sweep gas was discontinued for 4-12 hours whilst blood flow continued to prevent the membrane thrombosing. If the respiratory rate remained 25 or less with an arterial pH 7.35-7.45, then the $ECCO_2R$ device was stopped and the cannula removed. $ECCO_2R$ patients remained for observation overnight to exclude bleeding complications from the cannulation site.

The study workflow for the two limbs is displayed in figure 3.1.

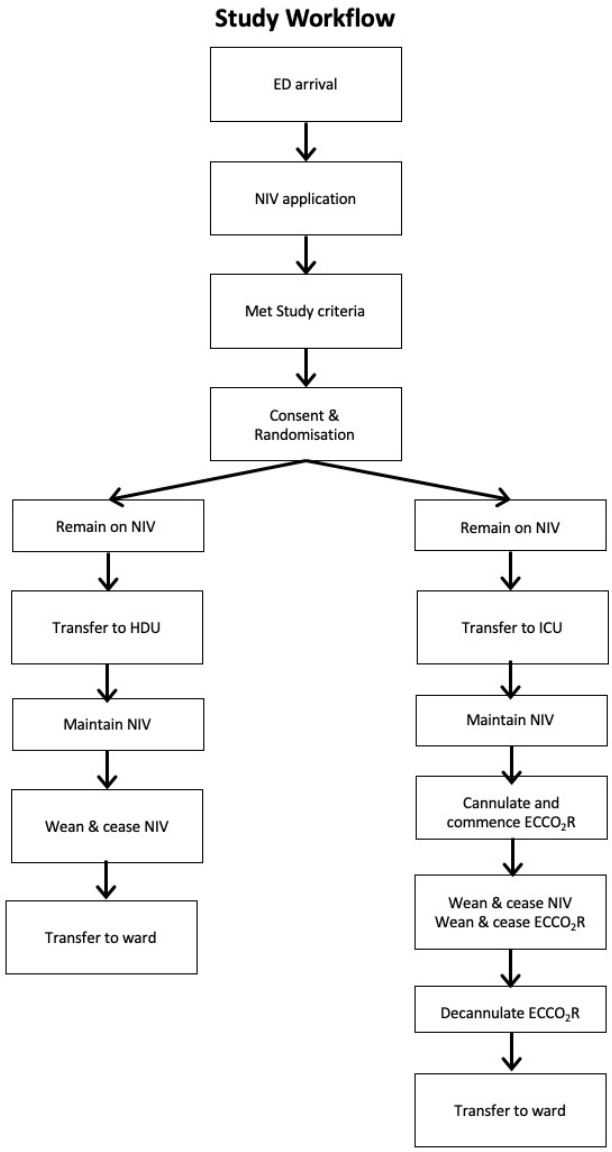

Figure 3.1: Study workflow.

3.2.6 Ethical approval

The trial protocol was approved by the Cambridge NHS Human Research Authority Research Ethics Committee (14/EE/0109).

3.2.7 Statistics

Statistical analysis was performed using Prism 9.5.1 for Mac (GraphPad, San Diego, USA). All data is presented as median (inter-quartile range). Categorical data were compared using a Chi-squared analysis. Survival was analysed using a log-rank test.

Statistical significance was defined as $p<0.05$. Given the relative size of the data sets, inferential statistics were not applied to the majority of the data.

3.3 Results

3.3.1 Recruitment

December 2017 and March 2020, 261 potentially eligible patients were screened, 32 patients met inclusion criteria, 18 consented and were randomised (figure 3.2). Nine were randomised to each group (figure 3.2, table 3.1). Two patients were lost to follow-up, one from each group, and were considered alive for the analysis (in accordance with mortality data from the UK NHS database). The trial was ceased early with the onset of the SARS-2 Coronavirus pandemic resulting in cessation of all non-COVID related research in the NHS.

3.3.2 Baseline characteristics

Patient characteristics at baseline are described in table 3.1. All patients had severe COPD (median GOLD stage 3 in each group). No patients were receiving domiciliary ventilation. Patients in both groups were broadly comparable, however baseline respiratory rate was higher in the $ECCO_2R$ group (29 (IQR 26-32) vs 24 (IQR 20-28) breaths/min), haemoglobin was higher in the $ECCO_2R$ group (151 (IQR 143-157) vs 130 (IQR 120-136) g/L), as was c-reactive protein (32 (IQR 30-51) vs 13 (IQR 3.5-16) vs mg/L).

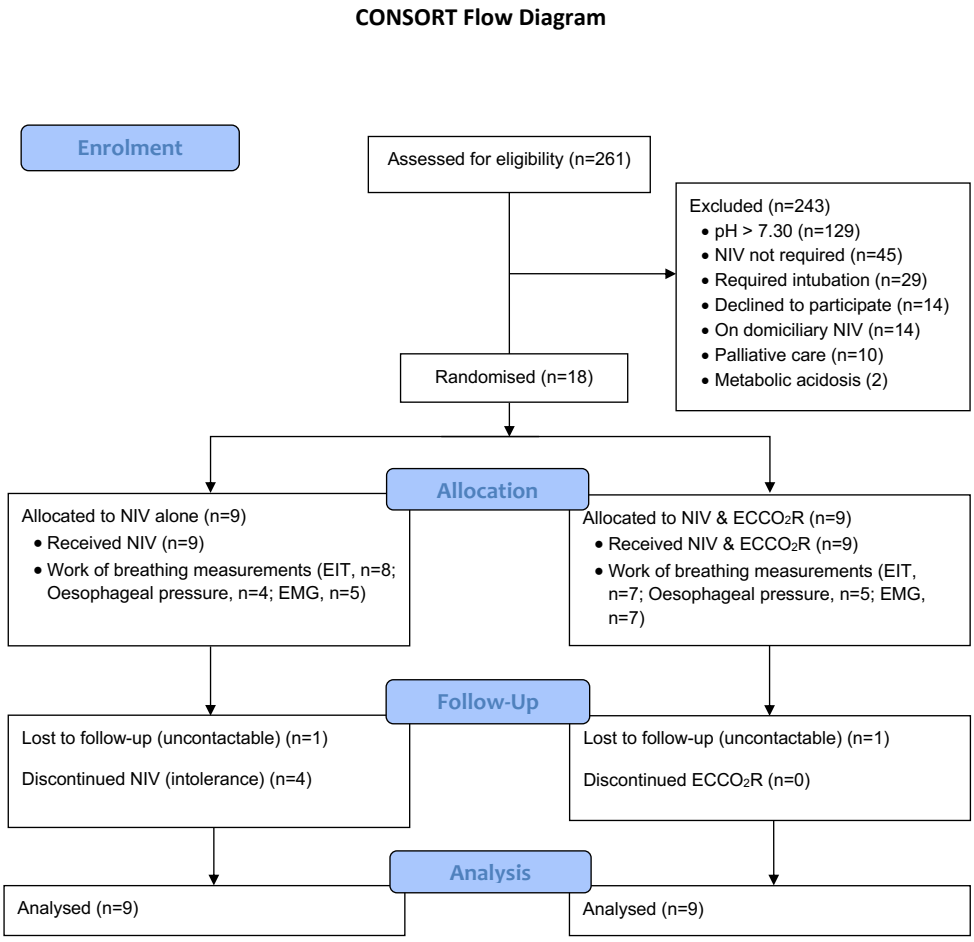

Figure 3.2: CONSORT flow diagram

	NIV	$ECCO_2R$
Demographic data		
Age (years)	69 (61-71)	65 (63-71)
BMI (kg/m^2)	22.19 (21.72-30.9)	24.67 (23.78-26.99)
Sex (F)	3	5
FEV1 (L)	0.84 (0.59-1.1)	0.97 (0.7-1.32)
FEV1 (% predicted) (%)	38 (21-45)	39.8 (39-46)
FVC (L)	2.3 (1.34-2.6)	2.6 (1.7-3.3)
FVC (% predicted) (%)	63 (33-105)	82 (63-92)
FEV1/FVC	48 (32-49)	44 (37-48)
GOLD stage	3 (3-4)	3 (3-3)
Pack years smoked	40 (20-60)	40 (39-45)
Baseline observations		
Systolic Blood pressure (mmHg)	120 (105-144)	130 (112-139)
Respiratory rate (breaths/min)	24 (20-28)	29 (26-32)
SpO_2 (%)	91 (90-92)	91 (87-93)
Heart rate (beats/min)	100 (86-113)	109 (100-116)
Presenting arterial blood gas		
PaO_2 (kPa)	8.67 (8.63-10.57)	7.33 (7.1-8.55)
$PaCO_2$ (kPa)	9.18 (8.94-10.31)	9.75 (8.14-9.78)
pH	7.23 (7.23-7.27)	7.26 (7.25-7.28)
HCO_3 (mmol/L)	31 (28.2-31.4)	29.5 (28.88-30.64)
Initial NIV settings		
EPAP (cmH_2O)	5 (5-5)	6 (5-6)
IPAP (cmH_2O)	18 (15-22)	18 (16-20)
FiO_2 (%)	32 (26-40)	35 (28-40)
Arterial blood gas after 1 hour NIV		
PaO_2 (kPa)	8.37 (8.05-8.83)	8.89 (7.9-9.41)
$PaCO_2$ (kPa)	9.16 (8.23-10.02)	9.34 (8.49-9.65)
pH	7.27 (7.24-7.27)	7.27 (7.25-7.27)
HCO_3 (mmol/L)	29.1 (26.7-30.8)	27.9 (27.7-30.52)
Baseline laboratory investigations		
Leukocytes ($x10^9/L$)	8.9 (6.8-10.4)	9.1 (8.3-11.8)
Haemoglobin (g/L)	130 (120-136)	151 (143-157)
Platelets ($x10^9/L$)	251 (172-288)	204 (163-308)
Creatinine (umol/L)	99 (57-136)	77 (69-80)
Bilirubin (umol/L)	6 (4-6)	7 (5.5-12)
C-reactive protein (mg/L)	13 (3.5-16)	32 (30-51)

Table 3.1: Baseline data. All data is presented as median (IQR).

3.3.3 $ECCO_2R$

All patients were cannulated via the femoral vein. Blood and sweep flow rates were all within the operating range of the device (table 3.2). $ECCO_2R$ was ceased after a median (IQR) of 96 (60-138) hours following successful weaning for all patients. CO_2 clearance through the membrane lung (VCO_2ML) was a median of 88 (83-104) mL/minute in the first hour and was maintained during the first 48 hours.

Hours	**4**	**8**	**12**	**24**	**48**
Pump RPM	1400 (1400-1400)	1400 (1400-1400)	1400 (1400-1400)	1400 (1400-1400)	1400 (1400-1400)
Blood flow (mL/min)	370 (357.5-380)	380 (380-395)	385 (377.5-400)	400 (365-410)	410 (395-420)
Sweep gas flow (L/min)	5 (3.5-8.5)	10 (6.5-10)	10 (7.5-10)	10 (10-10)	10 (7-10)
VCO_2 (mL/min)	78.5 (71.25-96.25)	88 (82.25-110.25)	90 (76.75-109.5)	95 (81.5-97)	86 (72.25-101.25)

Table 3.2: $ECCO_2R$ settings for the first 48 hours. All are median (IQR). VCO_2 is the reported membrane CO_2 clearance by the device.

3.3.4 NIV settings

The amount of pressure required (both expiratory and inspiratory) through the NIV circuit was not different between the two groups at baseline (table 3.1) or over the first 48 hours (table 3.3). However, in the $ECCO_2R$ group, NIV was ceased earlier and therefore comparative data was not available.

	NIV					
	Baseline	**4 hours**	**8 hours**	**12 hours**	**24 hours**	**48 hours**
NIV Observations						
EPAP (cmH_2O)	5 (5-5)	5 (5-5.25)	5 (5-6.5)	5.5 (5-6.5)	7 (5-8)	7.5 (6.5-8)
IPAP (cmH_2O)	18 (15-22)	17 (11.5-22.75)	18.5 (12-22)	20.5 (12-22)	19 (12-22)	20.5 (17.25-22.5)
FiO2 (%)	32 (26-40)	28 (26-40)	30 (28-32)	30 (28-32)	28 (24-28)	28 (27-28.5)
	$ECCO_2R$					
	Baseline	**4 hours**	**8 hours**	**12 hours**	**24 hours**	**48 hours**
$ECCO_2R$ Observations						
EPAP (cmH_2O)	6 (5-6)	5 (5-6)	5 (4.5-5)	5 (5-5)		
IPAP (cmH_2O)	18 (16-20)	18 (16-20)	18 (14.5-20.5)	20 (20-20)		
FiO_2 (%)	35 (28-40)	35 (30-40)	35 (28-40)	30 (28-40)	30 (25-40)	35 (35-40)

Table 3.3: NIV data over the first 48 hours in both groups.

3.3.5 Physiological changes post-randomisation

The respiratory rate appeared higher with $ECCO_2R$ compared with NIV at baseline and 12 hours post randomisation (22(20-24) vs 17 (15-19) breaths/min) (table 3.4, figure 3.3). The respiratory rate reduced in both groups initially and then plateaued (table 3.4, figure 3.3).

	NIV					
	Baseline	**4 hours**	**8 hours**	**12 hours**	**24 hours**	**48 hours**
RR (breaths/min)	24 (20-28)	20 (19-24)	19 (17-22)	17 (15-19)	17 (15-22)	20.5 (20-22.75)
SpO_2 (%)	90 (89-92)	90 (89-92)	91 (90-92)	92 (90-94)	93 (91-94)	94.5 (93.75-96)
HR (beats/min)	100 (90-105)	99 (99-105)	98 (91-104)	93 (87-101)	96 (91-99)	88 (82.5-93.75)
SBP (mmHg)	120 (105-144)	123 (119-137)	132 (117-138)	137 (114-138)	128 (115-145)	118 (109-130)
	$ECCO_2R$					
	Baseline	**4 hours**	**8 hours**	**12 hours**	**24 hours**	**48 hours**
RR (breaths/min)	29 (26-32)	22 (20-25)	20 (20-22)§	22 (20-24)	21 (20-23)	17 (16-23)
SpO_2 (%)	91 (87-93)	92 (88-96)	92 (91-94)	90 (86-91)	92 (90-93)	92 (91-95)
HR (beats/min)	101 (100-105)	101 (97-108)	93 (90-99)	87 (83-106)	88 (88-102)	92 (84-101)
SBP (mmHg)	130 (112-139)	142 (127-158)	141 (130-158)	123 (115-158)	123 (115-149)	119 (115-147)

Table 3.4: Physiological parameters over the first 48 hours in both groups.

3.3.6 Arterial blood gases

Arterial pH was similar between the two groups (figure 3.3, table 3.5). Arterial pH and CO_2 improved in both groups compared with baseline over time, although both pH and arterial CO2 may improve a little faster in the $ECCO_2R$ group.

	NIV					
	Baseline	**4 hours**	**8 hours**	**12 hours**	**24 hours**	**48 hours**
PaO_2 (kPa)	8.37 (8.05-9.35)	8.77 (7.74-8.95)	8.84 (7.93-10.15)	8.2 (8.01-8.6)	7.81 (7.55-8.14)	8.12 (7.54-8.68)
pH	7.27 (7.21-7.27)	7.3 (7.26-7.33)	7.32 (7.28-7.33)	7.34 (7.31-7.35)	7.36 (7.33-7.38)	7.38 (7.36-7.40)
$PaCO_2$ (kPa)	9.16 (8.23-10.02)	8.3 (7.74-9.3)	8.18 (7.63-8.7)	8.35 (7.6-9.45)	7.51 (7.16-8.92)	7.40 (7.16-8.08)
HCO_3 (mmol/L)	29.1 (26.7-33.6)	25.5 (22.2-30.4)	26.5 (24.2-29.2)	26.4 (25.5-31)	27.3 (26.1-30)	29.4 (29-30.175)
	$ECCO_2R$					
	Baseline	**4 hours**	**8 hours**	**12 hours**	**24 hours**	**48 hours**
PaO_2 (kPa)	8.89 (7.9-9.49)	7.77 (7-8.9)	8.45 (7.6-8.78)	7.67 (7.21-8.9)	9.02 (8.19-9.52)	8.8 (8.48-8.9)
pH	7.27 (7.25-7.29)	7.35 (7.31-7.37)	7.32 (7.32-7.38)	7.37 (7.35-7.41)	7.37 (7.33-7.39)	7.39 (7.37-7.42)
$PaCO_2$ (kPa)	9.34 (8.49-10.2)	6.8 (6.2-7.15)	8.13 (7.02-8.2)	7.99 (7.05-8.38)	7.51 (6.88-8.09)	8.02 (6.57-8.3)
HCO_3 (mmol/L)	27.9 (26.9-35.5)	24.7 (23.2-27.8)	25.7 (25-29)	26.5 (25.1-28.4)	26.6 (25.1-30.8)	29.7 (27.8-31.4)

Table 3.5: Arterial blood gases over the first 48 hours in each group.

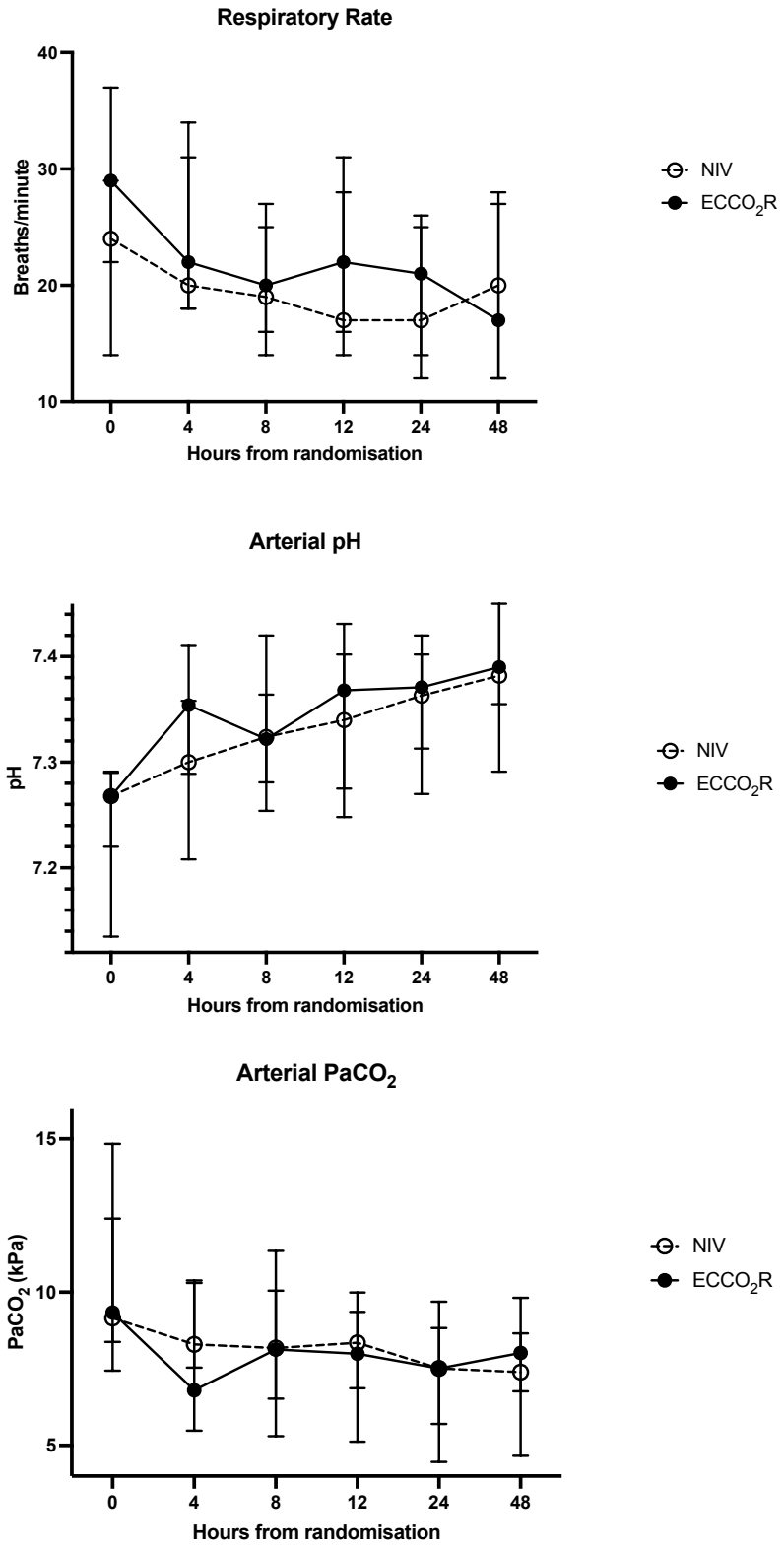

Figure 3.3: Respiratory rate, arterial pH and arterial PCO_2 between the two groups.

3.3.7 Time to event analysis

Median time from randomisation to cannulation and commencing $ECCO_2R$ was 2:30 (2:00-2:50) hours (table 3.6). Time from randomisation to pH >7.35 was lower with $ECCO_2R$ (5:32 (3:39-11:48) vs 23:58 (22:48-26:55) hours, p=0.024). Time to NIV discontinuation was shorter with $ECCO_2R$ (7:00 (6:18-8:30) vs 24:30 (18:15-49:45) hours, p=0.004) (table 3.6, figure 3.4). Four patients in the NIV arm ceased NIV against the treating clinician's advice. The ICU and hospital LOS were longer with $ECCO_2R$ than NIV (161:45 (132:27-174:50) vs 45:49 (40:22-53:00) hours, p=0.001 and 240:00 (219:52-337:31) vs 124:00 (103:38-213:15) hours, p=0.014).

	NIV	**$ECCO_2R$**	**p**
Cannulation		2:30 (2:00-2:50)	
Commencement $ECCO_2R$		2:30 (2:20-2:50)	
First time pH>7.35	23:58 (22:48-26:55)	5:32 (3:39-11:48)	0.0024
NIV ceased	24:30 (18:15-49:45)	7:00 (6:18-8:30)	0.004
$ECCO_2R$ ceased		97:30 (67:11-142:00)	
First sat out of bed	9:18 (7:05-30:22)	24:13 (21:08-105:50)	0.0721
First stand with assistance	21:00 (9:12-34:44)	24:13 (21:08-94:08)	0.3176
First walk with assistance	21:00 (7:52-43:29)	69:08 (21:56-147:43)	0.2222
First oral intake (not NG)	19:00 (12:03-26:58)	16:04 (13:42-33:40)	>0.9999
ICU discharge	45:49 (40:22-53:00)	161:45 (132:27-174:50)	0.0012
Hospital discharge	124:00 (103:38-213:15)	240:00 (219:52-337:31)	0.0142

Table 3.6: Time to event following randomisation. Median (IQR) time is presented in the format hours:minutes (*p<0.05)

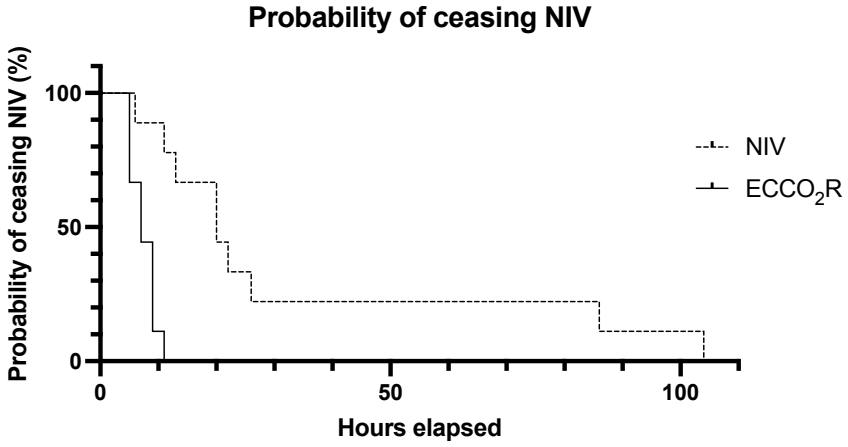

Hours	0	5	6	7	9	11	13	20	22	26	86
$ECCO_2R$	9	9		6	4	1					
NIV	9		9			8	7	6	4	3	2

Figure 3.4: Probability of remaining on NIV over time.

3.3.8 Subjective discomfort and dyspnoea

The results for visual analogue scores for both discomfort and dyspnoea are displayed in table 3.7 and figure 3.5. The onset of $ECCO_2R$ resulted in a reduction in VAS for discomfort (84 (78-87) vs 13 (4-65) and dyspnoea (85 (80-87) vs 20 (7-52).

	Pre-$ECCO_2R$	**Day 1**	**Day 2**
NIV			
Discomfort		56 (37-87)	50 (33-89)
Dyspnoea		41 (28-68)	24 (18-46)
$ECCO_2R$			
Discomfort	84 (78-87)	13 (4-65)	8 (1-67)
Dyspnoea	85 (80-87)	20 (7-52)	7 (2-28)

Table 3.7: Visual analogue scores for the two groups (median (IQR)).

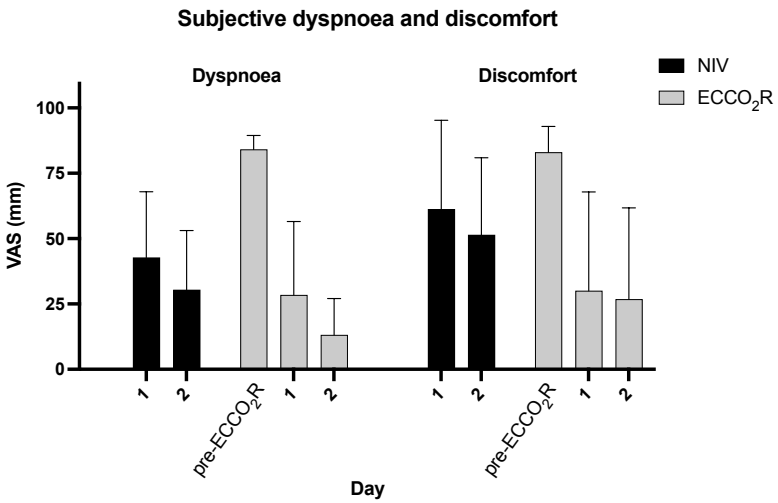

Figure 3.5: Subjective dyspnoea and discomfort over time in the NIV and $ECCO_2R$ groups using VAS.

3.3.9 Biochemistry and haematology data

Haematological, biochemical and coagulation parameters over the first 48 hours are described in table 3.8. Serum bilirubin levels appeared higher with $ECCO_2R$ compared with NIV at day two (14 (10-22) vs 5 (5-8) umol/L). The platelet count appeared lower with $ECCO_2R$ compared with NIV at day two (96 (73-124) vs 225 (169-244) $x10^9$/L). Fibrinogen appeared higher with $ECCO_2R$ compared with NIV at throughout the study period.

	NIV			$ECCO_2R$		
Day	**Baseline**	**Day 1**	**Day 2**	**Baseline**	**Day 1**	**Day 2**
Renal Biochemistry						
Sodium (mmol/L)	138 (132-141)	139 (135-141)	140 (139-141)	139 (138-142)	141 (140-143)	142 (142-143)
Potassium (mmol/L)	4.8 (4.6-5)	4.5 (4.2-4.6)	3.8 (3.7-4.4)	4.2 (3.8-4.5)	4.5 (4.3-4.5)	4.4 (4-5)
Creatinine (umol/L)	99 (57-136)	68.5 (52-92)	67 (55-93)	77 (69-80)	58 (49-76)	58 (51-74)
Hepatic function						
Alanine transaminase (IU/L)	20 (17-24)	22 (17-25)	21 (15-23)	19 (15-33)	24 (15-29)	22 (18-36)
Bilirubin (umol/L)	6 (4-6)	7 (4-9)	5 (5-8)	7 (6-12)	14 (8-26)	14 (10-22)
Inflammatory markers						
C-reactive protein (mg/L)	13 (4-21)	12 (5-64)	7 (3-66)	32 (30-51)	47 (20-56)	28 (23-41)
Haematology						
Leukocytes ($x10^9$/L)	8.9 (6.8-10.4)	9.2 (8.7-10.3)	9.6 (8.4-10.4)	9.1 (8.3-11.8)	9.1 (6.9-11.7)	8.5 (6.3-13.8)
Haemoglobin (g/L)	130 (120-136)	116 (107-126)	108 (100-117)	151 (143-157)	126 (113-127)	115 (105-125)
Platelets ($x10^9$/L)	251 (172-288)	224 (196-230)	225 (169-244)	204 (163-308)	138 (113-176)§	96 (73-124)
Plasma free-Hb (g/dL)				0.1 (0.1-0.1)	0.4 (0.2-0.5)	0.3 (0.3-0.6)
Coagulation						
APTTr	1 (1-1.1)	1 (0.9-1.1)	1.1 (1-1.1)	1 (1-1.1)	1 (1-1.5)	1.6 (1.4-2.7)
INR	1 (0.9-1.1)	1 (0.9-1.1)	1 (1-1.1)	1 (1-1.1)	1 (1-1.1)	1 (1-1)
Fibrinogen (g/L)	2.2 (1.5-2.3)	1.85 (1.5-2.4)	2 (1.8-2.6)	4.3 (4.1-5)	3.8 (3.4-4.4)	3.7 (3.2-4.7)

Table 3.8: Haematological, biochemical and coagulation parameters (median (IQR)).

3.3.10 Complications

There were no severe or life-threatening complications in either group. Complications are reported by device rather than by allocation group. The most frequent NIV-related complications were patient reported discomfort. Four patients stopped NIV due to discomfort. No patients stopped $ECCO_2R$. There were no patient complications related to cannulation for $ECCO_2R$, however one $ECCO_2R$ cannula thrombosed prior to commencement of $ECCO_2R$ and was changed. There was no significant bleeding in either group. No patients required red blood cell transfusion.

One patient with $ECCO_2R$ received a pool of platelets. No patient in either group underwent tracheal intubation and invasive mechanical ventilation whilst they were on therapy. One patient who had received $ECCO_2R$ required tracheal intubation and invasive mechanical ventilation later in the hospital stay due to development of pneumonia.

NIV (n=18)	**n**	**$ECCO_2R$ (n=9)**	**n**
NIV failure	0	Device failure	1
Aspiration pneumonia	0	Circuit change	0
Barotrauma	0	Cannula site bleeding	3
Hypotension (SBP <80mmHg)	0	Cannula site infection - clinical	0
Arm oedema	0	Cannula site infection – microbiological	0
CO_2 rebreathing	0	Air embolus	0
Claustrophobia	1	Haemolysis	3
Discomfort (patient reported)	13	Discomfort (patient reported)	1
Mechanical	1	Line position change	0
Nasal skin lesions	1	Circuit thrombus	0
Air leaks	8	Circuit fracture	0
Airway dryness	2	Intracranial haemorrhage	0
Gastric insufflation	0	Haemorrhage requiring 2 or more units	0
Vomiting	1	Venous insufficiency	0
Tracheal intubation required	0	Tracheal intubation required	1
Withdrew from therapy	4	Withdrew from therapy	0
Deep vein thrombosis	0	Deep vein thrombosis	0

Table 3.9: Adverse events relating to NIV and $ECCO_2R$, by device.

3.3.11 90-day survival and symptoms at follow-up

Survival with $ECCO_2R$ was 6/9 (ICU), 6/9 (hospital) and 5/9 at 90-day follow-up (table 3.10 and figure 3.6). Survival with NIV was 9/9 (ICU), 8/9 (hospital) and 7/9 at 90-day follow-up.

Results from the COPD assessment test (NIV: 22.5 (19.3-27.3), $ECCO_2R$ 26 (20-28)), St George's Respiratory Questionnaire (NIV: 71 (49.7-77.5), $ECCO_2R$: 55.3 (54.3-64.9)) and EuroQoL 5D-5L VAS (NIV: 37.5 (21.25-50), $ECCO_2R$: 45 (36.25-55)) were similar in the two groups.

	NIV	**$ECCO_2R$**
ICU survival	9/9 (100%)	6/9 (66%)
Hospital survival	8/9 (89%)	6/9 (66%)
90-day survival	7/9 (78%)	5/9 (56%)
CAT	22.5 (19.3-27.3)	26 (20-28)
EQ-5D	37.5 (21.25-50)	45 (36.25-55)
SGRQ	71 (49.7-77.5)	55.3 (54.3-64.9)

Table 3.10: Outcomes at ICU discharge, hospital discharge and 90 days.

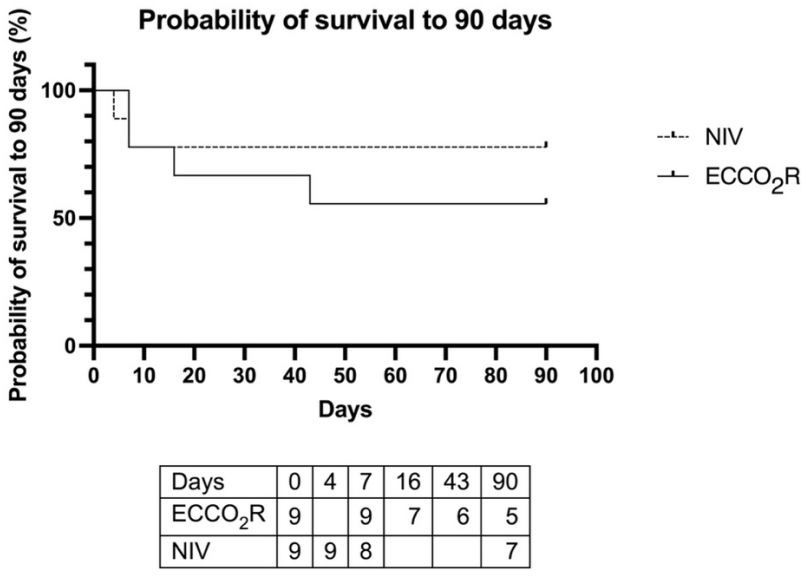

Figure 3.6: Probability of survival to 90 days.

3.4 Discussion

The present study is the first randomised controlled trial exploring the outcome of using $ECCO_2R$ in AECOPD. The data demonstrates that there was a resolution of hypercapnic respiratory failure over a similar timeframe in both groups. Similarly there was a reduction over time in subjective discomfort, subjective dyspnoea and tachypnoea. $ECCO_2R$ was associated with a reduction in time to ceasing NIV, however it was also associated with longer ICU and hospital stays.

The primary endpoint of the study was a reduction in the time taken to ceasing NIV of at least 12 hours. To achieve this primary endpoint with an alpha error of 5% and beta error of 20% with 5% loss to follow-up, it was estimated that 12 patients would be required to be randomised to each group. Although the study did not achieve its recruitment targets due to the COVID pandemic, the impact on NIV duration was greater than anticipated leading to 30 hours less NIV in the $ECCO_2R$ group (37 hours in the NIV group and 7 hours in the $ECCO_2R$ group). In clinical practice, time to NIV cessation, although meaningful for patients on the basis of comfort and for the ICU on the basis of resource utilisation, is a difficult composite endpoint. NIV is ceased for a number of reasons – stopped in accordance with hospital protocols by the nursing team due to improvement in pH, PCO_2 or respiratory rate, or stopped by the patient – this may be because they find NIV intolerable or because they felt their respiratory distress was improved. Four out of the nine patients in the NIV group withdrew from NIV before it was medically recommended, hence it is possible that the difference in time to removal of NIV between the two groups could have been greater.

Results demonstrate that the arterial pH and arterial CO_2 improved over time in both groups. The improvement in respiratory acidosis is consistent with results from observational studies exploring $ECCO_2R$ (Braune et al., 2016; Burki et al., 2013; Kluge et al., 2012; Moss et al., 2016). The early improvement in respiratory acidosis at 4 hours was followed by a reduction in pH again at 8 hours before restoration of normal pH at 10 hours in the $ECCO_2R$ group. The biphasic response to pH which occurred at

the same time as NIV was removed in the $ECCO_2R$ group suggests that the impact of NIV and $ECCO_2R$ are additive.

In keeping with improvement in pH and arterial CO2, the respiratory rate reduced initially in both groups and then remained relatively stable over the remaining 48 hours. This is in keeping with other studies which have demonstrated a reduction in respiratory rate associated with $ECCO_2R$ between 1 and 24 hours after commencement (Braune et al., 2016; Moss et al., 2016).

The VAS data is interesting – due to the enrolment of patients after commencement of NIV, there was no pre-NIV change in VAS which was able to be measured. The NIV and $ECCO_2R$ groups on day 1 and 2 had similar subjective dyspnoea and discomfort scores. What was also shown was that in the data which compared the immediately before and after $ECCO_2R$ data was that there was an improvement in subjective dyspnoea and discomfort (figure 3.5, table 3.7) as measured by the visual analogue scale (ATS, 1999). Dyspnoea is a complex symptom which is incompletely understood but likely relates to neural respiratory drive and is worsened by neuromechanical dissociation which is discussed further in chapter 4 (Jolley et al., 2009; Moxham & Jolley, 2009; Murphy et al., 2011; O'Donnell et al., 2009).

The optimal blood flow rate for provision of $ECCO_2R$ is currently a subject of significant debate. There is a limit for CO_2 clearance from whole blood with membrane efficiency plateauing at a ventilation/perfusion ratio of 10:1 and a linear increase in membrane dead space above a sweep gas flow rate of 2L/minute with the Hemolung (Barrett et al., 2020a, 2020b). This efficiency limitation has been noted in the literature with other devices (Gross-Hardt et al., 2019; Karagiannidis et al., 2014; Karagiannidis et al., 2017; Strassmann et al., 2019). These limitations have been particularly important in trying to understand the role of $ECCO_2R$ in acute respiratory distress syndrome (ARDS) (Combes et al., 2019; McNamee et al., 2017; McNamee et al., 2021). The key question following the publication of these studies, which did not support a role for $ECCO_2R$ in ARDS, was whether the blood flow of $ECCO_2R$ is adequate for the clinical purpose. The argument around optimal blood flow is important as higher blood flow devices require larger cannulae and may lead to greater shear

stress on blood with consequent injury to cellular components, although this depends on pump and membrane characteristics (Chandler, 2021; Sun et al., 2020). Higher blood flow devices require higher membrane surface areas to maintain efficiency leading to greater contact between blood and extracorporeal surface which leads to an increase in circuit induced inflammation and coagulation (Gross-Hardt et al., 2019; Karagiannidis et al., 2014; Karagiannidis et al., 2017; Strassmann et al., 2019; Sun et al., 2020). In the present study, the blood flow was a median of 400mL/min and the improvements in respiratory rate, $PaCO_2$ and respiratory acidosis suggests that in AECOPD in spontaneously breathing patients, the removal of CO_2 at an average rate of ~90 mL/minute (roughly equivalent 30-40% of the theoretical total CO_2 production of ~3mL/kg/minute) was clinically meaningful. This amount of CO_2 removal was associated with an earlier cessation of NIV, suggesting that the blood flow and CO_2 removal is adequate to achieve this endpoint.

No serious complications occurred in either group (table 3.9). The most common complications for NIV related to comfort – patient reported discomfort, claustrophobia, air leaks around the mask, airway dryness and nasal skin lesions. In total 72.2% of patients described a comfort-related complication of NIV. This type and frequency of complications is consistent with the literature (Consales et al., 2021; Demoule et al., 2006; Ko et al., 2015; Ozyilmaz et al., 2014; Pisani et al., 2016; Schnell et al., 2014). Discomfort relates to several different factors associated with NIV including the anchor system, the ventilatory settings, humidification (either too much leading to excessive facial moisture or too little leading to airway dryness), noise, psychological distress, anxiety, fear, pain and nasal/facial skin pressure lesions (Cammarota et al., 2022; Esquinas Rodriguez et al., 2013; Léotard et al., 2021; Patel et al., 2016; Sferrazza Papa et al., 2012). The discomfort associated with NIV may also be contributory to the significant improvement in comfort with the onset of $ECCO_2R$ (figure 3.5 and table 3.7) and may therefore have contributed to the marked improvement seen in the primary endpoint of time to NIV cessation in the $ECCO_2R$ group (table 3.6, figure 3.4). Discomfort is also commonly cited as a one of the root causes of NIV failure leading to tracheal intubation and mechanical ventilation (M. S. Stefan et al., 2015; Steriade et al., 2019; van Gemert et al., 2015). Only one patient in

the study required invasive mechanical ventilation and this patient was in the $ECCO_2R$ group, albeit after $ECCO_2R$ was weaned and ceased and was caused by a subsequent hospital acquired pneumonia. However, four patients in the NIV arm did elect to cease NIV prior to the normalisation of their respiratory rate and pH. In the $ECCO_2R$ group, most complications directly related to the device, including device failure, cannula site bleeding and haemolysis. Central line associated bacteraemia is a significant issue with complex underlying factors including duration of line insertion, site (femoral vein more problematic than internal jugular or subclavian), line care bundles and the infection control measures put in place at the time of insertion (Arvaniti et al., 2017; Couk et al., 2019; Hina & McDowell, 2017; Inhofer et al., 2022; Lai, Chaiyakunapruk, et al., 2016; Lai, Lai, et al., 2016; Velasquez Reyes et al., 2017). Despite the femoral vein cannulation site, no evidence of either microbiologically confirmed or clinically suspected line infection occurred.

Haemolysis was demonstrated to occur in the $ECCO_2R$ group with a rise in plasma free-Hb from 0.1 (0.1-0.1) to 0.4 (0.3-0.6) g/dL over the first 48 hours (table 3.8). Haemolysis is recognised to be a marker of blood trauma due to red cell injury as cells pass through the pump and membrane (Chandler, 2021). Blood trauma is a well-recognised complication of extracorporeal circuits and risk factors include blood flow at the higher or lower end of the pump operating range, pump revolutions of over 3000 per minute and negative access pressures (Schöps et al., 2021; Toomasian & Bartlett, 2011). The rise in plasma free-Hb leads to an increase in bilirubin and this was demonstrated in the $ECCO_2R$ group but not the NIV group over the first 48 hours and is in keeping with observational studies of $ECCO_2R$ (Burki et al., 2013; Combes et al., 2019; Kluge et al., 2012; Moss et al., 2016). Thrombocytopaenia is also associated with pumped extracorporeal circuits (Burki et al., 2013; Combes et al., 2019; Kluge et al., 2012; Moss et al., 2016) and was evident in this study (table 3.8). The underlying mechanisms are incompletely understood but may relate to platelet damage as blood transits the pump or platelet and fibrin films on the circuit or membrane (Chandler, 2021). Fibrinogen levels were elevated in the $ECCO_2R$ group compared with NIV. This is in keeping with the literature where high fibrinogen levels occur with excess inflammation, and low levels occur with excessive consumption (Burki et al., 2013;

Combes et al., 2019; Kluge et al., 2012; Moss et al., 2016). The mechanisms for the changes in fibrinogen are incompletely understood (Combes et al., 2019; Doyle et al., 2021). Despite the changes seen in platelets and fibrinogen, evidence of haemolysis and systemic anticoagulation with heparin there were no episodes of significant bleeding or thrombosis with $ECCO_2R$ and no need for transfusion of packed red blood cells. This is outwith the literature, where $ECCO_2R$ is associated with significant bleeding risk, including intracranial haemorrhage (Braune et al., 2016; Burki et al., 2013; Combes et al., 2019; Diehl, Augy, et al., 2020; Kluge et al., 2012; McNamee et al., 2017; Moss et al., 2016; Taccone et al., 2017).

Although the time to event data (table 3.6) demonstrated a shorter duration of NIV, ICU and hospital lengths of stay were both significantly longer in the $ECCO_2R$ than the NIV group. The longer stay was due to the longer stay in the ICU as time from ICU to home discharge was approximately 100 hours in both groups. This compares with other retrospective work which has found that the ICU LOS was shorter with $ECCO_2R$ (Braune et al., 2015). However, this was an observational study comparing $ECCO_2R$ with a retrospectively matched group of patients who required invasive mechanical ventilation. The longer ICU stay may be due to the baseline differences between the two groups with a higher respiratory rate, higher haemoglobin and c-reactive protein in the $ECCO_2R$ group suggesting that they may have been more unwell at baseline with a greater degree of infection and dehydration. The length of stay difference may also be contributed to by the differences in the hospital protocols of care between the techniques. NIV is a well-established therapy in my ICU and as such has clear, nurse-led weaning protocols allowing for weaning and cessation of NIV 24/7. Patients were discharged to the ward in the morning if they had been off NIV overnight. The clinical protocol for patients receiving $ECCO_2R$ did not allow nurse-led weaning or $ECCO_2R$ to be ceased overnight. Clinical $ECCO_2R$ protocols also mandated a period of observation – this led to a median of 8 hours (7-24) where the sweep gas flow was off but prior to decannulation. Clinical protocols also required a further overnight stay for observation. Finally, patients who had a persisting respiratory acidosis or tachypnoea but were assessed by the responsible clinician as having mental capacity and who declined ongoing NIV support were discharged to the ward for ongoing care.

These differences in clinical protocols and baseline physiology may have contributed to the increased length of stay but it is also possible that other factors, including the impact of $ECCO_2R$ on work of breathing also contributed.

The time to event data demonstrated that there was a delay to rehabilitation, time to sitting out of bed, first stand and first walk in the $ECCO_2R$ group (table 3.6). The median time to these events were lower than the median duration of $ECCO_2R$ indicating that rehabilitation was able to be undertaken despite the presence of a femoral cannula. This is important as there is ongoing controversy about mobilisation with femoral cannulae, especially larger diameter cannulae (Conceição et al., 2017; Leditschke et al., 2012; Perme et al., 2013). The time to rehabilitation is important as there is a clearly described benefit for early rehabilitation in critical illness (Hashem et al., 2016). One of benefits of NIV over mechanical ventilation with an oral endotracheal tube is that patients require less sedation are able to participate in active rehabilitation including standing, sitting in a chair and walking (Davidson et al., 2016). The importance of rehabilitation and the impact of $ECCO_2R$ on this outcome is a key consideration for future trials. The time to commence oral diet was similar in both groups. Nutrition is important in critical illness, especially in COPD where malnutrition is common, to prevent the consequences of the malnutrition associated with acute illness including muscle loss, inability to achieve rehabilitation goals and increased mortality (Kaegi-Braun et al., 2021; Kreymann et al., 2006; Singer, 2019). Early enteral nutrition, especially oral nutrition is preferred for both its nutritional and psychological benefits in critical illness (Fadeur et al., 2020; Singer et al., 2019).

The study was small and was not powered to detect a mortality difference. ICU, hospital and 90-day mortality were similar between the two groups (table 3.10 and figure 3.6). All in-hospital deaths were due to the underlying disease and no deaths were related to the provision of $ECCO_2R$. COPD is a chronic illness with a significant and progressive impact on quality of life. Patients in the study had severe symptoms (median GOLD stage 3), including dyspnoea on minimal exertion, with a consequent impact on quality of life. Exacerbations are known to contribute to a more rapid deterioration in quality of life (Camac et al., 2022; Camac et al., 2021; Gosker et al., 2021; Machado et al., 2022). There are several quality-of-life tools which have been

validated in patients with COPD, including the COPD assessment test (CAT) (Jones et al., 2009; Jones et al., 2012) and St George's Respiratory Questionnaire (SGRQ) (Nonato et al., 2015; Weatherall et al., 2009). The CAT results were similar between the two groups and indicate there was a high impact on symptoms due to the severity of the COPD. The CAT results are in keeping with the GOLD stage and the literature (Ghobadi et al., 2012). SGRQ measures the impact of disease on quality of life in COPD and a higher score represents a greater impact (Nonato et al., 2015; Weatherall et al., 2009). The minimally important difference in SGRQ in severe COPD is 8 (Welling et al., 2015), however although the scores were numerically different between the two groups. Similarly, the EuroQoL 5D-5L, a validated quality of life score (Devlin et al., 2018) shows that in both groups their quality of life was significantly impaired, however there was no difference between the groups. The impaired quality of life is also found in other patients with severe COPD (Guo et al., 2020; Morishita-Katsu et al., 2016).

This study is limited by the small sample size of only nine in each group, 3 patients short of the planned enrolment in each group. Despite this the primary end point of a reduction in time to cessation of NIV of at least 12 hours was met. The small numbers do reduce the strength of the interpretation of the study. Clearly there could have been unmeasured baseline differences that could have contributed to the study results. The small size limits the interpretation of the adverse consequences of $ECCO_2R$ as uncommon/infrequent complications may not be identified.

3.5 Conclusion

Overall, this data suggests physiological benefit associated with $ECCO_2R$ as an addition to NIV with the subsequent withdrawal of NIV as being equivalent to NIV alone. There is a potential patient-centred benefit relating to dyspnoea relief that needs further exploration. Overall the data suggests that ECCO2R may have a role in patients who do not tolerate NIV or who are deteriorating on NIV. However, the data also indicates that there was a longer ICU and hospital length of stay for patients when $ECCO_2R$ was added to NIV. The study was not powered to demonstrate a mortality benefit or a difference in the need for intubation and these need to be

explored in future larger trials. Although many patients did cease NIV shortly after commencing $ECCO_2R$, it is possible that there are benefits in adding $ECCO_2R$ to NIV but retaining NIV.

Chapter 4: Assessment of the impact of $ECCO_2R$ on distribution of ventilation and work of breathing in patients with an acute exacerbations of COPD

4.1 Introduction

The previous chapters have considered the efficacy of an extracorporeal membrane in clearing of CO_2 from the blood and the impact of $ECCO_2R$ added to NIV on patients' outcome. This chapter will describe the relative effects of $ECCO_2R$ on work of breathing and pulmonary gas distribution using three different methods – oesophageal pressure measurement, electrical impedance tomography (EIT) and parasternal electromyography (pEMG). An exacerbation of COPD is complex and each of the measurement devices explore different aspects of the exacerbation (figure 4.1). EIT describes the change in inspiratory time constants, distribution of aeration, dynamic hyperinflation and tidal volumes. Parasternal EMG describes changes in inspiratory effort and neural drive, whilst oesophageal pressure allows the estimation of the work of breathing. These methods are consequently complementary and will assist in developing a fuller picture of the relative impact of NIV and $ECCO_2R$ in AECOPD.

Acquiring physiological measurements in conscious critically ill patients is difficult and the more invasive the measurement the more difficult it is to acquire. Measuring oesophageal pressure using an oesophageal balloon requires tolerance of the insertion of the nasal tube and of the procedures involved, including the no-flow calibration and application of the pneumotachograph which requires active participation including breath holding. Although electrical impedance tomography is a non-invasive imaging method, it does require a band placed around the chest which may be perceived as restrictive and in the acute phases of respiratory distress poorly tolerated. The electrical environment in the ICU generates electrical noise and, although parasternal electromyography is easy to apply, the measurement of interpretable electromyographic signals can be unreliable. Finally, the condition of the patient and their ability to consent and to tolerate each examination fluctuates over time. Consequently, multiple different measurements that allow an

understanding of the potential impact of $ECCO_2R$ on regional and global ventilation as well as work of breathing are required (Barrett, Hart, et al., 2019).

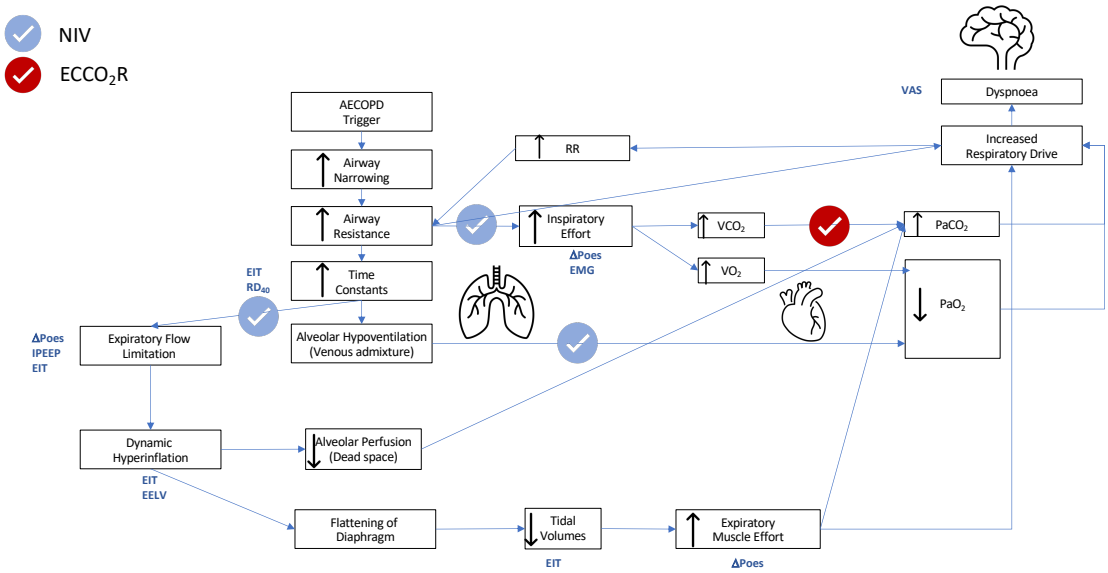

Figure 4.1: The use of oesophageal pressure, electromyography and electrical impedance tomography to explore different aspects of the potential impact of $ECCO_2R$ on the pathophysiology of COPD.

4.2 Oesophageal pressure measurement

4.2.1 Introduction

Oesophageal pressure measurement is undertaken using an air-filled balloon placed in the lower third of the oesophagus which is combined with a pneumotachograph to obtain simultaneous pressure, volume, time and flow data. The oesophageal pressure is a surrogate for pleural pressure and can be used to measure work of breathing, the pressure-time product and to assess the activity of the muscles of respiration (Akoumianaki et al., 2014; Banner et al., 1994; Cabello & Mancebo, 2006).

4.2.1.1 Equation of motion

At the beginning of respiration, the total pressure required for inspiration is the sum of the pressure required to overcome the elastance and resistance of the respiratory

system. The pressure at the start of inspiration (P_0) depends on whether the patient is mechanically ventilated (equal to PEEP) or breathing spontaneously (0 cmH_2O generally or > 0 cmH_2O if there is intrinsic PEEP). The total pressure necessary to move the respiratory system from a resting state to a given lung volume is described by the equation of motion (equation 4.1).

$$P_{TOTAL} = P_0 + (E_{RS} \times V) + (R_{RS} \times \dot{V}) \quad \text{[Eq 4.1]}$$

Equation 4.1: The equation of motion (Akoumianaki et al., 2014). P_{TOTAL} is the total pressure applied to the respiratory system, P_0 is the starting pressure (e.g., PEEP or 0 cmH_2O), E_{RS} is the elastance of the respiratory system, V is the tidal volume, R_{RS} is the resistance of the respiratory system and $\dot{V}$ is the inspiratory flow.

In spontaneously breathing patients without the assistance of mechanical ventilation, P_{AW} is 0 cmH_2O and in patients who are fully mechanically ventilated without any spontaneous effort, P_{MUS} is 0cmH_2O. For patients who are receiving NIV, there is a combination of intrinsic muscular effort and extrinsic work provided by the ventilator. The total pressure is thus also described as the sum of the airway pressure and the pressure generated by the muscles of respiration (equation 4.2).

$$P_{TOTAL} = P_{AW} + P_{MUS} \quad \text{[Eq 4.2]}$$

Equation 4.2: The equation of motion described using the pressure generated by the muscles of respiration (Akoumianaki et al., 2014). P_{TOTAL} is the total pressure applied to the respiratory system, P_{AW} is the pressure applied by the ventilator, P_{MUS} is the pressure generated by the patient's respiratory muscles.

4.2.1.2 Transpulmonary pressure

The change in airway pressure through muscular effort or mechanical ventilation, results in a pressure difference between the pleural space and the alveolus, the trans-pulmonary pressure. The pressure difference results in air flowing into the lungs (equation 4.3) (Akoumianaki et al., 2014; Banner et al., 1994; Cabello & Mancebo,

2006). In healthy humans, the transpulmonary pressure is negligible, however in patients with lung diseases the transpulmonary pressure increases significantly (Gattarello et al., 2023). The pleural pressure varies with gravity, body habitus, position and lung pathology, consequently, the pleural pressure is not the same throughout all regions (Akoumianaki et al., 2014; Bellani & Pesenti, 2014; Brochard, 2014; Hedenstierna, 2012; Krell & Rodarte, 1985; Pecchiari et al., 2013).

$$TPP = P_{AW} - P_{PL} \quad \text{[Eq 4.3]}$$

Equation 4.3: Transpulmonary pressure described using pleural pressure (Akoumianaki et al., 2014). TPP is transpulmonary pressure, P_{PL} is pleural pressure and P_{AW} is airway pressure.

4.2.1.3 Oesophageal pressure

Given that direct measurement of pleural pressure is not feasible in clinical conditions, oesophageal pressure is used as a surrogate (Agostoni & Hyatt, 1986; Akoumianaki et al., 2014). Oesophageal pressure (P_{ES}) may be measured using an inflated balloon placed in the lower oesophagus and attached to an air-filled pressure transducer. The balloon measures the pressure transmitted to the lower oesophagus and varies with lung volume, position, body habitus, oesophageal muscle tone, chest wall distortion and intrathoracic pathology (Akoumianaki et al., 2014; Bellani & Pesenti, 2014; Brochard, 2014; Hedenstierna, 2012; Krell & Rodarte, 1985; Pecchiari et al., 2013). The absolute oesophageal pressure is not an accurate measure of pleural pressure given the regional variations in pleural pressure and the single measurement point of the oesophageal pressure. However, tidal variations in oesophageal pressure correlate well with the equivalent changes in pleural pressure (Agostoni & Hyatt, 1986; Akoumianaki et al., 2014; Bellani & Pesenti, 2014; Benditt, 2005; Hedenstierna, 2012). Consequently, the difference between P_{ES} and P_{AW} is a reasonable estimate of transpulmonary pressure (equation 4.4) (Akoumianaki et al., 2014; Bellani & Pesenti, 2014; Hedenstierna, 2012).

$$TPP = P_{AW} - P_{ES} \quad \text{[Eq 4.4]}$$

Equation 4.4: Transpulmonary pressure described using oesophageal pressure (Akoumianaki et al., 2014). TPP is transpulmonary pressure, P_{ES} is oesophageal pressure and P_{AW} is airway pressure.

Oesophageal pressure measurement has several benefits. In addition to direct measurement of the oesophageal pressure, when combined with a pneumotachograph, lung volumes, pressures, air flow and the timing of inspiration/expiration can all be measured simultaneously. This allows the calculation of lung elastance (pressure change per litre of tidal volume) and resistance (pressure change per unit of flow (in litres) per second) as well as calculations of the work of breathing and pressure time product of the respiratory system. Additional calculations, including mechanical power (the total energy applied to the respiratory system every minute) and lung stress (the total distending pressure of the lung) can be performed. Given the demonstration of flow and pressure change over time, the relative timing of the onset of respiratory muscle contraction compared with the timing of the onset of airflow can also be measured which allows demonstration of the effort required to overcome airway resistance (Akoumianaki et al., 2014; Bellani & Pesenti, 2014; Blanch et al., 2005; Brochard, 2002, 2014; Purro et al., 1998; Ranieri et al., 1995).

4.2.1.4 Derived data from oesophageal pressure measurement

There are two accepted estimates of the activity of the muscles of respiration – work of breathing and the pressure-time product.

4.2.1.4.1 Work of Breathing

In patients receiving invasive or non-invasive mechanical ventilation, it is clear from the equation of motion that part of the pressure applied to the lung results from the pressure from ventilator (P_{AW}); and part from the patient's inspiratory muscles (P_{MUS}) (Bellani & Pesenti, 2014; Hedenstierna, 2012). The work performed by the respiratory muscles can be calculated by integrating the pressure and volume changes that occur

over time (Akoumianaki et al., 2014; Banner et al., 1994; Benditt, 2005; Cabello & Mancebo, 2006). Work is undertaken to overcome the resistive and elastic forces of the respiratory system (Banner et al., 1994; Cabello & Mancebo, 2006). Elastic work overcomes both the elastic recoil of the lung and the chest wall. Resistive work overcomes airway resistance which can be significant in exacerbations of COPD. Expiratory work is normally approximately 20% of the total due to stored potential energy in the elastic tissues, however for patients with exacerbations of COPD, there is activation of the expiratory muscles resulting in an increase in the work of breathing (Fritts et al., 1959; Milici-Emili & Petit, 1960; Yan et al., 2000). Unfortunately, oesophageal pressure monitoring only quantifies inspiratory work and for total work which includes that of expiratory muscle activation a more complex calculation through drawing of a Campbell's diagram is required (Pham et al., 2020).

Work is measured in Joules (J), or as J/L (Akoumianaki et al., 2014; Banner et al., 1994; Cabello & Mancebo, 2006). Work done over a unit of time is power and can be measured in Joules per minute (J/min) if the respiratory rate is known. The work of breathing is described by equation 4.5.

$$WOB = \int_0^{VT} P_{MUS}.\delta V \qquad \text{[Eq 4.5]}$$

Equation 4.5: Work of breathing (Akoumianaki et al., 2014). WOB is work of breathing measured in joules (J), VT is volume at time t, P_{MUS} is the pressure generated by the inspiratory muscles and δV is the tidal volume.

The pressure due to the contraction of the muscles of respiration (P_{MUS}) is the instantaneous difference between the static recoil pressure of the chest wall ($P_{CW, REL}$) at rest (i.e., static compliance of the chest wall multiplied by the instantaneous tidal volume), and the oesophageal pressure (P_{ES}), hence the work of breathing due to the muscular activity of the chest wall is given by equation 4.6.

$$WOB = \int_0^{VT} (P_{CW,REL(V)} - P_{ES(V)}).\delta V \qquad \text{[Eq 4.6]}$$

Equation 4.6: Work of breathing of the muscles of respiration (Akoumianaki et al., 2014). WOB is work of breathing measured in joules (J), VT is volume at time t, $P_{CW, REL}$ is the static recoil pressure of the chest wall at rest and is traditionally 4% of the predicted vital capacity and P_{ES} is the oesophageal pressure, VT is the tidal volume.

In patients who are spontaneously breathing, the static recoil pressure of the chest wall cannot be measured, and an estimate is required (Akoumianaki et al., 2014; Benditt, 2005). The static recoil pressure of the chest wall can be calculated using the tidal volume and an estimation of chest wall elastance which is generally equated to 4% of the theoretical vital capacity of that subject.

$$P_{CW,REL} = \frac{V}{(VC*0.04)} \qquad \text{[Eq 4.7]}$$

Equation 4.7: Estimating the static recoil pressure of the chest wall (Akoumianaki et al., 2014). $P_{CW, REL}$ is the static recoil pressure of the chest wall at rest, V is the tidal volume and VC is the theoretical vital capacity.

The theoretical vital capacity is calculated from height using equation 4.8a or 4.8b.

$$VC = height \times (21.78 - 0.101 \times age) \qquad \text{[Eq 4.8a]}$$

$$VC = height \times (27.63 - 0.112 \times age) \qquad \text{[Eq 4.8b]}$$

Equation 4.8a & 4.8b: Theoretical vital capacity (mL) (Baldwin et al., 1948). VC is theoretical vital capacity where height is measured in cm and age in years.

Work of breathing is commonly expressed as the work per breath, per minute or per litre. Work of breathing can also be calculated from the pressure-time product of a breath obtained from the oesophageal pressure (Gattinoni et al., 2017).

$$WOB/min = (PTP_{breath}/t_i)*RR*V*0.098 \quad [Eq\ 4.9a]$$

$$WOB/breath = (PTP_{breath}/t_i)*RR*V*0.098/RR \quad [Eq\ 4.9b]$$

$$WOB/litre = (PTP_{breath}/t_i)*RR*V*0.098/V_E \quad [Eq\ 4.9c]$$

Equation 4.9 a, b & c: Work of breathing in different formats (Gattinoni et al., 2017). WOB/min is the work of breathing per minute and is measured in J/min, WOB/breath is the work of breathing per breath and is measured in J and WOB/litre is the work of breathing per litre and is measured in J/L, PTP_{breath} is the pressure time product of the breath, measured in $cmH_2O.s$, t_i is the inspiratory time of the breath (s), RR is the respiratory rate (breaths/min) and V is the tidal volume (L), 0.098 is the constant to transfer $cmH_2O.L$ into Joules (J), V_E is the minute ventilation.

The relationship between pressure due to the respiratory muscles and volume can also described by Campbell's diagram (Cabello & Mancebo, 2006; Campbell, 1957). Campbell's diagram is a graphical analysis of the oesophageal pressure against tidal volume over the respiratory cycle. It separates work into inspiratory, expiratory, resistive and elastic components (Cabello & Mancebo, 2006; Campbell, 1957).

4.2.1.4.2 Pressure-time product

Respiratory muscle work can also be estimated using the pressure-time product of the oesophageal pressure (PTP_{ES}) (Akoumianaki et al., 2014; Bellani & Pesenti, 2014; Benditt, 2005; Collett et al., 1985; Hedenstierna, 2012). PTP_{ES} is the integral of pressure over time and is therefore the product of the change in pressure multiplied by the duration of the contraction (Akoumianaki et al., 2014; Bellani & Pesenti, 2014; Benditt, 2005; Collett et al., 1985; Hedenstierna, 2012). PTP_{ES} measures the activity related to all muscles of respiration (diaphragm and intercostal muscles). Work of breathing and PTP_{ES} are highly correlated provided that a volume is generated (Akoumianaki et al., 2014). The advantage of PTP_{ES} is that it provides an estimate of activity regardless of whether a volume is generated and therefore includes isometric contraction. PTP_{ES} has been shown to be better correlated with oxygen consumption

than other measures of work of breathing in the circumstance where significant isometric contraction occurs (Akoumianaki et al., 2014; Collett et al., 1985; Field et al., 1984). This is particularly important in AECOPD where airways resistance may need to be overcome to initiate a breath and work of breathing calculated from changes in volume and pressure underestimate this element (Akoumianaki et al., 2014; Annat et al., 1990; Brochard, 2002; Goldberg et al., 1995). Active expiration is also able to be identified and its work quantified if a gastric balloon is used in addition to the oesophageal balloon (Akoumianaki et al., 2014; Brochard, 2002). PTP_{ES} is measured in $cmH_2O.s$ and can be reported per breath, per minute or per litre of minute ventilation (Collett et al., 1985). PTP_{ES} can be partitioned into the different contributors to the PTP including the PTP due to the intrinsic PEEP, elastic PTP and resistive PTP.

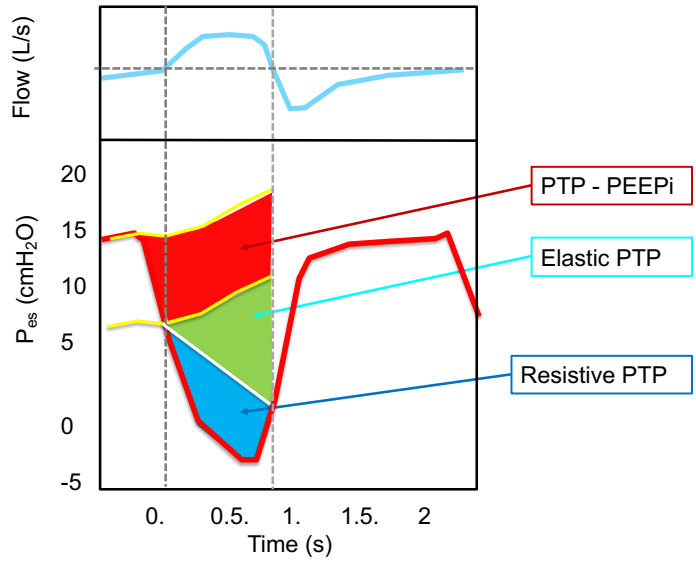

Figure 4.2: Contributors to the pressure time product – redrawn from (Pham et al., 2020). The red area represents the PTP due to intrinsic PEEP, the green area elastic PTP and the blue area resistive PTP. Flow is indicated in the upper portion of the graph and its relationship to the changes in oesophageal pressure is indicated by the dotted lines.

4.2.1.4.3 Oxygen consumption

The energy expended during quiet respiration is approximately 2-4J/minute (0.3-0.5J/L) of which 80% is expended during inspiration and 20% is expended during expiration (Fritts et al., 1959; Mancebo et al., 1995; Milici-Emili & Petit, 1960). The metabolic cost of respiration increases with increasing minute ventilation such that there is a progressively higher cost per litre of minute ventilation (Roussos, 1985; Roussos & Campbell, 2011). The efficiency of breathing is the ratio between the mechanical work of breathing and the energy expended by metabolism of the respiratory muscles (Roussos & Campbell, 2011). In healthy humans, the efficiency of the breathing is recorded as 10-25%, depending on position (Cherniack, 1959; McGregor & Becklake, 1961; Roussos & Campbell, 2011). In chronic lung diseases, including COPD, efficiency is approximately 1-2% (McGregor & Becklake, 1961; Roussos & Campbell, 2011). As minute ventilation increases, efficiency progressively reduces. It has been demonstrated that work of breathing correlates well with oxygen consumption and CO_2 production in health, exercise and in COPD (Akoumianaki et al., 2014; Brochard et al., 1989; Coast & Krause, 1993; Lewis et al., 1994; Robertson, Foster, et al., 1977; Robertson, Pagel, et al., 1977). However, the work of breathing is underestimated using the oesophageal balloon as work done on the elastic and inelastic forces of the chest wall are not measured, nor is displacement of the abdominal contents (Roussos & Campbell, 2011).

4.2.1.4.4 Total lung stress

Total lung stress is the sum of the pressures generated by the ventilator and the patient and can contribute to injury and inflammation within the lung parenchyma (Brochard et al., 2017; Otis et al., 1950). Total lung stress is calculated using the transpulmonary pressure and PEEP (equation 4.10) (Coppola et al., 2021).

$$\text{Total lung stress} = (\delta P_{AW} - \delta P_{ES}) + (PEEP * E_L/E_{RS}) \quad [Eq\ 4.10]$$

Equation 4.10: Total lung stress (Coppola et al., 2021). dP_{AW} is the change in airway pressure, δP_{ES} is the change in oesophageal pressure, PEEP is the positive end-expiratory pressure, E_L is the lung elastance and E_{RS} is the total elastance of the respiratory system.

4.2.1.4.5 Mechanical power

Mechanical power is the total amount of energy applied to the respiratory system during mechanical ventilation. In passively ventilated patients this energy comes entirely from the ventilator whilst in spontaneously breathing patients it come from the ventilator and the patient's own muscular effort (Coppola et al., 2021). Mechanical power is calculated using equation 4.11 (Coppola et al., 2021).

$$MP_{RS} = 0.098*RR*[VT^2*(E_L/E_{RS}*dP_{ES}/VT+RR*0.5)+VT*PEEP] \quad [Eq\ 4.11]$$

Equation 4.11: Mechanical power of the respiratory system (MP_{RS}) (Coppola et al., 2021). 0.098 is the constant to convert 1 cmH_2O into J/min, RR is respiratory rate (breaths/min), VT is the tidal volume (L), E_L is the lung elastance, E_{RS} is the respiratory system elastance, dP_{ES} is the change in oesophageal pressure and PEEP is positive end expiratory pressure.

4.2.1.4.6 Ventilatory ratio

The ventilatory ratio is a marker of impaired ventilation and is influenced by dead space fraction and carbon dioxide production (Sinha et al., 2019). It has been shown to correlate well with physiological dead space fraction (Sinha et al., 2019). A patient with healthy lungs would have a ventilatory ratio of approximately 1, however in COPD the ratio would be expected to be considerably higher due to the presence of increased physiological dead space. Ventilatory ratio is calculated using equation 4.12 (Sinha et al., 2019).

$$VR = V_{E\ measured} * PaCO_{2\ measured} / V_{E\ predicted} * PaCO_{2\ predicted} \quad [Eq\ 4.12]$$

where,

$V_{E\ predicted}$ = predicted body weight*100mL/kg/min

Predicted body weight = 45.5 + 0.91(height – 152.4) [female]

Predicted body weight = 50 + 0.91(height – 152.4) [male]

Equation 4.12: Ventilatory ratio (VR) (ARDSNET, 2000; Sinha et al., 2019). $V_{E\ measured}$ is the measured minute ventilation (L/min), $PaCO_{2\ measured}$ is the measured arterial partial pressure of carbon dioxide (kPa), $V_{E\ predicted}$ is the predicted minute ventilation (L/min), $PaCO_{2\ predicted}$ is the predicted normal partial pressure of carbon dioxide (5kPa) and height (cm).

4.2.1.4.7 Calculation of muscular effort

As discussed above, the pressure generated by the muscles of respiration needs to overcome the static recoil pressure of the chest wall and generate a pleural pressure to allow flow. P_{MUS} is equal to the elastic recoil pressure of the chest wall and the change in pleural or oesophageal pressure (equation 4.13).

$$P_{MUS} = P_{CW} + P_{ES} \quad [Eq\ 4.13]$$

Equation 4.13: Calculation of the total pressure generated by the muscles of respiration. P_{MUS} is the pressure generated by the muscles of respiration, P_{CW} is the elastic recoil of the chest wall and δP_{ES} is the change in oesophageal pressure.

The elastic recoil pressure of the chest wall is in turn calculated using the theoretical chest wall compliance (equation 4.14).

$$P_{CW} = V_{(t)}/C_{CW} \quad \text{[Eq 4.14]}$$

where,

$$C_{CW} = VC_{TH}*0.04$$

where,

$$VC_{TH} = \text{height} \times (21.78 - 0.101 \times \text{age})/1000 \text{ [female]}$$

$$VC_{TH} = \text{height} \times (27.63 - 0.112 \times \text{age})/1000 \text{ [male]}$$

Equation 4.14: Calculation of the elastic recoil of the chest wall. P_{CW} is the elastic recoil of the chest wall (cmH_2O), $V_{(t)}$ breath volume at time t (L), C_{CW} is the compliance of the chest wall (L/cmH_2O), VC_{TH} is the theoretical vital capacity (L), with height (cm) and age (years). There are separate calculations for males and females (Baldwin et al., 1948).

4.2.2 Methods

4.2.2.1 Contraindications

Oesophageal pressure monitoring was contraindicated where there is a lack of consent and in the presence of nasal or oesophageal pathology which precluded naso-oesophageal intubation (Akoumianaki et al., 2014; Benditt, 2005; Brochard, 2014; Sahetya & Brower, 2016).

4.2.2.2 Equipment

The oesophageal balloon catheter used was a 5Fr latex free catheter with balloon and polytetrafluoroethylene coated stillette (Cooper Surgical, Conneticut, USA). All signals were collected on a personal computer through a 12-bit analog-to-digital converter (National Instrument DAQCard 700, Austin, Texas) at a sampling frequency of 200 Hz (ICU-lab, KleisTEK Engineering, Bari, Italy). Flows, airway pressures and volumes were measured using a heated differential pneumotachograph (Hans Rudolph, Shawnee, Kansas) connected in line with the non-invasive ventilator with a

heat and moisture exchange bacterial/viral filter in the circuit to protect the patient. Data were analysed using ICU-Lab software.

4.2.2.3 Data collection

The following steps were undertaken:

- Consent was obtained.
- Topical anaesthetic (10% lignocaine spray) was offered to the patient.
- The catheter was placed transnasally into the oesophagus to a depth of at least 45 cm.
- Once the catheter was in place, the stillette was removed and the y-connector on the balloon was also removed.
- The transducer, LFE filter and laptop were turned on and the transducer was connected to the laptop.
- The pneumotachograph and port for the oesophageal balloon were connected to the transducer to allow calibration prior to connecting to the patient.
- Kleistek recorder was opened and the acquired channel setup opened.
- The channels were individually calibrated.
- The pneumotachograph was placed distal to the y-connector of the NIV circuit.
- The balloon catheter was connected to the transducer and 0.5-1mL of air was instilled into the balloon.
- The catheter was then repositioned to ensure that there was an oesophageal trace which became negative during inspiration and cardiac oscillations were present.
- In setup the file was recorded as COPD(patient number)OP(day)
- An inspiratory occlusion manoeuvre was then performed using an expiratory hold and asking the patient to take 3 maximal breaths and the traces were saved.
- The recorder was closed and the analyser opened.

- Following selection of the file, and auto-scaling of the traces, a breath taken during the maximal inspiratory effort was selected.
- Calibration was performed as described in section 4.2.2.4
- Once position was deemed adequate, 5 minutes of data was recorded. Data was recorded concurrently with electrical impedance tomography and parasternal electromyography.

4.2.2.4 Calibration of the oesophageal pressure position

Oesophageal pressure measurements require the passage of a catheter with a balloon trans-nasally into the lower oesophagus (Akoumianaki et al., 2014; Benditt, 2005; Brochard, 2014; Sahetya & Brower, 2016). Once in place, the balloon has 0.5-1.5 mL of air – based on the compliance characteristics of each balloon - instilled to allow optimal transmission of the pressure waveform. It is important to validate the position of the balloon using the dynamic occlusion test in the spontaneously breathing patient (figure 4.3) (Akoumianaki et al., 2014; Baydur et al., 1982; Benditt, 2005; Brochard, 2014; Sahetya & Brower, 2016). In this test, the patient breathes in against a closed inspiratory valve resulting in no airflow, and the ratio of the change in oesophageal pressure to change in airway pressure is assessed. A ratio approaching 1 (0.8-1.2) is considered to indicate appropriate placement (Baydur et al., 1982). The sequence of measurements are as follows:

- For the oesophageal pressure trace, the peak to trough difference was calculated (ΔP_{ES})
- For the airway pressure trace, the peak to trough difference was calculated (ΔP_{AW})
- The ratio $\Delta P_{ES}/\Delta P_{AW}$ was then calculated, if the ratio was 0.8-1.2, readings commenced, if not, then the catheter was repositioned, and the occlusion test was repeated.

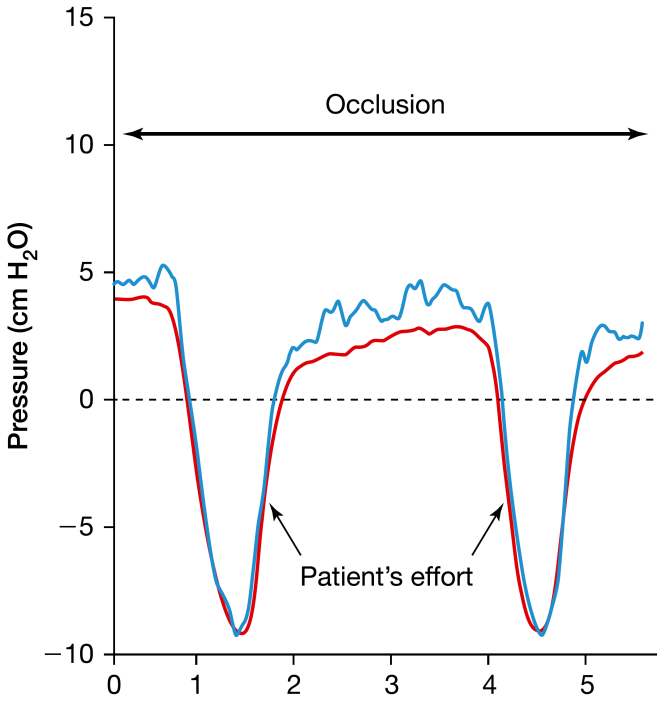

Figure 4.3: Occlusion test in a spontaneously breathing patient (Akoumianaki et al., 2014). Red is airway pressure, blue is oesophageal.

4.2.2.5 Data analysis

The data was analysed using automated proprietary software (ICU-lab, KleisTEK Engineering, Bari, Italy). The following data was measured:

- Time
    - start of inspiratory effort
    - start of expiratory effort
    - start of inspiratory flow
    - start of expiratory flow
- Volumes
    - inspiratory
    - expiratory
    - minute ventilation
- Respiratory rate
- Flow

    - peak inspiratory
    - mean inspiratory
    - peak expiratory flow
- Pressure
    - PEEP (total)
    - PEEP (intrinsic)
    - peak inspiratory airway pressure
    - mean airway pressure
    - oesophageal pressure

Calculated variables were:

- Elastance of the respiratory system and total lung
- Resistance of the respiratory system and total lung
- Pressure time product – chest wall, intrinsic PEEP, elastic and resistive, expressed per breath, per minute and per litre
- Elastic recoil pressure of the chest wall (equation 4.7)
- Pressure due to the muscles of respiration (equation 4.13)
- Total lung stress (equation 4.10)
- Transpulmonary pressure (equation 4.4)
- Work of breathing expressed per minute, per breath and per litre (equation 4.9)
- Mechanical power (equation 4.11)
- Ventilatory ratio (equation 4.12)

4.2.2.6 Ethical approval

The trial protocol was approved by the Cambridge NHS Human Research Authority Research Ethics Committee (14/EE/0109).

4.2.2.7 Statistical analysis

Statistical analysis was performed using Prism 9.5.1 for Mac (GraphPad, San Diego, USA). All data is presented as median (inter-quartile range). Data was compared

within and between the two arms grouped at 0-23 hours, 24-48 hours and 49-120 hours from randomisation.

4.2.3 Results

4.2.3.1 Demographics

Patient characteristics at baseline and who underwent oesophageal pressure measurements are displayed in table 4.1. All patients had severe COPD. Patients in both groups were comparable, apart from baseline respiratory rate which was higher in the $ECCO_2R$ group.

	NIV (n=4/9)	$ECCO_2R$ (n=5/9)
Demographic data		
Age (years)	63 (61-69)	70 (64-71)
BMI (kg/m^2)	19.2 (19.1-20.1)	23.8 (23.8-24.7)
Sex (F)	2	4
FEV1 (L)	1.13 (0.54-1.66)	0.97 (0.7-1.24)
FEV1 (% predicted) (%)	2.91 (2.018-3.88)	1.95 (1.7-3.12)
FVC (L)	34.5 (18-55.8)	39 (39-39.8)
FVC (% predicted) (%)	90.5 (53.5-119.3)	79.9 (63-82)
FEV1/FVC	39.5 (29.3-48)	47 (44-49)
GOLD stage	3 (2-4)	3 (3-3)
Baseline observations		
Systolic Blood pressure (mmHg)	118 (113-126)	123 (112-140)
Respiratory rate (breaths/min)	22 (19-25)	32 (30-35)
SpO_2 (%)	91 (89-92)	91 (87-94)
Heart rate (beats/min)	106.5 (98-117)	109 (91-125)
Presenting arterial blood gas		
PaO_2 (kPa)	9.2 (8.7-9.7)	9.4 (7.1-9.4)
$PaCO_2$ (kPa)	9.8 (9.2-10.4)	9.8 (9.7-9.9)
pH	7.23 (7.23-7.24)	7.25 (7.24-7.25)
HCO_3 (mmol/L)	31.2 (30.3-31.5)	29.7 (29.7-30.6)
Initial NIV settings		
EPAP (cmH_2O)	5 (5-5)	6 (5.25-6)
IPAP (cmH_2O)	15 (14-16)	18 (17-20)
FiO_2 (%)	34 (27-45)	35 (30-39)
Arterial blood gas after 1 hour NIV		
PaO_2 (kPa)	8.7 (8.1-9.8)	9.4 (8.9-9.4)
$PaCO_2$ (kPa)	8.7 (8.2-9.3)	8.9 (8.5-8.9)
pH	7.27 (7.26-7.28)	7.29 (7.28-7.29)
HCO_3 (mmol/L)	30 (28.5-30.9)	27.7 (27.7-27.9)

Table 4.1: Baseline demographics who had oesophageal pressure measurements in the NIV and $ECCO_2R$ groups. GOLD stage defines the severity of COPD and range from 1 (least severe) to 4 (the most severe). EPAP is expiratory positive airway pressure; IPAP is inspiratory positive airway pressure. All results are expressed as median (IQR).

4.2.3.2 Intra-group oesophageal pressure changes over time

Within group comparisons over time are described in table 4.2 for the $ECCO_2R$ group and table 4.3 for the NIV group.

In the $ECCO_2R$ group, there are 5 patients in the 0-23 hour period, 4 in the 24-48 hour period and 3 with measurements in the 49-120 hour period. There are reductions in

intrinsic PEEP, δP_{ES} and transpulmonary pressure over time. Over the three time periods, although the PTP/breath and PTP/L both reduce, the PTP/minute does not change. Overall, there is limited change in the work of breathing per minute. The ventilatory ratio and CO_2 removal remain stable over the three time periods

In the NIV group, there are n=4 patients in the 0-23 hour period and n=2 in the 24-48 hour period. The minute ventilation, airway pressures, intrinsic PEEP, transpulmonary pressure, δP_{ES} and P_{MUS} all increased over time. The pressure time product, work of breathing and ventilatory ratios also increased between the first and second day.

	$ECCO_2R$ 0-23 hours	$ECCO_2R$ 24-48 hours	$ECCO_2R$ 49-120 hours
N	5	4	3
T_{INSP} (s)	0.94 (0.79-1.08)	0.92 (0.73-1.06)	0.93 (0.86-1.08)
T_{TOT} (s)	2.64 (2.28-3.45)	2.24 (1.89-2.59)	2.62 (2.19-3.7)
T_{INSP}/T_{TOT}	0.34 (0.3-0.41)	0.41 (0.35-0.45)	0.34 (0.3-0.43)
δV (L)	0.51 (0.44-0.59)	0.56 (0.38-0.64)	0.61 (0.53-0.69)
RR (bpm)	22.73 (17.43-26.32)	26.84 (23.22-31.79)	22.91 (16.25-27.47)
Minute ventilation (L/min)	12.24 (8.51-13.9)	15.33 (12.85-17.15)	13.33 (9.12-19.12)
$PaCO_2$ (kPa)	7.59 (6.4-8.38)	8.47 (4.66-8.66)	8.34 (4.86-8.65)
pH	7.37 (7.28-7.38)	7.35 (7.35-7.49)	7.37 (7.34-7.46)
CO_2 removal (mL/min)	90 (83-103)	94 (80-94)	97 (28-97)
E_L (cmH_2O/L)	10 (4.1-17)	8.7 (4.1-15.7)	8.2 (4.7-18.2)
E_{RS} (cmH_2O/L)	13.59 (10.89-15.68)	14.17 (7.44-18.8)	11.52 (7.7-13.57)
R_L ($cmH_2O/L/s$)	10.3 (8.4-12.4)	10.3 (6.3-14.9)	9.1 (5.2-17.7)
R_{RS} ($cmH_2O/L/s$)	6.65 (5.82-8.53)	7.8 (4.92-8.65)	6.83 (4.5-7.96)
$P_{AW\ peak}$ (cmH_2O)	10.45 (9.3-12.7)	9.19 (6.37-10.56)	9.16 (7.05-9.72)
$P_{AW\ mean}$ (cmH_2O)	7.39 (6.66-9.16)	6 (4.41-7.9)	7.14 (4.26-7.54)
PEEPi (cmH_2O)	2.42 (1.36-4.4)	1.57 (0.94-2.69)	1.07 (0.36-1.93)
δP_{ES} (cmH_2O)	8.99 (4.69-13.43)	5.44 (3.98-9.71)	6.2 (3.35-16.49)
TPP (cmH_2O)	17.7 (9.84-21.33)	10.6 (8.87-19.55)	11.36 (8.66-24.01)
P_{CW} (cmH_2O)	4.18 (3.73-5.32)	4.31 (3.89-4.73)	4.7 (4.16-5.38)
P_{MUS} (cmH_2O)	15.08 (8.96-18.34)	10.22 (8.27-14.31)	11.5 (9.18-21.16)
Total lung stress (cmH_2O)	23.1 (14.96-29.61)	12.63 (10.14-22.13)	13.52 (10.24-30.93)
PTP_{CW} ($cmH_2O.s$)	0.97 (0.76-1.39)	1.08 (0.72-1.46)	1.26 (1.01-1.59)
PTP_{PEEPi} ($cmH_2O.s$)	2.26 (1.18-4.6)	1.44 (0.85-2.33)	1.03 (0.32-1.84)
PTP_E ($cmH_2O.s$)	3.37 (1.2-4.89)	2.18 (0.92-3.14)	6.58 (5.31-7.63)
PTP_R ($cmH_2O.s$)	3.29 (0.55-4.82)	2.31 (1.65-3.84)	4.61 (0.4-6.26)
PTP/breath ($cmH_2O.s$)	8.27 (5.01-10.36)	5.58 (3.88-8.37)	5.73 (4.19-14.59)
PTP/min ($cmH_2O.s/min$)	155.77 (99.87-249.73)	123.89 (91.83-228.4)	159.77 (75.81-317.72)
PTP/L ($cmH_2O.s/L$)	16.58 (8.74-21.35)	10.02 (6.92-18.84)	8.77 (6.42-24.33)
WOB/breath (J/breath)	0.42 (0.25-0.65)	0.32 (0.21-0.56)	0.42 (0.24-0.96)
WOB/min (J/min)	8.03 (4.8-15.94)	7.73 (5.07-17.43)	12.09 (3.23-20.5)
WOB/L (J/L)	0.82 (0.47-1.26)	0.52 (0.39-1.03)	0.6 (0.37-1.57)
Mechanical power (J/min)	25.23 (10.9-63.37)	23.74 (16.03-40.96)	38.89 (8.91-73.26)
Ventilatory ratio	2.36 (1.96-2.93)	2.29 (1.98-4.95)	2.93 (2.53-3.42)

Table 4.2: Changes in oesophageal pressure over time ($ECCO_2R$ group). T_{INSP} is the time for inspiration, T_{TOT} is the total time for the respiratory

cycle, δV is tidal volume, RR is respiratory rate, E_L is elastance of the lung, E_{RS} is elastance of the respiratory system, R_L is resistance of the lung, R_{RS} is resistance of the respiratory system, δP_{ES} is change in oesophageal pressure, TPP is transpulmonary pressure, P_{CW} is pressure due to the chest wall, P_{MUS} is pressure due to muscular effort, PTP_{CW} is pressure time product of the chest wall, PTP_E is pressure time product elastance, PTP_R is pressure time product resistance, PTP/breath is the pressure time product per breath, PTP/min is the pressure time product per minute, PTP/L is the pressure time product per litre, WOB/breath is the work of breathing per breath, WOB/minute is the work of breathing per minute and WOB/L is the work of breathing per litre of minute ventilation.

	NIV 0-23 hours	NIV 24-48 hours
N	4	2
T_{INSP} (s)	0.98 (0.83-1.71)	0.99 (0.85-1.11)
T_{TOT} (s)	2.88 (2.6-3.33)	3.06 (2.23-4.02)
T_{INSP}/T_{TOT}	0.36 (0.3-0.55)	0.33 (0.26-0.41)
δV (L)	0.77 (0.63-0.9)	0.74 (0.78-1.07)
RR (bpm)	20.86 (18.06-23.11)	19.61 (14.96-26.95)
Minute ventilation (L/min)	15.54 (13.14-18.48)	14.45 (9.55-18.93)
$PaCO_2$ (kPa)	8.37 (7.44-8.37)	7.47 (6.41-7.47)
pH	7.34 (7.34-7.35)	7.45 (7.43-7.45)
CO_2 removal (mL/min)	N/A	N/A
E_L (cmH_2O/L)	5.4 (1.3-8.3)	4.7 (3.7-6)
E_{RS} (cmH_2O/L)	8.79 (6.53-11.36)	7.25 (4.87-9.31)
R_L (cmH_2O/L/s)	6.3 (5.6-9.7)	4.9 (4.1-6.1)
R_{RS} (cmH_2O/L/s)	5.8 (5.1-6.12)	3.76 (3.05-6.27)
$P_{AW\ peak}$ (cmH_2O)	8.8 (8.02-11.01)	15.06 (10.72-15.4)
$P_{AW\ mean}$ (cmH_2O)	6.22 (5.11-7.09)	10.75 (7.7-11.16)
PEEPi (cmH_2O)	0.75 (0.19-1.29)	2.23 (1.08-5.4)
δP_{ES} (cmH_2O)	2.33 (1.22-3.87)	13.5 (8.88-16.85)
TPP (cmH_2O)	8.97 (8.37-10.49)	23.14 (16.95-26.9)
P_{CW} (cmH_2O)	5.43 (4.55-6.57)	5.52 (3.79-7.1)
P_{MUS} (cmH_2O)	7.98 (6.1-10.24)	16.94 (14.74-22.75)
Total lung stress (cmH_2O)	11.58 (10.13-13.37)	27.65 (20.48-34.02)
PTP_{CW} (cmH_2O.s)	1.46 (1.01-2.2)	2.73 (1.65-4.71)
PTP_{PEEPi} (cmH_2O.s)	1.01 (0.16-2.26)	2.39 (1.39-5)
PTP_E (cmH_2O.s)	0.16 (0.05-0.5)	1.95 (1.27-2.71)
PTP_R (cmH_2O.s)	0.62 (0.25-1.11)	4.47 (2.95-7.59)
PTP/breath (cmH_2O.s)	3.26 (1.98-6.02)	11.94 (9.59-17.41)
PTP/min (cmH_2O.s/min)	64.83 (42.45-125.51)	232.53 (182.61-317.72)
PTP/L (cmH_2O.s/L)	4.81 (2.73-7.19)	9.38 (8.44-10.43)
WOB/breath (J/breath)	0.22 (0.13-0.41)	0.86 (0.54-1.24)
WOB/min (J/min)	4.38 (2.76-7.27)	15.52 (11.93-21.6)
WOB/L (J/L)	0.3 (0.2-0.42)	1.46 (0.89-1.74)
Mechanical power (J/min)	19.58 (13.52-26.52)	37.63 (25.65-52.11)
Ventilatory ratio	3.89 (3.21-4.71)	3.06 (2.28-3.73)

Table 4.3: Changes in oesophageal pressure over time (NIV group). T_{INSP} is the time for inspiration, T_{TOT} is the total time for the respiratory cycle, δV is tidal volume, RR is respiratory rate, E_L is

elastance of the lung, E_{RS} is elastance of the respiratory system, R_L is resistance of the lung, R_{RS} is resistance of the respiratory system, δP_{ES} is change in oesophageal pressure, TPP is transpulmonary pressure, P_{CW} is pressure due to the chest wall, P_{MUS} is pressure due to muscular effort, PTP_{CW} is pressure time product of the chest wall, PTP_E is pressure time product elastance, PTP_R is pressure time product resistance, PTP/breath is the pressure time product per breath, PTP/min is the pressure time product per minute, PTP/L is the pressure time product per litre, WOB/breath is the work of breathing per breath, WOB/minute is the work of breathing per minute and WOB/L is the work of breathing per litre of minute ventilation.

4.2.3.3 Inter-group oesophageal pressure results

The results for the comparison of the two groups at 0-23 hours is described in table 4.4 and figures 4.4 and 4.5. Comparison at the 24-48 hour period is described in table 4.5. The minute ventilation in the $ECCO_2R$ group was lower, with a lower $PaCO_2$ and ventilatory ratio. Pressures were higher in the $ECCO_2R$ group with P_{MUS}, TPP, δP_{ES}, total lung stress and intrinsic PEEP all higher. Measures of work of breathing and pressure time product per breath, per minute and per litre were all higher in the $ECCO_2R$ group than in the NIV group in the 0-23 hour period. Figure 4.4 demonstrates the simple linear regression for work of breathing compared with pressure-time product. The lines have a similar slope but have a different x-intercept. The $ECCO_2R$ group has an x-intercept of 25.1 $cmH_2O.s/min$ compared with the NIV group having an x-intercept of -1.6 $cmH_2O.s/min$. Figure 4.5 demonstrates graphically a selection of the changes seen between the two groups in the 0-23 hour period.

	NIV 0-23 hours	$ECCO_2R$ 0-23 hours
N	4	5
T_{INSP} (s)	0.98 (0.83-1.71)	0.94 (0.79-1.08)
T_{TOT} (s)	2.88 (2.6-3.33)	2.64 (2.28-3.45)
T_{INSP}/T_{TOT}	0.36 (0.3-0.55)	0.34 (0.3-0.41)
δV (L)	0.77 (0.63-0.9)	0.51 (0.44-0.59)
RR (bpm)	20.86 (18.06-23.11)	22.73 (17.43-26.32)
Minute ventilation (L/min)	15.54 (13.14-18.48)	12.24 (8.51-13.9)
$PaCO_2$ (kPa)	8.37 (7.44-8.37)	7.59 (6.4-8.38)
pH	7.34 (7.34-7.35)	7.37 (7.28-7.38)
CO_2 removal (mL/min)	N/A	90 (83-103)
E_L (cmH_2O/L)	5.4 (1.3-8.3)	10 (4.1-17)
E_{RS} (cmH_2O/L)	8.79 (6.53-11.36)	13.59 (10.89-15.68)
R_L ($cmH_2O/L/s$)	6.3 (5.6-9.7)	10.3 (8.4-12.4)
R_{RS} ($cmH_2O/L/s$)	5.8 (5.1-6.12)	6.65 (5.82-8.53)
$P_{AW\ peak}$ (cmH_2O)	8.8 (8.02-11.01)	10.45 (9.3-12.7)
$P_{AW\ mean}$ (cmH_2O)	6.22 (5.11-7.09)	7.39 (6.66-9.16)
PEEPi (cmH_2O)	0.75 (0.19-1.29)	2.42 (1.36-4.4)
δP_{ES} (cmH_2O)	2.33 (1.22-3.87)	8.99 (4.69-13.43)
TPP (cmH_2O)	8.97 (8.37-10.49)	17.7 (9.84-21.33)
P_{CW} (cmH_2O)	5.43 (4.55-6.57)	4.18 (3.73-5.32)
P_{MUS} (cmH_2O)	7.98 (6.1-10.24)	15.08 (8.96-18.34)
Total lung stress (cmH_2O)	11.58 (10.13-13.37)	23.1 (14.96-29.61)
PTP_{CW} ($cmH_2O.s$)	1.46 (1.01-2.2)	0.97 (0.76-1.39)
PTP_{PEEPi} ($cmH_2O.s$)	1.01 (0.16-2.26)	2.26 (1.18-4.6)
PTP_E ($cmH_2O.s$)	0.16 (0.05-0.5)	3.37 (1.2-4.89)
PTP_R ($cmH_2O.s$)	0.62 (0.25-1.11)	3.29 (0.55-4.82)
PTP/breath ($cmH_2O.s$)	3.26 (1.98-6.02)	8.27 (5.01-10.36)
PTP/min ($cmH_2O.s/min$)	64.83 (42.45-125.51)	155.77 (99.87-249.73)
PTP/L ($cmH_2O.s/L$)	4.81 (2.73-7.19)	16.58 (8.74-21.35)
WOB/breath (J/breath)	0.22 (0.13-0.41)	0.42 (0.25-0.65)
WOB/min (J/min)	4.38 (2.76-7.27)	8.03 (4.8-15.94)
WOB/L (J/L)	0.3 (0.2-0.42)	0.82 (0.47-1.26)
Mechanical power (J/min)	19.58 (13.52-26.52)	25.23 (10.9-63.37)
Ventilatory ratio	3.89 (3.21-4.71)	2.36 (1.96-2.93)

Table 4.4: Comparison of oesophageal pressure over time in the NIV and $ECCO_2R$ groups on day 1 (0-23 hours). T_{INSP} is the time for inspiration, T_{TOT} is the total time for the respiratory cycle, δV is tidal volume, RR is

respiratory rate, E_L is elastance of the lung, E_{RS} is elastance of the respiratory system, R_L is resistance of the lung, R_{RS} is resistance of the respiratory system, δP_{ES} is change in oesophageal pressure, TPP is transpulmonary pressure, P_{CW} is pressure due to the chest wall, P_{MUS} is pressure due to muscular effort, PTP_{CW} is pressure time product of the chest wall, PTP_E is pressure time product elastance, PTP_R is pressure time product resistance, PTP/breath is the pressure time product per breath, PTP/min is the pressure time product per minute, PTP/L is the pressure time product per litre, WOB/breath is the work of breathing per breath, WOB/minute is the work of breathing per minute and WOB/L is the work of breathing per litre of minute ventilation.

	NIV 24-48 hours	$ECCO_2R$ 24-48 hours
N	2	4
T_{INSP} (s)	0.99 (0.85-1.11)	0.92 (0.73-1.06)
T_{TOT} (s)	3.06 (2.23-4.02)	2.24 (1.89-2.59)
T_{INSP}/T_{TOT}	0.33 (0.26-0.41)	0.41 (0.35-0.45)
δV (L)	0.74 (0.78-1.07)	0.56 (0.38-0.64)
RR (bpm)	19.61 (14.96-26.95)	26.84 (23.22-31.79)
Minute ventilation (L/min)	14.45 (9.55-18.93)	15.33 (12.85-17.15)
$PaCO_2$ (kPa)	7.47 (6.41-7.47)	8.47 (4.66-8.66)
pH	7.45 (7.43-7.45)	7.35 (7.35-7.49)
CO_2 removal (mL/min)		94 (80-94)
E_L (cmH_2O/L)	4.7 (3.7-6)	8.7 (4.1-15.7)
E_{RS} (cmH_2O/L)	7.25 (4.87-9.31)	14.17 (7.44-18.8)
R_L (cmH_2O/L/s)	4.9 (4.1-6.1)	10.3 (6.3-14.9)
R_{RS} (cmH_2O/L/s)	3.76 (3.05-6.27)	7.8 (4.92-8.65)
$P_{AW\ peak}$ (cmH_2O)	15.06 (10.72-15.4)	9.19 (6.37-10.56)
$P_{AW\ mean}$ (cmH_2O)	10.75 (7.7-11.16)	6 (4.41-7.9)
PEEPi (cmH_2O)	2.23 (1.08-5.4)	1.57 (0.94-2.69)
δP_{ES} (cmH_2O)	13.5 (8.88-16.85)	5.44 (3.98-9.71)
TPP (cmH_2O)	23.14 (16.95-26.9)	10.6 (8.87-19.55)
P_{CW} (cmH_2O)	5.52 (3.79-7.1)	4.31 (3.89-4.73)
P_{MUS} (cmH_2O)	16.94 (14.74-22.75)	10.22 (8.27-14.31)
Total lung stress (cmH_2O)	27.65 (20.48-34.02)	12.63 (10.14-22.13)
PTP_{CW} (cmH_2O.s)	2.73 (1.65-4.71)	1.08 (0.72-1.46)
PTP_{PEEPi} (cmH_2O.s)	2.39 (1.39-5)	1.44 (0.85-2.33)
PTP_E (cmH_2O.s)	1.95 (1.27-2.71)	2.18 (0.92-3.14)
PTP_R (cmH_2O.s)	4.47 (2.95-7.59)	2.31 (1.65-3.84)
PTP/breath (cmH_2O.s)	11.94 (9.59-17.41)	5.58 (3.88-8.37)
PTP/min (cmH_2O.s/min)	232.53 (182.61-317.72)	123.89 (91.83-228.4)
PTP/L (cmH_2O.s/L)	9.38 (8.44-10.43)	10.02 (6.92-18.84)
WOB/breath (J/breath)	0.86 (0.54-1.24)	0.32 (0.21-0.56)
WOB/min (J/min)	15.52 (11.93-21.6)	7.73 (5.07-17.43)
WOB/L (J/L)	1.46 (0.89-1.74)	0.52 (0.39-1.03)
Mechanical power (J/min)	37.63 (25.65-52.11)	23.74 (16.03-40.96)
Ventilatory ratio	3.06 (2.28-3.73)	2.29 (1.98-4.95)

Table 4.5: Comparison of oesophageal pressure over time in the NIV and $ECCO_2R$ groups on day 2 (24-48 hours). T_{INSP} is the time for inspiration, T_{TOT} is the total time for the respiratory cycle, δV is tidal volume, RR is

respiratory rate, E_L is elastance of the lung, E_{RS} is elastance of the respiratory system, R_L is resistance of the lung, R_{RS} is resistance of the respiratory system, δP_{ES} is change in oesophageal pressure, TPP is transpulmonary pressure, P_{CW} is pressure due to the chest wall, P_{MUS} is pressure due to muscular effort, PTP_{CW} is pressure time product of the chest wall, PTP_E is pressure time product elastance, PTP_R is pressure time product resistance, PTP/breath is the pressure time product per breath, PTP/min is the pressure time product per minute, PTP/L is the pressure time product per litre, WOB/breath is the work of breathing per breath, WOB/minute is the work of breathing per minute and WOB/L is the work of breathing per litre of minute ventilation.

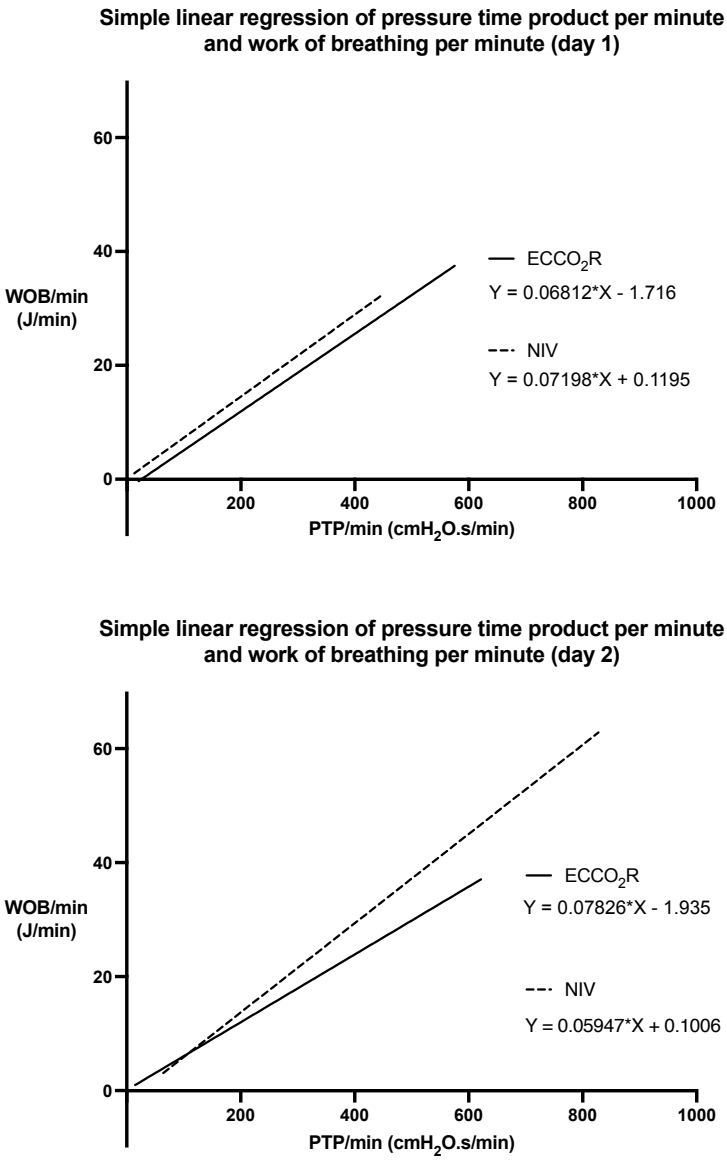

Figure 4.4: Linear regression of the pressure time product per minute and work of breathing per minute for the NIV and $ECCO_2R$ groups on day 1 and day 2.

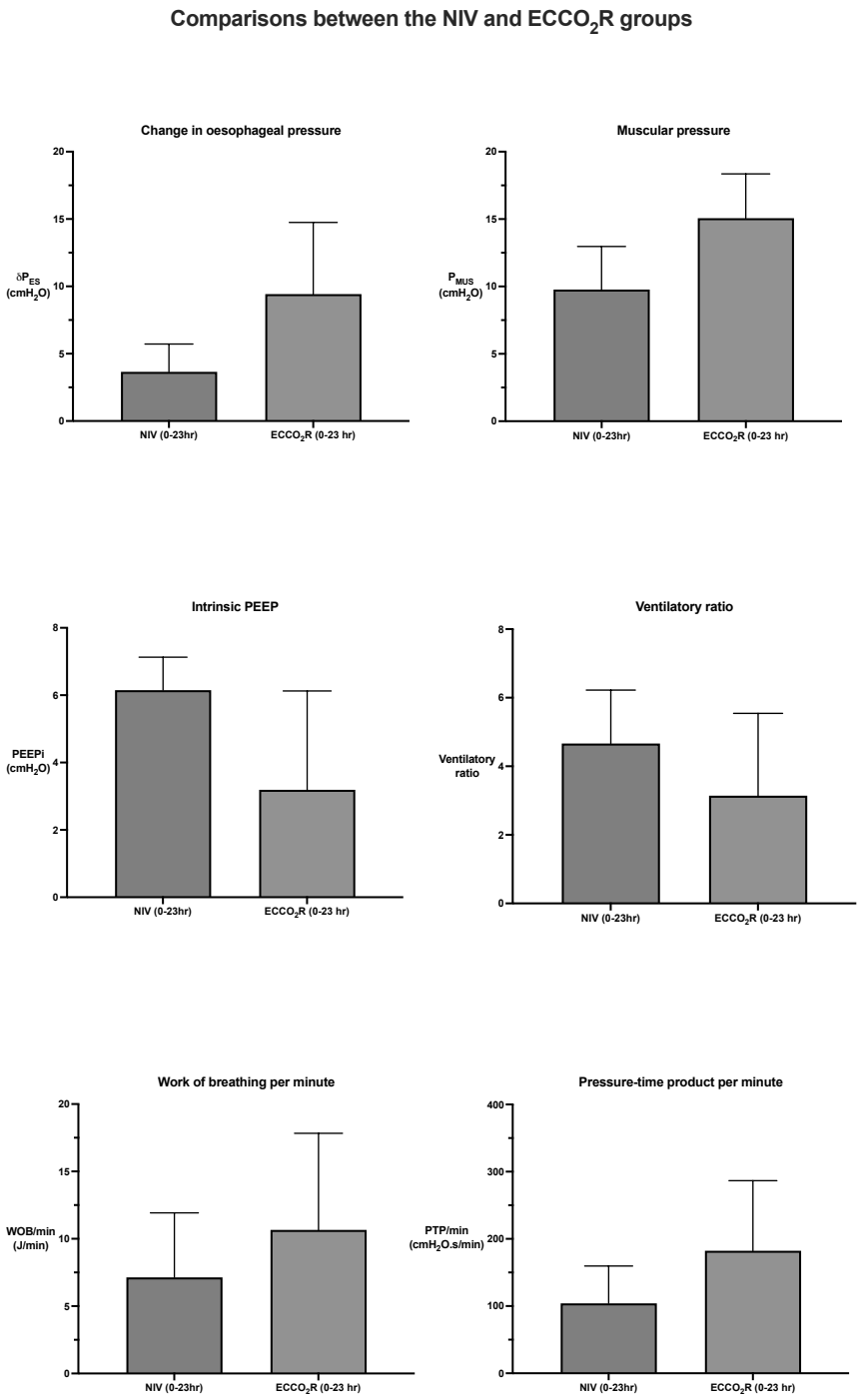

Figure 4.5: Comparisons between the NIV and $ECCO_2R$ groups in the 0-23 hour period.

4.2.3.4 $ECCO_2R$ combined with NIV compared with $ECCO_2R$ alone

In two patients, data was measured after commencement of $ECCO_2R$, on and off NIV (table 4.5 and figure 4.6). The elastance and resistance of both the lung and respiratory system increased. The intrinsic PEEP decreased but δP_{ES}, transpulmonary pressure, P_{MUS} and total lung stress all increased following the removal of NIV. PTP per breath, per minute and per litre all increased as did work of breathing. Figure 4.6 demonstrates the simple linear regression for work of breathing compared with pressure-time product. The lines have a different slope, and a different x-intercept. The $ECCO_2R$ group has an x-intercept through the origin compared with the $ECCO_2R$ and NIV group having an x-intercept of 38.5 $cmH_2O.s/min$.

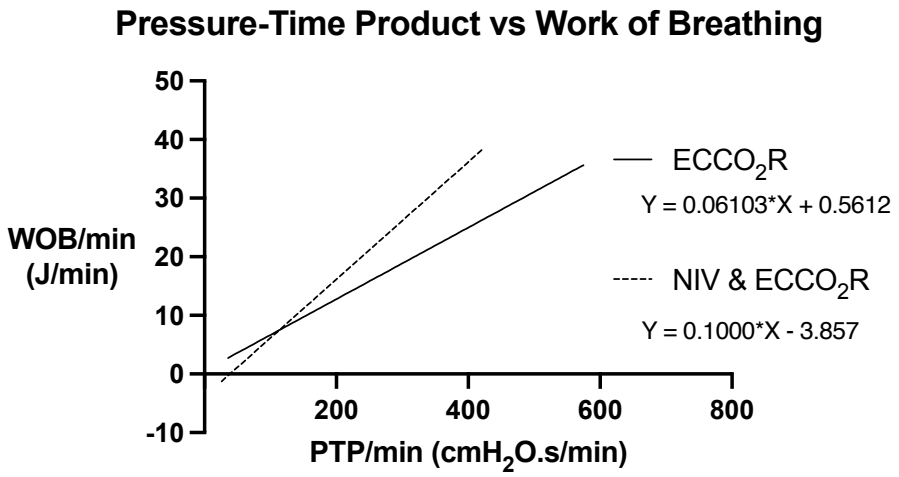

Figure 4.6: Linear regression of the pressure time product per minute and work of breathing per minute for patients in the $ECCO_2R$ group whilst the patients were still on NIV and after the removal of NIV.

	NIV & $ECCO_2R$	$ECCO_2R$
N	2	2
T_{INSP} (s)	0.88 (0.74-1)	1.03 (0.81-1.08)
T_{TOT} (s)	2.51 (2.22-3.09)	2.84 (2.34-3.54)
T_{INSP}/T_{TOT}	0.38 (0.3-0.41)	0.34 (0.28-0.42)
δV (L)	0.6 (0.52-0.64)	0.57 (0.46-0.73)
RR (bpm)	23.91 (19.44-27.03)	21.13 (16.98-25.7)
Minute ventilation (L/min)	13.5 (12-15.3)	11.9 (9.1-15.2)
$PaCO_2$ (kPa)	8.34 (8.34-9.09)	8.83 (8.59-8.83)
pH	7.34 (7.31-7.34)	7.31 (7.31-7.34)
CO_2 removal (mL/min)	N/A	119 (103-119)
E_L (cmH_2O/L)	4.8 (3.4-8.2)	7.7 (5.1-12)
E_{RS} (cmH_2O/L)	13.54 (11.24-16.26)	17.65 (13.74-22.49)
R_L (cmH_2O/L/s)	7.5 (7-9.9)	13.1 (11.9-14.2)
R_{RS} (cmH_2O/L/s)	5.91 (5.65-7)	8.91 (8.17-9.66)
$P_{AW\ peak}$ (cmH_2O)	9.72 (9.56-13.54)	12.48 (11.94-13.17)
$P_{AW\ mean}$ (cmH_2O)	7.52 (7.27-9.46)	8.59 (7.32-10.01)
PEEPi (cmH_2O)	3.92 (3.25-4.71)	2.81 (1.55-5.01)
δP_{ES} (cmH_2O)	6.6 (5.25-9.13)	10.61 (9.35-12.44)
TPP (cmH_2O)	13.31 (11.64-19.57)	20.44 (19.17-22.33)
P_{CW} (cmH_2O)	6.55 (5.77-6.98)	6.34 (5.03-8.14)
P_{MUS} (cmH_2O)	13.37 (11.37-15.89)	17.63 (16.1-19.2)
Total lung stress (cmH_2O)	14.36 (12.55-21.26)	22.64 (20.95-24.55)
PTP_{CW} (cmH_2O.s)	1.04 (0.82-1.24)	1.15 (0.71-1.79)
PTP_{PEEPi} (cmH_2O.s)	3.13 (2.49-3.81)	2.8 (1.68-4.44)
PTP_E (cmH_2O.s)	0.39 (0.33-0.55)	0.96 (0.56-1.67)
PTP_R (cmH_2O.s)	2.32 (1.34-2.94)	5.41 (4.56-5.97)
PTP/breath (cmH_2O.s)	5.64 (4.45-6.31)	8.83 (7.24-10.07)
PTP/min (cmH_2O.s/min)	123.24 (103-152.63)	186.88 (140.58-226.38)
PTP/L (cmH_2O.s/L)	9.56 (8.23-10.53)	15.7 (10.15-20.18)
WOB/min (J/min)	7.43 (6.08-10.19)	11.11 (8.11-15.15)
WOB/breath (J/breath)	0.35 (0.27-0.5)	0.54 (0.41-0.63)
WOB/L (J/L)	0.6 (0.47-0.81)	0.87 (0.76-1.03)
Mechanical power (J/min)	15.8 (13.45-22.34)	21.67 (13.67-31.84)
Ventilatory ratio	5.1 (4.53-5.98)	4.85 (3.54-6.87)

Table 4.6: Oesophageal pressure with the combination of NIV and $ECCO_2R$ and $ECCO_2R$ alone. T_{INSP} is the time for inspiration, T_{TOT} is the total time for the respiratory cycle, δV is tidal volume, RR is respiratory rate, E_L is

elastance of the lung, E_{RS} is elastance of the respiratory system, R_L is resistance of the lung, R_{RS} is resistance of the respiratory system, δP_{ES} is change in oesophageal pressure, TPP is transpulmonary pressure, P_{CW} is pressure due to the chest wall, P_{MUS} is pressure due to muscular effort, PTP_{CW} is pressure time product of the chest wall, PTP_E is pressure time product elastance, PTP_R is pressure time product resistance, PTP/breath is the pressure time product per breath, PTP/min is the pressure time product per minute, PTP/L is the pressure time product per litre, WOB/breath is the work of breathing per breath, WOB/min is the work of breathing per minute and WOB/L is the work of breathing per litre of minute ventilation.

4.2.4 Discussion

Oesophageal pressure measurements were obtained in approximately half of each group (4/9 in the NIV group and 5/9 in the $ECCO_2R$ group). Aside from the baseline difference in respiratory rate ($ECCO_2R$ 32 (30-35) bpm, vs NIV 22 (19-25) bpm), the groups were well matched.

4.2.4.1 NIV over time

The NIV group had lower P_{MUS}, transpulmonary pressure, lung stress and δP_{ES} on day 1 when compared with day 2 (table 4.3). On day 1 the median δP_{ES} in the NIV group was 2.4 cmH_2O, whilst on day 2 it was 13.5cmH_2O, similarly, the mean transpulmonary pressure rose from 9 to 23.2 cmH_2O, and the median P_{MUS} from 8 to 17 cmH_2O with median lung stress increasing from 11.6 to 27.7 cmH_2O. The literature describing δP_{ES} for patients with AECOPD receiving NIV describes findings more in keeping with the data measured on day 2 of NIV treatment. In a study of patients with AECOPD receiving non-invasive CPAP, (i.e., without pressure support), Goldberg and colleagues (1997) reported that the baseline δP_{ES} in unsupported patients was around 20 cmH_2O and this reduced to 15 cmH_2O with the commencement of CPAP (Goldberg et al., 1995). NIV administration in patients with AECOPD, has been shown to reduce δP_{ES} by half, from around 20 cmH_2O to 10 cmH_2O (Girault et al., 1997; Wysocki et al., 2002). A more recent study in patients with AECOPD on NIV explored

the changes in δP_{ES} over time and in variable body positions - supine or sitting upright (Steriade et al., 2022). The authors reported that the change between day 1 and day 3 was a reduction in δP_{ES} (upright) from a median of 17 to 13 cmH_2O and that the change in δP_{ES} moving from supine to upright was from 17.7 to 12 cmH_2O on day 3, suggesting that an increase in FRC reduces δP_{ES}. All the patients in the current study were studied in a semi-recumbent position of comfort and although this was not measured precisely will have been approximately 30-45 degrees. No patients had oesophageal pressure measurements taken either supine or fully upright.

Consistent with the pressure changes, the work of breathing and PTP rose between the first and second day. The work of breathing per minute increased from a median of 4.4J/min to a median of 15.6J/min, and PTP per minute increased from a median of 64.9 to a median of 232.6 cmH_2O.s/min between day 1 and day 2. Similar to δP_{ES}, the results reported in the literature for work of breathing and PTP in patients with AECOPD are more consistent with the results found on day 2 than day 1. One study on the use of NIV in AECOPD reported a work of breathing per minute 35 J/min with a PTP of 260cmH_2O.s/min in the NIV group (Wysocki et al., 2002). Another study demonstrated that the baseline work of breathing reduced from 17 J/min to 9.8 J/min with the application of NIV in AECOPD (Girault et al., 1997).

The literature suggests that the data obtained on day 2 is more consistent with reports of patients with exacerbations of COPD receiving NIV than the data from day 1. The pressures, work of breathing and PTP on day 1 are consistent with the findings from a healthy patient without respiratory failure or underlying lung pathology (Banner et al., 1994). In studies including patients with AECOPD who were intubated and passively ventilated on a fully supported mandatory mode, work of breathing was measured at 0.2J/breath (Sassoon et al., 1994). When the same patients started breathing spontaneously on pressure supported ventilation, the reported work of breathing was 4-5 times higher (0.8-1J/breath). Similarly, in a study comparing the relative impacts of assist control ventilation (with a mandatory rate and volume) and spontaneous ventilation with pressure support, the δP_{ES} was 9.8 cmH_2O and the work of breathing was 9.4J/min with pressure support, whilst in the assist control group, both δP_{ES} and the work of breathing were lower at 6 cmH_2O and 6.95 J/min

respectively (Girault et al., 1997). In a recent study exploring assisted ventilation in an invasively mechanically ventilated population which included patients with COPD, as the proportional assistance increased, progressively lower work of breathing, PTP and δP_{ES} were reported (Su et al., 2016).

Hence the data on day 1 in the NIV group is consistent with a low work of breathing despite refractory hypercapnic respiratory acidosis being present. One possible interpretation of this findings in is that patients were effectively mandatorily ventilated, and that the NIV was able to support their entire mechanical load and satisfy their drive.

Another possible interpretation for the low measured work of breathing on day 1 and the paradoxical increase in PTP, work of breathing, P_{MUS}, TPP and δP_{ES} on day 2 is that the patients were effectively ventilating close to their total lung capacity and were unable to generate additional pressure (Tobin et al., 2009). Patients in this study had either severe or very severe COPD by FEV_1 criteria (median predictedFEV_1 38% (21-45%)) (Halpin et al., 2021). Patients also had severe exacerbations with a median pH of 7.27 due to persistent respiratory acidosis after an hour of NIV (table 3.1) and are at risk of failure of NIV (Osadnik et al., 2017; Pejkovska et al., 2015). It is therefore surprising that the work of breathing was low on day 1. Hyperinflation can reduce force generation due to muscle shortening and diaphragmatic flattening and worsen the underlying diaphragmatic weakness seen in AECOPD (Clanton & Levine, 2009; De Troyer & Wilson, 2009; Newell et al., 1989; Tobin et al., 2009). Furthermore, a change in position from supine to upright increases FRC and simultaneously reduces δP_{ES} (Steriade et al., 2022). It is possible therefore that the lower P_{MUS}, TPP and δP_{ES} and associated work of breathing and PTP seen on day 1 represents respiratory muscle contractile fatigue. This is in keeping with the ongoing respiratory acidosis and the ventilatory ratio which suggests that physiological dead space is more than 75% (Maj et al., 2023). The measured intrinsic PEEP is low on the first day in the NIV group which is in keeping with the suggestion that patients are hyper-expanded and this would splint airway open and overcome the loss of radial traction of airways in COPD (Kallet & Diaz, 2009). During spontaneous breathing the intrinsic PEEP is the oesophageal pressure generated from the onset of muscular contraction to the point

of the commencement of flow. Consequently, measurement of intrinsic PEEP requires effort and will be underestimated if respiratory muscle fatigue is severe (Blanch et al., 2005).

4.2.4.2 $ECCO_2R$ over time

Oesophageal pressure measurements of were taken in the $ECCO_2R$ group over a period of up to 5 days (table 4.2). Over this period, there was a relatively stable minute ventilation, respiratory rate and pH. Extracorporeal CO_2 removal also remained constant throughout the study period for patients in whom oesophageal pressure was measured. Elastance and resistance of the respiratory system and lung also remained static. Over time, there was a reduction in intrinsic PEEP, transpulmonary pressure, P_{MUS}, δP_{ES} and total lung stress. The PTP/min remained stable, while PTP/breath and PTP/L reduced. The WOB/breath was overall constant, while the WOB per minute and WOB/L both increased on day 3-5 compared with day 1 due an increase in tidal volume. The ventilatory ratio – a proxy measure of dead-space ventilation - also increased over time. In a study of patients with AECOPD on invasive mechanical ventilation, the work of breathing was measured in five patients during a spontaneous breathing trial after the addition of $ECCO_2R$ (Diehl, Piquilloud, et al., 2020). In these patients work of breathing on $ECCO_2R$ was 0.59J/breath or 11.7 J/min, similar to the $ECCO_2R$ cohort in the current study. The CO_2 removal the study by Diehl and colleagues was 85mL/minute which is similar to the current study (90-100mL/minute) (Diehl, Piquilloud, et al., 2020). In a smaller study of two patients by the same group, the work of breathing per minute after the commencement of $ECCO_2R$ of one patient was approximately 14 J/min and in the other 2J/min (Diehl et al., 2016). Pisani and colleagues (2015) also explored $ECCO_2R$ in invasively mechanically ventilated patients AECOPD who had failed extubation (Pisani et al., 2015). In keeping with the present study, the authors found that there was an average of 78mL/minute of CO_2 removed. With $ECCO_2R$ the PTP per minute was between 80 and 199 $cmH_2O.s/min$, whilst work of breathing was between 5.2 and 8.4J/min. These results are in keeping with the PTP and work of breathing in the $ECCO_2R$ group in the current study. The work of breathing in the $ECCO_2R$ group is also consistent with or lower than that reported in studies of NIV alone (Girault et al.,

1997; Goldberg et al., 1995; Wysocki et al., 2002). The changes seen in work of breathing and δP_{ES} over time are consistent with the changes reported in the literature (Steriade et al., 2022). The improvement over time in the P_{MUS}, TPP and δP_{ES} can be interpreted as the gradual improvement in the exacerbation and this is consistent with the changes over time seen in the broader literature (Girault et al., 1997; Goldberg et al., 1995; Steriade et al., 2022; Wysocki et al., 2002). The lack of a consistent change in work of breathing and PTP may reflect the impact of $ECCO_2R$ – despite the elevated muscular and pleural pressures, the work of breathing is not as high as the literature would suggest, supporting a potential role for $ECCO_2R$ in reducing the chemical afferent effect on work of breathing.

4.2.4.3 NIV compared with $ECCO_2R$ over time

The comparison between NIV and $ECCO_2R$ are markedly different on day 1 and day 2 (table 4.4, 4.5, figure 4.5). On day 1, the comparison reveals a lower minute ventilation for the $ECCO_2R$ group but higher indices of muscular effort as well as higher PTP and work of breathing. On day 2 the situation is reversed with lower indices of muscular effort as well as lower PTP and work of breathing in the $ECCO_2R$ group. The groups also differed in their relationship between PTP and work of breathing. On day 1, in the $ECCO_2R$ group the PTP was 25 $cmH_2O.s$ when the work of breathing was 0 cmH_2O whilst for NIV the line passed through the origin. On day 2 the opposite is the case (figure 4.6).

Given the discussion above, these results support the hypothesis that the NIV results on day 1 reflect the limited muscular power that can be generated with significant hyperinflation and due to the lower changes in pressure, the measured PTP and work of breathing are lower (Clanton & Levine, 2009; De Troyer & Wilson, 2009; Newell et al., 1989; Tobin et al., 2009). Hence it is possible that in the $ECCO_2R$ group, removing CO_2 reduced minute ventilation, which in turn reduced dynamic hyperinflation and consequently allowed a higher PTP and respiratory work because of the greater pressure which could be generated. By day 2 the NIV group had a higher measured work of breathing, PTP and pressures (TPP, δP_{ES} and P_{MUS}) than the $ECCO_2R$ group. This changes in the NIV group despite their clinical improvement, may suggest that with the improvement of the COPD exacerbation over time, that dynamic

hyperinflation reduced, and the patients were able to generate changes in pressure and therefore increases in measured work of breathing and PTP. On day 2 in the $ECCO_2R$ group the lower work of breathing, PTP and pressures (TPP, δP_{ES} and P_{MUS}) suggests that the support provided by the removal of CO_2, with associated reductions in minute ventilation provides physiological benefits for patients.

The total lung stress and mechanical power also differ between the groups on different days. On day 1, the total lung stress was lower in the NIV group than the $ECCO_2R$ group (a median of 11.58 vs 23.1 cmH_2O), whilst on day 2 the opposite is found (a median of 27.65 vs 12.63 cmH_2O). This is in keeping the lower P_{MUS} and δP_{ES} on day 1 in the NIV group and day 2 in the $ECCO_2R$ group. The higher values of lung stress are consistent with that seen in patients with COPD who require mechanical ventilation (Blankman et al., 2016) however the total lung stress and δP_{ES} are higher than that seen in patients with COVID-related ARDS who failed NIV and progressed to invasive mechanical ventilation (Coppola et al., 2021). The prognostic significance of lung stress in the COPD population on NIV has not been reported.

The mechanical power is not different between day 1 NIV and $ECCO_2R$ but is higher in the NIV group on day 2 compared with both day 1 NIV and the $ECCO_2R$ group on day 2. In the present study, the range of mechanical power was substantial, with an upper quartile in the NIV group on day 2 of 52 J/min and elevated compared with patients with ARDS (Gattarello et al., 2023; Gattinoni et al., 2023; Gattinoni et al., 2016). Mechanical power describes the impact of airway pressures, tidal volume and respiratory rate, with higher values associated with injurious mechanical ventilation (Gattinoni et al., 2023; Gattinoni et al., 2016). The relevance of mechanical power in patients with COPD on NIV is unknown however in COVID-related ARDS higher mechanical power on NIV was associated with worse outcomes (Gattarello et al., 2023).

4.2.4.4 NIV and $ECCO_2R$ compared with $ECCO_2R$ alone

In a subset of patients (2/9) oesophageal pressure was able to be recorded after the commencement of $ECCO_2R$ but before NIV was removed and then subsequently, 4 hours later, the oesophageal pressure was re-measured to explore the relatively acute impact of the removal of NIV and the continuation of $ECCO_2R$ (table 4.6 and figure 4.6). With the removal of NIV, there is an increase in work of breathing, PTP and all measures of muscular effort (TPP, δP_{ES}, P_{MUS} and total lung stress). The work of breathing, PTP and pressures in the NIV and $ECCO_2R$ group are higher than the median discussed in the NIV-alone group above and in the broader literature (Girault et al., 1997; Goldberg et al., 1995; Steriade et al., 2022; Wysocki et al., 2002). The results are however similar to the changes seen with the combination of ventilation and $ECCO_2R$ in the weaning phase of invasive mechanical ventilation in patients with AECOPD (Diehl et al., 2016; Diehl, Piquilloud, et al., 2020; Pisani et al., 2015). The results in the $ECCO_2R$ group are also similar to that seen in the NIV literature (Girault et al., 1997; Goldberg et al., 1995; Steriade et al., 2022; Wysocki et al., 2002). The intrinsic PEEP was lower in the $ECCO_2R$ group which indicates there was a lower inspiratory threshold to ventilation. This is consistent with the relationship between PTP and work of breathing (figure 4.6) where $ECCO_2R$ alone results in the work of breathing and PTP passing through the origin, whereas $ECCO_2R$ and NIV results in a PTP of 38cmH_2O.s/min whilst the work of breathing is 0.0 J/min. This implies that there is isometric contraction of the respiratory muscles required to overcome intrinsic PEEP present in patients on NIV at the onset of $ECCO_2R$ and that this intrinsic PEEP has reduced several hours later (Akoumianaki et al., 2014; Annat et al., 1990; Field et al., 1984; Tobin et al., 2012). The addition of $ECCO_2R$ is also associated with a decrease in respiratory rate and minute ventilation, which will have decreased dynamic hyperinflation and therefore intrinsic PEEP. Hence there is reduced isometric contraction (figure 4.6). This change may also be contributed to by the passage of time and improvement in the underlying disease.

The data comparing NIV and $ECCO_2R$ with $ECCO_2R$ implies that the addition of $ECCO_2R$ to NIV is superior to $ECCO_2R$ alone and that the impact of the two therapies is additive but that the reduction in minute ventilation with $ECCO_2R$ may have facilitated a

reduction in dynamic hyperinflation and closer correlation between work of breathing and PTP.

4.2.4.5 Ventilatory ratio

Ventilatory ratio is a marker of ventilatory efficiency that correlates with physiological dead space (Sinha et al., 2019). In patients with ARDS, higher ventilatory ratios correlates with an increasing severity of disease and with increasing mortality (Maj et al., 2023; Sinha et al., 2019). A ventilatory ratio of 3 correlates with a physiological dead space ratio of 0.75 and is substantial (Maj et al., 2023). In the present study the ventilatory ratio varied between the groups. In the $ECCO_2R$ group ventilatory ratio was lower than in the NIV group (a median of 2.3-2.4 ($ECCO_2R$) compared with a median of 3.9-6.3 (NIV)). Ventilatory ratio is impacted by work of breathing and CO_2 production as CO_2 production rises with increasing work (Akoumianaki et al., 2014; Brochard et al., 1989; Coast & Krause, 1993; Lewis et al., 1994; Robertson, Foster, et al., 1977; Robertson, Pagel, et al., 1977). The $ECCO_2R$ group had a lower minute ventilation and work of breathing on day 2 when compared with NIV. The interpretation of the lower ventilatory ratio is potentially more complex. These relationships are altered during $ECCO_2R$ where the VCO_2 of the native lung does not reflect the entire metabolically produced CO_2 (as a proportion, ~ 1/3 is removed extracorporeally) and therefore $PaCO_2$ is uncoupled from the relationship between VCO_2 and alveolar ventilation. Nonetheless reductions in ventilatory ratio have been correlated with patient benefit in studies of $ECCO_2R$ in ARDS and in studies of AECOPD using high flow oxygen (Alessandri et al., 2023; Dianti et al., 2023; Ding et al., 2021; Ghiani et al., 2020; Goligher et al., 2019; Kronibus et al., 2022; Piquilloud et al., 2022; Zheng, 2023). A secondary analysis of the REST trial in ARDS found that the benefits of $ECCO_2R$ appeared to outweigh harm when patients had a ventilatory ratio of over 3 (Dianti et al., 2023). Similar findings were present in a secondary analysis of the SUPERNOVA trial where higher dead space/higher ventilatory ratios and lower respiratory system compliance predicted patients who were more likely to achieve benefit from $ECCO_2R$ (Goligher et al., 2019). This relationship should be further explored in future trials of AECOPD with and without $ECCO_2R$.

4.2.4.6 Limitations

There are several limitations to this data. Firstly, there is a change in the sample size involved in the individual groups over time which potentially biases the comparisons – it is certainly possible that the patients remaining in the study were more severely ill and therefore had different work of breathing and pressure indices that those who were not remaining. The sample size on day 1 are comparable to the numbers of patients included in many of the studies included in the literature, however on subsequent days this is smaller. It is recognised that patients with AECOPD have a elevated expiratory work of breathing and this was not estimated in my analysis of data from the oesophageal pressure monitoring. The natural history of AECOPD is to improve with time. Given the low number of subjects and the baseline difference in respiratory rate, it is possible that the $ECCO_2R$ group were more unwell and will have taken more time to improve and this may have biased results. To measure pressure and flow, a pneumotachograph was required and this was managed through the NIV circuit. In the $ECCO_2R$ group patients were only on NIV for the time that it took to record the measurements. It is possible that this may have impacted the measurements by reducing the apparent work of breathing due to the addition of NIV or increasing the apparent work of breathing by adding a degree of psychological distress. Patient position was not controlled for, however patients were semi-recumbent, generally 30-60 degrees rather than upright or supine and it is unlikely that this contributed to systematic bias.

Device performance is also an important consideration. Studies have shown that device characteristics including membrane surface area and blood flow make a significant difference to CO_2 extraction (Karagiannidis et al., 2017). Other work has shown that this difference in CO_2 extraction is associated with patient benefit in trials of ultra-low tidal ventilation in ARDS (Goligher et al., 2019). In the present study, CO_2 removal was 90mL/minute, which is approximately 30-40% of the theoretical CO_2 production of ~3mL/kg/min. Actual CO_2 production may have been higher due to the metabolic impact of the exacerbation. However, from the data presented here the impact of removing this amount of CO_2 results in physiological improvements. It is not known whether the use of devices with greater CO_2 extraction capability would

provide greater physiological impact, though given the data from the ARDS trials (Goligher et al., 2019), this would seem a reasonable assumption.

4.2.4.7 Conclusion

NIV and $ECCO_2R$ have different impacts on the work of breathing, PTP and pressure indices during AECOPD. By removing CO_2, $ECCO_2R$ facilitated a reduction in minute ventilation which reduced dynamic hyperinflation and isometric work acting mainly on the chemical stimulation of respiratory work. Application of $ECCO_2R$ was associated with a lower work of breathing than NIV alone on day 2, however the combination of NIV and $ECCO_2R$ was associated with the lowest work of breathing, PTP, P_{MUS}, δP_{ES} and TPP. NIV facilitates improvement through positive pressure, directly aiding inspiration and allowing a change in the mechanics of breathing over time. The additive effect of NIV and $ECCO_2R$ is a novel finding and if further explored may help with identification of patients who would benefit from $ECCO_2R$ even if tolerant of NIV. On the contrary, in patients intolerant or with contraindication to NIV, $ECCO_2R$ devices with higher CO_2 clearance may be required to impact on work of breathing and inspiratory effort.

4.3 Electrical impedance tomography

4.3.1 Introduction

Electrical impedance is a measure of the resistance to the flow of alternating electric current through any material (Bayford, 2006; Bayford & Tizzard, 2012; Bodenstein et al., 2009; Brown, 2003). The electrical impedance of tissue varies with the tissue composition with different cell size, orientation, membrane structure and the extracellular space all having effects on a tissue's impedance (Gabriel et al., 1996). The electrical impedance of normal tissue is different from that of a tissue with abnormal cellular structure (Bayford & Tizzard, 2012), allowing the detection of structural tissue abnormalities (e.g., malignancy). Tissue impedance varies with the electrical frequency applied – at low frequencies the impedance of the extracellular space predominates whilst at higher frequencies the impedance of the intracellular space and cell membrane affects the overall impedance.

Lungs have a particularly high electrical impedance due to the presence of air (Bayford, 2006; Bodenstein et al., 2009; Brown, 2003). Changes in impedance during the respiratory cycle are due to both the change in resistance due to changes in the air content as well as changes in the length of the fibres of the pulmonary parenchyma. As the lung fibres stretch during inspiration, the resistance to the electrical current in the lung increases in directly proportion to fibre length (Bayford, 2006; Bayford & Tizzard, 2012; Yerworth et al., 2016). The variation in tidal impedance provides quantitative data on the inspiratory changes in lung volume as well as the regional distribution of air within the lung and allows the recording of physiological phenomena with high temporal and functional resolution (Bayford, 2006; Bayford & Tizzard, 2012; Yerworth et al., 2016). This technique is particularly suitable for the analysis phenomena seen in COPD such as: heterogeneity of regional inspiratory and expiratory time-constants; and the dynamic changes in end-expiratory lung volume (hyperinflation) and response to therapies. EIT provides semi-continuous, real-time information about the regional distribution of the changes in electrical resistivity of the lung tissue due to variations in ventilation or blood flow in relation to a reference state (Bayford, 2006; Bodenstein et al., 2009; Brown, 2003).

4.3.1.1 EIT acquisition

EIT is acquired by repeatedly injecting small alternating electric currents (usually 5 mA) at high frequency of 50 – 80 kHz through a system of 16 skin electrodes applied circumferentially around the thorax in a single plane between the 4^{th} and 6^{th} intercostal space (Frerichs, Amato, et al., 2016; Frerichs et al., 2014). While an adjacent pair of electrodes 'injects' the current, the remaining passive electrode pairs measure the difference in electric potential. A resistivity (impedance) image is reconstructed from this data by a mathematical algorithm using a two-dimensional model and a simplified shape to represent the thoracic cross-section (Bayford, 2006; Bodenstein et al., 2009; Brown, 2003). The resulting image possesses a high temporal and functional resolution making it possible to monitor dynamic physiological change (e.g., delay in regional inflation or recruitment) on a breath-by-breath basis.

EIT images are based on image reconstruction techniques that require at least one measurement on a well-defined reference state (Frerichs, 2000; Frerichs et al., 2003; Frerichs et al., 2002; Frerichs et al., 2009). All quantitative data are related to this reference and therefore EIT can only quantify relative changes in local lung impedance rather than absolute changes. This also means that only structures that change over time are displayed.

4.3.1.2 EIT indices

EIT uses different measurements to help understand changes in ventilation as indicated by changes in impedance, either between inspiration and expiration or over time. There is consensus terminology used to describe each element (Frerichs, Amato, et al., 2016). EIT can also be used to describe global or regional changes (Frerichs, Amato, et al., 2016). Regions include dorsal right and left and ventral right and left. EIT measurements explore different facets of ventilation. Including the spatial and temporal distribution. Although there has been progress made in harmonising definitions and terminology (Frerichs, Amato, et al., 2016), some of the definitions are very much dependent upon individual devices and EIT definitions for the device used in the study (Krauss et al., 2021) are described below:

EIT indices averaging global/regional impedance include:

- End-expiratory lung impedance (EELI) is reflective of the impedance at end-expiration and is a surrogate for end-expiratory lung volume (EELV) (Adler et al., 1997; Frerichs, Amato, et al., 2016; Hinz et al., 2003; Marquis et al., 2006; März et al., 2015). Although increasing EELI indicates increasing EELV this is only a relative change rather than absolute lung volume (Krauss et al., 2021). The change in end-expiratory lung impedance (dEELI) reflects the impedance at the end of expiration and is measured as a change from the end of inspiration. Regional dEELI describes changes in impedance over time in the different regions of interest.
- Tidal impedance distribution (TID) represents the change in impedance during inspiration (end inspiration minus end expiration impedance). TID reflects the

average ventilation for a breath and is considered a surrogate for tidal volume (Frerichs, Amato, et al., 2016; Krauss et al., 2021; Shono & Kotani, 2019). Although increasing TID indicates increasing tidal ventilation, this is only a relative change rather than absolute volume (Krauss et al., 2021). Regional TID can be used to compare the impedance change in each region and correlates with the distribution of the tidal volume into each (Frerichs, Amato, et al., 2016; Shono & Kotani, 2019). Difference of tidal impedance distribution over time (dTID) is another way of expressing TID as it reflects the change of tidal impedance over time measured as a percent of baseline (assumed to be 0). Increases in dTID indicates increasing ventilation compared with baseline.

EIT indices used to analyse the spatial distribution of ventilation include:

- Surface of ventilated areas (SURF): describes the surface of ventilated areas or total aeration change within the lung because of impedance changes between inspiration and expiration. The larger the SURF the greater the aeration of the region (Krauss et al., 2021).
- Global inhomogeneity index (GI): represents the spatial distribution of the tidal breath (Krauss et al., 2021; Lynch et al., 2018). The larger the GI, the more heterogeneous the tidal volume is distributed within the ventilated area where a value of 0 represents perfectly homogenous ventilation (Becher et al., 2015; Becher et al., 2016; Zhao et al., 2009; Zhao et al., 2014). GI is a relative rather than absolute measure (Krauss et al., 2021).

EIT indices used to analyse the central position of ventilation include:

- Centre of gravity of ventilation distribution (CGVD): describes how ventilation is distributed vertically within the lung where 0% is the dorsal lung regions and 100% is the ventral regions (Frerichs et al., 2019; Krauss et al., 2021; Putensen et al., 2019). A value of 50 represents an equal distribution of ventilation between the ventral and the dorsal regions, whilst higher values indicate a more ventral distribution of ventilation (Becher et al., 2016; Frerichs et al., 2012; Vogt et al., 2012).

EIT indices used to analyse the temporal distribution of ventilation include:

- Regional ventilation delay (RVD): reflects the delay between the beginning of inspiration and reaching an impedance threshold set at a percent of final impedance. RVD40 is when 40% of final impedance is reached. RVD40 correlates with lung heterogeneity and recruited lung. Higher RVD40 indicates greater delay in ventilation and correlates with inspiratory time constants (Frerichs et al., 2012; Muders et al., 2012; Wrigge et al., 2008).

4.3.1.3 EIT in COPD

EIT has been studied in chronic stable COPD. End expiratory lung impedance and tidal impedance changes have been shown to correlate with traditional pulmonary function tests (e.g., FEV1 or FVC) (Balleza et al., 2009; Balleza-Ordaz et al., 2015).

Both spatial (GI) and temporal measurements (RVD) have been shown to differentiate between patients with and without COPD as well as differentiate between patients who do and do not respond to bronchodilators (Vogt et al., 2012; Vogt et al., 2016). The global inhomogeneity index is increased in patients with COPD (Trenk et al., 2016). The global inhomogeneity index can also differentiate those with COPD who respond to bronchodilator therapy from those who do not (Trenk et al., 2016; Vogt et al., 2012; Vogt et al., 2016).

The prolongation of the expiratory phase in COPD results in the development of dynamic hyperinflation and intrinsic PEEP. For patients who require non-invasive or invasive mechanical ventilation, the application of extrinsic PEEP may either improve or worsen dynamic hyperinflation depending on how well extrinsic and intrinsic PEEP are matched (Appendini et al., 1994; Brandolese et al., 1993; Laghi & Goyal, 2012). EELI correlates with end-expiratory lung volume and can be used to match extrinsic and intrinsic PEEP to reduce dynamic hyperinflation and optimize mechanical ventilation (Kostakou et al., 2016; Mauri, Bellani, Salerno, et al., 2013; Osadnik et al., 2017). The temporal measurements (e.g., RVD) available with EIT allow a better understanding of the distribution of inspiratory flow (Vogt et al., 2012; Vogt et al., 2016).

4.3.1.4 EIT data reconstruction

Following data acquisition, data analysis occurs using custom-made software and in accordance with the method described by the "Translational EIT development (TREND) study group" (Frerichs, Amato, et al., 2016) and in accordance with the Graz consensus Reconstruction algorithm for EIT (GREIT) (Adler et al., 2009). Five key stages of analysis are undertaken: (1) acquisition of EIT measurements (section 4.3.1.1), (2) generation of raw EIT images, (3) EIT waveforms and regions-of-interest (ROI), (4) functional EIT images and (5) EIT measures (Frerichs, Amato, et al., 2016). The process is schematically demonstrated in figure 4.6.

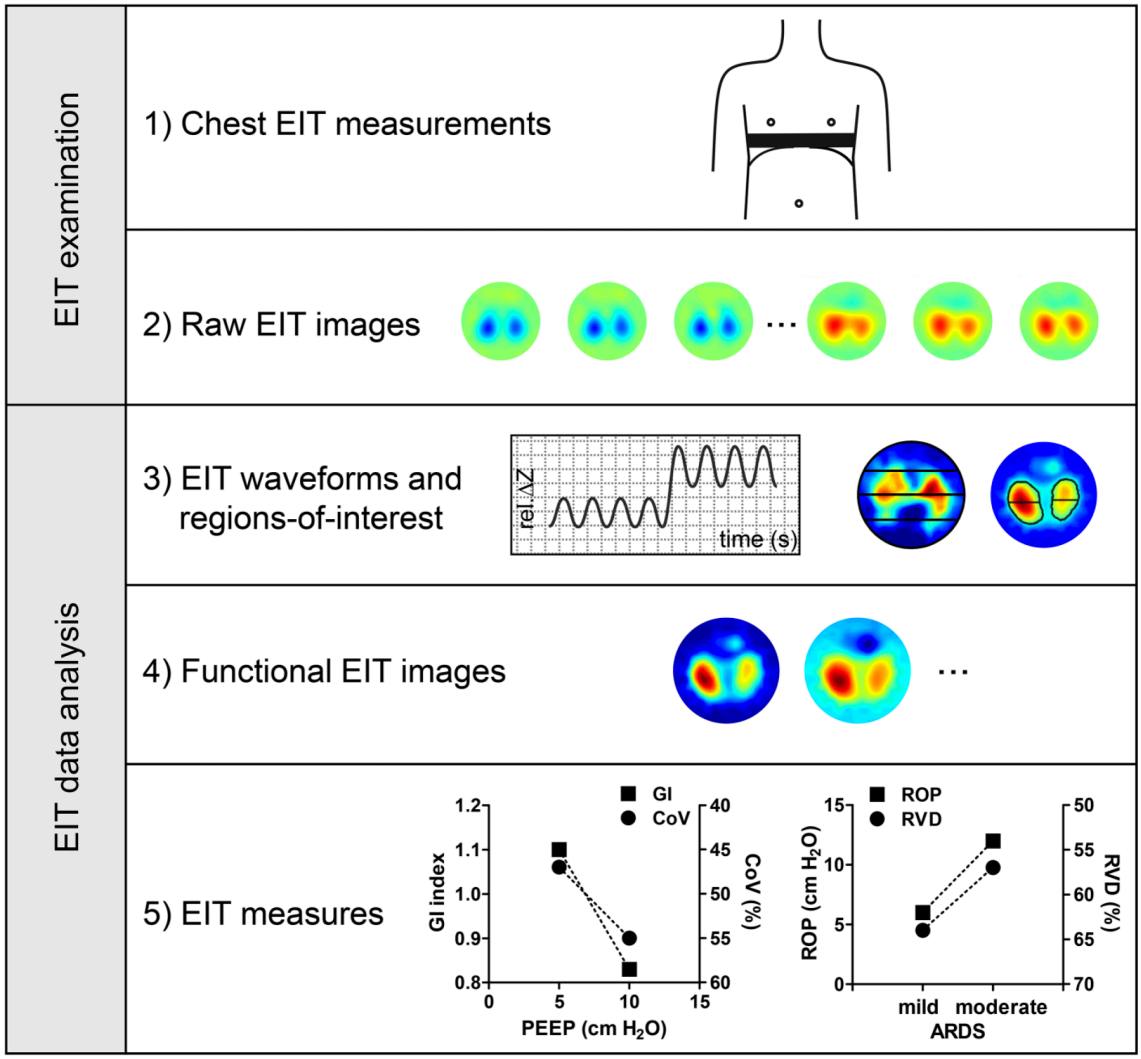

Figure 4.7: Schematic presentation of the chest EIT examination and data analysis (Frerichs, Amato, et al., 2016).

4.3.1.4.1 Generation of raw EIT images

Each EIT image shows the electrical tissue conductivity in a vertical slice roughly half the chest width (Rabbani & Kabir, 1991). The conductivity changes as the volume of air, blood or tissue within the field of view of the device changes. The raw data consists of voltage differences measured over time and this needs to be reconstructed into a 2-dimensional image through the plane of the electrodes (Lionheart, 2004). Images are generated through by comparing tissue properties in the current frame with the baseline frame using the GREIT image reconstruction algorithm, giving a time-difference EIT image (Adler et al., 2009; Frerichs, Amato, et al., 2016). The baseline image may be a mean of all images with the advantage that coughing or sighing causes less interference, however the presence of both positive and negative changes in impedance can make image interpretation more difficult (Frerichs, Amato, et al., 2016). The alternative is to select a physiological endpoint such as end inspiration or end-expiration (Frerichs, Amato, et al., 2016). This method makes images generally easier to interpret, however it has the disadvantage that events such as coughing make interpretation more difficult. Images are orientated in accordance with standard clinical radiological practice (i.e., the right side of the chest is on the left side of the image). The scale ranges from black (no change) through blue then white with increasing impedance and to purple with decrease in impedance (Frerichs, Amato, et al., 2016).

4.3.1.4.2 EIT waveforms and regions-of-interest (ROI)

EIT waveforms are the changes of impedance over time and are generated from raw EIT images (Frerichs et al., 2006). An image pixel is the basic unit for waveform data and data may be either grouped globally across the entire image or in smaller regions (Frerichs et al., 2006). Global waveforms are the average of all pixels in the image, whilst regional waveforms are generated from a subset of pixels. To improve analysis of the impedance changes within the lung, regions of interest (ROI) are usually identified (Becher et al., 2016; Frerichs, Amato, et al., 2016; Pulletz et al., 2006). The use of ROIs allows exclusion of non-pulmonary tissue and to allow comparison of different lung regions to demonstrate spatial heterogeneity (Frerichs et al., 2006;

Lowhagen et al., 2010). ROIs in the four quadrants of the lung between left dorsal and ventral, and right dorsal and ventral will be used to allow comparison between left and right dorsal and ventral lung regions to identify spatial heterogeneity and differences in expiratory time constants.

EIT images of the chest demonstrate changes in impedance in all the tissue under the electrodes, consequently, here are several potential sources of changes in impedance which do not relate to the lungs, including artefact from cardiac movement and changes in pulmonary perfusion. Although these physiological events cause a significantly smaller change in impedance than that due to ventilation, they do reduce signal quality and as they occur at a frequency significantly different to respiration they can be filtered out using digital frequency filtering (Frerichs, Amato, et al., 2016). Additional sources of noise include movement, loss of signal quality and interference from other electrical devices, particularly in the intensive care (Frerichs et al., 2011).

4.3.1.4.3 Functional EIT images

Functional EIT images are generated from the raw images and the waveforms using mathematical algorithms to generate physiologically relevant data (TREND). Data can then be displayed to visually demonstrate changes in tidal volume, end-expiratory lung volume, spatial distribution of gas and respiratory time constants (Frerichs et al., 2003; Mauri, Bellani, Confalonieri, et al., 2013; Miedema et al., 2012; Pulletz et al., 2012). The data can also be combined with other measurements for example airway pressure to generate system compliance (Frerichs et al., 2013; Miedema et al., 2011a, 2011b).

There are several useful functional EIT images in COPD. The first is the spatial distribution of ventilation within the lung. This can be shown using normalised tidal variation images where each pixel is displayed as a fraction of the overall tidal volume (Frerichs, Amato, et al., 2016). Volume difference function EIT images can demonstrate changes in end-expiratory lung volume if measured at the end of expiration (März et al., 2015). This allows within patient differences in end-expiratory lung volume to be measured over time. Ventilation delay can be demonstrated by

measuring the impedance of different pixels at different time points during inspiration and an image created (Muders et al., 2012). Similarly expiratory delay can be demonstrated by measuring regional impedance at different time-points during expiration (Crabb et al., 2016; Vogt et al., 2012; Vogt et al., 2016).

4.3.1.4.4 EIT measures

Functional EIT images display the changes within the lung regions, whilst EIT measures provide numerical descriptions of impedance changes over time. There are several groups of EIT measures. The first are the average of the region of interest examined in the functional image to quantify elements such as end-expiratory lung volume. The second are descriptors of the spatial distribution of ventilation including the global inhomogeneity index (Becher et al., 2015; Becher et al., 2016; Zhao et al., 2009; Zhao et al., 2014) and the coefficient of variation (Becher et al., 2016; Frerichs et al., 2012; Vogt et al., 2012). The impedance changes in different ROIs can also be compared. Additionally, the heterogeneity of ventilation can be quantified measuring regional respiratory time constants (Miedema et al., 2012; Pulletz et al., 2012), phase shifts in regional ventilation (Riedel et al., 2009), the ventilation delay index (Wrigge et al., 2008) and heterogeneity of expiratory times (Frerichs, Zhao, et al., 2016; Vogt et al., 2012; Vogt et al., 2016).

The global inhomogeneity index is the difference between the value of a pixel and the median value of all pixels normalised by the sum of impedance values within the lung.

$$GI = \Sigma(\text{pixel differences from median}) / \Sigma(\text{pixels}) \qquad \text{[Eq 4.15]}$$

In which:

$$\Sigma(\text{pixels}) = \Sigma\,(\Delta Zj), \text{ and}$$

$$\Sigma(\text{pixel differences from median}) = \Sigma\,(\Delta Zj - \Delta Z\text{median})$$

Equation 4.15: Global inhomogeneity index (Zhao et al., 2009). ΔZj is the functional EIT image value in pixel j, ΔZmedian is the median image value and all sums are calculated for all pixels j in the image.

The coefficient of variation describes the standard distribution in relation to the mean of the standard distribution and has been used to describe the global heterogeneity.

$$CV = SD(fEIT) / Mean(fEIT) \quad [Eq\ 4.16]$$

Equation 4.16: The coefficient of variation (Frerichs et al., 2012; Vogt et al., 2012). CV is the coefficient of variation, SD (fEIT) and mean (fEIT) are the standard deviation and mean of a given functional EIT image across all image pixels.

4.3.2 Methods

4.3.2.1 Contraindications

EIT was not performed if consent was declined or if a pacemaker was present.

4.3.2.2 Equipment

EIT examinations were performed using the Drager Pulmovista 500 EIT device (Pulmovista®; Draeger, Luebek, Germany). A silicone band consisting of 16 integrated cardiographic electrodes and 1 reference electrode was used to acquire the signals.

4.3.2.3 Data collection:

Data was collected using the following sequence in accordance with the standard methodology for EIT (Frerichs, Amato, et al., 2016):

- The EIT device was turned on and a device check was performed with the leads connected to the device;
- Once successfully completed, a new file was created and labelled using a standardised format: COPD (study number) EIT (day number of recording). The data recording was set to single for 5 minutes;
- The patient's thorax was measured using the EIT belt sizing tool from left mid-axilla to right mid-axilla and the appropriate belt was selected;

- The belt was applied to the thorax in the 4th intercostal space commencing with electrode one to the immediate left of the sternum and passing under the left axilla, around the back and ending at electrode 16 to the immediate right of the sternum. The belt was connected at both ends and the reference electrode was placed on the upper abdomen using an ECG electrode;
- 0.9% saline was applied between each electrode and the skin to reduce resistance;
- Once the belt was connected to the patient, the device leads were connected to the patient and the electrode signal was checked. If the signal was inadequate, additional 0.9% saline was placed between the electrode and the skin to reduce resistance;
- Once the signal check was adequate for all 16 electrodes and the reference electrode, the device was calibrated;
- 5 minutes of data was then recorded with a frame rate of 20 Hz. Any events were marked and labelled during the recording. A low-pass filter was set at a cut-off frequency of 50/min to exclude cardiac interference;
- The signal quality was checked constantly throughout the recording and any changes in signal viability resulted in a repeat recording following further application of 0.9% saline to the electrode;
- Data was backed up to an encrypted USB and transferred to an encrypted laptop for further processing.

For the NIV group, data was collected if the patient remained on NIV. For the $ECCO_2R$ group, data was collected if the patient remained on $ECCO_2R$, however two measurements were taken at each time point for each patient – a measurement on NIV and $ECCO_2R$ as well as a reading on $ECCO_2R$ alone. NIV was established for a period of 1 hour prior to taking the NIV and $ECCO_2R$ measurement and was removed for a period of 1 hour prior to taking the $ECCO_2R$ only measurement.

4.3.2.4 Data Analysis

The raw EIT data was analysed using a Matlab Tool EITdiag (MathWorks, Natick, MA, USA and Draeger, Luebek, Germany) and Microsoft Excel for Mac v16.71 (Microsoft, Seattle, WA, USA). The software undertakes analysis in accordance with the Graz consensus Reconstruction algorithm for EIT (GREIT) (Adler et al., 2009). Specific measurements obtained included tidal impedance, change in tidal impedance, surface volume, change in end-expiratory lung impedance, centre of gravity and regional ventilation delay set to 40% of maximum impedance. The EIT images were divided into four regions of interest – dorsal right (D/R), dorsal left (D/L), ventral right (V/R) and ventral left (V/L). Each region was of equal size and comprising 32 pixels. Ratios of global values were performed to compare the overall right-left and ventral-dorsal distribution of ventilation.

4.3.2.5 Ethical approval

The trial protocol was approved by the Cambridge NHS Human Research Authority Research Ethics Committee (14/EE/0109).

4.3.2.6 Statistical analysis

Statistical analysis was performed using Prism 9.5.1 for Mac (GraphPad, San Diego, USA). All data is presented as median (inter-quartile range). Data was compared within and between the two groups grouped at 0-23 hours, 24-48 hours and 49-120 hours.

4.3.3 Results

There were 8 patients in the NIV group and 7 patients in the $ECCO_2R$ group who underwent EIT measurements (figure 3.2, table 4.5). Measurements were taken daily whilst patients were on therapy. Inter- and intra-group comparisons were between the NIV and $ECCO_2R$ groups at 0-23 hours, 24-48 hours and 49-120 hours. Intra-group comparisons were between NIV with $ECCO_2R$ and $ECCO_2R$ alone using paired data.

4.3.3.1 Demographics

Patient characteristics at baseline and who underwent EIT measurements are displayed in table 4.5. All patients had severe COPD. Patients in both groups were comparable, however baseline respiratory rate was higher with $ECCO_2R$ (table 4.7).

	NIV (n=8/9)	$ECCO_2R$ (n=7/9)
Demographic data		
Age (years)	69.5 (65-73)	65 (63-71)
BMI (kg/m^2)	21.9 (21.1-28.5)	24.6 (24.2-29.5)
Sex (F)	2	4
FEV1 (L)	0.82 (0.58-1.24)	0.97 (0.825-1.32)
FEV1 (% predicted) (%)	33.5 (20.5-46.25)	39.8 (39-44.5)
FVC (L)	2.4 (1.2-2.8)	2.6 (1.8-3.2)
FVC (% predicted) (%)	68.5 (33-108)	82 (71.5-87)
FEV1/FVC	47.5 (31.75-48.25)	44 (37-48)
GOLD stage	4 (3-4)	3 (3-3)
Baseline observations		
Systolic Blood pressure (mmHg)	118 (105-134)	130 (118-140)
Respiratory rate (breaths/min)	24 (20-26)	30 (29-34)
SpO_2 (%)	92 (90-92)	91 (88-94)
Heart rate (beats/min)	101 (88-117)	109 (96-117)
Presenting arterial blood gas		
PaO_2 (kPa)	9.2 (8.7-10.9)	7.4 (7.1-8.9)
$PaCO_2$ (kPa)	9.7 (9-10.4)	9.8 (9-9.9)
pH	7.23 (7.23-7.25)	7.26 (7.25-7.27)
HCO_3 (mmol/L)	31.2 (27.4-31.8)	29.7 (29.5-31.09)
Initial NIV settings		
EPAP (cmH_2O)	5 (5-6)	6 (6-7)
IPAP (cmH_2O)	17 (14-21)	18 (16-19)
FiO_2 (%)	30 (26-43)	35 (29-38)
Arterial blood gas after 1 hour NIV		
PaO_2 (kPa)	8.5 (8.1-9.1)	8.9 (7.8-9.2)
$PaCO_2$ (kPa)	9.6 (8.2-10.1)	8.9 (8.5-9.1)
pH	7.27 (7.23-7.27)	7.29 (7.27-7.28)
HCO_3 (mmol/L)	29.9 (26.4-31.5)	27.9 (27.8-29.1)

Table 4.7: Baseline demographics in the NIV and $ECCO_2R$ group who had EIT measurements. All results are expressed as median (IQR).

4.3.3.2 Inter-group EIT results

Tables 4.8 and 4.9 demonstrates the changes over time within the NIV and $ECCO_2R$ groups. Tables 4.10 and 4.11 compare the two groups on day 1 and day 2 respectively.

In the $ECCO_2R$ group, EIT showed more inhomogeneous ventilation as demonstrated by an increase in GI and RVD40. There was a redistribution of volume from the ventral regions (decrease in dEELI of the ventral regions, with increase in the dorsal regions), with limited changes in overall aeration (SURF) and tidal ventilation (TID and dTID) over time. In the NIV group homogeneity was preserved and there was an increase in global dEELI and tidal impedance globally and regionally over time.

	NIV 0-23 hours	NIV 24-48 hours	NIV 49-120 hours
n	**8**	**7**	**2**
SpO_2 (%)	93 (92-94)	93 (91-93)	95 (94-95)
Resp rate (bpm)	21 (20-25)	20 (18-25)	19 (18-21)
FiO_2 (%)	28 (26-33)	29 (28-30)	29 (29-30)
IPAP (cmH_2O)	15 (10-21)	24 (16-25)	18 (15-21)
EPAP (cmH_2O)	5 (5-6)	5 (5-7)	6 (6-7)
CO_2 removal (mL/min)			
PaO_2 (kPa)	8.86 (7.71-9.61)	7.81 (7.60-8.28)	8.57 (8.33-8.80)
$PaCO_2$ (kPa)	8.37 (7.86-9.48)	7.33 (6.66-8.15)	7.55 (7.40-7.69)
pH	7.29 (7.25-7.33)	7.38 (7.35-7.40)	7.41 (7.40-7.42)
HCO_3 (mmol/L)	25.8 (23-29.6)	29.9 (27.9-31.7)	31.5 (31.4-31.5)
CO_2 Content (mmol/L)	27.3 (25.8-31.7)	30.3 (27.5-31.2)	30.9 (30.8-31)
TID (ΔZ AU)	100 (100-100)	122.9 (97.2-205.3)	170 (166.8-173.1)
SURF (pixels)	378.5 (330.8-414.8)	379 (362-413)	413 (405.5-420.5)
GI (%)	50.8 (47.3-59.2)	52.6 (49-56.2)	58 (55.4-60.5)
CGVD (%)	53.6 (51.2-59.8)	53.1 (51.3-54.4)	52.5 (51.8-53.2)
RVD40 (%Tinsp)	11.4 (10.2-13.6)	11.8 (10.3-20.4)	8.3 (6.4-10.3)
dTID (ΔZ AU)	0 (0-0)	22.9 (-2.8-105.3)	70 (66.8-73.1)
dEELI (ΔZ AU)	0 (0-0)	139.6 (12.9-559.3)	867.3 (552.3-1,182.3)
TID D/R (ΔZ AU)	24 (12-29.6)	26.4 (14.2-49.3)	39.6 (35.8-43.5)
TID D/L (ΔZ AU)	16.5 (13.6-20.5)	19.6 (17.8-31.9)	34.4 (34.3-34.6)
TID V/R (ΔZ AU)	26.4 (21.4-35)	42.3 (26.5-50.6)	37.3 (28.6-46)
TID V/L (ΔZ AU)	26.9 (25.1-44.7)	36.5 (30.8-52.6)	58.6 (56.7-60.5)
SURF D/R (pixels)	102 (54.5-110.3)	100 (83-116.5)	116 (104.5-127.5)
SURF D/L (pixels)	91.5 (71.3-98.3)	90 (70-101)	111.5 (109.3-113.8)
SURF V/R (pixels)	110 (83-118)	97 (92-114.5)	77.5 (64.8-90.3)
SURF V/L (pixels)	105.5 (95.3-123.8)	101 (90-115)	108 (102-114)
GI D/R (%)	13.4 (7.5-14.6)	10.5 (9-13.1)	11.6 (11.4-11.9)
GI D/L (%)	9.2 (7.7-10.5)	10.5 (8.7-12.6)	10.5 (9.8-11.3)
GI V/R (%)	14.6 (12.7-16.5)	13.4 (11.8-16)	15.2 (15-15.4)
GI V/L (%)	13 (11.2-22.7)	17.8 (10.2-23.4)	20.5 (18.7-22.3)
RVD40 D/R (%Tinsp)	10.3 (8-12.5)	11.4 (9.9-14.8)	9.1 (6.4-11.8)
RVD40 D/L (%Tinsp)	7.9 (6.9-8.7)	9.4 (6.7-14.3)	4.3 (3.8-4.9)
RVD40 V/R (%Tinsp)	16.1 (12.4-20.6)	17.3 (13.5-29.5)	15.9 (11.9-19.9)
RVD40 V/L (%Tinsp)	10.9 (9.3-13.8)	13.9 (7.6-18)	4.1 (3.5-4.6)
dTID D/R (ΔZ AU)	0 (0-0)	2.7 (0.7-21.3)	17.4 (9-25.9)
dTID D/L (ΔZ AU)	0 (0-0)	12 (1.7-16.2)	16.7 (14.7-18.6)
dTID V/R (ΔZ AU)	0 (0-0)	14.5 (7.6-22.3)	19.3 (12-26.6)
dTID V/L (ΔZ AU)	0 (0-0)	7.2 (-11-20.1)	16.5 (10.3-22.7)
dEELI D/R (ΔZ AU)	0 (0-0)	152.9 (19.7-265.3)	194.4 (152.3-236.5)
dEELI D/L (ΔZ AU)	0 (0-0)	15.4 (-1.8-140.9)	138.3 (123.9-152.6)
dEELI V/R (ΔZ AU)	0 (0-0)	3.1 (-65-89.8)	329.4 (172.5-486.2)
dEELI V/L (ΔZ AU)	0 (0-0)	24.3 (-22.3-104.4)	205.2 (75.3-335.2)

Table 4.8: Changes in EIT and physiological parameters over time for the NIV group. AU arbitrary units, ΔZ AU change in impedance arbitrary units, bpm breaths per minute, %Tinsp percentage of inspiratory time, D/L dorsal left region, D/R dorsal right region, V/L ventral left region, V/R ventral right region.

	$ECCO_2R$ 0-23 hours	$ECCO_2R$ 24-48 hours	$ECCO_2R$ 49-120 hours
n	**7**	**6**	**6**
SpO_2 (%)	92 (91-92)	93 (93-93)	92 (88-95)
Resp rate (bpm)	26 (20-30)	24 (23-27)	20 (18-23)
FiO_2 (%)	30 (28-40)	30 (30-40)	35 (30-35)
IPAP (cmH_2O)			
EPAP (cmH_2O)			
CO_2 removal (mL/min)	88 (79-93)	87 (80-95)	87 (61-97)
PaO_2 (kPa)	8.01 (7.44-8.82)	8.07 (7.66-8.48)	9.01 (8.49-9.69)
$PaCO_2$ (kPa)	7.99 (7.15-8.05)	7.51 (6.57-7.93)	7.98 (6.50-8.29)
pH	7.35 (7.31-7.39)	7.40 (7.32-7.45)	7.37 (7.36-7.41)
HCO_3 (mmol/L)	25 (24.2-27.7)	26.6 (25.6-30.8)	29.8 (29.3-30.7)
CO_2 Content (mmol/L)	26 (23.6-27)	27 (25.8-28.3)	30.3 (26.2-32.2)
TID (ΔZ AU)	100 (100-100)	88.7 (84.5-118.1)	117.8 (88.4-136.7)
SURF (pixels)	399 (394-466)	369 (321-403)	309.5 (277-404)
GI (%)	54.3 (46.1-64.1)	64.3 (59.9-71.3)	70.9 (66.2-82.3)
CGVD (%)	50 (48.7-50.2)	48.9 (48.2-51.5)	48.3 (45.5-49.5)
RVD40 (%Tinsp)	8.6 (7.6-16.5)	14.3 (9.9-14.8)	9.9 (7.4-13.1)
dTID (ΔZ AU)	0 (0-0)	-11.3 (-15.5-18.1)	17.8 (-11.6-36.7)
dEELI (ΔZ AU)	0 (0-0)	195.2 (67.3-269.2)	146.2 (68-342.2)
TID D/R (ΔZ AU)	25.9 (25.6-33.8)	22.9 (22-49.4)	35.1 (26.6-49.6)
TID D/L (ΔZ AU)	25.9 (24.1-27.4)	21.9 (21.6-25.1)	27.2 (18.9-39.2)
TID V/R (ΔZ AU)	21 (18.9-23.9)	24 (22.8-30.9)	23.3 (9.8-32.2)
TID V/L (ΔZ AU)	24.4 (18-27.2)	20.5 (19.6-25.7)	23.9 (21.4-33.4)
SURF D/R (pixels)	120 (97-122)	109 (88-117)	102.5 (94.5-121)
SURF D/L (pixels)	101 (87-130)	83 (71-110)	79.5 (66.3-96.3)
SURF V/R (pixels)	105 (91-106)	65 (65-118)	51 (40.3-96)
SURF V/L (pixels)	104 (86-107)	93 (50-94)	81.5 (61.8-97.3)
GI D/R (%)	18.7 (14-19.8)	25.2 (16.7-25.4)	21.6 (17.1-28.7)
GI D/L (%)	12.3 (12-14.7)	13.9 (13.7-13.9)	17.4 (15.6-21.6)
GI V/R (%)	10 (9.6-13.9)	16.5 (12-17.3)	15.8 (11.9-19.2)
GI V/L (%)	12.4 (11.6-12.8)	13.4 (11.5-14.8)	15.8 (13.8-17)
RVD40 D/R (%Tinsp)	11.1 (7.6-16)	10.6 (8.1-12.3)	11 (7.9-14.9)
RVD40 D/L (%Tinsp)	8.7 (7.9-9.9)	12.4 (8.7-17.6)	7.1 (6-9.8)
RVD40 V/R (%Tinsp)	12 (7.9-18.6)	13.3 (10-17.3)	7.2 (6-11)
RVD40 V/L (%Tinsp)	7 (6.6-16.4)	19 (9.3-24.1)	13.8 (6.5-17.5)
dTID D/R (ΔZ AU)	0 (0-0)	-1.3 (-3.6-15.6)	9.2 (3.5-21.1)
dTID D/L (ΔZ AU)	0 (0-0)	-4 (-5.7-5.6)	-0.6 (-4.2-15.5)
dTID V/R (ΔZ AU)	0 (0-0)	3.9 (-6.6-7)	-6.4 (-11.3-8.4)
dTID V/L (ΔZ AU)	0 (0-0)	-1.8 (-5.6-4.7)	6.2 (-3.8-9.2)
dEELI D/R (ΔZ AU)	0 (0-0)	172.3 (57.4-228.9)	45.7 (-129-141.8)
dEELI D/L (ΔZ AU)	0 (0-0)	146.8 (67.5-147.3)	22.2 (-3.7-91.6)
dEELI V/R (ΔZ AU)	0 (0-0)	-48.3 (-117.1-10.5)	56.9 (-19.1-169.1)
dEELI V/L (ΔZ AU)	0 (0-0)	-19.7 (-59.2--1.6)	3.6 (-38.9-179.8)

Table 4.9: Changes in EIT and physiological parameters over time for the $ECCO_2R$ group. AU arbitrary units, ΔZ AU change in impedance arbitrary units, bpm breaths per minute, %Tinsp percentage of inspiratory time, D/L dorsal left region, D/R dorsal right region, V/L ventral left region, V/R ventral right region.

	NIV 0-23 hours	$ECCO_2R$ 0-23 hours
n	**8**	**7**
SpO_2 (%)	93 (92-94)	91 (90-92)
Resp rate (bpm)	21 (20-25)	26 (25-32)
FiO_2 (%)	28 (26-33)	30 (28-38)
IPAP (cmH_2O)	15 (10-21)	0 (0-0)
EPAP (cmH_2O)	5 (5-6)	0 (0-0)
CO_2 Removal (mL/min)		88 (79-109)
PaO_2 (kPa)	8.86 (7.71-9.61)	8.01 (7.33-8.86)
$PaCO_2$ (kPa)	8.37 (7.86-9.48)	7.99 (6.88-8.13)
pH	7.29 (7.25-7.33)	7.35 (7.31-7.37)
HCO_3 (mmol/L)	25.8 (23-29.6)	25 (24.6-27.7)
CO_2 Content (mmol/L)	27.3 (25.8-31.7)	26 (23.6-27.8)
TID (DZ AU)	100 (100-100)	100 (100-100)
SURF (pixels)	378.5 (330.8-414.8)	394 (326.5-411.5)
GI (%)	50.8 (47.3-59.2)	59.1 (50.7-63.1)
CGVD (%)	53.6 (51.2-59.8)	50.2 (48.3-51.6)
RVD40 (%Tinsp)	11.4 (10.2-13.6)	8.6 (7.7-11.9)
dTID (ΔZ AU)	0 (0-0)	0 (0-0)
dEELI (ΔZ AU)	0 (0-0)	0 (0-0)
TID D/R (ΔZ AU)	24 (12-29.6)	25.6 (23.7-36.5)
TID D/L (ΔZ AU)	16.5 (13.6-20.5)	24.1 (21.3-27.1)
TID V/R (ΔZ AU)	26.4 (21.4-35)	22.9 (19.9-29.9)
TID V/L (ΔZ AU)	26.9 (25.1-44.7)	27.2 (18.6-28.6)
SURF D/R (pixels)	102 (54.5-110.3)	110 (92-120)
SURF D/L (pixels)	91.5 (71.3-98.3)	86 (71.5-107.5)
SURF V/R (pixels)	110 (83-118)	91 (77-105.5)
SURF V/L (pixels)	105.5 (95.3-123.8)	100 (70-105)
GI D/R (%)	13.4 (7.5-14.6)	18.7 (11.9-20)
GI D/L (%)	9.2 (7.7-10.5)	13.2 (11.1-14.7)
GI V/R (%)	14.6 (12.7-16.5)	13.9 (9.8-17.4)
GI V/L (%)	13 (11.2-22.7)	12.8 (9.7-16.6)
RVD40 D/R (%Tinsp)	10.3 (8-12.5)	10.4 (7.9-12.5)
RVD40 D/L (%Tinsp)	7.9 (6.9-8.7)	8.3 (4.4-9.3)
RVD40 V/R (%Tinsp)	16.1 (12.4-20.6)	12 (8.9-13)
RVD40 V/L (%Tinsp)	10.9 (9.3-13.8)	9.4 (6.8-12.3)
dTID D/R (ΔZ AU)	0 (0-0)	0 (0-0)
dTID D/L (ΔZ AU)	0 (0-0)	0 (0-0)
dTID V/R (ΔZ AU)	0 (0-0)	0 (0-0)
dTID V/L (ΔZ AU)	0 (0-0)	0 (0-0)
dEELI D/R (ΔZ AU)	0 (0-0)	0 (0-0)
dEELI D/L (ΔZ AU)	0 (0-0)	0 (0-0)
dEELI V/R (ΔZ AU)	0 (0-0)	0 (0-0)
dEELI V/L (ΔZ AU)	0 (0-0)	0 (0-0)

Table 4.10: Comparison in EIT and physiological parameters over time between the NIV and the $ECCO_2R$ group on day 1 (0-23 hours). AU

arbitrary units, ΔZ AU change in impedance arbitrary units, bpm breaths per minute, %Tinsp percentage of inspiratory time, D/L dorsal left region, D/R dorsal right region, V/L ventral left region, V/R ventral right region.

	NIV 24-48 hours	$ECCO_2R$ 24-48 hours
n	**7**	**6**
SpO_2 (%)	93 (91-93)	93 (92-93)
Resp rate (bpm)	20 (18-25)	23 (19-24)
FiO_2 (%)	29 (28-30)	40 (30-40)
IPAP (cmH_2O)	24 (16-25)	0 (0-0)
EPAP (cmH_2O)	5 (5-7)	0 (0-0)
CO_2 Removal (mL/min)		95 (80-100)
PaO_2 (kPa)	7.81 (7.60-8.28)	8.48 (7.66-8.99)
$PaCO_2$ (kPa)	7.33 (6.66-8.15)	7.93 (6.57-8.02)
pH	7.38 (7.35-7.40)	7.40 (7.34-7.45)
HCO_3 (mmol/L)	29.9 (27.9-31.7)	29 (26.6-30.8)
CO_2 Content (mmol/L)	30.3 (27.5-31.2)	28.3 (25.8-29.9)
TID (DZ AU)	122.9 (97.2-205.3)	91 (87.2-101.8)
SURF (pixels)	379 (362-413)	369 (321-403)
GI (%)	52.6 (49-56.2)	64.3 (54.5-71.3)
CGVD (%)	53.1 (51.3-54.4)	51.5 (48.9-53.6)
RVD40 (%Tinsp)	11.8 (10.3-20.4)	13.3 (11.2-14.3)
dTID (DZ AU)	22.9 (-2.8-105.3)	-9 (-12.8-1.8)
dEELI (DZ AU)	139.6 (12.9-559.3)	195.2 (67.3-269.2)
TID D/R (ΔZ AU)	26.4 (14.2-49.3)	21.5 (17.4-22.9)
TID D/L (ΔZ AU)	19.6 (17.8-31.9)	21 (16.4-21.9)
TID V/R (ΔZ AU)	42.3 (26.5-50.6)	24.9 (22.8-31.1)
TID V/L (ΔZ AU)	36.5 (30.8-52.6)	28.1 (20.5-31.4)
SURF D/R (pixels)	100 (83-116.5)	88 (85-109)
SURF D/L (pixels)	90 (70-101)	83 (56-106)
SURF V/R (pixels)	97 (92-114.5)	91 (65-112)
SURF V/L (pixels)	101 (90-115)	94 (67-99)
GI D/R (%)	10.5 (9-13.1)	16.7 (11.1-25.2)
GI D/L (%)	10.5 (8.7-12.6)	13.7 (11.1-13.9)
GI V/R (%)	13.4 (11.8-16)	17.3 (12-21)
GI V/L (%)	17.8 (10.2-23.4)	14.8 (13.4-21.5)
RVD40 D/R (%Tinsp)	11.4 (9.9-14.8)	10.8 (8.1-12.3)
RVD40 D/L (%Tinsp)	9.4 (6.7-14.3)	12.4 (8.7-14.9)
RVD40 V/R (%Tinsp)	17.3 (13.5-29.5)	13.3 (11.8-15.7)
RVD40 V/L (%Tinsp)	13.9 (7.6-18)	15.9 (12.3-19)
dTID D/R (ΔZ AU)	2.7 (0.7-21.3)	-2 (-3.4--1.3)
dTID D/L (ΔZ AU)	12 (1.7-16.2)	-2.5 (-4--0.9)
dTID V/R (ΔZ AU)	14.5 (7.6-22.3)	-0.3 (-4.5-4)
dTID V/L (ΔZ AU)	7.2 (-11-20.1)	-1.4 (-5.6-1.6)
dEELI D/R (ΔZ AU)	152.9 (19.7-265.3)	57.4 (-60.7-172.3)
dEELI D/L (ΔZ AU)	15.4 (-1.8-140.9)	97.3 (68.6-146.8)
dEELI V/R (ΔZ AU)	3.1 (-65-89.8)	3.8 (-76.4-146.3)
dEELI V/L (ΔZ AU)	24.3 (-22.3-104.4)	-19.7 (-59.2-32.5)

Table 4.11: Comparison in EIT and physiological parameters over time between the NIV and the $ECCO_2R$ group on day 2 (24-48 hours). AU

arbitrary units, ΔZ AU change in impedance arbitrary units, bpm breaths per minute, %Tinsp percentage of inspiratory time, D/L dorsal left region, D/R dorsal right region, V/L ventral left region, V/R ventral right region.

4.3.3.3 NIV and $ECCO_2R$ compared with $ECCO_2R$ alone

The comparison for the EIT measurements from NIV with $ECCO_2R$ and $ECCO_2R$ alone is displayed in tables 4.12 and 4.13, and figures 4.8 and 4.9. The results are from paired samples. The addition of NIV to $ECCO_2R$ resulted in an increase in end-expiratory lung volume (dEELI) both globally and regionally, with similar aeration (SURF) but lower tidal ventilation (TID and dTID). The homogeneity of ventilation (GI) was similar between the two groups overall. The global ratios (table 4.11) demonstrate that aspects of ventilation are more evenly distributed with the addition of NIV (CVHD, SURF and RVD40 ratios all approach 1) but with larger tidal variation (TID). There was greater ventilation ventrally than dorsally with NIV and $ECCO_2R$ combined with increases in ventral TID and SURF and corresponding decreases in dorsal TID and SURF along with the increase in CGVD indicating a ventral change in the distribution of ventilation. There was an increase in end expiratory lung volume dorsally (dEELI) and a decrease in inhomogeneity (lower GI). There was increased inhomogeneity ventrally (increased GI) with increasing regional ventilation delay (RVD40).

	ECCO$_2$R and NIV	ECCO$_2$R alone
TID (ΔZ AU)	91.3 (81.8-103.4)	100 (100-100)
SURF (pixels)	345 (297-394)	363 (251-417)
GI (%)	55 (50.9-69.6)	59.9 (47.9-73.3)
CGVD (%)	50.5 (47.3-52.9)	48.7 (46.2-50.7)
RVD40 (%Tinsp)	11.6 (9.1-12.5)	8.9 (7.4-13.1)
dTID (ΔZ AU)	-8.7 (-18.2-3.4)	0 (0-0)
dEELI (ΔZ AU)	65.9 (34.7-112.3)	0 (0-68)
TID D/R (ΔZ AU)	21.5 (17.3-25.5)	26.3 (22.9-42.9)
TID D/L (ΔZ AU)	21.6 (17.7-28)	26.1 (20.1-28.3)
TID V/R (ΔZ AU)	19.9 (14.4-27.6)	21 (13-26.6)
TID V/L (ΔZ AU)	27.6 (16.9-35.2)	22.4 (16.9-27.9)
SURF D/R (pixels)	97 (88-108)	99 (95-117)
SURF D/L (pixels)	86 (65-103)	87 (65-114)
SURF V/R (pixels)	87 (56-98)	65 (43-98)
SURF V/L (pixels)	96 (73-104)	90 (47-103)
GI D/R (%)	12.8 (10.6-20)	18.7 (12.2-22.6)
GI D/L (%)	12 (10.8-15.4)	12.3 (9.7-17.3)
GI V/R (%)	13.2 (10.5-16.6)	13.1 (10.5-19.4)
GI V/L (%)	16 (12.8-19.8)	13.5 (12.4-16.3)
RVD40 D/R (%Tinsp)	11.1 (7.6-14.3)	10.5 (7.8-12.6)
RVD40 D/L (%Tinsp)	9.3 (7.2-12.4)	8.7 (6.5-10.9)
RVD40 V/R (%Tinsp)	11.4 (7.9-13)	7.5 (6.6-12.1)
RVD40 V/L (%Tinsp)	11.1 (7.9-14.1)	9.3 (6.5-16.4)
dTID D/R (ΔZ AU)	-2.3 (-8.4-0)	0 (0-0)
dTID D/L (ΔZ AU)	-2.1 (-5.1-1.9)	0 (0-0)
dTID V/R (ΔZ AU)	-1.5 (-6.3-0.5)	0 (-3-0)
dTID V/L (ΔZ AU)	0 (-4-4.2)	0 (0-0)
dEELI D/R (ΔZ AU)	14.8 (0-79.9)	0 (0-0)
dEELI D/L (ΔZ AU)	19.1 (0-48.8)	0 (0-0)
dEELI V/R (ΔZ AU)	2.3 (-3.7-31.2)	0 (0-0)
dEELI V/L (ΔZ AU)	0 (-9.8-25.5)	0 (0-0)

Table 4.12: Comparison between EIT parameters between NIV with ECCO$_2$R and ECCO$_2$R alone, paired samples.

	Ventral/Dorsal Ratio		Right/Left Ratio	
	NIV & $ECCO_2R$	$ECCO_2R$	NIV & $ECCO_2R$	$ECCO_2R$
TID	1.25 (0.61-1.5)	0.86 (0.49-1.15)	0.89 (0.8-1.07)	1.02 (0.83-1.35)
SURF	1 (0.71-1.19)	0.73 (0.6-0.88)	0.96 (0.9-1.1)	1.04 (0.94-1.21)
GI	1.07 (0.66-1.62)	0.89 (0.67-1.28)	1.04 (0.84-1.19)	1.25 (0.94-1.4)
RVD40	1.1 (0.87-1.3)	1.08 (0.93-1.23)	1.05 (0.79-1.25)	1.01 (0.76-1.09)

Table 4.13: Ratio of global EIT parameters. The ratios compare the ventral/dorsal distribution and the right/left distribution of EIT parameters with the combination of NIV and $ECCO_2R$ and $ECCO_2R$ alone.

4.3.4 Discussion

4.3.4.1 NIV over time

The changes in the EIT signal varied between the two groups over the first 120 hours. The NIV group had an improvement in respiratory acidosis. The NIV group demonstrated preserved aeration (SURF) with preserved global homogeneity (GI). The NIV group also demonstrated an increase in tidal impedance (100-170 DZ AU) with an associated increase in dEELI (0-870 DZ AU). The change in dEELI was predominantly in the dorsal regions. dEELI has been demonstrated to be strongly correlated with and is a surrogate for end-expiratory lung volume (Adler et al., 1997; Frerichs, Amato, et al., 2016; Hinz et al., 2003; Marquis et al., 2006; März et al., 2015). However, dEELI reflects the changes in impedance between end of inspiration and end of expiration (Krauss et al., 2021). Hence although it is possible that there is an absolute change in end-expiratory lung volume over time, the change in dEELI implies that the relative lung volume change between the end of inspiration and end of expiration has increased and is therefore suggestive of increased aeration. This is in keeping with the minimal changes in surface volume (SURF), a marker of aeration suggesting that there has not been a marked increase in lung volumes (Krauss et al., 2021). It is also in keeping with the increase seen in tidal impedance (TID). TID reflects the average change in ventilation over the entire breath and correlates with and is considered a surrogate for tidal volume (Frerichs, Amato, et al., 2016; Krauss et al.,

2021; Shono & Kotani, 2019). This supports the concept that the increase in dEELI corresponds with increased ventilation rather than progressive overinflation. Global inhomogeneity (GI) also remains unchanged over time in the NIV group. GI represents the spatial distribution of the tidal breath (Becher et al., 2015; Becher et al., 2016; Krauss et al., 2021; Lynch et al., 2018; Zhao et al., 2009; Zhao et al., 2014). Other studies in COPD demonstrate that GI is, similar to the current study, higher in subjects with COPD compared with healthy subjects and that there is considerable variation between and within individuals with COPD over time (Frerichs et al., 2021; Zhao et al., 2020). The centre of gravity of ventilation does not change over time and values of 52.5-53.6% indicate a persisting but slightly ventral distribution of ventilation with NIV (Frerichs et al., 2019; Krauss et al., 2021; Putensen et al., 2019). RVD reduces over time. RVD measures the time for inspiration and is a surrogate for the inspiratory time constant (Frerichs et al., 2012; Muders et al., 2012; Wrigge et al., 2008). RVD is higher in patients with higher inhomogeneity and in patients with overinflation. The reduction seen therefore supports the concept that the changes in dEELI reflect improved aeration rather than increases in overinflation.

Overall, the EIT indices in the NIV group suggest that over time there is improving aeration and tidal ventilation with maintenance of aeration, homogeneity and minimal regional differences in aeration. This is likely due to the application of positive pressure throughout the respiratory cycle supporting inspiratory volumes and preventing airway collapse.

4.3.4.2 $ECCO_2R$ over time

In the $ECCO_2R$ group, there were relatively few changes in the impedance signal. There was an increase in the global dEELI over time with a small increase in tidal aeration consistent with improved aeration. The large changes in aeration seen in the NIV group over time were not replicated in the $ECCO_2R$ group (Adler et al., 1997; Frerichs, Amato, et al., 2016; Hinz et al., 2003; Marquis et al., 2006; März et al., 2015). There was a reduction in surface volume suggesting that the aerated pixels reduced with time. There was also an increase in inhomogeneity (GI) over the 5-day period. Inspiratory time varied over the 5 day period consistent with inhomogeneity (Becher

et al., 2015; Becher et al., 2016; Frerichs et al., 2012; Muders et al., 2012; Wrigge et al., 2008; Zhao et al., 2009; Zhao et al., 2014). The CGVD decreased, indicating that ventilation moved dorsally with time.

Overall, the EIT indices in the $ECCO_2R$ group over time suggest that controlling CO_2 without pressure support led to a movement of the ventilation dorsally with an increase in inhomogeneity and an increase in end-expiratory lung volume but maintenance of tidal ventilation suggesting that there was a degree of dynamic hyperinflation. Hence although $ECCO_2R$ may have improved the respiratory acidosis, the respiratory system was not necessarily offloaded.

4.3.4.3 NIV and $ECCO_2R$ compared with $ECCO_2R$ alone

The addition of NIV to $ECCO_2R$ resulted in an overall decrease in tidal impedance with higher dEELI and similar GI. The centre of gravity also shifted ventrally with NIV though this was back towards the midpoint at 50.5%. This suggests that the positive pressure of NIV induced a degree of overinflation that resulted in an increase in end expiratory lung volume and a corresponding decrease in tidal volume (Adler et al., 1997; Frerichs, Amato, et al., 2016; Hinz et al., 2003; Marquis et al., 2006; März et al., 2015). However, there was also a more homogenous spread of aeration throughout the lung with dorsal/ventral and right/left ratios close to 1 in the NIV and $ECCO_2R$ group for both surface volume and global inhomogeneity. The ratio graphs suggest that the $ECCO_2R$ group had a more dorsal distribution of lung volume with more inhomogeneous ventilation dorsally and with a greater proportion of tidal ventilation dorsally. The ratio graphs also indicate that both the inhomogeneity is greater in the right lung with $ECCO_2R$ alone and that the tidal ventilation change is shifted to the right as well.

Taken together this data suggests that although there was a small increase in overinflation that the application of positive pressure ventilation resulted in a more homogenous distribution of aeration throughout the lungs which was better centred in both the ventral/dorsal plane as well as the right/left plane.

4.3.4.4 Limitations

There are potential limitations to the current data and therefore its interpretation. Given the baseline difference between the respiratory rate in the two groups in both the EIT subset (table 4.5 and the overall group figure 3.2 and table 3.1), it is possible that the $ECCO_2R$ group were sicker, and this may have impacted results. The groups are also a subset of the overall group and this may have introduced bias.

4.3.4.5 Conclusions

The EIT data suggests that NIV provides more homogeneous global distribution of ventilation than $ECCO_2R$ alone and more homogeneously distributed aeration within the lung fields in both the ventral/dorsal regions as well as the right/left regions with NIV and $ECCO_2R$ compared with $ECCO_2R$, suggesting that there is a change in ventilation and aeration consequent to the addition of NIV to $ECCO_2R$.

4.4 Parasternal electromyography

4.4.1 Introduction

As discussed in chapter 1, COPD is characterised by expiratory flow limitation (O'Donnell et al., 2016) resulting in increased end-expiratory lung volume and dynamic hyperinflation. During an exacerbation there is an increase in airways resistance, worsening expiratory flow limitation, increase in end-expiratory lung volume and reduction in diaphragmatic function (figure 4.1) (M Orozco-Levi et al., 2001; M. Polkey et al., 1996). Together these result in a progressive increase in the subjective work of breathing, anxiety and tachypnoea further exacerbating dynamic hyperinflation (Calverley, 2003; D. O'Donnell & C. Parker, 2006; O'Donnell & Webb, 2003; O'Donnell et al., 2016). It has been demonstrated that patients with COPD have a high neural respiratory drive, which is worsened during an exacerbation (Jolley et al., 2015; Murphy et al., 2011; Suh et al., 2015).

The medulla co-ordinates both the voluntary and involuntary demands upon the respiratory system to generate of the respiratory pattern (Horn & Waldrop, 1998; Kinkead et al., 2014; Lopez-Barneo et al., 2008; Lumb, 2017; Masaoka & Homma,

2001). The outflow from the medulla results in the neural respiratory drive and as the load on the respiratory system increases, neural respiratory drive also increases (Druz & Sharp, 1982; Faisal et al., 2016; Jolley et al., 2015; Jolley et al., 2009; Luo et al., 2011; Reilly et al., 2013; Sinderby et al., 2001).

In humans the central neural drive of the brainstem respiratory centre cannot be directly measured however the neural signal to the muscles of respiration can be measured either at the level of the diaphragm or at the level of the parasternal intercostal muscles (Jolley et al., 2009; Murphy et al., 2011; Petit et al., 1960; Sinderby et al., 2001). The diaphragmatic electromyogram (EMG) can be recorded using a multipair electrode catheter placed via the oesophagus and is a well-validated measure of neural respiratory drive in COPD (A De Troyer et al., 1997; Druz & Sharp, 1982; Gorini et al., 1990; Luo et al., 2001; Luo & Moxham, 2005; Luo et al., 2008; Sinderby et al., 2001). However, diaphragmatic measurements are invasive (Jolley et al., 2009; Luo et al., 2008; Steier et al., 2010). The parasternal intercostal muscles have a much smaller bulk than the diaphragm and are activated simultaneously (De Troyer, 1984; De Troyer & Estenne, 1984; De Troyer & Sampson, 1982). Surface electrodes measuring EMG over the parasternal muscles is thus an alternative to diaphragmatic measurements (Hudson et al., 2010; Maarsingh et al., 2000). Parasternal EMG has been demonstrated to be a reproducible and well tolerated technique to assess neural respiratory drive (Duiverman et al., 2004; Maarsingh et al., 2006; Maarsingh et al., 2002; Reilly et al., 2012; Reilly et al., 2013; Reilly et al., 2011; Steier et al., 2011), particularly for patients with an exacerbation of COPD (Murphy et al., 2011; Suh et al., 2015).

The raw EMG signal depends on the size, type, depth of the muscle as well as the quality of the signal measured. The signal requires processing allow physiologically meaningful comparisons. The root mean square quantifies the intensity and duration of the contraction and has been shown to be linearly associated with increasing load on the muscle (Fridlund & Cacioppo, 1986; Fukuda et al., 2010). The root mean square of the parasternal EMG has been shown to have a high degree of correlation with the trans-oesophageal diaphragmatic EMG (Wu et al., 2017).

Additional measures to quantify the neural respiratory drive are the percentage of the EMG signal of the maximum EMG signal obtained ($EMG_{paramax\%}$) and the neural respiratory drive index (NRDI) (Murphy et al., 2011). The NRDI is the product of $EMG_{paramax\%}$ and the respiratory rate (equation 4.17) (Murphy et al., 2011). NRDI is a validated measure of work of breathing during an acute exacerbation and allows changes in work of breathing over time to be documented (Murphy et al., 2011; Suh et al., 2015).

$$NRDI = RMS\ EMG_{paramax\%} * RR \qquad [Eq\ 4.17]$$

Equation 4.17: Neural respiratory drive index (NRDI). RMS $EMG_{paramax\%}$ is the root mean square of the parasternal muscles as a percentage of maximum effort, RR is the respiratory rate (Murphy et al., 2011).

The acquisition of surface EMG can be problematic. The signal quality will depend upon quality of electrode contact with the skin, interference from other physiological electrical activity and from external electrical sources. The frequencies of the ECG and EMG overlap and consequently the ECG signal cannot be completely removed, however high-pass filtering at 20Hz does reduce cardiac artefact (Luo et al., 2008). Other voluntary and involuntary muscle activity from adjacent muscles can also cause interference (Ramsook et al., 2017). It is important to have the subject at rest with head, torso and arms appropriately supported. Electrical artefacts are common within critical care, although many of the actively transmitting devices have frequencies in the MHz-GHz range, (Lapinsky & Easty, 2006) however power line artefact occurs at 50Hz and can cause significant noise if cables are not shielded (Luo et al., 2008).

4.4.2 Methods

Following identification of the second intercostal space at the sternal edge by bony landmarks and skin preparation, wet gel electrodes (Neuroline 720, Ambu, Denmark) were connected via standard ECG leads to a high differential amplifier with band pass filters set at 10Hz and 2000Hz and an analogue 50Hz notch filter (1902, Cambridge

Electronic Design, Cambridge, UK). Amplified analogue signals were converted to digital signals (Powerlab, ADInstruments, Chalgrove, UK) attached to a computer. Digital filtering and post-processing occurred after data acquisition (LabChart v8.1, ADInstruments, Chalgrove, UK).

The following steps occurred to collect data:

- The USB cable was connected to the laptop.
- The EMG equipment was turned on.
- The encrypted laptop was then turned on.
- The second intercostal space was identified using bony landmarks.
- Skin was prepared with EMG contact gel (Nuprep, DO Weaver and Co, USA) and then wiped with alcoholic chlorhexidine swabs.
- Single use wet gel electrodes (Neuroline 720, Ambu, Denmark) were placed adjacent to the sternal edge in the second intercostal spaces and the shoulder.
- Electrodes were attached the shoulder (green), left 2nd intercostal space (white) and right 2nd intercostal space (black)
- Recordings were taken with the patient in bed seated at 30-45 degrees to the horizontal with arms and head supported and relaxed. The patient was instructed to breathe normally but not to talk or make any movements.
- LabChart7 (ADInstruments, Colorado, USA) was opened.
- A new file was created using a standardised format: COPD(study number) EMG (day number of recording).
- Channel settings were as follows:
    - Channel 1 set to 2V
    - Channel 3 set to 2mV, bioamp with high pass digital filter cut off at 20Hz.
    - Channel 17 used for the root mean square (RMS) analysis – set to arithmetic and equation 4.18 was used.
- The patient was encouraged to relax and then repositioned until the baseline signal in channel 17 was approximately 10 microvolts.

- Airflow was measured with a pneumotachograph connected to the Y-piece of the ventilator providing non-invasive ventilation.
- At the beginning and end of the recording patients were asked to sniff or take a maximal breath (depending on what they could tolerate) to provide a maximal signal. The measurement was repeated twice.
- Data was recorded for 5 minutes of quiet respiration.
- Data was backed up to an encrypted USB and transferred to an encrypted laptop for further processing.

4.4.2.1 Data Analysis

EMG signals were analysed in Labchart Reader (v8.1.8, ADInstruments, Chalgrove, UK). EMG_{para} signals were analysed using the root mean squared (RMS) of the raw EMG_{para} signal with a 40ms moving window. Signals were then normalised to the maximum RMS EMG_{para} value (RMS $EMG_{paramax}$). RMS $EMG_{paramax}$ was measured by selecting the RMS EMG_{para} during the maximum inspiratory effort manoeuvre. The maximum RMS of the EMG was measured for each breath by selecting the RMS EMG_{para} manually for each breath over a period of 1 minute (Murphy et al., 2011). The RMS $EMG_{paramax\%}$ was calculated as the mean maximum RMS EMG_{para} per breath as a percentage of RMS $EMG_{paramax}$. Dr Patrick Murphy taught me the technique and we undertook the analysis of one patient independently. This formed the basis of a rating of the inter-rater reliability. The NRDI was subsequently calculated per minute (equation 4.17) (Murphy et al., 2011).

4.4.2.2 Ethical approval

The trial protocol was approved by the Cambridge NHS Human Research Authority Research Ethics Committee (14/EE/0109).

4.4.2.3 Statistical analysis

Statistical analysis was performed using Prism 9.5.1 for Mac (GraphPad, San Diego, USA). All data is presented as median (inter-quartile range). Data was compared

within and between the two groups grouped at 0-23 hours, 24-48 hours and 49-120 hours. Inter-rater reliability was assessed using a Bland-Altman plot.

4.4.3 Results

There were 8 patients in the NIV group and 8 patients in the $ECCO_2R$ group who underwent parasternal EMG measurements, however only 5 of the patients in the NIV group and 7 in the $ECCO_2R$ group had EMG data which was interpretable due to significant electrical noise (figure 3.2, table 4.9). Measurements were taken daily whilst patients were on therapy. Inter- and intra-group comparisons were between the NIV and $ECCO_2R$ groups at 0-23 hours, 24-28 hours and 49-120 hours. Intra-group comparisons between NIV with $ECCO_2R$ and $ECCO_2R$ alone used paired data.

4.4.3.1 Demographics

Patient characteristics at baseline and who underwent EIT measurements are displayed in table 4.12. All patients had severe COPD. Patients in both groups were comparable, however baseline respiratory rate was higher with $ECCO_2R$ (24 (20-25) vs 30 (29-34) breaths/min).

	NIV (n=5/9)	$ECCO_2R$ (n=7/9)
Demographic data		
Age (years)	66 (61-78)	65 (62.5-70.5)
BMI (kg/m^2)	19.4 (19.4-23.5)	24.7 (24.2-29.5)
Sex (F)	0	4
FEV1 (L)	0.59 (0.55-1.66)	0.97 (0.825-1.32)
FEV1 (% predicted) (%)	2.41 (1.13-3.41)	2.6 (1.825-3.21)
FVC (L)	21 (19-50)	39.8 (39-44.5)
FVC (% predicted) (%)	63 (32-118)	82 (71.45-87)
FEV1/FVC	48 (31-48)	44 (37-48)
GOLD stage	4 (2-4)	3 (3-3)
Baseline observations		
Systolic Blood pressure (mmHg)	115 (105-120)	130 (118-140)
Respiratory rate (breaths/min)	24 (20-25)	30 (29-34)
SpO_2 (%)	92 (90-92)	91 (88-94)
Heart rate (beats/min)	102 (100-113)	109 (96-118)
Presenting arterial blood gas		
PaO_2 (kPa)	9.69 (8.67-13.51)	7.39 (7.07-8.91)
$PaCO_2$ (kPa)	10.31 (9.18-12.11)	9.8 (9.03-9.86)
pH	7.23 (7.19-7.23)	7.26 (7.25-7.27)
HCO_3 (mmol/L)	31.4 (31-32.1)	29.7 (29.5-31.09)
Initial NIV settings		
EPAP (cmH_2O)	5 (5-5)	6 (6-7)
IPAP (cmH_2O)	15 (15-18)	18 (16-19)
FiO_2 (%)	28 (25-40)	35 (29-38)
Arterial blood gas after 1 hour NIV		
PaO_2 (kPa)	8.5 (8.1-9.1)	8.9 (7.8-9.2)
$PaCO_2$ (kPa)	9.2 (8.2-10.8)	8.9 (8.5-9.1)
pH	7.27 (7.23-7.27)	7.29 (7.27-7.28)
HCO_3 (mmol/L)	30.8 (29.1-32.3)	27.9 (27.8-29.1)

Table 4.14: Baseline demographics in the NIV and $ECCO_2R$ group who had pEMG measurements. All results are expressed as median (IQR). * $p<0.05$

4.4.3.2 Inter-group EMG results

The $EMG_{paramax\%}$ and NRDI are compared between the NIV and $ECCO_2R$ groups over time (table 4.15 and 4.16). There is a reduction in the numerical value of $EMG_{paramax\%}$ in the NIV group over time. There is a reduction in the NRDI over time in the NIV group. There were no changes in NRDI or $EMG_{paramax\%}$ over time in the $ECCO_2R$ group.

	NIV 0-23 hours	NIV 24-48 hours	NIV 49-120 hours
n	**6**	**5**	**1**
$EMG_{paramax\%}$ (%)	67.3 (66.3-72.4)	53.9 (42.1-69.3)	24.3 (24.3-24.3)
NRDI (AU)	1163.8 (1085.5-1325.5)	757.6 (724.6-869.9)	388.7 (388.7-388.7)

Table 4.15: Parasternal EMG data in the NIV group over time. $EMG_{paramax\%}$ is the percentage of the maximum EMG signal obtained and NRDI is the neural respiratory drive index. AU is arbitrary units.

	$ECCO_2R$ 0-23 hours	$ECCO_2R$ 24-48 hours	$ECCO_2R$ 49-120 hours
n	**7**	**6**	**6**
$EMG_{paramax\%}$ (%)	61.5 (45.4-74.6)	64.2 (42.8-71.4)	76.4 (45.7-81.2)
NRDI (AU)	1093.8 (885.7-1258.7)	1,213.7 (908.7-1441.5)	886.9 (814.9-1293.3)

Table 4.16: Parasternal EMG data in the $ECCO_2R$ group over time. $EMG_{paramax\%}$ is the percentage of the maximum EMG signal obtained and NRDI is the neural respiratory drive index. AU is arbitrary units.

4.4.3.3 Intra-group EMG results

The $EMG_{paramax\%}$ and NRDI are shown in table 4.12. There is a lower numerical value of $EMG_{paramax\%}$ using the combination of NIV and $ECCO_2R$ compared with using $ECCO_2R$ alone. There is a lower NRDI using the combination of NIV and $ECCO_2R$ compared with using $ECCO_2R$ alone in the NRDI over time in the NIV group.

	NIV & $ECCO_2R$	$ECCO_2R$
$EMG_{paramax\%}$ (%)	42.2 (33.4-54.5)	62.8 (43.7-74.7)
NRDI (AU)	884.4 (684.7-967.3)	1321.1 (903.3-1575.3)

Table 4.17: Parasternal EMG data comparing NIV with $ECCO_2R$ and $ECCO_2R$ alone. $EMG_{paramax\%}$ is the percentage of the maximum EMG signal obtained and NRDI is the neural respiratory drive index. AU is arbitrary units.

4.4.3.4 Inter-rater reliability

The inter-rater reliability was assessed using a Bland-Altman plot for simultaneous but independent measurements of the EMG_{para} (figure 4.8). Agreement is acceptable.

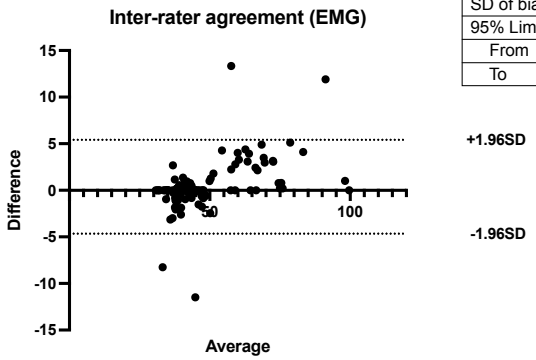

Bias	0.3781
SD of bias	2.570
95% Limits of Agreement	
From	-4.658
To	5.415

Figure 4.8: Bland-Altman plot of the inter-rater reliability of EMG_{para} measurements.

4.4.4 Discussion

The parasternal EMG results demonstrate that there is a reduction over time in the NRDI with NIV which is not demonstrated with $ECCO_2R$. There is a numerical reduction in $EMG_{paramax\%}$ with NIV and there is a numerical increase in $EMG_{paramax\%}$ with $ECCO_2R$. When comparing NIV with $ECCO_2R$ to $ECCO_2R$ alone, there is an increase in NRDI and $EMG_{paramax\%}$ when NIV is removed. Parasternal EMG and the neural respiratory drive index have been shown to be strongly correlated with neural respiratory drive (Duiverman et al., 2004; Maarsingh et al., 2006; Maarsingh et al., 2002; Reilly et al., 2012; Reilly et al., 2013; Reilly et al., 2011; Steier et al., 2011). In patients with an exacerbation of COPD a lack of improvement of both NRDI and $EMG_{paramax\%}$ has been associated with treatment non-responders and patients who are likely to be readmitted to hospital (Murphy et al., 2011; Suh et al., 2015).

These results suggest that the neural drive for patients with $ECCO_2R$ alone was higher than for patients with a combination of NIV and $ECCO_2R$ and therefore suggest that the addition of $ECCO_2R$ to positive pressure ventilation improved neural drive and hence inspiratory effort more than the clearance of CO_2 per se. It is also of note that

the subjective dyspnoea reported by patients fell with the commencement of $ECCO_2R$ (figure 3.4). Measurements of neural respiratory drive using parasternal EMG have correlated neuromechanical dissociation with symptomatic dyspnoea (Shah et al., 2022). This suggests that neuromechanical dissociation reduced with improvement in arterial partial pressure of CO_2 which occurred with the onset of $ECCO_2R$ (Moxham & Jolley, 2009).

4.4.4.1 Limitations

Limitations include the small numbers in the study – only 7/9 and 5/9 patients in the $ECCO_2R$ and NIV groups respectively had data available. This is due in part to patient refusal but also in part to electrical noise in the ICU environment making taking reliable measurements challenging. It is possible that the apparent differences between the two groups are impacted by the limited data which was available. It is possible that the baseline differences between the two groups impacted the inter-group comparisons. The respiratory rate in the NIV group was lower than that of the $ECCO_2R$ group – both the subset of those who had measurable EMG data and the total group (table 3.1 and 4.12). It is possible given the baseline difference that the $ECCO_2R$ group were a more unwell cohort despite the randomisation and this may have influenced the results.

4.4.4.2 Conclusions

Overall, the parasternal EMG results suggest that the neural respiratory drive remained stable with $ECCO_2R$, reduced over time with NIV and was improved with the combination of NIV and $ECCO_2R$ suggesting that a combination of direct CO_2 control and pressure support may be optimal.

4.5 Overall discussion and conclusions

The three different methods used in this thesis, i.e., EIT, oesophageal pressure and parasternal EMG are used to compare indices of work of breathing, regional distribution of ventilation and relative changes in lung volumes.

4.5.1 NIV alone

The oesophageal pressure measurements show that the work of breathing, PTP, P_{MUS}, dP_{ES} and TPP were lower on day 1 than day 2 in the NIV group. This is counter to the findings in the parasternal EMG data where the electrical signal - NRDI is higher on day 1 in the NIV group and then reduces with time. This paradoxical uncoupling between low inspiratory pressure generation but high parasternal accessory inspiratory muscle electrical activity, could be explained by a change in end-expiratory lung volume and diaphragmatic position. A hypothesis is that on admission, lung volume was high due to the high airway resistance and dynamic hyperinflation and is possible that these patients with severe AECOPD operated at end expiratory lung volumes closer to their total lung capacity. At these lung volumes, neural activation is generated by chemical stimulation and resistive work, but the inspiratory effort results in a limited transpulmonary pressure change. Neuromechanical dissociation has been shown to occur in the setting where dynamic hyperinflation increases lung volumes sufficiently to flatten the diaphragm and shorten the intercostal muscles resulting in greater neural drive which are not able to be met by the generation of muscular pressure (James et al., 2022; Moxham & Jolley, 2009; O'Donnell, 2006; O'Donnell et al., 2020; Sinderby et al., 2001). Neuromechanical dissociation is also known to contribute to dyspnoea (O'Donnell, 2006; Shah et al., 2022). The NIV group were symptomatically dyspnoeic and the non-concordance between the PTP and work of breathing in this group supports the concept of neuromechanical dissociation. Overall, the EIT indices in the NIV group suggest that over time there is improving aeration and tidal ventilation with maintenance of homogeneity of aeration the lung with and minimal regional differences. This is in keeping with the findings from the oesophageal pressure. It is important to recognise that the basis of EIT is the change in impedance during a

breath and over time (Adler et al., 2009; Frerichs, Amato, et al., 2016). Consequently, the lower dEELI, TID and dTID found on day 1 in the NIV group are in keeping with the proposition that patients had hyperinflation with limited tidal ventilation and measured work. As dynamic hyperinflation eased over day 2 and 3, TID and dEELI increased. A lack of intra-tidal change can also explain the lower SURF on day 1 than day 3 as SURF is also a relative rather than absolute measure.

4.5.2 $ECCO_2R$ alone

The findings of $ECCO_2R$ over time are also consistent among the three groups. In the oesophageal pressure group, the TPP, P_{MUS} dP_{ES} all decreased whilst the work of breathing and PTP remained relatively stable, with a small increase in the PTP/minute and WOB/minute. This is in keeping with the parasternal EMG findings where the NRDI remained relatively static over the same period. This broad correlation between the two methods suggests that there was no clear evidence of neuromechanical dissociation in this group (James et al., 2022; Moxham & Jolley, 2009; O'Donnell, 2006; O'Donnell et al., 2020; Sinderby et al., 2001). The reduction in reported dyspnoea with the onset of $ECCO_2R$ supports this given the relationship between dyspnoea and neuromechanical dissociation discussed above (O'Donnell, 2006). Overall, the EIT indices in the $ECCO_2R$ group over time suggest that controlling CO_2 without pressure support led to a movement of the ventilation dorsally with an increase in inhomogeneity and an increase in end-expiratory lung volume but maintenance of tidal ventilation suggesting that there was a degree of dynamic hyperinflation. This is in keeping with the disparity between PTP and work of breathing in the $ECCO_2R$ group which suggested that isometric contraction was required to overcome intrinsic PEEP.

4.5.3 Combination of $ECCO_2R$ and NIV

The comparison between the combination of NIV and $ECCO_2R$ with $ECCO_2R$ alone for oesophageal pressure data suggested that the impact was additive with a higher dP_{ES}, TPP, P_{MUS}, work of breathing and PTP for $ECCO_2R$ alone than with the combination. This is concordant with the parasternal EMG data where the addition of NIV was associated with a decrease in the NRDI. The concordance between the two

measurements suggests that the neural drive was matched by the increase in mechanical work and that neuromechanical dissociation is unlikely. The EIT data suggests that NIV provides results in a more homogenous distribution of ventilation and allows for overall greater aeration than $ECCO_2R$ alone. The data also suggests that ventilation is more balanced within the chest in both the ventral/dorsal plane as well as the right/left plane with NIV and $ECCO_2R$ compared with $ECCO_2R$, suggesting that there is an additive impact of NIV with $ECCO_2R$. Interestingly dEELI decreased with the removal of NIV suggesting that there was a lower end expiratory volume. This is in keeping with the finding that intrinsic PEEP was lower off NIV and that there was better concordance between work of breathing/minute and PTP/minute suggesting that there was less isometric contraction. Overall, these data suggests that the combination of NIV and $ECCO_2R$ resulted in a lower work of breathing and drive with more homogenous ventilation and therefore that the combination of the two support modalities was beneficial.

4.5.4 Conclusion

The clinical and physiological data supports the hypothetical impact of $ECCO_2R$ described in figure 4.1. The clinical and physiological data supports different but complementary impacts of NIV and $ECCO_2R$ in patients with AECOPD. NIV provided direct respiratory support but during the early phase of the exacerbation patients remained at end expiratory lung volumes close to total lung capacity and were unable to generate dP_{ES} or provide aeration of the lungs resulting in isometric contraction and neuromechanical dissociation. Over time as the exacerbation started to resolve, the ongoing physical support with NIV resulted in improved aeration which was homogenously distributed across the lung. As hyperinflation reduced, higher muscular pressures were able to be generated, acidosis was corrected, and the sensation of dyspnoea reduced. $ECCO_2R$ removed CO_2 from the venous blood and allowed an early reduction in dyspnoea with reduced respiratory rate, lowered dynamic hyperinflation and improved neuromechanical dissociation and isometric work. However, over time the physiological variables measured in the $ECCO_2R$ group remained relatively static with more inhomogeneous aeration, persisting hyperinflation, persistent neural drive and elevated work of breathing.

The combination of $ECCO_2R$ and NIV allowed elimination of a proportion of the metabolic CO_2 and a reduction in the requirements of alveolar ventilation and results in a lower work of breathing, lower neural respiratory drive, less dyspnoea and more homogenously distributed ventilation.

Conclusion

This thesis has considered multiple aspects of $ECCO_2R$ from bench to bedside, including the physiology of membrane gas exchange, the risks and benefits of $ECCO_2R$ in patients with exacerbations of COPD and the impact of $ECCO_2R$ on respiratory physiology. The bench and basic membrane work has shown that in both in vivo and in vitro CO_2 removal from the device with a 400mL blood flow is clinically relevant, that there is a plateau in CO_2 removal from the device and that the CO_2 clearance reported by the device is accurate. These are both clinically relevant findings which have now been published. The results from the clinical trial are the first results from a prospective randomised controlled trial. The key differences were improvements in respiratory rate, pH, $PaCO_2$ and in patient sensations of dyspnoea with $ECCO_2R$, however ICU and hospital length of stay were longer with $ECCO_2R$ and mortality, which the trial was not powered for, was no different. The physiological studies demonstrated that there are differential physiological effects for NIV and $ECCO_2R$ individually with additive effects when NIV and $ECCO_2R$ are used simultaneously. NIV provides mechanical support for breathing and allows the patient time to recover but with severe exacerbations persisting dynamic hyperinflation can result in neuromechanical dissociation. The addition of $ECCO_2R$ to the NIV allows elimination of a proportion of the metabolic CO_2 and a reduction in the requirements of alveolar ventilation. This results in the resolution of the neuromechanical dissociation, improves dyspnoea and allows better aeration of the lungs. $ECCO_2R$ alone without NIV results in a higher work of breathing and muscular effort but maintains concordance between respiratory drive and muscular effort.

Taken together, this thesis has demonstrated the degree and regulation of gas exchange across a specific $ECCO_2R$ device and explored its efficiency of gas exchange. The use of $ECCO_2R$ has led to improvements in key clinical markers including respiratory acidosis and symptomatic dyspnoea and has reduced neuromechanical dissociation. It appears that the combination of NIV and $ECCO_2R$ is likely to lead to the greatest physiological and potentially clinical benefits for patients. This potential

benefit appears to be recognised by patients who have requested $ECCO_2R$ on subsequent admissions with AECOPD.

My period as a part-time post-graduate student has been stimulating and challenging in several anticipated and unanticipated ways. I have been Clinical Lead for ICU since 2018 and more recently Clinical Director for Pulmonary, Adult Critical Care and Sleep at Guy's and St Thomas' NHS Foundation Trust giving me a significant managerial burden in addition to my clinical and research duties. I have also had the unanticipated additional burden of leading critical care during the COVID-19 pandemic. As the trial coincided with the REST trial which used the same device and circuit, there were issues with the timeliness of supply of the disposables which impacted the timeliness of at least one patient having access to therapy. The pandemic impacted this work significantly. The original clinical trial was designed to enrol 24 patients, 12 in each treatment limb. With the onset of the pandemic enrolment to clinical trials involving non-COVID patients ceased in the NHS so that urgent and necessary COVID-19 research could be carried out as quickly as possible. This was especially true for studies based in the ICU. In addition, patients without COVID-19 were encouraged not to seek hospital care unless necessary. Furthermore, patients with severe COPD in the UK were asked to shield for nearly 2 years, many continued to shield afterwards, and this has impacted the presentation of patients with acute exacerbations to the hospital. As a group these patients are difficult to include in research given the extremis in which they present and the fact that they commonly lack capacity at presentation meaning that consultee assent is often required. This added an additional barrier to recruitment as families tend to be more conservative about their family members being included in trials than patients are. All in all, I was delighted that I gained as much data from patients as I did. I gained significantly during the PhD by learning new techniques, especially electrical impedance tomography, parasternal electromyography and oesophageal pressure.

The work I have undertaken will lead into other areas of exploration relating to my clinical interests. The question of the clinical role of $ECCO_2R$ continues to be an open research question, both in COPD and ARDS with the flow rates and amount of extracorporeal CO_2 removal being key questions. There is also additional growing

interest in using $ECCO_2R$ in a way analogous to renal dialysis – a sort of "respiratory dialysis". The aim is to remove as much CO_2 from non-blood CO_2 stores as possible (mainly muscle and bones) so that most of the CO_2 accumulated in the interdialytic time is served to replenish such stores and will not impact dissolved CO_2. This is likely to represent a potentially useful addition to NIV in patients who are NIV dependent or are poorly controlled with NIV. There is also the question about the optimal patient – other groups including post-pneumonectomy patients may well benefit. In terms of the physiological techniques, there is significant scope for using them in the ICU, especially in patients on ECMO where optimal lung protective ventilation on respiratory ECMO and weaning from respiratory ECMO are both key questions that would be well suited to physiological research.

References

Abdo, W. F., & Heunks, L. M. (2012). Oxygen-induced hypercapnia in COPD: myths and facts. *Crit Care*, *16*(5), 323. https://doi.org/10.1186/cc11475

Abrams, D., & Brodie, D. (2013). Emerging indications for extracorporeal membrane oxygenation in adults with respiratory failure. *Ann Am Thorac Soc*, *10*(4), 371-377. https://doi.org/10.1513/AnnalsATS.201305-113OT

Abroug, F., Ouanes-Besbes, L., Hammouda, Z., Benabidallah, S., Dachraoui, F., Ouanes, I., & Jolliet, P. (2017). Noninvasive ventilation with helium-oxygen mixture in hypercapnic COPD exacerbation: aggregate meta-analysis of randomized controlled trials. *Ann Intensive Care*, *7*(1), 59. https://doi.org/10.1186/s13613-017-0273-6

Adler, A., Amyot, R., Guardo, R., Bates, J. H., & Berthiaume, Y. (1997). Monitoring changes in lung air and liquid volumes with electrical impedance tomography. *J Appl Physiol (1985)*, *83*(5), 1762-1767.

Adler, A., Arnold, J. H., Bayford, R., Borsic, A., Brown, B., Dixon, P., Faes, T. J., Frerichs, I., Gagnon, H., Garber, Y., Grychtol, B., Hahn, G., Lionheart, W. R., Malik, A., Patterson, R. P., Stocks, J., Tizzard, A., Weiler, N., & Wolf, G. K. (2009). GREIT: a unified approach to 2D linear EIT reconstruction of lung images. *Physiol Meas*, *30*(6), S35-55. https://doi.org/10.1088/0967-3334/30/6/s03

Adler, D., & Janssens, J. P. (2019). The Pathophysiology of Respiratory Failure: Control of Breathing, Respiratory Load, and Muscle Capacity. *Respiration*, *97*(2), 93-104. https://doi.org/10.1159/000494063

Agostoni, E., & Hyatt, R. (1986). Static behavior of the respiratory system. In A. Fishman, P. Macklem, & J. Mead (Eds.), *Handbook of physiology* (pp. 113–130). American Physiological Society.

Akoumianaki, E., Maggiore, S. M., Valenza, F., Bellani, G., Jubran, A., Loring, S. H., Pelosi, P., Talmor, D., Grasso, S., Chiumello, D., Guerin, C., Patroniti, N., Ranieri, V. M., Gattinoni, L., Nava, S., Terragni, P. P., Pesenti, A., Tobin, M., Mancebo, J., & Brochard, L. (2014). The application of esophageal pressure

measurement in patients with respiratory failure. *Am J Respir Crit Care Med*, *189*(5), 520-531. https://doi.org/10.1164/rccm.201312-2193CI

Al-Rawas, N., Banner, M. J., Euliano, N. R., Tams, C. G., Brown, J., Martin, A. D., & Gabrielli, A. (2013). Expiratory time constant for determinations of plateau pressure, respiratory system compliance, and total resistance. *Crit Care*, *17*(1), R23. https://doi.org/10.1186/cc12500

Alessandri, F., Tonetti, T., Pistidda, L., Busani, S., Borrazzo, C., Fanelli, V., Polzoni, M., Piazza, O., Lorini, L., Cattaneo, S., Ricci, D., Zanoni, A., Girardis, M., Terragni, P., Tempesta, M., Di Luca, M., Pugliese, F., & Ranieri, V. M. (2023). Extracorporeal CO 2 Removal During Renal Replacement Therapy to Allow Lung-Protective Ventilation in Patients With COVID-19-Associated Acute Respiratory Distress Syndrome. *Asaio j*, *69*(1), 36-42. https://doi.org/10.1097/mat.0000000000001803

Ankjaergaard, K. L., Maibom, S. L., & Wilcke, J. T. (2016). Long-term non-invasive ventilation reduces readmissions in COPD patients with two or more episodes of acute hypercapnic respiratory failure. *Eur Clin Respir J*, *3*, 28303. https://doi.org/10.3402/ecrj.v3.28303

Ankjaergaard, K. L., Rasmussen, D. B., Schwaner, S. H., Andreassen, H. F., Hansen, E. F., & Wilcke, J. T. (2017). COPD: Mortality and Readmissions in Relation to Number of Admissions with Noninvasive Ventilation. *Copd*, *14*(1), 30-36. https://doi.org/10.1080/15412555.2016.1181160

Ankjaergaard, K. L., Tonnesen, P., Laursen, L. C., Hansen, E. F., Andreassen, H. F., & Wilcke, J. T. (2016). Home Non Invasive Ventilation (NIV) treatment for COPD patients with a history of NIV-treated exacerbation; a randomized, controlled, multi-center study. *BMC Pulm Med*, *16*, 32. https://doi.org/10.1186/s12890-016-0184-6

Annat, G. J., Viale, J. P., Dereymez, C. P., Bouffard, Y. M., Delafosse, B. X., & Motin, J. P. (1990). Oxygen cost of breathing and diaphragmatic pressure-time index. Measurement in patients with COPD during weaning with pressure support ventilation. *Chest*, *98*(2), 411-414.

Anzueto, A. (2009). Impact of exacerbations on COPD. *Eur Respir Rev*, *19*(116), 113-118.

Anzueto, A., Leimer, I., & Kesten, S. (2009). Impact of frequency of COPD exacerbations on pulmonary function, health status and clinical outcomes. *Int J Chron Obstruct Pulmon Dis*, *4*, 245-251.

Appendini, L., Patessio, A., Zanaboni, S., Carone, M., Gukov, B., & Donner, C. (1994). Physiologic effects of positive endexpiratory pressure and mask pressure support during exacerbations of chronic obstructive pulmonary disease. *Am J Respir Crit Care Med*, *149*(5), 1069–1076.

Arazawa, D. T., Kimmel, J. D., Finn, M. C., & Federspiel, W. J. (2015). Acidic sweep gas with carbonic anhydrase coated hollow fiber membranes synergistically accelerates CO2 removal from blood. *Acta Biomater*, *25*, 143-149. https://doi.org/10.1016/j.actbio.2015.07.007

ARDSNET. (2000). Ventilation with Lower Tidal Volumes as Compared with Traditional Tidal Volumes for Acute Lung Injury and the Acute Respiratory Distress Syndrome. *New England Journal of Medicine*, *342*(18), 1301-1308. https://doi.org/10.1056/nejm200005043421801

Arthurs, G. J., & Sudhakar, M. (2005). Carbon dioxide transport. *Continuing Education in Anaesthesia, Critical Care & Pain*, *5*(6), 207-210.

Arvaniti, K., Lathyris, D., Blot, S., Apostolidou-Kiouti, F., Koulenti, D., & Haidich, A. B. (2017). Cumulative Evidence of Randomized Controlled and Observational Studies on Catheter-Related Infection Risk of Central Venous Catheter Insertion Site in ICU Patients: A Pairwise and Network Meta-Analysis. *Crit Care Med*, *45*(4), e437-e448. https://doi.org/10.1097/ccm.0000000000002092

ATS. (1999). Dyspnea. Mechanisms, assessment, and management: a consensus statement. American Thoracic Society. *Am J Respir Crit Care Med*, *159*(1), 321-340. https://doi.org/10.1164/ajrccm.159.1.ats898

Aubier, M., Murciano, D., Milic-Emili, J., Touaty, E., Daghfous, J., Pariente, R., & Derenne, J. P. (1980). Effects of the administration of O2 on ventilation and blood gases in patients with chronic obstructive pulmonary disease during

acute respiratory failure. *Am Rev Respir Dis*, *122*(5), 747-754. https://doi.org/10.1164/arrd.1980.122.5.747

Austin, M. A., Wills, K. E., Blizzard, L., Walters, E. H., & Wood-Baker, R. (2010). Effect of high flow oxygen on mortality in chronic obstructive pulmonary disease patients in prehospital setting: randomised controlled trial. *Bmj*, *341*, c5462.

Baldwin, E. D., Cournand, A., & Richards, D. W., Jr. (1948). Pulmonary insufficiency; physiological classification, clinical methods of analysis, standard values in normal subjects. *Medicine (Baltimore)*, *27*(3), 243-278.

Balleza, M., Calaf, N., Feixas, T., Gonzalez, M., Anton, D., Riu, P. J., & Casan, P. (2009). [Measuring breathing pattern in patients with chronic obstructive pulmonary disease by electrical impedance tomography]. *Arch Bronconeumol*, *45*(7), 320-324. https://doi.org/10.1016/j.arbres.2009.01.013 (Medicion del patron ventilatorio mediante tomografia por impedancia electrica en pacientes con EPOC.)

Balleza-Ordaz, M., Perez-Alday, E., Vargas-Luna, M., & Riu, J. (2015). Tidal volume monitoring by electrical impedance tomography (EIT) using different regions of interest (ROI): Calibration equations. *Biomedical Signal Processing and Control*, *18*, 102-109.

Banner, M., & Lampotang, S. (1988). Clinical use of inspiratory and expiratory

waveforms. In R. Kacmarek & J. Stoller (Eds.), *Current Respiratory Care.* (pp. 137). Decker.

Banner, M. J., Jaeger, M. J., & Kirby, R. R. (1994). Components of the work of breathing and implications for monitoring ventilator-dependent patients. *Crit Care Med*, *22*(3), 515-523. https://doi.org/10.1097/00003246-199403000-00024

Barbera, J. A., Roca, J., Ferrer, A., Felez, M. A., Diaz, O., Roger, N., & Rodriguez-Roisin, R. (1997). Mechanisms of worsening gas exchange during acute exacerbations of chronic obstructive pulmonary disease. *Eur Respir J*, *10*(6), 1285-1291.

Barrett, N. A., & Camporota, L. (2017). The evolving role and practical application of extracorporeal carbon dioxide removal in critical care. *Crit Care Resusc*, *19*(Suppl 1), 62-67.

Barrett, N. A., Hart, N., & Camporota, L. (2019). Assessment of Work of Breathing in Patients with Acute Exacerbations of Chronic Obstructive Pulmonary Disease. *Copd*, *16*(5-6), 418-428. https://doi.org/10.1080/15412555.2019.1681390

Barrett, N. A., Hart, N., & Camporota, L. (2020a). In vivo carbon dioxide clearance of a low-flow extracorporeal carbon dioxide removal circuit in patients with acute exacerbations of chronic obstructive pulmonary disease. *Perfusion*, *35*(5), 436-441. https://doi.org/10.1177/0267659119896531

Barrett, N. A., Hart, N., & Camporota, L. (2020b). In-vitro performance of a low flow extracorporeal carbon dioxide removal circuit. *Perfusion*, *35*(3), 227-235. https://doi.org/10.1177/0267659119865115

Barrett, N. A., Hart, N., Daly, K. J. R., Marotti, M., Kostakou, E., Carlin, C., Lua, S., Singh, S., Bentley, A., Douiri, A., & Camporota, L. (2022). A randomised controlled trial of non-invasive ventilation compared with extracorporeal carbon dioxide removal for acute hypercapnic exacerbations of chronic obstructive pulmonary disease. *Ann Intensive Care*, *12*(1), 36. https://doi.org/10.1186/s13613-022-01006-8

Barrett, N. A., Kostakou, E., Hart, N., Douiri, A., & Camporota, L. (2019). Extracorporeal carbon dioxide removal for acute hypercapnic exacerbations of chronic obstructive pulmonary disease: study protocol for a randomised controlled trial. *Trials*, *20*(1), 465. https://doi.org/10.1186/s13063-019-3548-4

Bartlett, R. H. (2017). Physiology of Gas Exchange During ECMO for Respiratory Failure. *J Intensive Care Med*, *32*(4), 243-248. https://doi.org/10.1177/0885066616641383

Batchinsky, A. I., Jordan, B. S., Regn, D., Necsoiu, C., Federspiel, W. J., Morris, M. J., & Cancio, L. C. (2011). Respiratory dialysis: reduction in dependence on

mechanical ventilation by venovenous extracorporeal CO2 removal. *Crit Care Med*, *39*(6), 1382-1387.

Baydur, A., Behrakis, P. K., Zin, W. A., Jaeger, M., & Milic-Emili, J. (1982). A simple method for assessing the validity of the esophageal balloon technique. *Am Rev Respir Dis*, *126*(5), 788-791. https://doi.org/10.1164/arrd.1982.126.5.788

Bayford, R. (2006). Bioimpedance tomography (electrical impedance tomography). *Annual review of biomedical engineering*, *8*, 63-91.

Bayford, R., & Tizzard, A. (2012). Bioimpedance imaging: an overview of potential clinical applications. *Analyst*, *137*(20), 4635-4643. https://doi.org/10.1039/c2an35874c

Becher, T., Kott, M., Schadler, D., Vogt, B., Meinel, T., Weiler, N., & Frerichs, I. (2015). Influence of tidal volume on ventilation inhomogeneity assessed by electrical impedance tomography during controlled mechanical ventilation. *Physiol Meas*, *36*(6), 1137-1146. https://doi.org/10.1088/0967-3334/36/6/1137

Becher, T., Vogt, B., Kott, M., Schadler, D., Weiler, N., & Frerichs, I. (2016). Functional Regions of Interest in Electrical Impedance Tomography: A Secondary Analysis of Two Clinical Studies. *PLoS One*, *11*(3), e0152267. https://doi.org/10.1371/journal.pone.0152267

Bein, T., Weber, F., Philipp, A., Prasser, C., Pfeifer, M., Schmid, F. X., Butz, B., Birnbaum, D., Taeger, K., & Schlitt, H. J. (2006). A new pumpless extracorporeal interventional lung assist in critical hypoxemia/hypercapnia. *Crit Care Med*, *34*(5), 1372-1377.

Bein, T., Zimmermann, M., Hergeth, K., Ramming, M., Rupprecht, L., Schlitt, H. J., & Slutsky, A. S. (2009). Pumpless extracorporeal removal of carbon dioxide combined with ventilation using low tidal volume and high positive end-expiratory pressure in a patient with severe acute respiratory distress syndrome. *Anaesthesia*, *64*(2), 195-198.

Bellani, G., & Pesenti, A. (2014). Assessing effort and work of breathing. *Curr Opin Crit Care*, *20*(3), 352-358. https://doi.org/10.1097/mcc.0000000000000089

Benditt, J. O. (2005). Esophageal and gastric pressure measurements. *Respir Care*, *50*(1), 68-75; discussion 75-77.

Bhowmik, A., Seemungal, T. A., Sapsford, R. J., & Wedzicha, J. A. (2000). Relation of sputum inflammatory markers to symptoms and lung function changes in COPD exacerbations. *Thorax*, *55*(2), 114-120. https://doi.org/10.1136/thorax.55.2.114

Blanch, L., Bernabe, F., & Lucangelo, U. (2005). Measurement of air trapping, intrinsic positive end-expiratory pressure, and dynamic hyperinflation in mechanically ventilated patients. *Respir Care*, *50*(1), 110-123; discussion 123-114.

Bland, J. M., & Altman, D. G. (1986). Statistical methods for assessing agreement between two methods of clinical measurement. *Lancet*, *1*(8476), 307-310.

Blankman, P., Hasan, D., Bikker, I. G., & Gommers, D. (2016). Lung stress and strain calculations in mechanically ventilated patients in the intensive care unit. *Acta Anaesthesiol Scand*, *60*(1), 69-78. https://doi.org/10.1111/aas.12589

Bodenstein, M., David, M., & Markstaller, K. (2009). Principles of electrical impedance tomography and its clinical application. *Crit Care Med*, *37*(2), 713-724. https://doi.org/10.1097/CCM.0b013e3181958d2f

Bohr, C. (1891). U¨ ber die Lungeatmung. *Skand Arch Physiol*, *2*, 236-238 (Article in German).

Bouferrache, K., & Vieillard-Baron, A. (2011). Acute respiratory distress syndrome, mechanical ventilation, and right ventricular function. *Curr Opin Crit Care*, *17*(1), 30-35. https://doi.org/10.1097/MCC.0b013e328342722b

Bourgoin, P., Baudin, F., Brossier, D., Emeriaud, G., Wysocki, M., & Jouvet, P. (2017). Assessment of Bohr and Enghoff Dead Space Equations in Mechanically Ventilated Children. *Respir Care*, *62*(4), 468-474. https://doi.org/10.4187/respcare.05108

Brandolese, R., Broseghini, C., Polese, G., Bernasconi, M., Brandi, G., Milic-Emili, J., & Rossi, A. (1993). Effects of intrinsic PEEP on pulmonary gas exchange in mechanically-ventilated patients. *Eur Respir J*, *6*(3), 358-363.

Braune, S., Burchardi, H., Engel, M., Nierhaus, A., Ebelt, H., Metschke, M., Rosseau, S., & Kluge, S. (2015). The use of extracorporeal carbon dioxide removal to avoid intubation in patients failing non-invasive ventilation--a cost analysis. *BMC Anesthesiol*, *15*, 160. https://doi.org/10.1186/s12871-015-0139-0

Braune, S., Sieweke, A., Brettner, F., Staudinger, T., Joannidis, M., Verbrugge, S., Frings, D., Nierhaus, A., Wegscheider, K., & Kluge, S. (2016). The feasibility and safety of extracorporeal carbon dioxide removal to avoid intubation in patients with COPD unresponsive to noninvasive ventilation for acute hypercapnic respiratory failure (ECLAIR study): multicentre case-control study. *Intensive Care Med*, *42*(9), 1437-1444. https://doi.org/10.1007/s00134-016-4452-y

Brochard, L. (2002). Intrinsic (or auto-) positive end-expiratory pressure during spontaneous or assisted ventilation. *Intensive Care Med*, *28*(11), 1552-1554.

Brochard, L. (2014). Measurement of esophageal pressure at bedside: pros and cons. *Curr Opin Crit Care*, *20*(1), 39-46. https://doi.org/10.1097/mcc.0000000000000050

Brochard, L., Harf, A., Lorino, H., & Lemaire, F. (1989). Inspiratory pressure support prevents diaphragmatic fatigue during weaning from mechanical ventilation. *Am Rev Respir Dis*, *139*(2), 513-521. https://doi.org/10.1164/ajrccm/139.2.513

Brochard, L., Isabey, D., Piquet, J., Amaro, P., Mancebo, J., Messadi, A. A., Brun-Buisson, C., Rauss, A., Lemaire, F., & Harf, A. (1990). Reversal of acute exacerbations of chronic obstructive lung disease by inspiratory assistance with a face mask. *N Engl J Med*, *323*(22), 1523-1530. https://doi.org/10.1056/nejm199011293232204

Brochard, L., Mancebo, J., Wysocki, M., Lofaso, F., Conti, G., Rauss, A., Simonneau, G., Benito, S., Gasparetto, A., Lemaire, F., & et al. (1995). Noninvasive ventilation for acute exacerbations of chronic obstructive pulmonary disease. *N Engl J Med*, *333*(13), 817-822. https://doi.org/10.1056/nejm199509283331301

Brochard, L., Slutsky, A., & Pesenti, A. (2017). Mechanical Ventilation to Minimize Progression of Lung Injury in Acute Respiratory Failure. *Am J Respir Crit Care Med*, *195*(4), 438-442. https://doi.org/10.1164/rccm.201605-1081CP

Broseghini, C., Brandolese, R., Poggi, R., Polese, G., Manzin, E., Milic-Emili, J., & Rossi, A. (1988). Respiratory mechanics during the first day of mechanical ventilation in patients with pulmonary edema and chronic airway obstruction. *Am Rev Respir Dis*, *138*(2), 355-361. https://doi.org/10.1164/ajrccm/138.2.355

Brown, B. H. (2003). Electrical impedance tomography (EIT): a review. *J Med Eng Technol*, *27*(3), 97-108. https://doi.org/10.1080/0309190021000059687

Brunet, F., Belghith, M., Mira, J. P., Lanore, J. J., Vaxelaire, J. F., Dall'ava Santucci, J., & Dhainaut, J. F. (1993). Extracorporeal carbon dioxide removal and low-frequency positive-pressure ventilation. Improvement in arterial oxygenation with reduction of risk of pulmonary barotrauma in patients with adult respiratory distress syndrome. *Chest*, *104*(3), 889-898.

Brusasco, V., & Martinez, F. (2014). Chronic Obstructive Pulmonary Disease. *Compr Physiol*, *4*, 1-31.

Burge, S., & Wedzicha, J. A. (2003). COPD exacerbations: definitions and classifications. *Eur Respir J Suppl*, *41*, 46s-53s.

Burki, N. K., Mani, R. K., Herth, F. J., Schmidt, W., Teschler, H., Bonin, F., Becker, H., Randerath, W. J., Stieglitz, S., Hagmeyer, L., Priegnitz, C., Pfeifer, M., Blaas, S. H., Putensen, C., Theuerkauf, N., Quintel, M., & Moerer, O. (2013). A novel extracorporeal CO(2) removal system: results of a pilot study of hypercapnic respiratory failure in patients with COPD. *Chest*, *143*(3), 678-686.

Cabello, B., & Mancebo, J. (2006). Work of breathing. *Intensive Care Med*, *32*(9), 1311-1314. https://doi.org/10.1007/s00134-006-0278-3

Calverley, P. (2003). Respiratory failure in chronic obstructive pulmonary disease. *Eur Respir J*, *22*, 26-30S.

Camac, E. R., Stumpf, N. A., Voelker, H. K., & Criner, G. J. (2022). Short-Term Impact of the Frequency of COPD Exacerbations on Quality of Life. *Chronic Obstr Pulm Dis*, *9*(3), 298-308. https://doi.org/10.15326/jcopdf.2021.0280

Camac, E. R., Voelker, H., & Criner, G. J. (2021). Impact of COPD exacerbations leading to hospitalization on general and disease-specific quality of life. *Respir Med*, *186*, 106526. https://doi.org/10.1016/j.rmed.2021.106526

Cammarota, G., Simonte, R., & De Robertis, E. (2022). Comfort During Non-invasive Ventilation. *Front Med (Lausanne)*, *9*, 874250. https://doi.org/10.3389/fmed.2022.874250

Campbell, E. (1957). *The respiratory muscles and the mechanics of breathing* (Vol. 43). Lloyd-Luke. https://doi.org/10.1113/expphysiol.1958.sp001324

Camporota, L., & Barrett, N. (2016). Current Applications for the Use of Extracorporeal Carbon Dioxide Removal in Critically Ill Patients. *Biomed Res Int*, *2016*, 9781695. https://doi.org/10.1155/2016/9781695

Cardenas, V. J., Jr., Lynch, J. E., Ates, R., Miller, L., & Zwischenberger, J. B. (2009). Venovenous carbon dioxide removal in chronic obstructive pulmonary disease: experience in one patient. *Asaio j*, *55*(4), 420-422.

Cardoso, D. M., Gass, R., Sbruzzi, G., Berton, D. C., & Knorst, M. M. (2020). Effect of the expiratory positive airway pressure on dynamic hyperinflation and exercise capacity in patients with COPD: a meta-analysis. *Sci Rep*, *10*(1), 13292. https://doi.org/10.1038/s41598-020-70250-4

Carratu, P., Bonfitto, P., Dragonieri, S., Schettini, F., Clemente, R., Di Gioia, G., Loponte, L., Foschino Barbaro, M. P., & Resta, O. (2005). Early and late failure of noninvasive ventilation in chronic obstructive pulmonary disease with acute exacerbation. *Eur J Clin Invest*, *35*(6), 404-409.

Carrera, M., Marin, J. M., Anton, A., Chiner, E., Alonso, M. L., Masa, J. F., Marrades, R., Sala, E., Carrizo, S., Giner, J., Gomez-Merino, E., Teran, J., Disdier, C., Agusti, A. G., & Barbe, F. (2009). A controlled trial of noninvasive ventilation for chronic obstructive pulmonary disease exacerbations. *J Crit Care*, *24*(3), 473.e477-414. https://doi.org/10.1016/j.jcrc.2008.08.007

Carron, M., Freo, U., BaHammam, A. S., Dellweg, D., Guarracino, F., Cosentini, R., Feltracco, P., Vianello, A., Ori, C., & Esquinas, A. (2013). Complications of non-invasive ventilation techniques: a comprehensive qualitative review of randomized trials. *Br J Anaesth*, *110*(6), 896-914. https://doi.org/10.1093/bja/aet070

Celli, B., & Wedzicha, J. A. (2019). Update on Clinical Aspects of Chronic Obstructive Pulmonary Disease. *New England Journal of Medicine*, *381*, 1257-1266.

Celli, B. R., & MacNee, W. (2004). Standards for the diagnosis and treatment of patients with COPD: a summary of the ATS/ERS position paper. *Eur Respir J*, *23*(6), 932-946.

Chandler, W. L. (2021). Platelet, Red Cell, and Endothelial Activation and Injury During Extracorporeal Membrane Oxygenation. *Asaio j*. https://doi.org/10.1097/mat.0000000000001320

Chandra, D., Stamm, J. A., Taylor, B., Ramos, R. M., Satterwhite, L., Krishnan, J. A., Mannino, D., Sciurba, F. C., & Holguin, F. (2012). Outcomes of noninvasive ventilation for acute exacerbations of chronic obstructive pulmonary disease in the United States, 1998-2008. *Am J Respir Crit Care Med*, *185*(2), 152-159.

Chen, Z., Eldridge, F., & Wagner, P. (1992). Respiratory-associated thalamic activity is related to level of respiratory drive. *Resp Physiol 90*, 99-113.

Cherniack, N., & Longobardo, G. (1970). Oxygen and carbon dioxide gas stores of the body. *Physiol Rev.*, *50*(2), 196-243.

Cherniack, R. M. (1959). The oxygen consumption and efficiency of the respiratory muscles in health and emphysema. *J Clin Invest*, *38*(3), 494-499. https://doi.org/10.1172/jci103826

Cherpanath, T. G., Landburg, P. P., Lagrand, W. K., Schultz, M. J., & Juffermans, N. P. (2016). Effect of extracorporeal CO2 removal on right ventricular and hemodynamic parameters in a patient with acute respiratory distress syndrome. *Perfusion*, *31*(6), 525-529. https://doi.org/10.1177/0267659115621783

Clanton, T. L., & Levine, S. (2009). Respiratory muscle fiber remodeling in chronic hyperinflation: dysfunction or adaptation? *J Appl Physiol (1985)*, *107*(1), 324-335. https://doi.org/10.1152/japplphysiol.00173.2009

Coast, J. R., & Krause, K. M. (1993). Relationship of oxygen consumption and cardiac output to work of breathing. *Med Sci Sports Exerc*, *25*(3), 335-340.

Collett, P. W., Perry, C., & Engel, L. A. (1985). Pressure-time product, flow, and oxygen cost of resistive breathing in humans. *J Appl Physiol (1985)*, *58*(4), 1263-1272. https://doi.org/10.1152/jappl.1985.58.4.1263

Collins, P. D., Giosa, L., Camarda, V., & Camporota, L. (2023). Physiological adaptations during weaning from veno-venous extracorporeal membrane oxygenation. *Intensive Care Med Exp*, *11*(7), 1-18.

Combes, A., Fanelli, V., Pham, T., & Ranieri, V. M. (2019). Feasibility and safety of extracorporeal CO2 removal to enhance protective ventilation in acute respiratory distress syndrome: the SUPERNOVA study. *Intensive Care Med*. https://doi.org/10.1007/s00134-019-05567-4

Conceição, T., Gonzáles, A. I., Figueiredo, F., Vieira, D. S. R., & Bündchen, D. C. (2017). Safety criteria to start early mobilization in intensive care units. Systematic review. *Rev Bras Ter Intensiva*, *29*(4), 509-519. https://doi.org/10.5935/0103-507x.20170076 (Critérios de segurança para iniciar a mobilização precoce em unidades de terapia intensiva. Revisão sistemática.)

Confalonieri, M., Garuti, G., Cattaruzza, M. S., Osborn, J. F., Antonelli, M., Conti, G., Kodric, M., Resta, O., Marchese, S., Gregoretti, C., & Rossi, A. (2005). A chart of failure risk for noninvasive ventilation in patients with COPD exacerbation. *Eur Respir J*, *25*(2), 348-355.

Consales, G., Zamidei, L., Turani, F., Atzeni, D., Isoni, P., Boscolo, G., Saggioro, D., Resta, M. V., & Ronco, C. (2021). Combined Renal-Pulmonary Extracorporeal Support with Low Blood Flow Techniques: A Retrospective Observational Study (CICERO Study). *Blood Purif*, 1-10. https://doi.org/10.1159/000517280

Conti, G., Antonelli, M., Navalesi, P., Rocco, M., Bufi, M., Spadetta, G., & Meduri, G. U. (2002). Noninvasive vs. conventional mechanical ventilation in patients

with chronic obstructive pulmonary disease after failure of medical treatment in the ward: a randomized trial. *Intensive Care Med*, *28*(12), 1701-1707. https://doi.org/10.1007/s00134-002-1478-0

Contou, D., Fragnoli, C., Cordoba-Izquierdo, A., Boissier, F., Brun-Buisson, C., & Thille, A. W. (2013). Noninvasive ventilation for acute hypercapnic respiratory failure: intubation rate in an experienced unit. *Respir Care*, *58*(12), 2045-2052.

Cooper, C. B., & Celli, B. (2008). Venous admixture in COPD: pathophysiology and therapeutic approaches. *Copd*, *5*(6), 376-381. https://doi.org/10.1080/15412550802522783

Coppola, S., Chiumello, D., Busana, M., Giola, E., Palermo, P., Pozzi, T., Steinberg, I., Roli, S., Romitti, F., Lazzari, S., Gattarello, S., Palumbo, M., Herrmann, P., Saager, L., Quintel, M., Meissner, K., Camporota, L., Marini, J. J., Centanni, S., & Gattinoni, L. (2021). Role of total lung stress on the progression of early COVID-19 pneumonia. *Intensive Care Med*, *47*(10), 1130-1139. https://doi.org/10.1007/s00134-021-06519-7

Couk, J., Chernetsky Tejedor, S., Steinberg, J. P., Robichaux, C., & Jacob, J. T. (2019). Impact of multiple concurrent central lines on central-line-associated bloodstream infection rates. *Infect Control Hosp Epidemiol*, *40*(9), 1019-1023. https://doi.org/10.1017/ice.2019.180

Cove, M. E., & Federspiel, W. J. (2015). Veno-venous extracorporeal CO2 removal for the treatment of severe respiratory acidosis. *Crit Care*, *19*, 176. https://doi.org/10.1186/s13054-015-0769-0

Crabb, M., Grychtol, B., Lionheart, W., & Camporota, L. (2016). EIT regional time constants.

D'Albo, R., Romitti, F., Camporota, L., Moerer, O., Busana, M., & Gattinoni, L. Gas volumes corrections in Intensive Care Unit: needed or pointless? *J Appl Physiol*, *0*(0), null. https://doi.org/10.1152/japplphysiol.00225.2023

Davidson, A. C., Banham, S., Elliott, M., Kennedy, D., Gelder, C., Glossop, A., Church, A. C., Creagh-Brown, B., Dodd, J. W., Felton, T., Foëx, B., Mansfield, L., McDonnell, L., Parker, R., Patterson, C. M., Sovani, M., & Thomas, L. (2016).

BTS/ICS guideline for the ventilatory management of acute hypercapnic respiratory failure in adults. *Thorax*, *71 Suppl 2*, ii1-35. https://doi.org/10.1136/thoraxjnl-2015-208209

Davies, L., Angus, R. M., & Calverley, P. M. (1999). Oral corticosteroids in patients admitted to hospital with exacerbations of chronic obstructive pulmonary disease: a prospective randomised controlled trial. *Lancet*, *354*(9177), 456-460.

De Troyer, A. (1984). Actions of the respiratory muscles or how the chest wall moves in upright man. *Bull Eur Physiopathol Respir*, *20*(5), 409-413.

De Troyer, A., & Estenne, M. (1984). Coordination between rib cage muscles and diaphragm during quiet breathing in humans. *J Appl Physiol Respir Environ Exerc Physiol*, *57*(3), 899-906. https://doi.org/10.1152/jappl.1984.57.3.899

De Troyer, A., Leeper, J., & McKenzie, D. (1997). Neural drive to the diaphragm in patients with severe COPD. *Am J Respir Crit Care Med*, *155*, 1335-1340.

De Troyer, A., Leeper, J. B., McKenzie, D. K., & Gandevia, S. C. (1997). Neural drive to the diaphragm in patients with severe COPD. *Am J Respir Crit Care Med*, *155*(4), 1335-1340. https://doi.org/10.1164/ajrccm.155.4.9105076

De Troyer, A., & Sampson, M. G. (1982). Activation of the parasternal intercostals during breathing efforts in human subjects. *J Appl Physiol Respir Environ Exerc Physiol*, *52*(3), 524-529. https://doi.org/10.1152/jappl.1982.52.3.524

De Troyer, A., & Wilson, T. A. (2009). Effect of acute inflation on the mechanics of the inspiratory muscles. *J Appl Physiol (1985)*, *107*(1), 315-323. https://doi.org/10.1152/japplphysiol.91472.2008

de Villiers Hugo, J., Sharma, A. S., Ahmed, U., & Weerwind, P. W. (2017). Quantification of Carbon Dioxide Removal at Low Sweep Gas and Blood Flows. *J Extra Corpor Technol*, *49*(4), 257-261.

Del Sorbo, L., Pisani, L., Filippini, C., Fanelli, V., Fasano, L., Terragni, P., Dell'Amore, A., Urbino, R., Mascia, L., Evangelista, A., Antro, C., D'Amato, R., Sucre, M. J., Simonetti, U., Persico, P., Nava, S., & Ranieri, V. M. (2015). Extracorporeal Co2

removal in hypercapnic patients at risk of noninvasive ventilation failure: a matched cohort study with historical control. *Crit Care Med*, *43*(1), 120-127. https://doi.org/10.1097/ccm.0000000000000607

Demoule, A., Girou, E., Richard, J. C., Taille, S., & Brochard, L. (2006). Increased use of noninvasive ventilation in French intensive care units. *Intensive Care Med*, *32*(11), 1747-1755. https://doi.org/10.1007/s00134-006-0229-z

Devlin, N. J., Shah, K. K., Feng, Y., Mulhern, B., & van Hout, B. (2018). Valuing health-related quality of life: An EQ-5D-5L value set for England. *Health Econ*, *27*(1), 7-22. https://doi.org/10.1002/hec.3564

Di Lascio, G., Prifti, E., Messai, E., Peris, A., Harmelin, G., Xhaxho, R., Fico, A., Sani, G., & Bonacchi, M. (2017). Extracorporeal membrane oxygenation support for life-threatening acute severe status asthmaticus. *Perfusion*, *32*(2), 157-163. https://doi.org/10.1177/0267659116670481

Dianti, J., McNamee, J. J., Slutsky, A. S., Fan, E., Ferguson, N. D., McAuley, D. F., & Goligher, E. C. (2023). Determinants of Effect of Extracorporeal CO₂ Removal in Hypoxemic Respiratory Failure. *NEJM Evidence*, *2*(5), EVIDoa2200295. https://doi.org/doi:10.1056/EVIDoa2200295

Díaz, O., Bégin, P., Torrealba, B., Jover, E., & Lisboa, C. (2002). Effects of noninvasive ventilation on lung hyperinflation in stable hypercapnic COPD. *Eur Respir J*, *20*(6), 1490-1498. https://doi.org/10.1183/09031936.02.00034402

Diaz, O., Iglesia, R., Ferrer, M., Zavala, E., Santos, C., Wagner, P. D., Roca, J., & Rodriguez-Roisin, R. (1997). Effects of noninvasive ventilation on pulmonary gas exchange and hemodynamics during acute hypercapnic exacerbations of chronic obstructive pulmonary disease. *Am J Respir Crit Care Med*, *156*(6), 1840-1845. https://doi.org/10.1164/ajrccm.156.6.9701027

Diehl, J. L., Augy, J. L., Rivet, N., Guerin, C., Chocron, R., & Smadja, D. M. (2020). Severity of endothelial dysfunction is associated with the occurrence of hemorrhagic complications in COPD patients treated by extracorporeal CO(2) removal. *Intensive Care Med*, *46*(10), 1950-1952. https://doi.org/10.1007/s00134-020-06138-8

Diehl, J. L., Piquilloud, L., Richard, J. M., Mancebo, J., & Mercat, A. (2016). Effects of extracorporeal carbon dioxide removal on work of breathing in patients with chronic obstructive pulmonary disease. *Intensive Care Med*, *42*(5), 951-952. https://doi.org/10.1007/s00134-015-4166-6

Diehl, J. L., Piquilloud, L., Vimpere, D., Aissaoui, N., Guerot, E., Augy, J. L., Pierrot, M., Hourton, D., Arnoux, A., Richard, C., Mancebo, J., & Mercat, A. (2020). Physiological effects of adding ECCO(2)R to invasive mechanical ventilation for COPD exacerbations. *Ann Intensive Care*, *10*(1), 126. https://doi.org/10.1186/s13613-020-00743-y

Ding, X., Chen, H., Zhao, H., Zhang, H., He, H., Cheng, W., Wang, C., Jiang, W., Ma, J., Qin, Y., Liu, Z., Wang, J., Yan, X., Li, T., Zhou, X., Long, Y., & Zhang, S. (2021). ECCO(2)R in 12 COVID-19 ARDS Patients With Extremely Low Compliance and Refractory Hypercapnia. *Front Med (Lausanne)*, *8*, 654658. https://doi.org/10.3389/fmed.2021.654658

Domino, K. B., Wetstein, L., Glasser, S. A., Lindgren, L., Marshall, C., Harken, A., & Marshall, B. E. (1983). Influence of mixed venous oxygen tension (PVO2) on blood flow to atelectatic lung. *Anesthesiology*, *59*(5), 428-434.

Donaldson, G. C., Seemungal, T. A., Bhowmik, A., & Wedzicha, J. A. (2002). Relationship between exacerbation frequency and lung function decline in chronic obstructive pulmonary disease. *Thorax*, *57*(10), 847-852.

Dorrington, K. L., McRae, K. M., Gardaz, J. P., Dunnill, M. S., Sykes, M. K., & Wilkinson, A. R. (1989). A randomized comparison of total extracorporeal CO2 removal with conventional mechanical ventilation in experimental hyaline membrane disease. *Intensive Care Med*, *15*(3), 184-191.

Douglas, A. R., Jones, N. L., & Reed, J. W. (1988). Calculation of whole blood CO2 content. *J Appl Physiol (1985)*, *65*(1), 473-477.

Doyle, A. J., Hunt, B. J., Sanderson, B., Zhang, J., Mak, S. M., Benedetti, G., Breen, K. A., Camporota, L., Barrett, N. A., & Retter, A. (2021). A Comparison of Thrombosis and Hemorrhage Rates in Patients With Severe Respiratory Failure Due to Coronavirus Disease 2019 and Influenza Requiring

Extracorporeal Membrane Oxygenation. *Crit Care Med*. https://doi.org/10.1097/ccm.0000000000004971

Dreher, M., Ekkernkamp, E., Walterspacher, S., Walker, D., Schmoor, C., Storre, J. H., & Windisch, W. (2011). Noninvasive ventilation in COPD: impact of inspiratory pressure levels on sleep quality. *Chest*, *140*(4), 939-945. https://doi.org/10.1378/chest.11-0253

Dreher, M., Storre, J. H., Schmoor, C., & Windisch, W. (2010). High-intensity versus low-intensity non-invasive ventilation in patients with stable hypercapnic COPD: a randomised crossover trial. *Thorax*, *65*(4), 303-308. https://doi.org/10.1136/thx.2009.124263

Druz, W. S., & Sharp, J. T. (1982). Electrical and mechanical activity of the diaphragm accompanying body position in severe chronic obstructive pulmonary disease. *Am Rev Respir Dis*, *125*(3), 275-280. https://doi.org/10.1164/arrd.1982.125.3.275

Duan, J., Wang, S., Liu, P., Han, X., Tian, Y., Gao, F., Zhou, J., Mou, J., Qin, Q., Yu, J., Bai, L., Zhou, L., & Zhang, R. (2019). Early prediction of noninvasive ventilation failure in COPD patients: derivation, internal validation, and external validation of a simple risk score. *Ann Intensive Care*, *9*(1), 108. https://doi.org/10.1186/s13613-019-0585-9

Duiverman, M. L., van Eykern, L. A., Vennik, P. W., Koeter, G. H., Maarsingh, E. J., & Wijkstra, P. J. (2004). Reproducibility and responsiveness of a noninvasive EMG technique of the respiratory muscles in COPD patients and in healthy subjects. *J Appl Physiol (1985)*, *96*(5), 1723-1729. https://doi.org/10.1152/japplphysiol.00914.2003

Dunham-Snary, K. J., Wu, D., Sykes, E. A., Thakrar, A., Parlow, L. R. G., Mewburn, J. D., Parlow, J. L., & Archer, S. L. (2017). Hypoxic Pulmonary Vasoconstriction: From Molecular Mechanisms to Medicine. *Chest*, *151*(1), 181-192. https://doi.org/10.1016/j.chest.2016.09.001

Echevarria, C., Steer, J., Hartley, T., Lane, N., & Bourke, S. C. (2020). Predictors of NIV Treatment in Patients with COPD Exacerbation Complicated by Respiratory

Acidaemia. *Copd*, *17*(5), 492-498. https://doi.org/10.1080/15412555.2020.1823358

Elliot, S. C., Paramasivam, K., Oram, J., Bodenham, A. R., Howell, S. J., & Mallick, A. (2007). Pumpless extracorporeal carbon dioxide removal for life-threatening asthma. *Crit Care Med*, *35*(3), 945-948.

Elliott, M. W., Aquilina, R., Green, M., Moxham, J., & Simonds, A. K. (1994). A comparison of different modes of noninvasive ventilatory support: effects on ventilation and inspiratory muscle effort. *Anaesthesia*, *49*(4), 279-283. https://doi.org/10.1111/j.1365-2044.1994.tb14173.x

EMC. (2018). *Summary of product characteristics: Plasmalyte solution for infusion*. Retrieved 14/7/2023 from https://www.medicines.org.uk/emc/product/1795/smpc#gref

Engel, L. (1986). Dynamic distribution of gas flow. In P. Macklem & M. J (Eds.), *Handbook of Physiology. The respiratory system.* (Vol. 3, pp. 575). American Physiologic Society.

Engel, M., Albrecht, H., & Volz, S. (2016). Use of Extracorporeal CO2 Removal to Avoid Invasive Mechanical Ventilation in Hypercapnic Coma and Failure of Noninvasive Ventilation. *J Pulm Respir Med*, *6*, 357.

Enghoff, H. (1938). Volumen inefficax: bemerkungen zur frage des schadlichen raumes. *Upsala La¨k-Fo¨ren Fo¨rh*, *44*, 191-218 (Article in German).

Esquinas Rodriguez, A. M., Papadakos, P. J., Carron, M., Cosentini, R., & Chiumello, D. (2013). Clinical review: Helmet and non-invasive mechanical ventilation in critically ill patients. *Crit Care*, *17*(2), 223. https://doi.org/10.1186/cc11875

Fadeur, M., Preiser, J. C., Verbrugge, A. M., Misset, B., & Rousseau, A. F. (2020). Oral Nutrition during and after Critical Illness: SPICES for Quality of Care! *Nutrients*, *12*(11). https://doi.org/10.3390/nu12113509

Faisal, A., Alghamdi, B. J., Ciavaglia, C. E., Elbehairy, A. F., Webb, K. A., Ora, J., Neder, J. A., & O'Donnell, D. E. (2016). Common Mechanisms of Dyspnea in Chronic

Interstitial and Obstructive Lung Disorders. *Am J Respir Crit Care Med*, *193*(3), 299-309. https://doi.org/10.1164/rccm.201504-0841OC

Fanelli, V., Ranieri, M. V., Mancebo, J., Moerer, O., Quintel, M., Morley, S., Moran, I., Parrilla, F., Costamagna, A., Gaudiosi, M., & Combes, A. (2016). Feasibility and safety of low-flow extracorporeal carbon dioxide removal to facilitate ultra-protective ventilation in patients with moderate acute respiratory distress sindrome. *Crit Care*, *20*, 36. https://doi.org/10.1186/s13054-016-1211-y

Federspiel, W. J., & Hattler, B. G. (1996). Sweep gas flowrate and CO2 exchange in artificial lungs. *Artif Organs*, *20*(9), 1050-1052.

Field, S., Sanci, S., & Grassino, A. (1984). Respiratory muscle oxygen consumption estimated by the diaphragm pressure-time index. *J Appl Physiol Respir Environ Exerc Physiol*, *57*(1), 44-51. https://doi.org/10.1152/jappl.1984.57.1.44

Fischer, S., Hoeper, M., Bein, T., Simon, A., Gottlieb, J., Wisser, W., Frey, L., Van Raemdonck, D., Welte, T., Haverich, A., & Strueber, M. (2008). Interventional lung assist: a new concept of protective ventilation in bridge to lung transplantation. *ASAIO J 54*, 3-10.

Fitzgerald, M., Millar, J., Blackwood, B., Davies, A., Brett, S. J., McAuley, D. F., & McNamee, J. J. (2014). Extracorporeal carbon dioxide removal for patients with acute respiratory failure secondary to the acute respiratory distress syndrome: a systematic review. *Crit Care*, *18*(3), 222. https://doi.org/10.1186/cc13875

Frerichs, I. (2000). Electrical impedance tomography (EIT) in applications related to lung and ventilation: a review of experimental and clinical activities. *Physiol Meas*, *21*(2), R1-21.

Frerichs, I., Achtzehn, U., Pechmann, A., Pulletz, S., Schmidt, E. W., Quintel, M., & Weiler, N. (2012). High-frequency oscillatory ventilation in patients with acute exacerbation of chronic obstructive pulmonary disease. *J Crit Care*, *27*(2), 172-181. https://doi.org/10.1016/j.jcrc.2011.04.008

Frerichs, I., Amato, M. B., van Kaam, A. H., Tingay, D. G., Zhao, Z., Grychtol, B., Bodenstein, M., Gagnon, H., Bohm, S. H., Teschner, E., Stenqvist, O., Mauri,

T., Torsani, V., Camporota, L., Schibler, A., Wolf, G. K., Gommers, D., Leonhardt, S., & Adler, A. (2016). Chest electrical impedance tomography examination, data analysis, terminology, clinical use and recommendations: consensus statement of the TRanslational EIT developmeNt stuDy group. *Thorax*. https://doi.org/10.1136/thoraxjnl-2016-208357

Frerichs, I., Dargaville, P. A., Dudykevych, T., & Rimensberger, P. C. (2003). Electrical impedance tomography: a method for monitoring regional lung aeration and tidal volume distribution? *Intensive Care Med*, *29*(12), 2312-2316. https://doi.org/10.1007/s00134-003-2029-z

Frerichs, I., Dargaville, P. A., & Rimensberger, P. C. (2013). Regional respiratory inflation and deflation pressure-volume curves determined by electrical impedance tomography. *Physiol Meas*, *34*(6), 567-577. https://doi.org/10.1088/0967-3334/34/6/567

Frerichs, I., Dargaville, P. A., & Rimensberger, P. C. (2019). Regional pulmonary effects of bronchoalveolar lavage procedure determined by electrical impedance tomography. *Intensive Care Med Exp*, *7*(1), 11. https://doi.org/10.1186/s40635-019-0225-6

Frerichs, I., Dargaville, P. A., van Genderingen, H., Morel, D. R., & Rimensberger, P. C. (2006). Lung volume recruitment after surfactant administration modifies spatial distribution of ventilation. *Am J Respir Crit Care Med*, *174*(7), 772-779. https://doi.org/10.1164/rccm.200512-1942OC

Frerichs, I., Hinz, J., Herrmann, P., Weisser, G., Hahn, G., Dudykevych, T., Quintel, M., & Hellige, G. (2002). Detection of local lung air content by electrical impedance tomography compared with electron beam CT. *J Appl Physiol (1985)*, *93*(2), 660-666. https://doi.org/10.1152/japplphysiol.00081.2002

Frerichs, I., Lasarow, L., Strodthoff, C., Vogt, B., Zhao, Z., & Weiler, N. (2021). Spatial Ventilation Inhomogeneity Determined by Electrical Impedance Tomography in Patients With Chronic Obstructive Lung Disease [Brief Research Report]. *Frontiers in Physiology*, *12*. https://doi.org/10.3389/fphys.2021.762791

Frerichs, I., Pulletz, S., Elke, G., Gawelczyk, B., Frerichs, A., & Weiler, N. (2011). Patient examinations using electrical impedance tomography--sources of interference in the intensive care unit. *Physiol Meas*, *32*(12), L1-10. https://doi.org/10.1088/0967-3334/32/12/f01

Frerichs, I., Pulletz, S., Elke, G., Reifferscheid, F., Schadler, D., Scholz, J., & Weiler, N. (2009). Assessment of changes in distribution of lung perfusion by electrical impedance tomography. *Respiration*, *77*(3), 282-291. https://doi.org/10.1159/000193994

Frerichs, I., Zhao, Z., Becher, T., Zabel, P., Weiler, N., & Vogt, B. (2016). Regional lung function determined by electrical impedance tomography during bronchodilator reversibility testing in patients with asthma. *Physiol Meas*, *37*(6), 698-712. https://doi.org/10.1088/0967-3334/37/6/698

Frerichs, I. z., Becher, T., & Weiler, N. (2014). Methodology of electrical impedance tomography-derived measures of regional lung ventilation. 1-1. https://doi.org/10.1186/s13054-014-0635-5

Fridlund, A. J., & Cacioppo, J. T. (1986). Guidelines for human electromyographic research. *Psychophysiology*, *23*(5), 567-589.

Fritts, H. W., Jr., Filler, J., Fishman, A. P., & Cournand, A. (1959). The efficiency of ventilation during voluntary hyperpnea: studies in normal subjects and in dyspneic patients with either chronic pulmonary emphysema or obesity. *J Clin Invest*, *38*(8), 1339-1348. https://doi.org/10.1172/jci103909

Fukuda, T., Echeimberg, J., Pompeu, J., Lucareli, P., Garbelotti, S., Gimenes, R., & Apolinário, A. (2010). Root Mean Square Value of the Electromyographic Signal in the Isometric Torque of the Quadriceps, Hamstrings and Brachial Biceps Muscles in Female Subjects. *Journal of Applied Research*, *10*(1), 32-39.

Gabriel, C., Gabriel, S., & Corthout, E. (1996). The dielectric properties of biological tissues: I. Literature survey. *Phys Med Biol*, *41*(11), 2231-2249.

Garcia, J. P., Kon, Z. N., Evans, C., Wu, Z., Iacono, A. T., McCormick, B., & Griffith, B. P. (2011). Ambulatory veno-venous extracorporeal membrane oxygenation: innovation and pitfalls. *J Thorac Cardiovasc Surg*, *142*(4), 755-761.

Garcia-Aymerich, J., Farrero, E., Felez, M. A., Izquierdo, J., Marrades, R. M., & Anto, J. M. (2003). Risk factors of readmission to hospital for a COPD exacerbation: a prospective study. *Thorax*, *58*(2), 100-105.

Gattarello, S., Coppola, S., Chiodaroli, E., Pozzi, T., Camporota, L., Saager, L., Chiumello, D., & Gattinoni, L. (2023). Mechanical Power Ratio and Respiratory Treatment Escalation in COVID-19 Pneumonia: A Secondary Analysis of a Prospectively Enrolled Cohort. *Anesthesiology*, *138*(3), 289-298. https://doi.org/10.1097/aln.0000000000004465

Gattinoni, L. (2016). Ultra-protective ventilation and hypoxemia. *Critical Care*, *20*, 130. https://doi.org/10.1186/s13054-016-1310-9

Gattinoni, L., Collino, F., & Camporota, L. (2023). Mechanical power: meaning, uses and limitations. *Intensive Care Med*, *49*(4), 465-467. https://doi.org/10.1007/s00134-023-06991-3

Gattinoni, L., Kolobow, T., Agostoni, A., Damia, G., Pelizzola, A., Rossi, G. P., Langer, M., Solca, M., Citterio, R., Pesenti, A., Fox, U., & Uziel, L. (1979). Clinical application of low frequency positive pressure ventilation with extracorporeal CO2 removal (LFPPV-ECCO2R) in treatment of adult respiratory distress syndrome (ARDS). *Int J Artif Organs*, *2*(6), 282-283.

Gattinoni, L., Kolobow, T., Damia, G., Agostoni, A., & Pesenti, A. (1979). Extracorporeal carbon dioxide removal (ECCO2R): a new form of respiratory assistance. *Int J Artif Organs*, *2*(4), 183-185.

Gattinoni, L., Kolobow, T., Tomlinson, T., Iapichino, G., Samaja, M., White, D., & Pierce, J. (1978). Low-frequency positive pressure ventilation with extracorporeal carbon dioxide removal (LFPPV-ECCO2R): an experimental study. *Anesth Analg*, *57*(4), 470-477.

Gattinoni, L., Kolobow, T., Tomlinson, T., White, D., & Pierce, J. (1978). Control of intermittent positive pressure breathing (IPPB) by extracorporeal removal of carbon dioxide. *Br J Anaesth*, *50*(8), 753-758.

Gattinoni, L., Marini, J. J., Collino, F., Maiolo, G., Rapetti, F., Tonetti, T., Vasques, F., & Quintel, M. (2017). The future of mechanical ventilation: lessons from the

present and the past. *Crit Care*, *21*(1), 183. https://doi.org/10.1186/s13054-017-1750-x

Gattinoni, L., Pesenti, A., Mascheroni, D., Marcolin, R., Fumagalli, R., Rossi, F., Iapichino, G., Romagnoli, G., Uziel, L., Agostoni, A., & et al. (1986). Low-frequency positive-pressure ventilation with extracorporeal CO2 removal in severe acute respiratory failure. *Jama*, *256*(7), 881-886.

Gattinoni, L., Solca, M., Pesenti, A., Marcolin, R., Riboni, A., Gavazzeni, V., Bassi, F., Giuffrida, A., & Prato, P. (1983). Combined use of artificial lung and kidney in the treatment of terminal acute respiratory distress syndrome. *Life Support Syst*, *1 Suppl 1*, 365-367.

Gattinoni, L., Tonetti, T., Cressoni, M., Cadringher, P., Herrmann, P., Moerer, O., Protti, A., Gotti, M., Chiurazzi, C., Carlesso, E., Chiumello, D., & Quintel, M. (2016). Ventilator-related causes of lung injury: the mechanical power. *Intensive Care Med*, *42*(10), 1567-1575. https://doi.org/10.1007/s00134-016-4505-2

Ghiani, A., Paderewska, J., Sainis, A., Crispin, A., Walcher, S., & Neurohr, C. (2020). Variables predicting weaning outcome in prolonged mechanically ventilated tracheotomized patients: a retrospective study. *J Intensive Care*, *8*, 19. https://doi.org/10.1186/s40560-020-00437-4

Ghobadi, H., Ahari, S. S., Kameli, A., & Lari, S. M. (2012). The Relationship between COPD Assessment Test (CAT) Scores and Severity of Airflow Obstruction in Stable COPD Patients. *Tanaffos*, *11*(2), 22-26.

Girault, C., Richard, J. C., Chevron, V., Tamion, F., Pasquis, P., Leroy, J., & Bonmarchand, G. (1997). Comparative physiologic effects of noninvasive assist-control and pressure support ventilation in acute hypercapnic respiratory failure. *Chest*, *111*(6), 1639-1648. https://doi.org/10.1378/chest.111.6.1639

Goldberg, P., Reissmann, H., Maltais, F., Ranieri, M., & Gottfried, S. B. (1995). Efficacy of noninvasive CPAP in COPD with acute respiratory failure. *Eur Respir J*, *8*(11), 1894-1900.

Goligher, E. C., Combes, A., Brodie, D., Ferguson, N. D., Pesenti, A. M., Ranieri, V. M., Slutsky, A. S., Beale, R., Brochard, L., Chiche, J.-D., Fan, E., de Backer, D., Francois, G., Laffey, J., Mercat, A., McAuley, D. F., Müller, T., Quintel, M., Vincent, J.-L., . . . for the , SUPERNOVA i. a. f. t. I. E. N. (2019). Determinants of the effect of extracorporeal carbon dioxide removal in the SUPERNOVA trial: implications for trial design. *Intensive Care Med*, *45*(9), 1219-1230. https://doi.org/10.1007/s00134-019-05708-9

Gorini, M., Misuri, G., Corrado, A., Duranti, R., Iandelli, I., De Paola, E., & Scano, G. (1996). Breathing pattern and carbon dioxide retention in severe chronic obstructive pulmonary disease. *Thorax*, *51*(7), 677-683. https://doi.org/10.1136/thx.51.7.677

Gorini, M., Spinelli, A., Ginanni, R., Duranti, R., Gigliotti, F., & Scano, G. (1990). Neural respiratory drive and neuromuscular coupling in patients with chronic obstructive pulmonary disease (COPD). *Chest*, *98*(5), 1179-1186.

Gosker, H. R., Langen, R. C., & Simons, S. O. (2021). Role of acute exacerbations in skeletal muscle impairment in COPD. *Expert Rev Respir Med*, *15*(1), 103-115. https://doi.org/10.1080/17476348.2021.1843429

Gross-Hardt, S., Hesselmann, F., Arens, J., Steinseifer, U., Vercaemst, L., Windisch, W., Brodie, D., & Karagiannidis, C. (2019). Low-flow assessment of current ECMO/ECCO(2)R rotary blood pumps and the potential effect on hemocompatibility. *Crit Care*, *23*(1), 348. https://doi.org/10.1186/s13054-019-2622-3

Gruffydd-Jones, K. (2008). A national strategy for the management of chronic obstructive pulmonary disease (COPD) in England: aiming to improve the quality of care for patients. *Primary Care Respiratory Journal*, *17*(1), s8-s10.

Guérin, C., Coussa, M. L., Eissa, N. T., Corbeil, C., Chassé, M., Braidy, J., Matar, N., & Milic-Emili, J. (1993). Lung and chest wall mechanics in mechanically ventilated COPD patients. *J Appl Physiol (1985)*, *74*(4), 1570-1580. https://doi.org/10.1152/jappl.1993.74.4.1570

Guo, J., Chen, Y., Zhang, W., Tong, S., & Dong, J. (2020). Moderate and severe exacerbations have a significant impact on health-related quality of life, utility, and lung function in patients with chronic obstructive pulmonary disease: A meta-analysis. *Int J Surg*, *78*, 28-35. https://doi.org/10.1016/j.ijsu.2020.04.010

Halpin, D. M. G., Criner, G. J., Papi, A., Singh, D., Anzueto, A., Martinez, F. J., Agusti, A. A., & Vogelmeier, C. F. (2021). Global Initiative for the Diagnosis, Management, and Prevention of Chronic Obstructive Lung Disease. The 2020 GOLD Science Committee Report on COVID-19 and Chronic Obstructive Pulmonary Disease. *Am J Respir Crit Care Med*, *203*(1), 24-36. https://doi.org/10.1164/rccm.202009-3533SO

Haluszka, J., Chartrand, D., & Grassino, A. (1990). Intrinsic PEEP and arterial PCO2 in stable patients with chronic obstructive pulmonary disease. . *Am Rev Respir Dis*, *141*, 1194–1197.

Hanson, C. W., 3rd, Marshall, B. E., Frasch, H. F., & Marshall, C. (1996). Causes of hypercarbia with oxygen therapy in patients with chronic obstructive pulmonary disease. *Crit Care Med*, *24*(1), 23-28. https://doi.org/10.1097/00003246-199601000-00007

Hashem, M. D., Parker, A. M., & Needham, D. M. (2016). Early Mobilization and Rehabilitation of Patients Who Are Critically Ill. *Chest*, *150*(3), 722-731. https://doi.org/10.1016/j.chest.2016.03.003

Hedenstierna, G. (2012). Esophageal pressure: benefit and limitations. *Minerva Anestesiol*, *78*(8), 959-966.

Hill, J. D., O'Brien, T. G., Murray, J. J., Dontigny, L., Bramson, M. L., Osborn, J. J., & Gerbode, F. (1972). Prolonged extracorporeal oxygenation for acute post-traumatic respiratory failure (shock-lung syndrome). Use of the Bramson membrane lung. *N Engl J Med*, *286*(12), 629-634.

Hilty, M. P., Riva, T., Cottini, S. R., Kleinert, E. M., Maggiorini, A., & Maggiorini, M. (2017). Low flow veno-venous extracorporeal CO2 removal for acute

hypercapnic respiratory failure. *Minerva Anestesiol*, *83*(8), 812-823. https://doi.org/10.23736/s0375-9393.17.11524-5

Hina, H. R., & McDowell, J. R. S. (2017). Minimising central line-associated bloodstream infection rate in inserting central venous catheters in the adult intensive care units. *J Clin Nurs*, *26*(23-24), 3962-3973. https://doi.org/10.1111/jocn.13824

Hinz, J., Hahn, G., Neumann, P., Sydow, M., Mohrenweiser, P., Hellige, G., & Burchardi, H. (2003). End-expiratory lung impedance change enables bedside monitoring of end-expiratory lung volume change. *Intensive Care Med*, *29*(1), 37-43. https://doi.org/10.1007/s00134-002-1555-4

Horn, E. M., & Waldrop, T. G. (1998). Suprapontine control of respiration. *Respir Physiol*, *114*(3), 201-211.

Horton, S., Thuys, C., Bennett, M., Augustin, S., Rosenberg, M., & Brizard, C. (2004). Experience with the Jostra Rotaflow and QuadroxD oxygenator for ECMO. *Perfusion*, *19*(1), 17-23. https://doi.org/10.1191/0267659104pf702oa

Hout, M. S., Hattler, B. G., & Federspiel, W. J. (2000). Validation of a model for flow-dependent carbon dioxide exchange in artificial lungs. *Artif Organs*, *24*(2), 114-118.

Hudson, A. L., Butler, J. E., Gandevia, S. C., & De Troyer, A. (2010). Interplay between the inspiratory and postural functions of the human parasternal intercostal muscles. *J Neurophysiol*, *103*(3), 1622-1629. https://doi.org/10.1152/jn.00887.2009

Hurst, J. R., Perera, W. R., Wilkinson, T. M., Donaldson, G. C., & Wedzicha, J. A. (2006). Systemic and upper and lower airway inflammation at exacerbation of chronic obstructive pulmonary disease. *Am J Respir Crit Care Med*, *173*(1), 71-78. https://doi.org/10.1164/rccm.200505-704OC

Husain-Syed, F., Birk, H. W., Wilhelm, J., Ronco, C., Ranieri, V. M., Karle, B., Kuhnert, S., Tello, K., Hecker, M., Morty, R. E., Herold, S., Kehl, O., Walmrath, H. D., Seeger, W., & Vadász, I. (2020). Extracorporeal Carbon Dioxide Removal Using a Renal Replacement Therapy Platform to Enhance Lung-Protective

Ventilation in Hypercapnic Patients With Coronavirus Disease 2019-Associated Acute Respiratory Distress Syndrome. *Front Med (Lausanne)*, *7*, 598379. https://doi.org/10.3389/fmed.2020.598379

Ikeda, K., Kawakami, K., Onimaru, H., Okada, Y., Yokota, S., Koshiya, N., Oku, Y., Iizuka, M., & Koizumi, H. (2017). The respiratory control mechanisms in the brainstem and spinal cord: integrative views of the neuroanatomy and neurophysiology. *J Physiol Sci*, *67*(1), 45-62. https://doi.org/10.1007/s12576-016-0475-y

Inhofer, J., Bertasi, A., Gangidine, M., Repas, S. J., Holmes, J., Harris, M., Stull, M., & Marco, C. (2022). Incidence of central line associated bloodstream infection following central venous catheter placement in the emergency department. *Am J Emerg Med*, *51*, 338-341. https://doi.org/10.1016/j.ajem.2021.11.018

ISO. (2016). ISO standard 7199: Cardiovascular implants and artificial organs — Blood-gas exchangers (oxygenators). In (pp. 1-20): International Standards Organisation.

James, M. D., Phillips, D. B., Vincent, S. G., Abdallah, S. J., Donovan, A. A., de-Torres, J. P., Neder, J. A., Smith, B. M., Jensen, D., & O'Donnell, D. E. (2022). Exertional dyspnoea in patients with mild-to-severe chronic obstructive pulmonary disease: neuromechanical mechanisms. *J Physiol*, *600*(18), 4227-4245. https://doi.org/10.1113/jp283252

Javaheri, S., & Kazemi, H. (1987). Metabolic alkalosis and hypoventilation in humans. *Am Rev Respir Dis*, *136*(4), 1011-1016. https://doi.org/10.1164/ajrccm/136.4.1011

Jeffries, R., Mussin, Y., Bulanin, D., Lund, L., Kocyildirim, E., Zhumadilov, Z., Olzhayev, F., Federspiel, W., & Wearden, P. (2014). HHS Public Access. *Pre-clinical evaluation of an adult extracorporeal carbon dioxide removal system with active mixing for pediatric respiratory support*, *37*(12), 888-899. https://doi.org/10.5301/ijao.5000372

Jeffries, R. G., Lund, L., Frankowski, B., & Federspiel, W. J. (2017). An extracorporeal carbon dioxide removal (ECCO2R) device operating at hemodialysis blood flow rates. 1-12. https://doi.org/10.1186/s40635-017-0154-1

Jiang, C., Galaydick, J., Fernandez, H., & Caronia, J. (2017). Adjunctive extracorporeal carbon dioxide removal in refractory status asthmaticus. *BMJ Case Rep*, *2017*. https://doi.org/10.1136/bcr-2017-220693

Jolley, C. J., Luo, Y. M., Steier, J., Rafferty, G. F., Polkey, M. I., & Moxham, J. (2015). Neural respiratory drive and breathlessness in COPD. *Eur Respir J*, *45*(2), 355-364. https://doi.org/10.1183/09031936.00063014

Jolley, C. J., Luo, Y. M., Steier, J., Reilly, C., Seymour, J., Lunt, A., Ward, K., Rafferty, G. F., Polkey, M. I., & Moxham, J. (2009). Neural respiratory drive in healthy subjects and in COPD. *Eur Respir J*, *33*(2), 289-297. https://doi.org/10.1183/09031936.00093408

Jones, P. W., Harding, G., Berry, P., Wiklund, I., Chen, W.-H., & Kline Leidy, N. (2009). Development and first validation of the COPD Assessment Test. *European Respiratory Journal*, *34*(3), 648-654. https://doi.org/10.1183/09031936.00102509

Jones, P. W., Harding, G., Wiklund, I., Berry, P., Tabberer, M., Yu, R., & Leidy, N. K. (2012). Tests of the responsiveness of the COPD assessment test following acute exacerbation and pulmonary rehabilitation. *Chest*, *142*(1), 134-140. https://doi.org/10.1378/chest.11-0309

Jones, P. W., Quirk, F. H., & Baveystock, C. M. (1991). The St George's Respiratory Questionnaire. *Respir Med*, *85 Suppl B*, 25-31; discussion 33-27. https://doi.org/10.1016/s0954-6111(06)80166-6

Joyce, C. J., Shekar, K., & Cook, D. A. (2018). A mathematical model of CO2, O2 and N2 exchange during venovenous extracorporeal membrane oxygenation. *Intensive Care Med Exp*, *6*(1), 25. https://doi.org/10.1186/s40635-018-0183-4

Jubran, A., Van de Graaff, W. B., & Tobin, M. J. (1995). Variability of patient-ventilator interaction with pressure support ventilation in patients with chronic

obstructive pulmonary disease. *Am J Respir Crit Care Med*, *152*(1), 129-136. https://doi.org/10.1164/ajrccm.152.1.7599811

Kaegi-Braun, N., Mueller, M., Schuetz, P., Mueller, B., & Kutz, A. (2021). Evaluation of Nutritional Support and In-Hospital Mortality in Patients With Malnutrition. *JAMA Netw Open*, *4*(1), e2033433. https://doi.org/10.1001/jamanetworkopen.2020.33433

Kallet, R. H., & Diaz, J. V. (2009). The physiologic effects of noninvasive ventilation. *Respir Care*, *54*(1), 102-115.

Kanner, R. E., Anthonisen, N. R., & Connett, J. E. (2001). Lower respiratory illnesses promote FEV(1) decline in current smokers but not ex-smokers with mild chronic obstructive pulmonary disease: results from the lung health study. *Am J Respir Crit Care Med*, *164*(3), 358-364.

Karagiannidis, C., Hesselmann, F., & Fan, E. (2019). Physiological and Technical Considerations of Extracorporeal CO2 Removal. *Crit Care*, *23*(1), 75. https://doi.org/10.1186/s13054-019-2367-z

Karagiannidis, C., Kampe, K. A., Sipmann, F. S., Larsson, A., Hedenstierna, G., Windisch, W., & Mueller, T. (2014). Veno-venous extracorporeal CO2 removal for the treatment of severe respiratory acidosis: pathophysiological and technical considerations. *Crit Care*, *18*(3), R124. https://doi.org/10.1186/cc13928

Karagiannidis, C., Strassmann, S., Brodie, D., Ritter, P., Larsson, A., Borchardt, R., & Windisch, W. (2017). Impact of membrane lung surface area and blood flow on extracorporeal CO2 removal during severe respiratory acidosis. *Intensive Care Med Exp*, *5*(1), 34. https://doi.org/10.1186/s40635-017-0147-0

Karagiannidis, C., Strassmann, S., Schwarz, S., Merten, M., Fan, E., Beck, J., Sinderby, C., & Windisch, W. (2019). Control of respiratory drive by extracorporeal CO(2) removal in acute exacerbation of COPD breathing on non-invasive NAVA. *Crit Care*, *23*(1), 135. https://doi.org/10.1186/s13054-019-2404-y

Kessler, R., Stahl, E., Vogelmeier, C., Haughney, J., Trudeau, E., Lofdahl, C. G., & Partridge, M. R. (2006). Patient understanding, detection, and experience of

COPD exacerbations: an observational, interview-based study. *Chest*, *130*(1), 133-142.

Kesten, S., Celli, B., Decramer, M., Liu, D., & Tashkin, D. (2011). Adverse health consequences in COPD patients with rapid decline in FEV1 - evidence from the UPLIFT trial. *Respir Res*, *12*, 129.

Kinkead, R., Tenorio, L., Drolet, G., Bretzner, F., & Gargaglioni, L. (2014). Respiratory manifestations of panic disorder in animals and humans: a unique opportunity to understand how supramedullary structures regulate breathing. *Respir Physiol Neurobiol*, *204*, 3-13. https://doi.org/10.1016/j.resp.2014.06.013

Kluge, S., Braune, S. A., Engel, M., Nierhaus, A., Frings, D., Ebelt, H., Uhrig, A., Metschke, M., Wegscheider, K., Suttorp, N., & Rousseau, S. (2012). Avoiding invasive mechanical ventilation by extracorporeal carbon dioxide removal in patients failing noninvasive ventilation. *Intensive Care Med*, *38*(10), 1632-1639.

Ko, B. S., Ahn, S., Lim, K. S., Kim, W. Y., Lee, Y. S., & Lee, J. H. (2015). Early failure of noninvasive ventilation in chronic obstructive pulmonary disease with acute hypercapnic respiratory failure. *Intern Emerg Med*, *10*(7), 855-860. https://doi.org/10.1007/s11739-015-1293-6

Köhnlein, T., Windisch, W., & Kohler, D. (2014). Non-invasive positive pressure ventilation for the treatment of severe stable chronic obstructive pulmonary disease: a prospective, multicentre, randomised, controlled clinical trial. . *Lancet Respir Med.* , *2*(9), 698-705.

Kolobow, T., & Bowman, R. L. (1963). Construction and evaluation of an alveolar membrane artificial heart-lung. *Trans Am Soc Artif Intern Organs*, *9*, 238-243.

Kolobow, T., Gattinoni, L., Tomlinson, T., & Pierce, J. (1977). Control breathing using an extracorporeal membrane lung. *Anaesthesia*, *46*, 138-141.

Kostakou, E., Barrett, N., & Camporota, L. (2016). Electrical impedance tomography to determine optimal positive end-expiratory pressure in severe chronic

obstructive pulmonary disease. *Critical Care*, 1-2. https://doi.org/10.1186/s13054-016-1475-2

Kramer, N., Meyer, T. J., Meharg, J., Cece, R. D., & Hill, N. S. (1995). Randomized, prospective trial of noninvasive positive pressure ventilation in acute respiratory failure. *Am J Respir Crit Care Med*, *151*(6), 1799-1806. https://doi.org/10.1164/ajrccm.151.6.7767523

Krauss, E., van der Beck, D., Schmalz, I., Wilhelm, J., Tello, S., Dartsch, R. C., Mahavadi, P., Korfei, M., Teschner, E., Seeger, W., & Guenther, A. (2021). Evaluation of Regional Pulmonary Ventilation in Spontaneously Breathing Patients with Idiopathic Pulmonary Fibrosis (IPF) Employing Electrical Impedance Tomography (EIT): A Pilot Study from the European IPF Registry (eurIPFreg). *J Clin Med*, *10*(2). https://doi.org/10.3390/jcm10020192

Krell, W. S., & Rodarte, J. R. (1985). Effects of acute pleural effusion on respiratory system mechanics in dogs. *J Appl Physiol (1985)*, *59*(5), 1458-1463. https://doi.org/10.1152/jappl.1985.59.5.1458

Kreymann, K. G., Berger, M. M., Deutz, N. E., Hiesmayr, M., Jolliet, P., Kazandjiev, G., Nitenberg, G., van den Berghe, G., Wernerman, J., Ebner, C., Hartl, W., Heymann, C., & Spies, C. (2006). ESPEN Guidelines on Enteral Nutrition: Intensive care. *Clin Nutr*, *25*(2), 210-223. https://doi.org/10.1016/j.clnu.2006.01.021

Krohn, F., Novello, M., van der Giessen, R. S., De Zeeuw, C. I., Pel, J. J. M., & Bosman, L. W. J. (2023). The integrated brain network that controls respiration. *Elife*, *12*. https://doi.org/10.7554/eLife.83654

Kronibus, N., Seiler, F., Danziger, G., Muellenbach, R. M., Reyher, C., Becker, A. P., Kamphorst, M., Rixecker, T. M., Metz, C., Bals, R., Lepper, P. M., & Mang, S. (2022). Respiratory Physiology of COVID-19 and Influenza Associated Acute Respiratory Distress Syndrome. *J Clin Med*, *11*(21). https://doi.org/10.3390/jcm11216237

Kumar, S., Khilnani, G. C., Banga, A., & Sharma, S. K. (2013). Predictors of requirement of mechanical ventilation in patients with chronic obstructive pulmonary disease with acute respiratory failure. *Lung India*, *30*(3), 178-182.

Laghi, F., & Goyal, A. (2012). Auto-PEEP in respiratory failure. *Minerva Anestesiol*, *78*(2), 201-221.

Laghi, F., & Tobin, M. J. (2003). Disorders of the respiratory muscles. *Am J Respir Crit Care Med*, *168*(1), 10-48. https://doi.org/10.1164/rccm.2206020

Lai, N. M., Chaiyakunapruk, N., Lai, N. A., O'Riordan, E., Pau, W. S., & Saint, S. (2016). Catheter impregnation, coating or bonding for reducing central venous catheter-related infections in adults. *Cochrane Database Syst Rev*, *3*(3), Cd007878. https://doi.org/10.1002/14651858.CD007878.pub3

Lai, N. M., Lai, N. A., O'Riordan, E., Chaiyakunapruk, N., Taylor, J. E., & Tan, K. (2016). Skin antisepsis for reducing central venous catheter-related infections. *Cochrane Database Syst Rev*, *7*(7), Cd010140. https://doi.org/10.1002/14651858.CD010140.pub2

Lapinsky, S. E., & Easty, A. C. (2006). Electromagnetic interference in critical care. *J Crit Care*, *21*(3), 267-270. https://doi.org/10.1016/j.jcrc.2006.03.010

Leditschke, I. A., Green, M., Irvine, J., Bissett, B., & Mitchell, I. A. (2012). What are the barriers to mobilizing intensive care patients? *Cardiopulm Phys Ther J*, *23*(1), 26-29.

Lehle, K., Philipp, A., Hiller, K. A., Zeman, F., Buchwald, D., Schmid, C., Dornia, C., Lunz, D., Muller, T., & Lubnow, M. (2014). Efficiency of gas transfer in venovenous extracorporeal membrane oxygenation: analysis of 317 cases with four different ECMO systems. *Intensive Care Med*, *40*(12), 1870-1877. https://doi.org/10.1007/s00134-014-3489-z

Léotard, A., Lebret, M., Daabek, N., Prigent, H., Destors, M., Saint-Raymond, C., Sagniez, A., Leroux, K., Tamisier, R., Lofaso, F., Pépin, J. L., & Borel, J. C. (2021). Impact of Interface Type on Noninvasive Ventilation Efficacy in Patients With Neuromuscular Disease: A Randomized Cross-Over Trial. *Arch Bronconeumol (Engl Ed)*, *57*(4), 273-280. https://doi.org/10.1016/j.arbres.2020.05.024

Lewis, M. I., Belman, M. J., Monn, S. A., Elashoff, J. D., & Koerner, S. K. (1994). The relationship between oxygen consumption and work rate in patients with airflow obstruction. *Chest*, *106*(2), 366-372. https://doi.org/10.1378/chest.106.2.366

Lightowler, J. V., Wedzicha, J. A., Elliott, M. W., & Ram, F. S. (2003). Non-invasive positive pressure ventilation to treat respiratory failure resulting from exacerbations of chronic obstructive pulmonary disease: Cochrane systematic review and meta-analysis. *Bmj*, *326*(7382), 185.

Lionheart, W. (2004). EIT reconstruction algorithms: pitfalls, challenges and recent developments. . *Physiol Meas*, *25*, 125-142.

Livigni, S., Maio, M., Ferretti, E., Longobardo, A., Potenza, R., Rivalta, L., Selvaggi, P., Vergano, M., & Bertolini, G. (2006). Efficacy and safety of a low-flow veno-venous carbon dioxide removal device: results of an experimental study in adult sheep. *Crit Care*, *10*(5), R151.

Lopez-Barneo, J., Ortega-Saenz, P., Pardal, R., Pascual, A., & Piruat, J. I. (2008). Carotid body oxygen sensing. *Eur Respir J*, *32*(5), 1386-1398. https://doi.org/10.1183/09031936.00056408

Lougheed, D. M., Webb, K. A., & O'Donnell, D. E. (1995). Breathlessness during induced lung hyperinflation in asthma: the role of the inspiratory threshold load. *Am J Respir Crit Care Med*, *152*(3), 911-920. https://doi.org/10.1164/ajrccm.152.3.7663804

Lougheed, M. D., Lam, M., Forkert, L., Webb, K. A., & O'Donnell, D. E. (1993). Breathlessness during acute bronchoconstriction in asthma. Pathophysiologic mechanisms. *Am Rev Respir Dis*, *148*(6 Pt 1), 1452-1459. https://doi.org/10.1164/ajrccm/148.6_Pt_1.1452

Lowhagen, K., Lundin, S., & Stenqvist, O. (2010). Regional intratidal gas distribution in acute lung injury and acute respiratory distress syndrome--assessed by electric impedance tomography. *Minerva Anestesiol*, *76*(12), 1024-1035.

Lukacsovits, J., Szollosi, G., & Varga, J. T. (2023). Cardiovascular effects of exercise induced dynamic hyperinflation in COPD patients-Dynamically hyperinflated

and non-hyperinflated subgroups. *PLoS One*, *18*(1), e0274585. https://doi.org/10.1371/journal.pone.0274585

Lumb, A. (2017). *Nunn's Applied Respiratory Physiology* (8 ed.). Elsevier.

Lund, L. W., & Federspiel, W. J. (2013). Removing extra CO(2) in COPD patients. *Curr Respir Care Rep*, *2*(3), 131-138. https://doi.org/10.1007/s13665-013-0057-x

Luo, Y. M., Hart, N., Mustfa, N., Lyall, R. A., Polkey, M. I., & Moxham, J. (2001). Effect of diaphragm fatigue on neural respiratory drive. *J Appl Physiol (1985)*, *90*(5), 1691-1699. https://doi.org/10.1152/jappl.2001.90.5.1691

Luo, Y. M., Li, R., Jolley, C., Wu, H. D., Steier, J., Moxham, J., & Zhong, N. S. (2011). Neural Respiratory Drive in Patients with COPD during Exercise Tests. *Respiration*, *81*, 294-301.

Luo, Y. M., & Moxham, J. (2005). Measurement of neural respiratory drive in patients with COPD. *Respir Physiol Neurobiol*, *146*(2-3), 165-174. https://doi.org/10.1016/j.resp.2004.12.014

Luo, Y. M., Moxham, J., & Polkey, M. I. (2008). Diaphragm electromyography using an oesophageal catheter: current concepts. *Clin Sci (Lond)*, *115*(8), 233-244. https://doi.org/10.1042/cs20070348

Lynch, D. A., Sverzellati, N., Travis, W. D., Brown, K. K., Colby, T. V., Galvin, J. R., Goldin, J. G., Hansell, D. M., Inoue, Y., Johkoh, T., Nicholson, A. G., Knight, S. L., Raoof, S., Richeldi, L., Ryerson, C. J., Ryu, J. H., & Wells, A. U. (2018). Diagnostic criteria for idiopathic pulmonary fibrosis: a Fleischner Society White Paper. *Lancet Respir Med*, *6*(2), 138-153. https://doi.org/10.1016/s2213-2600(17)30433-2

Maarsingh, E. J., Oud, M., van Eykern, L. A., Hoekstra, M. O., & van Aalderen, W. M. (2006). Electromyographic monitoring of respiratory muscle activity in dyspneic infants and toddlers. *Respir Physiol Neurobiol*, *150*(2-3), 191-199. https://doi.org/10.1016/j.resp.2005.05.029

Maarsingh, E. J., van Eykern, L. A., de Haan, R. J., Griffioen, R. W., Hoekstra, M. O., & van Aalderen, W. M. (2002). Airflow limitation in asthmatic children assessed with a non-invasive EMG technique. *Respir Physiol Neurobiol*, *133*(1-2), 89-97.

Maarsingh, E. J., van Eykern, L. A., Sprikkelman, A. B., Hoekstra, M. O., & van Aalderen, W. M. (2000). Respiratory muscle activity measured with a noninvasive EMG technique: technical aspects and reproducibility. *J Appl Physiol (1985)*, *88*(6), 1955-1961. https://doi.org/10.1152/jappl.2000.88.6.1955

Machado, A., Barusso, M., De Brandt, J., Quadflieg, K., Haesevoets, S., Daenen, M., Thomeer, M., Ruttens, D., Marques, A., & Burtin, C. (2022). Impact of acute exacerbations of COPD on patients' health status beyond pulmonary function: A scoping review. *Pulmonology*. https://doi.org/10.1016/j.pulmoe.2022.04.004

Macklem, P. T., Fraser, R. G., & Brown, W. G. (1965). BRONCHIAL PRESSURE MEASUREMENTS IN EMPHYSEMA AND BRONCHITIS. *J Clin Invest*, *44*(6), 897-905. https://doi.org/10.1172/jci105206

MacLaren, G. (2012). Lessons in advanced extracorporeal life support. *Crit Care Med*, *40*(9), 2729-2731. https://doi.org/10.1097/CCM.0b013e31825ae6dc

Maj, R., Palermo, P., Gattarello, S., Brusatori, S., D'Albo, R., Zinnato, C., Velati, M., Romitti, F., Busana, M., Wieditz, J., Herrmann, P., Moerer, O., Quintel, M., Meissner, K., Sanderson, B., Chiumello, D., Marini, J. J., Camporota, L., & Gattinoni, L. (2023). Ventilatory ratio, dead space, and venous admixture in patients with acute respiratory distress syndrome. *Br J Anaesth*, *130*(3), 360-367. https://doi.org/10.1016/j.bja.2022.10.035

Makris, D., Desrousseaux, B., Zakynthinos, E., Durocher, A., & Nseir, S. (2011). The impact of COPD on ICU mortality in patients with ventilator-associated pneumonia. *Respir Med*, *105*(7), 1022-1029.

Mallick, A., Elliot, S., McKinlay, J., & Bodenham, A. (2007). Extracorporeal carbon dioxide removal using the Novalung in a patient with intracranial bleeding. *Anaesthesia*, *62*(1), 72-74.

Maltais, F., Ostinelli, J., Bourbeau, J., Tonnel, A. B., Jacquemet, N., Haddon, J., Rouleau, M., Boukhana, M., Martinot, J. B., & Duroux, P. (2002). Comparison of nebulized budesonide and oral prednisolone with placebo in the treatment of acute exacerbations of chronic obstructive pulmonary disease: a randomized controlled trial. *Am J Respir Crit Care Med*, *165*(5), 698-703.

Mamary, A. J., Kondapaneni, S., Vance, G. B., Gaughan, J. P., Martin, U. J., & Criner, G. J. (2011). Survival in Patients Receiving Prolonged Ventilation: Factors that Influence Outcome. *Clin Med Insights Circ Respir Pulm Med*, *5*, 17-26.

Mancebo, J., Isabey, D., Lorino, H., Lofaso, F., Lemaire, F., & Brochard, L. (1995). Comparative effects of pressure support ventilation and intermittent positive pressure breathing (IPPB) in non-intubated healthy subjects. *Eur Respir J*, *8*(11), 1901-1909. https://doi.org/10.1183/09031936.95.08111901

Marquis, F., Coulombe, N., Costa, R., Gagnon, H., Guardo, R., & Skrobik, Y. (2006). Electrical impedance tomography's correlation to lung volume is not influenced by anthropometric parameters. *J Clin Monit Comput*, *20*(3), 201-207. https://doi.org/10.1007/s10877-006-9021-4

Marthan, R., Castaing, Y., Manier, G., & Guenard, H. (1985). Gas exchange alterations in patients with chronic obstructive lung disease. *Chest*, *87*(4), 470-475. https://doi.org/10.1378/chest.87.4.470

Martin-Gonzalez, F., Gonzalez-Robledo, J., Sanchez-Hernandez, F., Moreno-Garcia, M. N., & Barreda-Mellado, I. (2016). Effectiveness and predictors of failure of noninvasive mechanical ventilation in acute respiratory failure. *Med Intensiva*, *40*(1), 9-17. https://doi.org/10.1016/j.medin.2015.01.007

März, A., Ukere, A., Wodack, K., Trepte, C., Waldmann, A., Böhm, S., & Reuter, D. (2015). Perioperative assessment of regional ventilation during changing body positions and ventilation conditions by electrical impedance tomography with increased spatial resolution and signal quality. . *Critical Care 19*(Suppl 1), P249.

Masaoka, Y., & Homma, I. (2001). The effect of anticipatory anxiety on breathing and metabolism in humans. *Respir Physiol*, *128*(2), 171-177.

Mathews, A. M., Wysham, N. G., Xie, J., Qin, X., Giovacchini, C. X., Ekström, M., & MacIntyre, N. R. (2020). Hypercapnia in Advanced Chronic Obstructive Pulmonary Disease: A Secondary Analysis of the National Emphysema Treatment Trial. *Chronic Obstr Pulm Dis*, *7*(4), 336-345. https://doi.org/10.15326/jcopdf.7.4.2020.0176

Mauri, T., Bellani, G., Confalonieri, A., Tagliabue, P., Turella, M., Coppadoro, A., Citerio, G., Patroniti, N., & Pesenti, A. (2013). Topographic distribution of tidal ventilation in acute respiratory distress syndrome: effects of positive end-expiratory pressure and pressure support. *Crit Care Med*, *41*(7), 1664-1673. https://doi.org/10.1097/CCM.0b013e318287f6e7

Mauri, T., Bellani, G., Salerno, D., Mantegazza, F., & Pesenti, A. (2013). Regional distribution of air trapping in chronic obstructive pulmonary disease. *Am J Respir Crit Care Med*, *188*(12), 1466-1467. https://doi.org/10.1164/rccm.201303-0463IM

May, A. G., Jeffries, R. G., Frankowski, B. J., Burgreen, G. W., & Federspiel, W. J. (2018). Bench Validation of a Compact Low-Flow CO2 Removal Device. *Intensive Care Med Exp*, *6*(1), 34. https://doi.org/10.1186/s40635-018-0200-7

McGregor, M., & Becklake, M. R. (1961). The relationship of oxygen cost of breathing to respiratory mechanical work and respiratory force. *J Clin Invest*, *40*(6), 971-980. https://doi.org/10.1172/jci104336

McHardy, G. J. (1967). The relationship between the differences in pressure and content of carbon dioxide in arterial and venous blood. *Clin Sci*, *32*(2), 299-309.

McNamee, J. J., Gillies, M. A., Barrett, N. A., Agus, A. M., Beale, R., Bentley, A., Bodenham, A., Brett, S. J., Brodie, D., Finney, S. J., Gordon, A. J., Griffiths, M., Harrison, D., Jackson, C., McDowell, C., McNally, C., Perkins, G. D., Tunnicliffe, W., Vuylsteke, A., . . . McAuley, D. F. (2017). pRotective vEntilation with veno-venouS lung assisT in respiratory failure: A protocol for a multicentre randomised controlled trial of extracorporeal carbon dioxide removal in

patients with acute hypoxaemic respiratory failure. *J Intensive Care Soc*, *18*(2), 159-169. https://doi.org/10.1177/1751143716681035

McNamee, J. J., Gillies, M. A., Barrett, N. A., Perkins, G. D., Tunnicliffe, W., Young, D., Bentley, A., Harrison, D. A., Brodie, D., Boyle, A. J., Millar, J. E., Szakmany, T., Bannard-Smith, J., Tully, R. P., Agus, A., McDowell, C., Jackson, C., & McAuley, D. F. (2021). Effect of Lower Tidal Volume Ventilation Facilitated by Extracorporeal Carbon Dioxide Removal vs Standard Care Ventilation on 90-Day Mortality in Patients With Acute Hypoxemic Respiratory Failure: The REST Randomized Clinical Trial. *Jama*, *326*(11), 1013-1023. https://doi.org/10.1001/jama.2021.13374

Mekontso Dessap, A., Charron, C., Devaquet, J., Aboab, J., Jardin, F., Brochard, L., & Vieillard-Baron, A. (2009). Impact of acute hypercapnia and augmented positive end-expiratory pressure on right ventricle function in severe acute respiratory distress syndrome. *Intensive Care Med*, *35*(11), 1850-1858. https://doi.org/10.1007/s00134-009-1569-2

Miedema, M., de Jongh, F. H., Frerichs, I., van Veenendaal, M. B., & van Kaam, A. H. (2011a). Changes in lung volume and ventilation during lung recruitment in high-frequency ventilated preterm infants with respiratory distress syndrome. *J Pediatr*, *159*(2), 199-205.e192. https://doi.org/10.1016/j.jpeds.2011.01.066

Miedema, M., de Jongh, F. H., Frerichs, I., van Veenendaal, M. B., & van Kaam, A. H. (2011b). Changes in lung volume and ventilation during surfactant treatment in ventilated preterm infants. *Am J Respir Crit Care Med*, *184*(1), 100-105. https://doi.org/10.1164/rccm.201103-0375OC

Miedema, M., de Jongh, F. H., Frerichs, I., van Veenendaal, M. B., & van Kaam, A. H. (2012). Regional respiratory time constants during lung recruitment in high-frequency oscillatory ventilated preterm infants. *Intensive Care Med*, *38*(2), 294-299. https://doi.org/10.1007/s00134-011-2410-2

Milici-Emili, G., & Petit, J. M. (1960). Mechanical efficiency of breathing. *J Appl Physiol*, *15*, 359-362. https://doi.org/10.1152/jappl.1960.15.3.359

Morelli, A., Del Sorbo, L., Pesenti, A., Ranieri, V. M., & Fan, E. (2017). Extracorporeal carbon dioxide removal (ECCO(2)R) in patients with acute respiratory failure. *Intensive Care Med*, *43*(4), 519-530. https://doi.org/10.1007/s00134-016-4673-0

Morishita-Katsu, M., Nishimura, K., Taniguchi, H., Kimura, T., Kondoh, Y., Kataoka, K., Ogawa, T., Watanabe, F., Arizono, S., Nishiyama, O., Nakayasu, K., Imaizumi, K., & Hasegawa, Y. (2016). The COPD assessment test and St George's Respiratory Questionnaire: are they equivalent in subjects with COPD? *Int J Chron Obstruct Pulmon Dis*, *11*, 1543-1551. https://doi.org/10.2147/copd.S104947

Morris, A. H., Wallace, C. J., Menlove, R. L., Clemmer, T. P., Orme, J. F., Jr., Weaver, L. K., Dean, N. C., Thomas, F., East, T. D., Pace, N. L., Suchyta, M. R., Beck, E., Bombino, M., Sittig, D. F., Bohm, S., Hoffmann, B., Becks, H., Butler, S., Pearl, J., & Rasmusson, B. (1994). Randomized clinical trial of pressure-controlled inverse ratio ventilation and extracorporeal CO2 removal for adult respiratory distress syndrome. *Am J Respir Crit Care Med*, *149*(2 Pt 1), 295-305.

Mortola, J. P. (2019). How to breathe? Respiratory mechanics and breathing pattern. *Respir Physiol Neurobiol*, *261*, 48-54. https://doi.org/10.1016/j.resp.2018.12.005

Moss, C. E., Galtrey, E. J., Camporota, L., Meadows, C., Gillon, S., Ioannou, N., & Barrett, N. A. (2016). A Retrospective Observational Case Series of Low-Flow Venovenous Extracorporeal Carbon Dioxide Removal Use in Patients with Respiratory Failure. *Asaio j*, *62*(4), 458-462. https://doi.org/10.1097/mat.0000000000000386

Moxham, J., & Jolley, C. (2009). Breathlessness, fatigue and the respiratory muscles. *Clin Med (Lond)*, *9*(5), 448-452.

Muders, T., Luepschen, H., Zinserling, J., Greschus, S., Fimmers, R., Guenther, U., Buchwald, M., Grigutsch, D., Leonhardt, S., Putensen, C., & Wrigge, H. (2012). Tidal recruitment assessed by electrical impedance tomography and

computed tomography in a porcine model of lung injury*. *Crit Care Med*, *40*(3), 903-911. https://doi.org/10.1097/CCM.0b013e318236f452

Muller, T., Lubnow, M., Philipp, A., Bein, T., Jeron, A., Luchner, A., Rupprecht, L., Reng, M., Langgartner, J., Wrede, C. E., Zimmermann, M., Birnbaum, D., Schmid, C., Riegger, G. A., & Pfeifer, M. (2009). Extracorporeal pumpless interventional lung assist in clinical practice: determinants of efficacy. *Eur Respir J*, *33*(3), 551-558. https://doi.org/10.1183/09031936.00123608

Murphy, P. B., Kumar, A., Reilly, C., Jolley, C., Walterspacher, S., Fedele, F., Hopkinson, N. S., Man, W. D., Polkey, M. I., Moxham, J., & Hart, N. (2011). Neural respiratory drive as a physiological biomarker to monitor change during acute exacerbations of COPD. *Thorax*, *66*(7), 602-608. https://doi.org/10.1136/thx.2010.151332

Murphy, P. B., Rehal, S., Arbane, G., Bourke, S., Calverley, P. M. A., Crook, A. M., Dowson, L., Duffy, N., Gibson, G. J., Hughes, P. D., Hurst, J. R., Lewis, K. E., Mukherjee, R., Nickol, A., Oscroft, N., Patout, M., Pepperell, J., Smith, I., Stradling, J. R., . . . Hart, N. (2017). Effect of Home Noninvasive Ventilation With Oxygen Therapy vs Oxygen Therapy Alone on Hospital Readmission or Death After an Acute COPD Exacerbation: A Randomized Clinical Trial. *Jama*, *317*(21), 2177-2186. https://doi.org/10.1001/jama.2017.4451

Nagaraj, C., Tabeling, C., Nagy, B. M., Jain, P. P., Marsh, L. M., Papp, R., Pienn, M., Witzenrath, M., Ghanim, B., Klepetko, W., Weir, E. K., Heschl, S., Kwapiszewska, G., Olschewski, A., & Olschewski, H. (2017). Hypoxic vascular response and ventilation/perfusion matching in end-stage COPD may depend on p22phox. *Eur Respir J*, *50*(1). https://doi.org/10.1183/13993003.01651-2016

Nava, S., Ambrosino, N., Clini, E., Prato, M., Orlando, G., Vitacca, M., Brigada, P., Fracchia, C., & Rubini, F. (1998). Noninvasive mechanical ventilation in the weaning of patients with respiratory failure due to chronic obstructive pulmonary disease. A randomized, controlled trial. *Ann Intern Med*, *128*(9), 721-728.

Newell, S. Z., McKenzie, D. K., & Gandevia, S. C. (1989). Inspiratory and skeletal muscle strength and endurance and diaphragmatic activation in patients with chronic airflow limitation. *Thorax*, *44*(11), 903-912. https://doi.org/10.1136/thx.44.11.903

Nguyen, P. L., Uddin, M. M., Mir, T., Khalil, A., Regmi, N., Pervaiz, A., Hussain, T., Babu, M. A., Ullah, I., Patel, P., Lohia, P., Saydain, G., Koul, P. A., & Soubani, A. O. (2021). Trends in Incidence, and Mortality of Acute Exacerbation of Chronic Obstructive Pulmonary Disease in the United States Emergency Department (2010-2018). *Copd*, 1-9. https://doi.org/10.1080/15412555.2021.1979500

NICE. (2011). Chronic obstructive pulmonary disease costing report. www.nice.org.uk/nicemedia/live/13029/53292/53292.pdf

Niewoehner, D. E. (2008). Oral prednisolone was not inferior to intravenous prednisolone for treatment failure in chronic obstructive pulmonary disease exacerbation. *Evid Based Med*, *13*(5), 145.

Niewoehner, D. E., Erbland, M. L., Deupree, R. H., Collins, D., Gross, N. J., Light, R. W., Anderson, P., & Morgan, N. A. (1999). Effect of systemic glucocorticoids on exacerbations of chronic obstructive pulmonary disease. Department of Veterans Affairs Cooperative Study Group. *N Engl J Med*, *340*(25), 1941-1947.

Nonato, N. L., Díaz, O., Nascimento, O. A., Dreyse, J., Jardim, J. R., & Lisboa, C. (2015). Behavior of Quality of Life (SGRQ) in COPD Patients According to BODE Scores. *Arch Bronconeumol*, *51*(7), 315-321. https://doi.org/10.1016/j.arbres.2014.02.017

O'Donnell, D., Chau, L., & Bertley, J. (1997). Qualitative aspects of exertional breathlessness in chronic airflow limitation: pathophysiologic mechanisms. *Am J Respir Crit Care Med*, *155*, 109-115.

O'Donnell, D., & Parker, C. (2006). COPD Exacerbations: Pathophysiology. *Thorax*, *61*, 354-361.

O'Donnell, D., Revill, S., & Webb, K. (2001). Dynamic hyperinflation and exercise intolerance in COPD. *Am J Respir Crit Care Med*

, *164*, 770-777.

O'Donnell, D., & Webb, K. (2003). Chronic obstructive pulmonary disease. In P. Calverley, W. MacNee, N. Pride, & S. Rennard (Eds.), *Exercise* (2 ed., pp. 243–269). Arnold.

O'Donnell, D. E. (2006). Hyperinflation, dyspnea, and exercise intolerance in chronic obstructive pulmonary disease. *Proc Am Thorac Soc*, *3*(2), 180-184. https://doi.org/10.1513/pats.200508-093DO

O'Donnell, D. E., D'Arsigny, C., Fitzpatrick, M., & Webb, K. A. (2002). Exercise hypercapnia in advanced chronic obstructive pulmonary disease: the role of lung hyperinflation. *Am J Respir Crit Care Med*, *166*(5), 663-668. https://doi.org/10.1164/rccm.2201003

O'Donnell, D. E., Milne, K. M., James, M. D., de Torres, J. P., & Neder, J. A. (2020). Dyspnea in COPD: New Mechanistic Insights and Management Implications. *Adv Ther*, *37*(1), 41-60. https://doi.org/10.1007/s12325-019-01128-9

O'Donnell, D. E., Neder, J. A., & Elbehairy, A. F. (2016). Physiological impairment in mild COPD. *Respirology*, *21*(2), 211-223. https://doi.org/10.1111/resp.12619

O'Donnell, D. E., Ora, J., Webb, K. A., Laveneziana, P., & Jensen, D. (2009). Mechanisms of activity-related dyspnea in pulmonary diseases. *Respir Physiol Neurobiol*, *167*(1), 116-132. https://doi.org/10.1016/j.resp.2009.01.010

O'Donnell, D. E., & Parker, C. M. (2006a). COPD exacerbations . 3: Pathophysiology. *Thorax*, *61*(4), 354-361. https://doi.org/10.1136/thx.2005.041830

O'Donnell, D. E., & Parker, C. M. (2006b). COPD exacerbations: Pathophysiology. *Thorax*, *61*(4), 354-361. https://doi.org/10.1136/thx.2005.041830

O'Neill, D. P., & Robbins, P. A. (2017). A mechanistic physicochemical model of carbon dioxide transport in blood. *J Appl Physiol (1985)*, *122*(2), 283-295. https://doi.org/10.1152/japplphysiol.00318.2016

Ohtake, S., Kawashima, Y., Hirose, H., Matsuda, H., Nakano, S., Kaku, K., & Okuda, A. (1983). Experimental evaluation of pumpless arteriovenous ECMO with

polypropylene hollow fiber membrane oxygenator for partial respiratory support. *Trans Am Soc Artif Intern Organs*, *29*, 237-241.

Ontario, H. Q. (2010). Extracorporeal Lung Support Technologies – Bridge to Recovery and Bridge to Lung Transplantation in Adult Patients: An Evidence-Based Analysis. *Ont Health Technol Assess Ser*, *10*(5), 1-47.

Orozco-Levi, M., Gea, J., Lloreta, J. L., Félez, M., Minguella, J., Serrano, S., & Broquetas, J. M. (1999). Subcellular adaptation of the human diaphragm in chronic obstructive pulmonary disease. *Eur Respir J*, *13*(2), 371-378. https://doi.org/10.1183/09031936.99.13237199

Orozco-Levi, M., Lloreta, J., & Minguella, J. (2001). Injury of the human diaphragm associated with exertion and chronic obstructive pulmonary disease. *Am J Respir Crit Care Med*, *164*, 1734–1739.

Orozco-Levi, M., Lloreta, J., Minguella, J., Serrano, S., Broquetas, J. M., & Gea, J. (2001). Injury of the human diaphragm associated with exertion and chronic obstructive pulmonary disease. *Am J Respir Crit Care Med*, *164*(9), 1734-1739. https://doi.org/10.1164/ajrccm.164.9.2011150

Osadnik, C. R., Tee, V. S., Carson-Chahhoud, K. V., Picot, J., Wedzicha, J. A., & Smith, B. J. (2017). Non-invasive ventilation for the management of acute hypercapnic respiratory failure due to exacerbation of chronic obstructive pulmonary disease. *Cochrane Database Syst Rev*, *7*, Cd004104. https://doi.org/10.1002/14651858.CD004104.pub4

Otis, A. B., Fenn, W. O., & Rahn, H. (1950). Mechanics of breathing in man. *J Appl Physiol*, *2*(11), 592-607. https://doi.org/10.1152/jappl.1950.2.11.592

Ozsancak Ugurlu, A., & Habesoglu, M. A. (2017). Epidemiology of NIV for Acute Respiratory Failure in COPD Patients: Results from the International Surveys vs. the "Real World". *Copd*, *14*(4), 429-438. https://doi.org/10.1080/15412555.2017.1336527

Ozyilmaz, E., Ugurlu, A. O., & Nava, S. (2014). Timing of noninvasive ventilation failure: causes, risk factors, and potential remedies. *BMC Pulm Med*, *14*, 19-19. https://doi.org/10.1186/1471-2466-14-19

Pare, P., Brooks, L., & Bates, J. H. (1982). Exponential analysis of the lung pressure-volume curve as a predictor of pulmonary emphysema. *Am Rev Respir Dis*, *126*, 54-61.

Park, M., Costa, E. L., Maciel, A. T., Silva, D. P., Friedrich, N., Barbosa, E. V., Hirota, A. S., Schettino, G., & Azevedo, L. C. (2013). Determinants of oxygen and carbon dioxide transfer during extracorporeal membrane oxygenation in an experimental model of multiple organ dysfunction syndrome. *PLoS One*, *8*(1), e54954. https://doi.org/10.1371/journal.pone.0054954

Patel, B. K., Wolfe, K. S., Pohlman, A. S., Hall, J. B., & Kress, J. P. (2016). Effect of Noninvasive Ventilation Delivered by Helmet vs Face Mask on the Rate of Endotracheal Intubation in Patients With Acute Respiratory Distress Syndrome: A Randomized Clinical Trial. *Jama*, *315*(22), 2435-2441. https://doi.org/10.1001/jama.2016.6338

Pauwels, R. A., Buist, A. S., Calverley, P. M., Jenkins, C. R., & Hurd, S. S. (2001). Global strategy for the diagnosis, management, and prevention of chronic obstructive pulmonary disease. NHLBI/WHO Global Initiative for Chronic Obstructive Lung Disease (GOLD) Workshop summary. *Am J Respir Crit Care Med*, *163*(5), 1256-1276.

Pecchiari, M., Loring, S. H., & D'Angelo, E. (2013). Esophageal pressure as an estimate of average pleural pressure with lung or chest distortion in rats. *Respir Physiol Neurobiol*, *186*(2), 229-235. https://doi.org/10.1016/j.resp.2013.02.006

Pejkovska, S., Kaeva, B. J., Goseva, Z., Arsovski, Z., Janeva, J. J., & Zeynel, S. (2015). Predictive Factors for the Effect of Treatment by Noninvasive Ventilation in Patients with Respiratory Failure as a Result of Acute Exacerbation of the Chronic Obstructive Pulmonary Disease. *Open Access Maced J Med Sci*, *3*(4), 655-660. https://doi.org/10.3889/oamjms.2015.115

Pellegrino, R., Violante, B., Nava, S., Rampulla, C., Brusasco, V., & Rodarte, J. R. (1993). Expiratory airflow limitation and hyperinflation during methacholine-induced bronchoconstriction. *J Appl Physiol (1985)*, *75*(4), 1720-1727. https://doi.org/10.1152/jappl.1993.75.4.1720

Penuelas, O., Frutos-Vivar, F., Fernandez, C., Anzueto, A., Epstein, S. K., Apezteguia, C., Gonzalez, M., Nin, N., Raymondos, K., Tomicic, V., Desmery, P., Arabi, Y., Pelosi, P., Kuiper, M., Jibaja, M., Matamis, D., Ferguson, N. D., & Esteban, A. (2011). Characteristics and outcomes of ventilated patients according to time to liberation from mechanical ventilation. *Am J Respir Crit Care Med*, *184*(4), 430-437.

Perme, C., Nalty, T., Winkelman, C., Kenji Nawa, R., & Masud, F. (2013). Safety and Efficacy of Mobility Interventions in Patients with Femoral Catheters in the ICU: A Prospective Observational Study. *Cardiopulm Phys Ther J*, *24*(2), 12-17.

Pesenti, A., Patroniti, N., & Fumagalli, R. (2010). Carbon dioxide dialysis will save the lung. *Crit Care Med*, *38*(10 Suppl), S549-554. https://doi.org/10.1097/CCM.0b013e3181f1fe0c

Petit, J. M., Milic-Emili, G., & Delhez, L. (1960). Role of the diaphragm in breathing in conscious normal man: an electromyographic study. *J Appl Physiol*, *15*, 1101-1106. https://doi.org/10.1152/jappl.1960.15.6.1101

Pham, T. M., Telias, I., & Beitler, J. R. (2020). Esophageal Manometry. *Respir Care*, *65*(6), 772-792. https://doi.org/10.4187/respcare.07425

PHE. (2023). *COPD: QOF prevalance (all ages) 2021/22*. https://fingertips.phe.org.uk/profile/inhale/data#page/3/gid/8000008/pat/15/par/E92000001/ati/167/are/E38000006/iid/253/age/1/sex/4/cat/-1/ctp/-1/yrr/1/cid/4/tbm/1/page-options/car-do-0

Piquilloud, L., Olivier, P. Y., Richard, J. C., Thepot-Seegers, V., Brochard, L., Mercat, A., & Beloncle, F. (2022). High flow nasal cannula improves breathing efficiency and ventilatory ratio in COPD patients recovering from an exacerbation. *J Crit Care*, *69*, 154023. https://doi.org/10.1016/j.jcrc.2022.154023

Pisani, L., Corcione, N., & Nava, S. (2016). Management of acute hypercapnic respiratory failure. *Curr Opin Crit Care*, *22*(1), 45-52. https://doi.org/10.1097/mcc.0000000000000269

Pisani, L., Fasano, L., Corcione, N., Comellini, V., Guerrieri, A., Ranieri, M. V., & Nava, S. (2015). Effects of Extracorporeal CO2 Removal on Inspiratory Effort and

Respiratory Pattern in Patients Who Fail Weaning from Mechanical Ventilation. *Am J Respir Crit Care Med*, *192*(11), 1392-1394. https://doi.org/10.1164/rccm.201505-0930LE

Plant, P. K., Owen, J. L., & Elliott, M. W. (2000). Early use of non-invasive ventilation for acute exacerbations of chronic obstructive pulmonary disease on general respiratory wards: a multicentre randomised controlled trial. *Lancet*, *355*(9219), 1931-1935.

Plant, P. K., Owen, J. L., & Elliott, M. W. (2001). Non-invasive ventilation in acute exacerbations of chronic obstructive pulmonary disease: long term survival and predictors of in-hospital outcome. *Thorax*, *56*(9), 708-712. https://doi.org/10.1136/thorax.56.9.708

Polkey, M., Kyroussis, D., & Hamnegard, C. (1996). Diaphragm strength in chronic obstructive pulmonary disease. *Am J Respir Crit Care Med*, *154*, 1310-1317.

Polkey, M. I., Kyroussis, D., Hamnegard, C. H., Mills, G. H., Green, M., & Moxham, J. (1996). Diaphragm strength in chronic obstructive pulmonary disease. *Am J Respir Crit Care Med*, *154*(5), 1310-1317. https://doi.org/10.1164/ajrccm.154.5.8912741

Prinianakis, G., Delmastro, M., Carlucci, A., Ceriana, P., & Nava, S. (2004). Effect of varying the pressurisation rate during noninvasive pressure support ventilation. *Eur Respir J*, *23*(2), 314-320. https://doi.org/10.1183/09031936.03.00010203

Pulletz, S., Kott, M., Elke, G., dler, D. S., Vogt, B., Weiler, N., & Frerichs, I. z. (2012). Dynamics of regional lung aeration determined by electrical impedance tomography in patients with acute respiratory distress syndrome. *7*(1), 1-1. https://doi.org/10.1186/2049-6958-7-44

Pulletz, S., van Genderingen, H. R., Schmitz, G., Zick, G., Schadler, D., Scholz, J., Weiler, N., & Frerichs, I. (2006). Comparison of different methods to define regions of interest for evaluation of regional lung ventilation by EIT. *Physiol Meas*, *27*(5), S115-127. https://doi.org/10.1088/0967-3334/27/5/s10

Purro, A., Appendini, L., Patessio, A., Zanaboni, S., Gudjonsdottir, M., Rossi, A., & Donner, C. F. (1998). Static intrinsic PEEP in COPD patients during spontaneous breathing. *Am J Respir Crit Care Med*, *157*(4 Pt 1), 1044-1050. https://doi.org/10.1164/ajrccm.157.4.9702007

Putensen, C., Hentze, B., Muenster, S., & Muders, T. (2019). Electrical Impedance Tomography for Cardio-Pulmonary Monitoring. *J Clin Med*, *8*(8). https://doi.org/10.3390/jcm8081176

Quon, B. S., Gan, W. Q., & Sin, D. D. (2008). Contemporary management of acute exacerbations of COPD: a systematic review and metaanalysis. *Chest*, *133*(3), 756-766.

Rabbani, K., & Kabir, A. (1991). Studies on the effect of the third dimension on a two-dimensional electrical impedance tomography system. *Clin Phys Physiol Meas*, *12*(293-402).

Raluy-Callado, M., Lambrelli, D., MacLachlan, S., & Khalid, J. M. (2015). Epidemiology, severity, and treatment of chronic obstructive pulmonary disease in the United Kingdom by GOLD 2013. *Int J Chron Obstruct Pulmon Dis*, 925-937.

Ram, F. S., Picot, J., Lightowler, J., & Wedzicha, J. A. (2004). Non-invasive positive pressure ventilation for treatment of respiratory failure due to exacerbations of chronic obstructive pulmonary disease. *Cochrane Database Syst Rev*(3), Cd004104. https://doi.org/10.1002/14651858.CD004104.pub3

Ramos, R. P., Alencar, M. C., Treptow, E., Arbex, F., Ferreira, E. M., & Neder, J. A. (2013). Clinical usefulness of response profiles to rapidly incremental cardiopulmonary exercise testing. *Pulm Med*, *2013*, 359021. https://doi.org/10.1155/2013/359021

Ramsook, A. H., Mitchell, R. A., Bell, T., Calli, S., Kennedy, C., Lehmann, J., Thompson, M., Puyat, J. H., & Guenette, J. A. (2017). Is parasternal intercostal EMG an accurate surrogate of respiratory neural drive and biomarker of dyspnea during cycle exercise testing? *Respir Physiol Neurobiol*, *242*, 40-44. https://doi.org/10.1016/j.resp.2017.03.003

Ranieri, V. M., Grasso, S., Mascia, L., Martino, S., Fiore, T., Brienza, A., & Giuliani, R. (1997). Effects of proportional assist ventilation on inspiratory muscle effort in patients with chronic obstructive pulmonary disease and acute respiratory failure. *Anesthesiology*, *86*(1), 79-91. https://doi.org/10.1097/00000542-199701000-00012

Ranieri, V. M., Mascia, L., Petruzzelli, V., Bruno, F., Brienza, A., & Giuliani, R. (1995). Inspiratory effort and measurement of dynamic intrinsic PEEP in COPD patients: effects of ventilator triggering systems. *Intensive Care Med*, *21*(11), 896-903.

Reilly, C. C., Jolley, C. J., Elston, C., Moxham, J., & Rafferty, G. F. (2012). Measurement of parasternal intercostal electromyogram during an infective exacerbation in patients with cystic fibrosis. *Eur Respir J*, *40*(4), 977-981. https://doi.org/10.1183/09031936.00163111

Reilly, C. C., Jolley, C. J., Ward, K., MacBean, V., Moxham, J., & Rafferty, G. F. (2013). Neural respiratory drive measured during inspiratory threshold loading and acute hypercapnia in healthy individuals. *Exp Physiol*, *98*(7), 1190-1198. https://doi.org/10.1113/expphysiol.2012.071415

Reilly, C. C., Ward, K., Jolley, C. J., Lunt, A. C., Steier, J., Elston, C., Polkey, M. I., Rafferty, G. F., & Moxham, J. (2011). Neural respiratory drive, pulmonary mechanics and breathlessness in patients with cystic fibrosis. *Thorax*, *66*(3), 240-246. https://doi.org/10.1136/thx.2010.142646

Reis Miranda, D., van Thiel, R., Brodie, D., & Bakker, J. (2015). Right ventricular unloading after initiation of venovenous extracorporeal membrane oxygenation. *Am J Respir Crit Care Med*, *191*(3), 346-348. https://doi.org/10.1164/rccm.201408-1404LE

Retter, A., Wyncoll, D., Pearse, R., Carson, D., McKechnie, S., Stanworth, S., Allard, S., Thomas, D., & Walsh, T. (2013). Guidelines on the management of anaemia and red cell transfusion in adult critically ill patients. *Br J Haematol*, *160*(4), 445-464. https://doi.org/10.1111/bjh.12143

Riedel, T., Kyburz, M., Latzin, P., Thamrin, C., & Frey, U. (2009). Regional and overall ventilation inhomogeneities in preterm and term-born infants. *Intensive Care Med*, *35*(1), 144-151. https://doi.org/10.1007/s00134-008-1299-x

Riley, R. L., & Cournand, A. (1949). Ideal alveolar air and the analysis of ventilation-perfusion relationships in the lungs. *J Appl Physiol*, *1*(12), 825-847. https://doi.org/10.1152/jappl.1949.1.12.825

Riley, R. L., & Cournand, A. (1951). Analysis of factors affecting partial pressures of oxygen and carbon dioxide in gas and blood of lungs; theory. *J Appl Physiol*, *4*(2), 77-101. https://doi.org/10.1152/jappl.1951.4.2.77

Robertson, C. H., Jr., Foster, G. H., & Johnson, R. L., Jr. (1977). The relationship of respiratory failure to the oxygen consumption of, lactate production by, and distribution of blood flow among respiratory muscles during increasing inspiratory resistance. *J Clin Invest*, *59*(1), 31-42. https://doi.org/10.1172/jci108619

Robertson, C. H., Jr., Pagel, M. A., & Johnson, R. L., Jr. (1977). The distribution of blood flow, oxygen consumption, and work output among the respiratory muscles during unobstructed hyperventilation. *J Clin Invest*, *59*(1), 43-50. https://doi.org/10.1172/jci108620

Robinson, T. D., Freiberg, D. B., Regnis, J. A., & Young, I. H. (2000). The role of hypoventilation and ventilation-perfusion redistribution in oxygen-induced hypercapnia during acute exacerbations of chronic obstructive pulmonary disease. *Am J Respir Crit Care Med*, *161*(5), 1524-1529. https://doi.org/10.1164/ajrccm.161.5.9904119

Rochwerg, B., Brochard, L., Elliott, M. W., Hess, D., Hill, N. S., Nava, S., Navalesi, P. M. O. T. S. C., Antonelli, M., Brozek, J., Conti, G., Ferrer, M., Guntupalli, K., Jaber, S., Keenan, S., Mancebo, J., Mehta, S., & Raoof, S. M. O. T. T. F. (2017). Official ERS/ATS clinical practice guidelines: noninvasive ventilation for acute respiratory failure. *Eur Respir J*, *50*(2). https://doi.org/10.1183/13993003.02426-2016

Roussos, C. (1985). Structure and function of the thorax: energetics. In C. Roussos & P. T. Macklem (Eds.), *The Thorax* (pp. 437-492). Dekker.

Roussos, C., & Campbell, E. J. M. (2011). Respiratory Muscle Energetics. In *Compr Physiol* (pp. 481-509). https://doi.org/https://doi.org/10.1002/cphy.cp030328

Roussos, C., & Koutsoukou, A. (2003). Respiratory failure. *Eur Respir J Suppl*, *47*, 3s-14s. https://doi.org/10.1183/09031936.03.00038503

Ruberto, F., Pugliese, F., D'Alio, A., Perrella, S., D'Auria, B., Ianni, S., Anile, M., Venuta, F., Coloni, G. F., & Pietropaoli, P. (2009). Extracorporeal removal CO2 using a venovenous, low-flow system (Decapsmart) in a lung transplanted patient: a case report. *Transplant Proc*, *41*(4), 1412-1414.

Sahetya, S. K., & Brower, R. G. (2016). The promises and problems of transpulmonary pressure measurements in acute respiratory distress syndrome. *Curr Opin Crit Care*, *22*(1), 7-13. https://doi.org/10.1097/mcc.0000000000000268

Sapey, E., & Stockley, R. A. (2006). COPD exacerbations . 2: aetiology. *Thorax*, *61*(3), 250-258.

Sassoon, C. S. H., Del Rosario, N., Fei, R., Rheeman, C. H., Gruer, S. E., & Mahutte, K. C. (1994). Influence of pressure- and flow-triggered synchronous intermittent mandatory ventilation on inspiratory muscle work. *Crit Care Med*, *22*(12), 1933-1941. https://journals.lww.com/ccmjournal/Fulltext/1994/12000/Influence_of_pressure_and_flow_triggered.8.aspx

Saure, E. W., Eagan, T. M., Jensen, R. L., Voll-Aanerud, M., Aukrust, P., Bakke, P. S., & Hardie, J. A. (2012). Explained variance for blood gases in a population with COPD. *Clin Respir J*, *6*(2), 72-80. https://doi.org/10.1111/j.1752-699X.2011.00248.x

Scaravilli, V., Kreyer, S., Belenkiy, S., Linden, K., Zanella, A., Li, Y., Dubick, M. A., Cancio, L. C., Pesenti, A., & Batchinsky, A. I. (2016). Extracorporeal Carbon Dioxide Removal Enhanced by Lactic Acid Infusion in Spontaneously Breathing

Conscious Sheep. *Anesthesiology*, *124*(3), 674-682. https://doi.org/10.1097/aln.0000000000000995

Scaravilli, V., Kreyer, S., Linden, K., Belenkiy, S., Pesenti, A., Zanella, A., Cancio, L. C., & Batchinsky, A. I. (2015). Enhanced Extracorporeal CO2 Removal by Regional Blood Acidification: Effect of Infusion of Three Metabolizable Acids. *Asaio j*, *61*(5), 533-539. https://doi.org/10.1097/mat.0000000000000238

Schettino, G., Altobelli, N., & Kacmarek, R. M. (2008). Noninvasive positive-pressure ventilation in acute respiratory failure outside clinical trials: experience at the Massachusetts General Hospital. *Crit Care Med*, *36*(2), 441-447.

Schmidt, M., Jaber, S., Zogheib, E., Godet, T., Capellier, G., & Combes, A. (2018). Feasibility and safety of low-flow extracorporeal CO2 removal managed with a renal replacement platform to enhance lung-protective ventilation of patients with mild-to-moderate ARDS. *Crit Care*, *22*(1), 122. https://doi.org/10.1186/s13054-018-2038-5

Schnell, D., Timsit, J. F., Darmon, M., Vesin, A., Goldgran-Toledano, D., Dumenil, A. S., Garrouste-Orgeas, M., Adrie, C., Bouadma, L., Planquette, B., Cohen, Y., Schwebel, C., Soufir, L., Jamali, S., Souweine, B., & Azoulay, E. (2014). Noninvasive mechanical ventilation in acute respiratory failure: trends in use and outcomes. *Intensive Care Med*, *40*(4), 582-591. https://doi.org/10.1007/s00134-014-3222-y

Schöps, M., Groß-Hardt, S. H., Schmitz-Rode, T., Steinseifer, U., Brodie, D., Clauser, J. C., & Karagiannidis, C. (2021). Hemolysis at low blood flow rates: in-vitro and in-silico evaluation of a centrifugal blood pump. *Journal of Translational Medicine*, *19*(1), 2. https://doi.org/10.1186/s12967-020-02599-z

Schulman, S., & Kearon, C. (2005). Definition of major bleeding in clinical investigations of antihemostatic medicinal products in non-surgical patients. *J Thromb Haemost*, *3*(4), 692-694. https://doi.org/10.1111/j.1538-7836.2005.01204.x

Seemungal, T., & Sykes, A. (2008). Recent advances in exacerbations of COPD. *Thorax*, *63*(10), 850-852.

Seemungal, T. A., Donaldson, G. C., Bhowmik, A., Jeffries, D. J., & Wedzicha, J. A. (2000). Time course and recovery of exacerbations in patients with chronic obstructive pulmonary disease. *Am J Respir Crit Care Med*, *161*(5), 1608-1613.

SEL. (2012). *Power calculator for continuous outcome superiority trial.* https://www.sealedenvelope.com/power/continuous-superiority/

Sferrazza Papa, G. F., Di Marco, F., Akoumianaki, E., & Brochard, L. (2012). Recent advances in interfaces for non-invasive ventilation: from bench studies to practical issues. *Minerva Anestesiol*, *78*(10), 1146-1153.

Shah, C. H., Onukwugha, E., Zafari, Z., Villalonga-Olives, E., Park, J. E., & Slejko, J. F. (2021). Economic burden of comorbidities among COPD Patients hospitalized for acute exacerbations: an analysis of a commercially insured population. *Expert Rev Pharmacoecon Outcomes Res*, 1-8. https://doi.org/10.1080/14737167.2021.1981291

Shah, N. M., Hart, N., & Kaltsakas, G. (2022). Managing breathlessness in end-stage COPD: a neural respiratory drive approach. *J Bras Pneumol*, *48*(4), e20220264. https://doi.org/10.36416/1806-3756/e20220264

Shono, A., & Kotani, T. (2019). Clinical implication of monitoring regional ventilation using electrical impedance tomography. *J Intensive Care*, *7*(1), 4. https://doi.org/10.1186/s40560-019-0358-4

Siggaard-Andersen, O. (1971). An acid-base chart for arterial blood with normal and pathophysiological reference areas. *Scand J Clin Lab Invest*, *27*(3), 239-245.

Similowski, T., Yan, S., Gauthier, A. P., Macklem, P. T., & Bellemare, F. (1991). Contractile properties of the human diaphragm during chronic hyperinflation. *N Engl J Med*, *325*(13), 917-923. https://doi.org/10.1056/nejm199109263251304

Sinderby, C., Spahija, J., Beck, J., Kaminski, D., Yan, S., Comtois, N., & Sliwinski, P. (2001). Diaphragm activation during exercise in chronic obstructive pulmonary disease. *Am J Respir Crit Care Med*, *163*(7), 1637-1641. https://doi.org/10.1164/ajrccm.163.7.2007033

Singer, P. (2019). Preserving the quality of life: nutrition in the ICU. *Crit Care*, *23*(Suppl 1), 139. https://doi.org/10.1186/s13054-019-2415-8

Singer, P., Blaser, A. R., Berger, M. M., Alhazzani, W., Calder, P. C., Casaer, M. P., Hiesmayr, M., Mayer, K., Montejo, J. C., Pichard, C., Preiser, J. C., van Zanten, A. R. H., Oczkowski, S., Szczeklik, W., & Bischoff, S. C. (2019). ESPEN guideline on clinical nutrition in the intensive care unit. *Clin Nutr*, *38*(1), 48-79. https://doi.org/10.1016/j.clnu.2018.08.037

Sinha, P., Calfee, C. S., Beitler, J. R., Soni, N., Ho, K., Matthay, M. A., & Kallet, R. H. (2019). Physiologic Analysis and Clinical Performance of the Ventilatory Ratio in Acute Respiratory Distress Syndrome. *Am J Respir Crit Care Med*, *199*(3), 333-341. https://doi.org/10.1164/rccm.201804-0692OC

Sklar, M. C., Beloncle, F., Katsios, C. M., Brochard, L., & Friedrich, J. O. (2015). Extracorporeal carbon dioxide removal in patients with chronic obstructive pulmonary disease: a systematic review. *Intensive Care Med*, *41*(10), 1752-1762. https://doi.org/10.1007/s00134-015-3921-z

Smith, J. C. (2022). Respiratory rhythm and pattern generation: Brainstem cellular and circuit mechanisms. *Handb Clin Neurol*, *188*, 1-35. https://doi.org/10.1016/b978-0-323-91534-2.00004-7

Soo Hoo, G. W. (2010). Noninvasive ventilation in adults with acute respiratory distress: a primer for the clinician. *Hosp Pract (Minneap)*, *38*(1), 16-25.

Soo Hoo, G. W., Santiago, S., & Williams, A. J. (1994). Nasal mechanical ventilation for hypercapnic respiratory failure in chronic obstructive pulmonary disease: determinants of success and failure. *Crit Care Med*, *22*(8), 1253-1261.

Spencer, S., Calverley, P. M., Burge, P. S., & Jones, P. W. (2004). Impact of preventing exacerbations on deterioration of health status in COPD. *Eur Respir J*, *23*(5), 698-702.

Spinelli, E., Crotti, S., Zacchetti, L., Bottino, N., Berto, V., Russo, R., Chierichetti, M., Protti, A., & Gattinoni, L. (2013). Effect of extracorporeal CO2 removal on respiratory rate in spontaneously breathing patients with chronic obstructive pulmonary disease exacerbation. *Critical Care*, *17*(S2), P128.

Spinelli, E., Mauri, T., Beitler, J. R., Pesenti, A., & Brodie, D. (2020). Respiratory drive in the acute respiratory distress syndrome: pathophysiology, monitoring, and therapeutic interventions. *Intensive Care Med*, *46*, 606–618.

Stefan, M., Nathanson, B., Higgins, T., Steingrub, J., Lagu, T., & Rothberg, M. (2015). Comparative effectiveness of noninvasive and invasive ventilation in critically ill patients with acute exacerbation of chronic obstructive pulmonary disease. *Crit Care Med*, *43*, 1386–1394.

Stefan, M. S., Shieh, M. S., Pekow, P. S., Hill, N., Rothberg, M. B., & Lindenauer, P. K. (2015). Trends in mechanical ventilation among patients hospitalized with acute exacerbations of COPD in the United States, 2001 to 2011. *Chest*, *147*(4), 959-968. https://doi.org/10.1378/chest.14-1216

Steier, J., Jolley, C. J., Polkey, M. I., & Moxham, J. (2011). Nocturnal asthma monitoring by chest wall electromyography. *Thorax*, *66*(7), 609-614. https://doi.org/10.1136/thx.2010.152462

Steier, J., Jolley, C. J., Seymour, J., Ward, K., Luo, Y. M., Polkey, M. I., & Moxham, J. (2010). Increased load on the respiratory muscles in obstructive sleep apnea. *Respir Physiol Neurobiol*, *171*(1), 54-60. https://doi.org/10.1016/j.resp.2010.01.012

Steriade, A. T., Gologanu, M., Bumbacea, R. S., Bogdan, S. N., & Bumbacea, D. (2022). Esophageal Pressure Measurement in Acute Hypercapnic Respiratory Failure Due to Severe COPD Exacerbation Requiring NIV-A Pilot Safety Study. *J Clin Med*, *11*(22). https://doi.org/10.3390/jcm11226810

Steriade, A. T., Johari, S., Sargarovschi, N., Necula, D., Tudose, C. E., Ionita, D., Bogdan, M. A., & Bumbacea, D. (2019). Predictors of outcome of noninvasive ventilation in severe COPD exacerbation. *BMC Pulm Med*, *19*(1), 131. https://doi.org/10.1186/s12890-019-0892-9

Strassmann, S., Merten, M., Schafer, S., de Moll, J., Brodie, D., Larsson, A., Windisch, W., & Karagiannidis, C. (2019). Impact of sweep gas flow on extracorporeal CO2 removal (ECCO2R). *Intensive Care Med Exp*, *7*(1), 17. https://doi.org/10.1186/s40635-019-0244-3

Su, P. L., Kao, P. S., Lin, W. C., Su, P. F., & Chen, C. W. (2016). Limited predictability of maximal muscular pressure using the difference between peak airway pressure and positive end-expiratory pressure during proportional assist ventilation (PAV). *Crit Care*, *20*(1), 382. https://doi.org/10.1186/s13054-016-1554-4

Suarez-Sipmann, F., Santos, A., Böhm, S. H., Borges, J. B., Hedenstierna, G., & Tusman, G. (2013). Corrections of Enghoff's dead space formula for shunt effects still overestimate Bohr's dead space. *Respir Physiol Neurobiol*, *189*(1), 99-105. https://doi.org/10.1016/j.resp.2013.06.020

Suh, E. S., Mandal, S., Harding, R., Ramsay, M., Kamalanathan, M., Henderson, K., O'Kane, K., Douiri, A., Hopkinson, N. S., Polkey, M. I., Rafferty, G., Murphy, P. B., Moxham, J., & Hart, N. (2015). Neural respiratory drive predicts clinical deterioration and safe discharge in exacerbations of COPD. *Thorax*, *70*(12), 1123-1130. https://doi.org/10.1136/thoraxjnl-2015-207188

Sun, L., Kaesler, A., Fernando, P., Thompson, A. J., Toomasian, J. M., & Bartlett, R. H. (2018). CO2 clearance by membrane lungs. *Perfusion*, *33*(4), 249-253. https://doi.org/10.1177/0267659117736379

Sun, W., Wang, S., Chen, Z., Zhang, J., Li, T., Arias, K., Griffith, B. P., & Wu, Z. J. (2020). Impact of high mechanical shear stress and oxygenator membrane surface on blood damage relevant to thrombosis and bleeding in a pediatric ECMO circuit. *Artif Organs*, *44*(7), 717-726. https://doi.org/10.1111/aor.13646

Tabak, Y. P., Sun, X., Johannes, R. S., Gupta, V., & Shorr, A. F. (2009). Mortality and need for mechanical ventilation in acute exacerbations of chronic obstructive pulmonary disease: development and validation of a simple risk score. *Arch Intern Med*, *169*(17), 1595-1602.

Taccone, F. S., Malfertheiner, M. V., Ferrari, F., Di Nardo, M., Swol, J., Broman, L. M., Vercaemst, L., Barrett, N., Pappalardo, F., Belohlavek, J., Mueller, T., Lorusso, R., & Belliato, M. (2017). Extracorporeal CO2 removal in critically ill patients: a systematic review. *Minerva Anestesiol*, *83*(7), 762-772. https://doi.org/10.23736/s0375-9393.17.11835-3

Tantucci, C., Corbeil, C., Chassé, M., Braidy, J., Matar, N., & Milic-Emili, J. (1991). Flow resistance in patients with chronic obstructive pulmonary disease in acute respiratory failure. Effects of flow and volume. *Am Rev Respir Dis*, *144*(2), 384-389. https://doi.org/10.1164/ajrccm/144.2.384

Terragni, P., Maiolo, G., & Ranieri, V. M. (2012). Role and potentials of low-flow CO(2) removal system in mechanical ventilation. *Curr Opin Crit Care*, *18*(1), 93-98. https://doi.org/10.1097/MCC.0b013e32834f17ef

Terragni, P. P., Birocco, A., Faggiano, C., & Ranieri, V. M. (2010). Extracorporeal CO2 removal. *Contrib Nephrol*, *165*, 185-196. https://doi.org/10.1159/000313758

Terragni, P. P., Del Sorbo, L., Mascia, L., Urbino, R., Martin, E. L., Birocco, A., Faggiano, C., Quintel, M., Gattinoni, L., & Ranieri, V. M. (2009). Tidal volume lower than 6 ml/kg enhances lung protection: role of extracorporeal carbon dioxide removal. *Anesthesiology*, *111*(4), 826-835.

Terry, P. B., Traystman, R. J., Newball, H. H., Batra, G., & Menkes, H. A. (1978). Collateral ventilation in man. *N Engl J Med*, *298*(1), 10-15. https://doi.org/10.1056/nejm197801052980103

Thompson, W. H., Nielson, C. P., Carvalho, P., Charan, N. B., & Crowley, J. J. (1996). Controlled trial of oral prednisone in outpatients with acute COPD exacerbation. *Am J Respir Crit Care Med*, *154*(2 Pt 1), 407-412.

Tipton, M. J., Harper, A., Paton, J. F. R., & Costello, J. T. (2017). The human ventilatory response to stress: rate or depth? *J Physiol*, *595*(17), 5729-5752. https://doi.org/10.1113/jp274596

Tobin, M. J., Laghi, F., & Brochard, L. (2009). Role of the respiratory muscles in acute respiratory failure of COPD: lessons from weaning failure. *J Appl Physiol*, *107*(3), 962-970. https://doi.org/10.1152/japplphysiol.00165.2009

Tobin, M. J., Laghi, F., & Jubran, A. (2012). Ventilatory failure, ventilator support, and ventilator weaning. *Compr Physiol*, *2*(4), 2871-2921. https://doi.org/10.1002/cphy.c110030

Toft-Petersen, A. P., Torp-Pedersen, C., Weinreich, U. M., & Rasmussen, B. S. (2017). Trends in assisted ventilation and outcome for obstructive pulmonary disease exacerbations. A nationwide study. *PLoS One*, *12*(2), e0171713. https://doi.org/10.1371/journal.pone.0171713

Toomasian, J. M., & Bartlett, R. H. (2011). Hemolysis and ECMO pumps in the 21st Century. *Perfusion*, *26*(1), 5-6. https://doi.org/10.1177/0267659110396015

Trenk, F., Mendes, L., Carvalho, P., Paiva, R. P., Henriques, J., Maglaveras, N., Chouvarda, I., Tsara, V., & Teixeira, C. A. (2016). Evaluation of lung ventilation distribution in chronic obstructive pulmonary disease patients using the global inhomogeneity index. *Conf Proc IEEE Eng Med Biol Soc*, *2016*, 5286-5289. https://doi.org/10.1109/embc.2016.7591920

Turri, F., & Yanagihara, J. I. (2011). Computer-assisted numerical analysis for oxygen and carbon dioxide mass transfer in blood oxygenators. *Artif Organs*, *35*(6), 579-592. https://doi.org/10.1111/j.1525-1594.2010.01150.x

Tusman, G., Sipmann, F. S., & Bohm, S. H. (2012). Rationale of dead space measurement by volumetric capnography. *Anesth Analg*, *114*(4), 866-874. https://doi.org/10.1213/ANE.0b013e318247f6cc

Tusman, G., Sipmann, F. S., Borges, J. B., Hedenstierna, G., & Bohm, S. H. (2011). Validation of Bohr dead space measured by volumetric capnography. *Intensive Care Med*, *37*(5), 870-874. https://doi.org/10.1007/s00134-011-2164-x

van Gemert, J. P., Brijker, F., Witten, M. A., & Leenen, L. P. (2015). Intubation after noninvasive ventilation failure in chronic obstructive pulmonary disease: associated factors at emergency department presentation. *Eur J Emerg Med*, *22*(1), 49-54. https://doi.org/10.1097/mej.0000000000000141

Van Slyke, D. D., Sendroy, J., & Liu, S. H. (1932). MANOMETRIC ANALYSIS OF GAS MIXTURES: III. MANOMETRIC DETERMINATION OF CARBON DIOXIDE TENSION AND pHs OF BLOOD. *Journal of Biological Chemistry*, *95*(2), 547-568. https://doi.org/https://doi.org/10.1016/S0021-9258(18)76334-5

Vaporidi, K., Akoumianaki, E., Telias, I., Goligher, E. C., Brochard, L., & Georgopoulos, D. (2020). Respiratory drive in critically ill patients. Pathophysiology and clinical implications. *Am J Respir Crit Care Med*, *201*, 20–32.

Vasques, F., Camporota, L., & Barrett, N. A. (2020). Nonantibiotic Pharmacological Treatment of Severe Chronic Obstructive Pulmonary Disease Exacerbations. *Semin Respir Crit Care Med*. https://doi.org/10.1055/s-0040-1714379

Velasquez Reyes, D. C., Bloomer, M., & Morphet, J. (2017). Prevention of central venous line associated bloodstream infections in adult intensive care units: A systematic review. *Intensive Crit Care Nurs*, *43*, 12-22. https://doi.org/10.1016/j.iccn.2017.05.006

Vestbo, J., Hurd, S. S., Agusti, A. G., Jones, P. W., Vogelmeier, C., Anzueto, A., Barnes, P. J., Fabbri, L. M., Martinez, F. J., Nishimura, M., Stockley, R. A., Sin, D. D., & Rodriguez-Roisin, R. (2013). Global strategy for the diagnosis, management, and prevention of chronic obstructive pulmonary disease: GOLD executive summary. *Am J Respir Crit Care Med*, *187*(4), 347-365. https://doi.org/10.1164/rccm.201204-0596PP

Visser, B. F. (1960). Pulmonary Diffusion of Carbon Dioxide. *Physics in Medicine & Biology*, *5*(2), 155. https://doi.org/10.1088/0031-9155/5/2/305

Vogt, B., Pulletz, S., Elke, G., Zhao, Z., Zabel, P., Weiler, N., & Frerichs, I. (2012). Spatial and temporal heterogeneity of regional lung ventilation determined by electrical impedance tomography during pulmonary function testing. *J Appl Physiol (1985)*, *113*(7), 1154-1161. https://doi.org/10.1152/japplphysiol.01630.2011

Vogt, B., Zhao, Z., Zabel, P., Weiler, N., & Frerichs, I. (2016). Regional lung response to bronchodilator reversibility testing determined by electrical impedance tomography in chronic obstructive pulmonary disease. *Am J Physiol Lung Cell Mol Physiol*, *311*(1), L8-l19. https://doi.org/10.1152/ajplung.00463.2015

Wagers, S., & Jaffe, E. (2003). Development structure and physiology in normal

and asthmatic lung. In N. J. Adkinson, J. Yunginger, W. Busse, B. Bochner, S. Holgate, & F. Simons (Eds.), *Middleton's Allergy: Principles and Practice* (6th ed.). Mosby, Inc.

Wagner, P. D. (2008). Causes of a high physiological dead space in critically ill patients. *Crit Care*, *12*(3), 148. https://doi.org/10.1186/cc6888

Wagner, P. D., Dantzker, D. R., Dueck, R., Clausen, J. L., & West, J. B. (1977). Ventilation-perfusion inequality in chronic obstructive pulmonary disease. *J Clin Invest*, *59*(2), 203-216. https://doi.org/10.1172/jci108630

Wearden, P. D., Federspiel, W. J., Morley, S. W., Rosenberg, M., Bieniek, P. D., Lund, L. W., & Ochs, B. D. (2012). Respiratory dialysis with an active-mixing extracorporeal carbon dioxide removal system in a chronic sheep study [Article]. *Intensive Care Med*, *38*(10), 1705-1711. https://doi.org/10.1007/s00134-012-2651-8

Weatherall, M., Marsh, S., Shirtcliffe, P., Williams, M., Travers, J., & Beasley, R. (2009). Quality of life measured by the St George's Respiratory Questionnaire and spirometry. *European Respiratory Journal*, *33*(5), 1025-1030. https://doi.org/10.1183/09031936.00116808

Wedzicha, J. A., & Seemungal, T. A. (2007). COPD exacerbations: defining their cause and prevention. *Lancet*, *370*(9589), 786-796. https://doi.org/10.1016/s0140-6736(07)61382-8

Welling, J. B. A., Hartman, J. E., Ten Hacken, N. H. T., Klooster, K., & Slebos, D.-J. (2015). The minimal important difference for the St George's Respiratory Questionnaire in patients with severe COPD. *European Respiratory Journal*, *46*(6), 1598-1604. https://doi.org/10.1183/13993003.00535-2015

West, J. B. (2011). Causes of and Compensations for Hypoxemia and Hypercapnia. *Compr Physiol*, *1*, 1541-1553.

West, J. B., Dollery, C. T., & Naimark, A. (1964). Distribution of Blood Flow in Isolated Lung; Relation to vascular and alveolar pressures. *J Appl Physiol*, *19*, 713-724. https://doi.org/10.1152/jappl.1964.19.4.713

West, J. B., & Wagner, P. D. (1998). Pulmonary gas exchange. *Am J Respir Crit Care Med*, *157*(4 Pt 2), S82-87. https://doi.org/10.1164/ajrccm.157.4.nhlbi-4

Whittaker, H., Rubino, A., Müllerová, H., Morris, T., Varghese, P., Xu, Y., De Nigris, E., & Quint, J. K. (2022). Frequency and Severity of Exacerbations of COPD Associated with Future Risk of Exacerbations and Mortality: A UK Routine Health Care Data Study. *Int J Chron Obstruct Pulmon Dis*, *17*, 427-437. https://doi.org/10.2147/copd.S346591

Wier, L., Elixhauser, A., Pfuntner, A., & Au, D. (2011). Overview of Hospitalizations among Patients with COPD, 2008: Statistical Brief #106. . *Healthcare Cost and Utilization Project (HCUP) Statistical Briefs 106*. http://www.ncbi.nlm.nih.gov/books/NBK53969/

Windisch, W., Storre, J. H., & Köhnlein, T. (2015). Nocturnal non-invasive positive pressure ventilation for COPD. . *Expert Rev Respir Med.*, *9*(3), 295–308.

Wrigge, H., Zinserling, J., Muders, T., Varelmann, D., Gunther, U., von der Groeben, C., Magnusson, A., Hedenstierna, G., & Putensen, C. (2008). Electrical impedance tomography compared with thoracic computed tomography during a slow inflation maneuver in experimental models of lung injury. *Crit Care Med*, *36*(3), 903-909. https://doi.org/10.1097/ccm.0b013e3181652edd

Wu, W., Guan, L., Li, X., Lin, L., Guo, B., Yang, Y., Liang, Z., Wang, F., Zhou, L., & Chen, R. (2017). Correlation and compatibility between surface respiratory electromyography and transesophageal diaphragmatic electromyography measurements during treadmill exercise in stable patients with COPD. *Int J Chron Obstruct Pulmon Dis*, *12*, 3273-3280. https://doi.org/10.2147/copd.s148980

Wysocki, M., Richard, J. C., & Meshaka, P. (2002). Noninvasive proportional assist ventilation compared with noninvasive pressure support ventilation in hypercapnic acute respiratory failure. *Crit Care Med*, *30*(2), 323-329. https://doi.org/10.1097/00003246-200202000-00010

Yan, S., Sinderby, C., Bielen, P., Beck, J., Comtois, N., & Sliwinski, P. (2000). Expiratory muscle pressure and breathing mechanics in chronic obstructive pulmonary

disease. *Eur Respir J*, *16*(4), 684-690. https://doi.org/10.1034/j.1399-3003.2000.16d20.x

Yerworth, R. J., Frerichs, I., & Bayford, R. (2016). Analysis and compensation for errors in electrical impedance tomography images and ventilation-related measures due to serial data collection. *J Clin Monit Comput*. https://doi.org/10.1007/s10877-016-9920-y

Zanella, A., Giani, M., Redaelli, S., Mangili, P., Scaravilli, V., Ormas, V., Costanzi, M., Albertini, M., Bellani, G., Patroniti, N., & Pesenti, A. (2013). Infusion of 2.5 meq/min of Lactic Acid minimally increases CO2 production compared to an isocaloric glucose infusion in healthy anesthetized, mechanically ventilated pigs. *Crit Care*, *17*(6), R268. https://doi.org/10.1186/cc13098

Zanella, A., Patroniti, N., Isgro, S., Albertini, M., Costanzi, M., Pirrone, F., Scaravilli, V., Vergnano, B., & Pesenti, A. (2009). Blood acidification enhances carbon dioxide removal of membrane lung: an experimental study. *Intensive Care Med*, *35*(8), 1484-1487. https://doi.org/10.1007/s00134-009-1513-5

Zhao, Z., Chang, M. Y., Frerichs, I., Zhang, J. H., Chang, H. T., Gow, C. H., & Möller, K. (2020). Regional air trapping in acute exacerbation of obstructive lung diseases measured with electrical impedance tomography: a feasibility study. *Minerva Anestesiol*, *86*(2), 172-180. https://doi.org/10.23736/s0375-9393.19.13732-7

Zhao, Z., Moller, K., Steinmann, D., Frerichs, I., & Guttmann, J. (2009). Evaluation of an electrical impedance tomography-based Global Inhomogeneity Index for pulmonary ventilation distribution. *Intensive Care Med*, *35*(11), 1900-1906. https://doi.org/10.1007/s00134-009-1589-y

Zhao, Z., Pulletz, S., Frerichs, I., Muller-Lisse, U., & Moller, K. (2014). The EIT-based global inhomogeneity index is highly correlated with regional lung opening in patients with acute respiratory distress syndrome. *BMC Res Notes*, *7*, 82. https://doi.org/10.1186/1756-0500-7-82

Zheng, M. (2023). Dead space ventilation-related indices: bedside tools to evaluate the ventilation and perfusion relationship in patients with acute respiratory

distress syndrome. *Critical Care*, *27*(1), 46. https://doi.org/10.1186/s13054-023-04338-4

Zimmermann, M., Bein, T., Arlt, M., Philipp, A., Rupprecht, L., Mueller, T., Lubnow, M., Graf, B., & Schlitt, H. (2009). Pumpless extracorporeal interventional lung assist in patients with acute respiratory distress syndrome: a prospective pilot study. *Crit Care*, *13*, R10.

Zimmermann, M., Bein, T., Philipp, A., Ittner, K., Foltan, M., Drescher, J., Weber, F., & Schmid, F. X. (2006). Interhospital transportation of patients with severe lung failure on pumpless extracorporeal lung assist. *Br J Anaesth*, *96*(1), 63-66.

Zwischenberger, J. B., & Alpard, S. K. (2002). Artificial lungs: a new inspiration. *Perfusion*, *17*(4), 253-268.

Zwischenberger, J. B., Alpard, S. K., Tao, W., Deyo, D. J., & Bidani, A. (2001). Percutaneous extracorporeal arteriovenous carbon dioxide removal improves survival in respiratory distress syndrome: a prospective randomized outcomes study in adult sheep. *J Thorac Cardiovasc Surg*, *121*(3), 542-551.

Zwischenberger, J. B., Savage, C., Witt, S. A., Alpard, S. K., Harper, D. D., & Deyo, D. J. (2002). Arterio-venous CO2 removal (AVCO2R) perioperative management: rapid recovery and enhanced survival. *J Invest Surg*, *15*(1), 15-21.

Appendix – study publications

Barrett, N. A., and L. Camporota. 2017. The evolving role and practical application of extracorporeal carbon dioxide removal in critical care, *Crit Care Resusc*, 19: 62-67.

Barrett, N. A., N. Hart, and L. Camporota. 2019. Assessment of Work of Breathing in Patients with Acute Exacerbations of Chronic Obstructive Pulmonary Disease, *COPD*, 16: 418-28.

Barrett, N. A., N. Hart, and L. Camporota. 2020a. In vivo carbon dioxide clearance of a low-flow extracorporeal carbon dioxide removal circuit in patients with acute exacerbations of chronic obstructive pulmonary disease, *Perfusion*, 35: 436-41.

Barrett, N. A., N. Hart, and L. Camporota. 2020b. In-vitro performance of a low flow extracorporeal carbon dioxide removal circuit, *Perfusion*, 35: 227-35.

Barrett, N. A., N. Hart, K. J. R. Daly, M. Marotti, E. Kostakou, C. Carlin, S. Lua, S. Singh, A. Bentley, A. Douiri, and L. Camporota. 2022. A randomised controlled trial of non-invasive ventilation compared with extracorporeal carbon dioxide removal for acute hypercapnic exacerbations of chronic obstructive pulmonary disease, *Ann Intensive Care*, 12: 36.

Barrett, N. A., E. Kostakou, N. Hart, A. Douiri, and L. Camporota. 2019. Extracorporeal carbon dioxide removal for acute hypercapnic exacerbations of chronic obstructive pulmonary disease: study protocol for a randomised controlled trial, *Trials*, 20: 465.